



# University of HUDDERSFIELD

## University of Huddersfield Repository

Zheng, Lin

Model-based Condition Monitoring of Anti-lock Braking Systems

### Original Citation

Zheng, Lin (2014) Model-based Condition Monitoring of Anti-lock Braking Systems. Doctoral thesis, University of Huddersfield.

This version is available at <http://eprints.hud.ac.uk/id/eprint/20331/>

The University Repository is a digital collection of the research output of the University, available on Open Access. Copyright and Moral Rights for the items on this site are retained by the individual author and/or other copyright owners. Users may access full items free of charge; copies of full text items generally can be reproduced, displayed or performed and given to third parties in any format or medium for personal research or study, educational or not-for-profit purposes without prior permission or charge, provided:

- The authors, title and full bibliographic details is credited in any copy;
- A hyperlink and/or URL is included for the original metadata page; and
- The content is not changed in any way.

For more information, including our policy and submission procedure, please contact the Repository Team at: [E.mailbox@hud.ac.uk](mailto:E.mailbox@hud.ac.uk).

<http://eprints.hud.ac.uk/>

# **Model-based Condition Monitoring of Anti-lock Braking Systems**

**This thesis is submitted to the University of Huddersfield  
in Partial Fulfilment of the Requirements for  
the degree of Doctor of Philosophy  
in the School of Computing and Engineering**

**2014**

**Lin Zheng**

# LIST OF CONTENTS

<b>LIST OF CONTENTS</b> .....	2
<b>LIST OF FIGURES</b> .....	9
<b>LIST OF TABLES</b> .....	19
<b>LIST OF NOMENCLATURE</b> .....	20
<b>ABSTRACT</b> .....	24
<b>DECLARATION</b> .....	26
<b>COPYRIGHT STATEMENT</b> .....	27
<b>ACKNOWLEDGEMENT</b> .....	28
<b>PUBLICATIONS</b> .....	29
<b>CHAPTER ONE</b>	
<b>INTRODUCTION</b> .....	32
1.1 INTRODUCTION TO ABS RELIABILITY .....	33
1.2 INTRODUCTION TO CONDITION MONITORING.....	35
1.3 INTRODUCTION TO THE MODEL-BASED APPROACH .....	36
1.4 INTRODUCTION TO THE KALMAN FILTER .....	37
1.5 RESEARCH AIMS AND OBJECTIVES .....	38
1.6 STRUCTURE OF THIS THESIS .....	40
<b>CHAPTER TWO</b>	
<b>LITERATURE REVIEW</b> .....	42
2.1 THE MODEL-BASED APPROACH FOR CONDITION	

MONITORING.....	43
2.1.1 Development of Model-based Methods .....	43
2.1.2 Basic Theory of the Model-based Approach .....	45
2.1.3 A General Introduction to Residual Generation in the Model-based Approach.....	49
2.1.4 Fault Modelling and Fault Testing.....	51
2.1.5 Advantages of using a Model-based Approach for Condition Monitoring .....	52
2.2 OVERVIEW OF ABS .....	53
2.2.1 Introduction.....	53
2.2.2 The Development of ABS.....	53
2.2.3 The Basic Theory of ABS.....	55
2.2.4 Technical Requirements and Evaluation Methods of ABS .	61
2.3 THE BASIC COMPOSITION AND WORKING PRINCIPLES OF ABS.....	62
2.3.1 The Components of ABS .....	62
2.3.2 Working Process of ABS .....	64
2.4 THE CONTROL PRINCIPLES OF ABS.....	67
2.4.1 Control Methods .....	68
2.4.2 Control Channel Layout on Vehicle Dynamics .....	69
2.5 MODEL-BASED CONDITION MONITORING OF ABS.....	70
2.6 SUMMARY .....	72

## **CHAPTER THREE**

### **THEORETICAL MODEL OF**

### **THE ANTI-LOCK BRAKING SYSTEM .....74**

#### **3.1 DYNAMIC ANALYSIS OF THE THREE STEPS OF ABS**

#### **CONTROL.....75**

##### **3.1.1 The Pressure Increasing Mode.....75**

##### **3.1.2 The Pressure Decreasing Mode .....79**

##### **3.1.3 The Pressure Holding Mode .....80**

##### **3.1.4 Parameter Setting for the Three Steps of the ABS .....82**

#### **3.2 CONTROL CYCLES OF ABS .....82**

#### **3.3 GENERAL FAULTS OF ABS .....85**

##### **3.3.1 Wheel Speed Sensor Failure .....85**

##### **3.3.2 Solenoid Valve Sticking or Stuck .....86**

##### **3.3.3 Fluid Leakage .....86**

##### **3.3.4 Pump Efficiency Loss .....87**

##### **3.3.5 Pressure Hysteresis .....87**

##### **3.3.6 Air Blister Inclusion in Brake Fluid .....88**

#### **3.4 FRICTION COEFFICIENT CALCULATION .....88**

#### **3.5 THE KALMAN FILTER FOR VELOCITY ESTIMATION .....90**

##### **3.5.1 The Kalman Filter Algorithm .....90**

##### **3.5.2 The Kalman Filter of Wheel Velocity .....92**

##### **3.5.3 The Kalman Filter of Vehicle Velocity .....93**

3.5.4 Parameter Adaptive Kalman Filter .....	95	
3.6 SUMMARY .....	96	
<b>CHAPTER FOUR</b>		
<b>THE SIMULATION MODEL OF</b>		
<b>THE ANTI-LOCK BRAKING SYSTEM .....</b>		<b>98</b>
4.1 THE ABS CONTROL MODEL .....	99	
4.1.1 The Calculation Module of Slip Rate .....	99	
4.1.2 The Dynamic Model of the Vehicle .....	99	
4.1.3 Friction Coefficient Calculation .....	100	
4.1.4 The Braking Simulation without ABS .....	102	
4.2 THE SIMULATION MODEL WITHOUT PRESSURE-HOLDING PROCESS .....	102	
4.3 THE SIMULATION MODEL WITH PRESSURE-HOLDING PROCESS .....	105	
4.4 THE FAULT SIMULATION.....	110	
4.4.1 Wheel Speed Sensor Failure .....	110	
4.4.2 Solenoid Valve Sticking or Stuck .....	111	
4.4.3 Fluid Leakage .....	112	
4.4.4 Pump Efficiency Loss .....	113	
4.5 SUMMARY .....	114	

**CHAPTER FIVE**

**SIMULATION RESULTS OF**

<b>THE ANTI-LOCK BRAKING SYSTEM .....</b>	<b>116</b>
5.1 SIMULATION RESULTS WITHOUT ABS.....	117
5.2 SIMULATION RESULTS WITHOUT PRESSURE-HOLDING PROCESS .....	119
5.3 SIMULATION RESULTS WITH PRESSURE-HOLDING PROCESS .....	123
5.4 COMPARISON RESULTS .....	127
5.5 THE SIMULATION RESULTS WITH SPEED SENSOR FAILURE .....	131
5.6 THE SIMULATION RESULTS WITH SOLENOID VALVE STICKING OR STUCK .....	136
5.7 THE SIMULATION RESULTS WITH FLUID LEAKAGE .....	141
5.8 THE SIMULATION RESULTS WITH PUMP EFFICIENCY LOSS .....	146
5.9 SUMMARY .....	152
 <b>CHAPTER SIX</b>	
 <b>TEST RIG DEVELOPMENT OF</b>	
 <b>THE ANTI-LOCK BRAKING SYSTEM .....</b>	<b>153</b>
6.1 THE OBJECTIVES OF THE TEST RIG .....	154
6.2 DSPACE MICROAUTOBOX II .....	154
6.3 THE DESIGN OF THE ABS TEST RIG.....	156
6.3.1 The Overall Design.....	156

6.3.2 Speed Signal Collection.....	158
6.3.3 Schematic Diagrams of the Three Steps.....	163
6.3.4 Data Acquisition Component.....	165
6.3.5 Other Components .....	168
6.4 AUTONOMOUS CONTROL OF THE ABS SYSTEM USING THE DSPACE TOOLBOX.....	171
6.5 TEST RESULTS OF ABS SYSTEM UNDER AUTONOMOUS CONTROL.....	172
6.6 SUMMARY .....	174
<b>CHAPTER SEVEN</b>	
<b>ABS MONITORING USING THE KALMAN FILTER .....</b>	<b>175</b>
7.1 TEST RESULTS UNDER NORMAL CONDITION.....	176
7.1.1 Comparison Results between the Simulation and the Kalman Filter Estimation .....	177
7.1.2 Comparison Results between the Measurement and the Kalman Filter Estimation.....	181
7.2 TEST RESULTS OF WHEEL SPEED SENSOR FAILURE .....	185
7.2.1 Vehicle Velocity with Speed Sensor Failure.....	185
7.2.2 Wheel Velocity with Speed Sensor Failure .....	188
7.3 TEST RESULTS OF SOLENOID VALVE STICKING OR STUCK .....	191

7.3.1 Vehicle Velocity with Solenoid Valve Sticking or Stuck Fault	191
7.3.2 Wheel Velocity with Solenoid Valve Sticking or Stuck Fault	193
7.4 TEST RESULTS OF LIQUID LEAKAGE	195
7.4.1 Vehicle Velocity with Liquid Leakage Fault	195
7.4.2 Wheel Velocity with Liquid Leakage Fault	198
7.5 TEST RESULTS OF PUMPEFFICIENCY LOSS	200
7.5.1 Vehicle Velocity with Pump Efficiency Loss	200
7.5.2 Wheel Velocity with Pump Efficiency Loss	202
7.6 SUMMARY	204
<b>CHAPTER EIGHT</b>	
<b>CONCLUSIONS AND FUTURE WORK</b>	205
8.1 REVIEW OF PROJECT OBJECTIVES AND ACHIEVEMENTS	206
8.2 CONCLUSIONS	210
8.3 CONTRIBUTION TO KNOWLEDGE	213
8.4 FUTURE WORK	214
<b>REFERENCES</b>	217

# LIST OF FIGURES

Figure 2.1 Factors applied on the actual system.....	46
Figure 2.2 The scheme of the model-based condition monitoring approach.....	49
Figure 2.3 Redundant signal structure in residual generation .....	50
Figure 2.4 Typical ABS components .....	55
Figure 2.5 The simplified model of a wheel.....	56
Figure 2.6 Illustration of the relationship between the braking coefficient and wheel slip .....	60
Figure 2.7 Structure of an Anti-lock Braking System .....	64
Figure 2.8 Sketch of solenoid valve .....	66
Figure 3.1 Schematic diagram of brake pedal and master cylinder .....	75
Figure 3.2 Sketch of the pressure increasing process of ABS .....	77
Figure 3.3 Sketch of the pressure decreasing process of ABS .....	79
Figure 3.4 Pressure holding process structure diagram.....	81
Figure 3.5 Control cycles of the ABS system with hydraulic brakes.....	84
Figure 3.6 Typical slip rate – friction coefficient characteristics .....	88
Figure 4.1 Simulation module of slip rate .....	99
Figure 4.2 Simulation model of the vehicle .....	100
Figure 4.3 Simulink module of friction coefficient with input of slip rate .....	101

Figure 4.4 Simulation model of hydraulic pressure braking without ABS .....	102
Figure 4.5 Braking torque logic controller module without the pressure-holding process.....	104
Figure 4.6 Simulation model of logic control without the pressure-holding process.....	105
Figure 4.7 Simulation model of logic control with the pressure-holding process.....	107
Figure 4.8 Braking torque controller with pressure-holding process .....	107
Figure 4.9 Braking torque subsystem with dSpace DAC module.....	108
Figure 4.10 Disconnection problem of dSpace .....	108
Figure 4.11 Stateflow of logic control on high friction coefficient road	110
Figure 4.12 Simulink model of speed sensor failure in braking torque subsystem.....	111
Figure 4.13 Simulink model of valve stuck failure in braking torque subsystem.....	112
Figure 4.14 Simulink model of liquid leakage in braking torque subsystem.....	113
Figure 4.15 Simulink model of pump efficiency loss in braking torque subsystem.....	114
Figure 5.1 Velocity in braking without ABS .....	117
Figure 5.2 Braking distance without ABS .....	118

Figure 5.3 Slip rate in braking without ABS ..... 118

Figure 5.4 Braking torque without ABS ..... 119

Figure 5.5 Velocity under logic control without the pressure-holding process.....120

Figure 5.6 Braking distance under logic control without the pressure-holding process.....121

Figure 5.7 Slip rate under logic control without the pressure-holding process.....121

Figure 5.8 Braking torque under logic control without the pressure-holding process.....122

Figure 5.9 Braking torque comparison with memory and real-time without the pressure-holding process .....122

Figure 5.10 Zoom in of Figure 5.9 .....123

Figure 5.11 Velocity under logic control with the pressure-holding process.....124

Figure 5.12 Braking distance with the pressure-holding process.....124

Figure 5.13 Slip rate under logic control with the pressure-holding process.....125

Figure 5.14 Braking torque under logic control with the pressure-holding process.....126

Figure 5.15 Wheel acceleration under logic control with the pressure-holding process.....126

Figure 5.16 Action choice of Stateflow with the pressure-holding process .....	127
Figure 5.17 Comparison of vehicle velocity .....	128
Figure 5.18 Comparison of wheel velocity .....	129
Figure 5.19 Comparison of braking distance.....	129
Figure 5.20 Comparison of slip rate .....	130
Figure 5.21 Comparison of braking torque .....	131
Figure 5.22 Vehicle velocity with speed sensor failure .....	132
Figure 5.23 Residual of vehicle velocity with speed sensor failure.....	132
Figure 5.24 Wheel velocity with speed sensor failure.....	133
Figure 5.25 Residual of a wheel velocity with speed sensor failure .....	133
Figure 5.26 Braking distance with speed sensor failure.....	134
Figure 5.27 Slip rate with speed sensor failure .....	135
Figure 5.28 Braking torque with speed sensor failure.....	135
Figure 5.29 Vehicle velocity with valve stuck.....	137
Figure 5.30 Residual of vehicle velocity with valve stuck.....	137
Figure 5.31 Wheel velocity with valve stuck .....	138
Figure 5.32 Residual of wheel velocity with valve stuck.....	139
Figure 5.33 Braking distance with valve stuck.....	139
Figure 5.34 Slip rate with valve stuck fault.....	140
Figure 5.35 Wheel acceleration with valve stuck.....	140
Figure 5.36 Vehicle velocity with fluid leakage .....	142

Figure 5.37 Residual of the vehicle velocity with fluid leakage .....	142
Figure 5.38 Wheel velocity with fluid leakage.....	143
Figure 5.39 Residual of wheel velocity with fluid leakage .....	143
Figure 5.40 Braking distance with fluid leakage.....	144
Figure 5.41 Slip rate with fluid leakage.....	145
Figure 5.42 Braking torque with fluid leakage.....	145
Figure 5.43 Wheel acceleration with fluid leakage .....	146
Figure 5.44 Vehicle velocity with pump efficiency loss.....	147
Figure 5.45 Residual of vehicle velocity with pump efficiency loss ...	148
Figure 5.46 Wheel velocity with pump efficiency loss .....	149
Figure 5.47 Residual of wheel velocity with pump efficiency loss .....	149
Figure 5.48 Braking distance with pump efficiency loss .....	150
Figure 5.49 Slip rate with pump efficiency loss .....	150
Figure 5.50 Braking torque with pump efficiency loss .....	151
Figure 5.51 Wheel acceleration with pump efficiency loss.....	151
Figure 6.1 Top view of dSpace MicroAutoBoxII .....	155
Figure 6.2 dSpace MicroAutoBoxII I/O connector .....	155
Figure 6.3 dSpace MicroAutoBoxII I/O connector with hub .....	156
Figure 6.4 The entire design of the ABS test rig .....	157
Figure 6.5 Construction of the ABS test rig .....	158
Figure 6.6 Speed sensor of front wheel .....	159
Figure 6.7 Speed sensor of rear wheel.....	159

Figure 6.8 Speed sensor of rear wheel on test rig .....	159
Figure 6.9 The principle of the wheel speed sensor .....	160
Figure 6.10 Wheel speed sensor signal voltage comparison .....	161
Figure 6.11 Speed sensor data of the vehicle at 20km/h .....	162
Figure 6.12 Speed sensor data of the vehicle at 30km/h .....	162
Figure 6.13 Speed sensor data of the vehicle at 40km/h .....	163
Figure 6.14 Pressure increasing sketch.....	164
Figure 6.15 Pressure holding sketch.....	164
Figure 6.16 Pressure decrease sketch .....	165
Figure 6.17 The National Instruments Data Acquisition Card .....	166
Figure 6.18 Signal label application diagram of NI DAQ.....	166
Figure 6.19 The ABS controller.....	168
Figure 6.20 The ABS control unit.....	169
Figure 6.21 The master cylinder .....	169
Figure 6.22 The vacuum booster and the accumulator.....	170
Figure 6.23 The DC motor.....	170
Figure 6.24 The liquid pressure sensor.....	171
Figure 6.25 An ABS system driven by the dSpace MicroAutoBoxII.....	172
Figure 6.26 Interface for ABS condition monitoring by using dSpace toolbox .....	172
Figure 6.27 Braking pressure in the ABS valve under step control .....	173
Figure 6.28 Braking pressure when the normally closed solenoid valve is	

in the open condition.....174

Figure 7.1 Scheme of Kalman filter application under fault-free condition  
.....176

Figure 7.2 Scheme of Kalman filter application under faulty conditions  
.....177

Figure 7.3 Comparison of vehicle velocity between the simulation and the  
Kalman filter .....178

Figure 7.4 Residual of vehicle velocity between the simulation and the  
Kalman filter .....179

Figure 7.5 Comparison of wheel velocity between the simulation and the  
Kalman filter .....180

Figure 7.6 Residual of wheel velocity between the simulation and the  
Kalman filter .....180

Figure 7.7 Measurement results of the vehicle velocity under normal  
condition .....182

Figure 7.8 Comparison between the measurement and the Kalman filter  
of vehicle velocity under normal condition .....183

Figure 7.9 Measurement results of the wheel velocity under normal  
condition .....184

Figure 7.10 Comparison results and the residual results between the  
measurement and the Kalman filter of vehicle velocity under normal  
condition .....185

Figure 7.11 Measurement results of the vehicle velocity with speed sensor failure .....186

Figure 7.12 Comparison results between the measurement and the Kalman filter of vehicle velocity with speed sensor failure .....187

Figure 7.13 Fault detection threshold of vehicle velocity with speed sensor failure.....188

Figure 7.14 Measurement results of the wheel velocity with speed sensor failure .....189

Figure 7.15 Comparison results between the measurement and the Kalman filter of wheel velocity with speed sensor failure .....189

Figure 7.16 Fault detection threshold of wheel velocity with speed sensor failure .....190

Figure 7.17 Measurement results of the vehicle velocity with valve sticking or stuck fault.....191

Figure 7.18 Comparison results between the measurement and the Kalman filter of vehicle velocity with valve sticking or stuck fault .....192

Figure 7.19 Fault detection threshold of vehicle velocity with valve sticking or stuck fault.....193

Figure 7.20 Measurement results of the wheel velocity with valve sticking or stuck fault.....194

Figure 7.21 Comparison results between the measurement and the Kalman filter of wheel velocity with valve sticking or stuck fault .....194

Figure 7.22 Fault detection threshold of wheel velocity with valve sticking or stuck fault.....195

Figure 7.23 Measurement results of the vehicle velocity with liquid leakage fault .....196

Figure 7.24 Comparison results between the measurement and the Kalman filter of vehicle velocity with liquid leakage fault .....197

Figure 7.25 Fault detection threshold of the vehicle velocity with liquid leakage fault .....197

Figure 7.26 Measurement results of the wheel velocity with liquid leakage fault .....198

Figure 7.27 Comparison results between the measurement and the Kalman filter of wheel velocity with liquid leakage fault .....199

Figure 7.28 Fault detection threshold of the wheel velocity with liquid leakage fault .....199

Figure 7.29 Measurement results of the vehicle velocity with pump efficiency loss .....200

Figure 7.30 Comparison results between the measurement and the Kalman filter of vehicle velocity with pump efficiency loss.....201

Figure 7.31 Fault detection threshold of vehicle velocity with pump efficiency loss .....202

Figure 7.32 Measurement results of the wheel velocity with pump efficiency loss .....202

Figure 7.33 Comparison results between the measurement and the  
Kalman filter of wheel velocity with pump efficiency loss.....203

Figure 7.34 Fault detection threshold of wheel velocity with pump  
efficiency loss .....204

## LIST OF TABLES

Table 1.1 Definitions of terms related to condition monitoring .....	37
Table 2.1 Useful concepts of the model-based approach .....	51
Table 2.2 Components list of Figure 2.8 .....	66
Table 3.1 Definition of threshold parameters .....	83
Table 3.2 Control phases with transfer conditions and pressure status ....	85
Table 3.3 Parameters for friction coefficient characteristics (Burckhardt) .....	89
Table 4.1 Control logic of ABS logic threshold .....	109
Table 6.1 The appellations of components of the ABS test rig .....	157
Table 6.2 Analogue terminal assignments of NI DAQ .....	157
Table 6.3 Digital terminal assignments of NI DAQ .....	168

## LIST OF NOMENCLATURE

- $A$  -- The  $n \times n$  state variable coefficient matrix
- $A_a$  -- The effective area of the piston inside the brake cylinder
- $A_b$  -- The effective area of the piston inside the accumulator
- $A_B$  -- The flow area of the release valve
- $A_d$  -- The area of the brake drum
- $A_m$  -- The effective area of the piston inside the master cylinder
- $A_i$  -- The effective cross-sectional area of the solenoid valve orifice
- $A_T$  -- The flow area of the supply valve
- $A_1$  -- The wheel acceleration threshold of first pressure-decrease
- $A_2$  -- The wheel acceleration threshold from pressure-decrease to pressure-holding
- $A_3$  -- The wheel acceleration threshold from pressure-holding to pressure-decrease
- $B$  -- The  $n \times l$  state variable coefficient matrix
- $C_B$  -- The flow rate coefficient of the release valve
- $C_d$  -- The discharge coefficient of the throttle
- $C_T$  -- The flow rate coefficient of the supply valve
- $Dth_{KFV}$  -- The vehicle velocity estimation threshold
- $Dth_{KFW}$  -- The wheel velocity estimation threshold
- $Dth_{MV}$  -- The vehicle velocity measurement threshold
- $Dth_{MW}$  -- The wheel velocity measurement threshold
- $Ed$  -- The unknown inputs to the actuators and to the dynamic process

- $F$  -- The force on brake pedal from driver
- $F_a$  -- The braking force on one side of the disc of the wheel
- $F_d$  -- The unknown input to a sensor
- $F_x$  -- The friction force of the tyre
- $F_z$  -- The normal force of the wheel
- $G^f$  -- The sensor faults
- $H$  -- The  $m \times n$  state variable coefficient matrix
- $J$  -- The moment of inertia of the wheel
- $k$  -- The index of the supply valve with a value from 0.5 to 1.0
- $K$  -- The fluid bulk modulus
- $K_b$  -- The spring stiffness of the accumulator
- $K^f$  -- The actuator and component faults
- $K_f$  -- The gain of the force on brake pedal (pedal ratio)
- $K_{pb}$  -- The braking efficacy coefficient
- $K_v$  -- The discharge coefficient
- $M_b$  -- The mass of the piston inside the accumulator
- $m_s$  -- The mass of the spring of the accumulator
- $P_a$  -- The brake oil pressure of the brake cylinder
- $p_a$  -- The intensity pressure of the brake drum
- $P_b$  -- The brake oil pressure of the accumulator
- $P_m$  -- The pressure generated in the master cylinder when braking
- $\Delta P_t$  -- The pressure difference between the front and rear of the supply/inlet solenoid valve

- $Q_L$  -- The leakage flow rate
- $Q_i$  -- The volumetric flow rate from the master cylinder to the supply/inlet valve
- $Q_v$  -- The flow rate of the brake oil out from brake cylinder
- $Q_w$  -- The flow rate of the brake oil out from pump
- $Q_{w0}$  -- The theoretical flow rate in the pump
- $r$  -- The rolling radius of the wheel
- $R$  -- The discharge coefficient
- $R_e$  -- The flow resistance of the throttle (Reynolds Number of brake oil)
- $stdev_{KFV}$  -- The standard deviation of vehicle velocity estimation
- $stdev_{KFW}$  -- The standard deviation of wheel velocity estimation
- $stdev_{MV}$  -- The standard deviation of vehicle velocity measurement
- $stdev_{MW}$  -- The standard deviation of wheel velocity measurement
- $S_{opt}$  -- The optimal wheel slip rate
- $S_\lambda$  -- The wheel slip ratio
- $S_\eta$  -- The wheel rolling ratio
- $S_1$  -- The slip rate threshold of first pressure-decrease
- $S_2$  -- The slip rate from pressure-holding to step-pressure-increase
- $S_3$  -- The slip rate threshold from step-pressure-increase to pressure-decrease
- $T_b$  -- The braking torque of wheel
- $u$  -- The  $l \times 1$  input vector
- $v$  -- The forward linear vehicle velocity
- $V$  -- The total volume of the brake cylinder and fluid pipes
- $v_0$  -- The initial vehicle velocity

$V_a$  -- The volume of brake oil volume from the supply/inlet valve to the brake chamber

$x$  -- The  $n \times 1$  state vector

$X_b$  -- The displacement of the piston inside the accumulator

$X_{KFV}$  -- The vehicle velocity data of the Kalman filter estimation results

$X_{KFW}$  -- The wheel velocity data of the Kalman filter estimation results

$X_m$  -- The displacement of the piston inside the master cylinder

$X_{modelV}$  -- The vehicle velocity data of the simulation results

$X_{modelW}$  -- The wheel velocity data of the simulation results

$X_{MV}$  -- The vehicle velocity data of the smoothed measurement results

$X_{MW}$  -- The wheel velocity data of the smoothed measurement results

$y$  -- The  $m \times 1$  output vector

$z^{-1}$  -- Delay function

$\beta_e$  -- The effective bulk /volume modulus of the brake oil

$\beta_{e0}$  -- The ideal bulk /volume modulus of brake oil

$\phi$  -- The index of the release valve

$\rho$  -- The density of the brake oil

$\tau_0$  -- The time delay constant

$\eta$  -- The pump efficiency

$\omega$  -- The wheel angular speed

$\mu_b$  -- The longitudinal friction coefficient

## ABSTRACT

The Anti-lock Braking System (ABS) is one of the most important safety features in modern vehicles. It is a device integrating complicated electronic systems, hydraulic systems and mechanical components. It is possible to produce faults in these systems due to extreme vehicle operating conditions, which may lead to the failure of the ABS. However, there has, not been an effective mechanism available in current operation and service facilities, which allows the performance of the ABS to be checked on-board or at a service base.

This research therefore aims to investigate and develop approaches which allow the ABS systems to be monitored in different ways. As the ABS is a highly integrated system, conventional monitoring methods cannot be applied to it directly. The primary objective of this research is to develop a condition monitoring model for a typical ABS system under different conditions and then to monitor the dynamic characteristics and the performance of the ABS according to simulation and experimental results. The Rapid Control Prototype (RCP) technique is used by applying dSpace MicroAutoBox II on the ABS controller. A full mathematical model has been developed to simulate the ABS system under different conditions and seeded fault conditions. This results in a full understanding of the characteristics of measurable variables such as wheel velocity and vehicle velocity. This work has led to the conclusion that a model-based condition monitoring approach is the method with the most potential for the monitoring of ABS systems.

To overcome inevitable measurement noise and model uncertainties, a Kalman filter (KF) has been designed and evaluated through both simulation data and experimental results. This has been found to have acceptable performance and has subsequently been incorporated into the model-based condition monitoring system.

The performance of the model-based condition monitoring system has been evaluated using an ABS test system. The ABS test rig consists of the basic ABS components and also the dSpace MicroAutoBox II components, together with NI data acquisition equipment. The ABS test rig developed in this research is highly flexible to allow experimental investigations under different fault conditions with different severities. It has demonstrated that the monitoring system can reliably detect different possible faults in the ABS such as speed sensor failure, solenoid valve sticking or stuck, hydraulic fluid leakage and pump efficiency loss. All these faults occur with high possibility according to a systematic failure mode analysis based on that of similar components.

Obviously, there is still considerable work which needs to be carried out to adopt this system in industry. For example, interfaces to integrate this new system into existing vehicle electronics should be investigated. In addition, specific fault conditions from different vehicle manufacturers should be simulated to tailor the system to specific vehicles specifically.

# DECLARATION

No portion of the work referred to in this thesis has been submitted in support of an application for another degree or qualification of the University of Huddersfield or any other university or other institute of learning.

# COPYRIGHT STATEMENT

1. The author of this thesis (including any appendices and/or schedules to this thesis) owns any copyright in it (the “Copyright”) and she has given The University of Huddersfield the right to use such Copyright for any administrative, promotional, educational and/or teaching purposes.
2. Copies of this thesis, either in full or in extracts, may be made only in accordance with the regulations of the University Library. Details of these regulations may be obtained from the Librarian. This page must form part of any such copies made.
3. The ownership of any patents, designs, trade marks and any and all other intellectual property rights except for the Copyright (the “Intellectual Property Rights”) and any reproductions of copyright works, for example graphs and tables (“Reproductions”), which may be described in this thesis, may not be owned by the author and may be owned by third parties. Such Intellectual Property Rights and Reproductions cannot and must not be made available for use without the prior written permission of the owner(s) of the relevant Intellectual Property Rights and/or Reproductions.

# ACKNOWLEDGEMENT

I would like to sincerely thank my academic supervisor, **Professor Andrew Ball** at the University of Huddersfield. His inspiration, guidance and constant encouragement have made an unforgettable impression to me and made my research valuable. This thesis would not have been finished without his kind support.

I am grateful to my co-supervisors, **Professor. Zhanqun Shi** and **Dr. Fengshou Gu**, for their sincere and warm-hearted help on both academic research and career advice. With support from Professor. Zhanqun Shi, some test results were carried out in the laboratory of Hebei University of Technology in China. Our many discussions have made this thesis fruitful. With help from Dr. Fengshou Gu during my study, some significant improvements of my project have been made successfully. His strictness in scientific work influenced me deeply.

I am also indebted to my other colleagues at the Centre for Efficiency and Performance Engineering in School of Computing and Engineering.

Last but not least, most grateful thanks are extended to my family: my father **Chengzhong Zheng**, my mother **Lihong Wang** and my husband **Honghao Zu**. Special thanks are also due to my relatives and friends for their high expectations and encouragement.

## PUBLICATIONS

1. **Lin Zheng**, Zhanqun Shi & Andrew Ball. (2013) Fault Detection and Diagnosis of Anti-lock Braking System using filter Technology. Journal of the Chinese Society of Mechanical Engineers. (Under Review)
2. **Lin Zheng**, Zhanqun Shi & Andrew Ball. (2013) Fuzzy logic control under high-frequency transformation between high-adhesion coefficient and low-adhesion coefficient roads of Anti-lock Braking System. 2014 International Conference on Computer, Intelligent Computing and Education Technology (CICET 2014). (Accepted)
3. **Lin Zheng**, Zhanqun Shi, Xueming Gu & Andrew Ball. (2013) Condition Monitoring of Anti-lock Braking System using dSpace Component for Fault Detection using Kalman filter. 2014 International Conference on Frontiers of Advanced Materials and Engineering Technology (FAMET 2014). (Accepted)
4. **Lin Zheng**, Zhanqun Shi, Andrew Ball. (2013) Vehicle Anti-lock Braking System Performance using dSPACE. SCE Diamond Jubilee Researchers' Conference 2013. The University of Huddersfield School of Computing and Engineering Annual Researchers' Conference on December 2013. pp.1-6. Prize of Best Presentation of Annual Researchers' Conference (CEARC's)  
ISBN: 978-86218-121-2
5. **Lin Zheng**, Liangliang Wu, X.Gu, Z.Shi & Andrew Ball. (2013) Application of EKF for an Electro-hydraulic Servo System using Model-based Approach. Proceedings of 5<sup>th</sup> International Conference on Mechanical and Electronic Engineering ICMEE, 2013. Tianjin, China, August 2013. Journal of Applied Mechanics and Materials. Main Theme: Applied Scientific Research and

Engineering Development for Industry. Volumes 385-386. pp. 609-613

ISSN: 1660-9336

Published by: Trans Tech Publications Ltd, Switzerland

6. **Lin Zheng**, Zhanqun Shi, Xueming Gu, Andrew Ball. (2013) Sliding Mode Control of Anti-Lock Braking System. Proceedings of 2<sup>nd</sup> International Conference on Computer, Mechatronics, Control and Electronic Engineering (ICCMCEE 2013). Xi'an, China, July 2013. Journal of Applied Mechanics and Materials. Main Theme: Mechanical Engineering, Industrial Electronics and Information Technology Application in Industry. Volumes 427-429. pp. 85-89

ISSN: 1660-9336

Published by: Trans Tech Publications Ltd, Switzerland

7. Yan Yuqing, Shi Zhanqun, **Zheng Lin**. (2013) Analysis of Influence Factors for Axial Piston Hydraulic Pump Flow Fluctuation Based on AMESim. Journal of Chinese Hydraulics & Pneumatics. (Accepted)

ISSN: 1000-4858

Published by: Beijing Research Institute of Automation for Machinery Industry

8. **Lin Zheng**, Zhanqun Shi, L. Lidstone, Fengshou Gu & Andrew Ball. (2007) Model-based Fault Detection for an Electro-hydraulic Servo System Using an Extended Kalman filter. Published by WCEAM CM 2007: The 2nd World Congress on Engineering Asset Management (EAM) and the 4th International Conference on Condition Monitoring, Harrogate, U.K., 2007. pp. 2216-2226

ISBN-13: 978-1-901892-22-2.

ISBN-10: 1-901892-22-0.

Published by: Coxmoor Publishing Company

9. **Lin Zheng**, Zhanqun Shi, Liam Lidstone & Andrew Ball. (2007) Development of a Fault Prognostics Model of a Non-linear Control System using the Extended

Kalman filter. Published by WCEAM CM 2007: The 2nd World Congress on Engineering Asset Management (EAM) and the 4th International Conference on Condition Monitoring, Harrogate, U.K.,2007. pp. 2205-2215

ISBN-13: 978-1-901892-22-2

ISBN-10: 1-901892-22-0

Published by: Coxmoor Publishing Company

10. Shi Zhanqun, Higson Andrew, **Zheng Lin**, Gu Fengshou, Ball Andrew. (2006) Automatic fault detection using a model-based approach in the frequency domain. Published by 8<sup>th</sup> Biennial ASME Conference on Engineering Systems Design and Analysis, ESDA 2006. Torino, Italy, July 2006. Volume 2006, pp.849-855.

ISBN-10: 079837793

ISBN-13: 9780791837795

Publisher: American Society of Mechanical Engineering, Three Park Avenue, New York, NY 10016-5990, United States

---

# CHAPTER ONE

## INTRODUCTION

---

**This chapter gives a brief introduction to the research project which solves a number of problems often encountered when applying a model-based condition monitoring approach to the Anti-lock Braking System using filtering technology. A brief outline of ABS reliability, the model-based condition monitoring approach, as well as the Kalman filter is provided in this chapter. The research objectives for this project are then outlined in detail, along with an explanation of the structure of this thesis.**

## 1.1 INTRODUCTION TO ABS RELIABILITY

The earliest principles of Anti-lock Braking System (ABS) were developed for the aircraft industry. Landing at high speeds could cause problems such as tyre flattening and explosion when a wheel locked at high landing speeds. Before the introduction of ABS, the problem was addressed using an overly cautious use of brakes at touchdown, resulting in longer stopping distances. In the 1950s, the aircraft industry succeeded in developing an experimental system to prevent wheel lock during braking [1]. The use of this experimental system showed a more stable performance on the runway. The success of ABS's use in the aircraft industry prompted an interest in its application in automobiles. Since then, several manufacturers introduced anti-lock systems but only a small number of these systems entered phased production. They did not gain great popularity for two main reasons: firstly, comprehensive durability tests carried out before introduction of the system showed much lower performance and reliability than was expected in everyday service life; secondly, the concept was always that of an add-on unit to the existing braking systems, resulting in a complicated and expensive total package. These factors were instrumental in delaying the introduction of such systems on a mass scale.

Improvements in vehicle design over the years have led to increased speeds and a higher number of fatal accidents. Severe and frequent braking leads to the locking of wheels resulting in loss of vehicle control. The results of recent investigations have shown that it is possible to avoid roughly 7% of all traffic accidents involving passenger cars and to mitigate the consequences of another 15% through the use of the ABS systems [2]. The potential of the ABS for increasing traffic safety is recognized by a number of automotive insurance companies as many grant a discount on fully comprehensive insurance for vehicles equipped with ABS. This in turn has made it worth whilst for automotive companies to expand the use of ABS outside of performance and luxury cars to the average cars used in day to day life.

The technology and understanding of ABS systems are continually evolving. Recent advances in electronics such as, acceleration sensor for example, have made an enormous contribution to the advancement of the reliability, performance and cost of ABS systems [3]. The initial analogue electronic circuits, which were sensitive to manufacturing variations and temperature changes, have been replaced by digital circuits mitigating these issues. The number of components and connections has also been reduced to improve reliability. From a safety stand point, considerable amount of effort is now put into brake diagnostics: any failure in the ABS unit is detected and the system will then revert to normal braking mode [4] [5]. Upgrading to a combined ABS and traction control system, can have the potential benefits of a low incremental cost, a better pedal feel, a smaller size, higher flexibility for packaging, versatility for application in different vehicles, less noise and vibrations, comfortable drive and intelligent diagnosis capability. This further development serves to create the technical and economic conditions under which the system can be used on a wide scale in all vehicles.

At the moment, there is no effective method to predict or check the ABS's mechanical conditions routinely to ensure its functionality [6]. Due to the ABS system only works above a particular velocity during emergency brakes, current brake test facilities are not adequate to test ABS systems [6] [7]. Besides this, it would not be acceptable to use a public road to implement such a practice for condition monitoring because of the dangers involved, so an alternative means must be sought [6] [8]. In order to provide a convenient and safe enough solution, this project proposes a novel method that the vehicle is stationary. In this situation, a model-based condition monitoring approach is applied to predict various faults of ABS system especially focused on its hydraulic components. A mathematical model is therefore developed to describe the dynamic performance of vehicle. The operating processes of the ABS system in both healthy condition and faulty conditions are included during model development. An autonomous control strategy is also designed to actuate the control module independently although there is not quite detailed knowledge of the control algorithms

embedded in the ABS control module [6]. In order to carry out the application, this approach is then evaluated through a Simulink simulation in this project.

## **1.2 INTRODUCTION TO CONDITION MONITORING**

The condition monitoring technique began in the 1960s [9]. It is concerned with extracting information from a monitored system to indicate its condition and to enable it to be operated and maintained with safety and economy [10] [11] [12] [13]. Condition monitoring is the process of monitoring a parameter of the condition of machinery, where a significant change is indicative of a developing failure. It is a major part of predictive maintenance [14].

The advantages of condition monitoring include [15][16][17][18][19]:

- Avoiding unexpected catastrophic breakdowns with expensive or dangerous consequences;
- Reducing maintenance costs by reducing the number of machine overhauls to a minimum;
- Eliminating unnecessary intervention and the subsequent risk of introducing faults on previously healthy machines; and
- Reducing the intervention time and thereby minimizing production loss (as the fault can be detected before it causes damage to the system). In addition, the application of condition monitoring has led to the development of a vast number of techniques for condition monitoring.

Condition monitoring techniques vary widely to meet the requirements of different types of processes and maintenance objectives [20]. These objectives and the costs of

monitoring must be taken into consideration when choosing a condition monitoring technique [21]. Some of the commonly used condition monitoring techniques consist of: visual inspection, trend monitoring, performance monitoring, vibration monitoring, and model-based technique [22]. The most frequently used technique in control system monitoring is the model-based technique, which includes the observer-based approach [23] and the parameter estimation approach [24]. In this thesis, a model-based condition monitoring approach has been chosen for the ABS control system.

## **1.3 INTRODUCTION TO THE MODEL-BASED APPROACH**

The basic theory of the model-based approach will be explored in detail in Chapter Two. This section, however, provides the relevant concepts and advantages as well as statistical information concerning the application of the model-based approach.

A mathematical model is needed for condition monitoring because the system model is developed and calibrated in accordance with the normal behaviour of the system. During implementation, the residual signals (differences) can be obtained by comparing the model outputs with the real outputs [25]. By analysing these residual signals, it is possible to get information about the system's condition.

The central theme of the model-based condition monitoring approach is the design of residual signals, which generate information on the location and time of faults. The residual can then be used to monitor faults when they occur in systems or processes. The related terms are listed in Table 1.1 below:

Table 1.1 Definitions of terms related to condition monitoring [26]

Residual	A fault indicator, based on a deviation between measurements and model-equation-based computations
Disturbance	An unknown and uncontrolled input acting on a system
Fault	An unexpected deviation of at least one characteristic property or parameter of the system from the acceptable, usual or standard condition
Failure	A permanent interruption of a system's ability to perform a required function under specified operating conditions
Symptom	A change of an observable quantity outside normal behaviour patterns
Error	A deviation from a measured or computed value and the specified or theoretically correct value

## 1.4 INTRODUCTION TO THE KALMAN FILTER

Amongst the significant range of mathematical tools (such as the Bayesian Parameter Estimation, Least Square Estimation or the Linear Minimum Mean Square Error Estimation), that can be used for random signal estimation from noisy sensor measurements, one of the most well-known and widely used is the Kalman filter [27]. The Kalman filter is named after Rudolph E. Kalman, who in 1960 published a paper presenting a recursive solution to the discrete-data linear filtering problem [28]. Although it was originally derived for a linear problem, the Kalman filter is habitually applied to many nonlinear problems without loss of performances [29]. These extensions generally use partial derivatives as linear approximations of nonlinear relations. Schmidt [30] introduced the idea of evaluating these partial derivatives at the estimated value of the state variables. This approach is generally called the Extended Kalman filter (EKF).

The Kalman filter is widely used in navigational and guidance systems, radar tracking, sonar ranging, and satellite orbit determination (for example, it can be seen in the Ranger, Apollo, and Mariner missions), as well as in fields as diverse as seismic data processing, nuclear power plant instrumentation, and econometrics [31].

## 1.5 RESEARCH AIMS AND OBJECTIVES

The research objectives established for the project are focused on developing condition monitoring for the automotive ABS systems based on model-based techniques. It will focus on the main objectives as follows:

- **Objective 1:** To review and understand existing techniques in the model-based condition monitoring of control systems. A potential technique will be chosen for implementation in this project.
- **Objective 2:** To investigate the background and algorithm of the Kalman filter. New applications of the Kalman filter will be introduced in order to exploit the filter with the ABS.
- **Objective 3:** To develop a normal model of a typical ABS system for implementing ABS process control. The control strategies will focus on improving controllability, stability and stopping distance under a wide variety of driving conditions.
- **Objective 4:** To develop fault models for the ABS control system. The faults designed in the models should be ones which are not easily detected by common methods. The seeded faults should be fully controlled in fault type and in fault severity, and furthermore, should not cause any damage to the test facility or simulation hardware.

- **Objective 5:** To set up a test facility for the implementation of the ABS system. This work will allow control of the ABS system when different strategies are applied, in order to monitor and estimate the system, with the same user interface, and moreover, to seed faults in the system.
  
- **Objective 6:** To design different road conditions in a Simulink model in order to test scenarios for road and driving conditions. The road type chosen for the design should be classical and realistic.
  
- **Objective 7:** To combine a dSpace MicroAutoBox II with the ABS system test rig together with advanced data acquisition components. The targets for the application of this hardware are flexible of design and modelling, and stability of operation and control.
  
- **Objective 8:** To investigate Kalman filtering techniques for application to the condition monitoring of the ABS system. Based on this study, novel schemes will be recommended for the model-based approach.
  
- **Objective 9:** To perform a comprehensive data analysis for the ABS system for fault detection and diagnosis. Both normal condition and faulty conditions are to be demonstrated based on the control algorithm designed for the ABS system.
  
- **Objective 10:** According to the results and experience gained during this programme of work, to suggest potential future work which will extend the research for integration of more advanced technologies in this field.

## **1.6 STRUCTURE OF THIS THESIS**

Chapter one gives background information and discusses the evolution of ABS and a model-based condition monitoring approach. It defines the motivation, objectives, and scope of the problem and then discusses the approach followed to meet the objectives. The structure of this thesis is also listed in this chapter.

Chapter Two reviews model-based condition monitoring technology. The principle and the procedure as well as the concepts in the model-based approach are also discussed in detail in this chapter. The principles of the ABS system including the function and performance characteristics of the ABS system as well as the mathematical models are involved. The different forces acting on the vehicle and wheels during braking are discussed.

Chapter Three details the theoretical model of an ABS system including the dynamic analysis and Simulink model building. Three steps of ABS control are simulated to complete the control cycle. The control strategies are then developed and their implications are discussed. Some general faults that occur in ABS are also introduced. Finally, the principles of the Kalman filter, together with the equations for estimation of both vehicle velocity and wheel velocity are introduced in this chapter.

Chapter Four shows the Simulink model based on the algorithm discussed in Chapter Three. The Simulink models in both normal and faulty conditions such as wheel speed sensor failure, solenoid valve sticking or stuck, fluid leakage and pump efficiency loss, are also developed in this chapter.

Chapter Five describes the simulation results of the ABS system. The results of no ABS, ABS with and without the pressure-holding process are discussed separately. The simulation results of ABS with faults as introduced in Chapter Four, are also

listed in this chapter.

Chapter Six details the test rig development of a real ABS system together with control unit and data acquisition. The dSpace MicroAutoBox II components that takes place of the Electronic Control Unit (ECU) of vehicle are introduced, and the performance of vehicles during braking is discussed.

Chapter Seven discusses ABS monitoring using the Kalman filter. The comparisons of the test results under normal and then under faulty conditions are described separately.

Chapter Eight draws together conclusions from the current research and makes recommendations for future work.

---

## CHAPTER TWO

# LITERATURE REVIEW

---

**This chapter provides an overview of the model-based condition monitoring approach firstly. The residual generation in the model-based approach is also reviewed. The development, basic theory, technical requirements and evaluation methods of the ABS system is introduced in details. The key backgrounds of ABS in this research, such as the components and working principles of the ABS system, are discussed. The control methods and control channel layout on vehicle dynamics are also laid out in this chapter.**

## **2.1 THE MODEL-BASED APPROACH FOR CONDITION MONITORING**

The model-based condition monitoring is gaining a parallel development with the advancement of automatic manufacturing processes in the last thirty years [32]. The development of an effective condition monitoring system that can detect faults in a timely manner is complicated due to the operating condition variation, the significant variability/uncertainty of the control system, and the measurement noise [33]. The researchers would need to collect a huge amount of baseline data under all different varying conditions if a non-model-based scheme is used, which would be extremely costly and even infeasible [33]. The concepts in model-based approach such as, faults, failures, malfunctions, errors, fault diagnosis, detection, isolation and identification are used, but can be misinterpreted [3]. For example, it may prove difficult to establish the differences between errors, failures, faults and malfunctions. It is, therefore, both beneficial and necessary to give a brief review of the model-based condition monitoring method and its related concepts, including usage.

### **2.1.1 Development of Model-based Methods**

The model-based approach was established in the 1970s firstly [34]. At beginning, the model-based approach was mainly applied to linear systems within the time domain [13]. This method for fault detection is developed by using input and output signals and applying dynamic process models [35]. After that, the newly emerging methods and their potential capability of model-based approach mainly in stochastic dynamical systems are summarized by Willsky [36]. During that period, the majority of model-based control methods used in industry relies on linear dynamic model developed from data generated from a dedicated plant test [37].

Subsequently, many different methods were carried out for the model-based condition monitoring such as, parameter estimation methods, parity space methods, observer-based methods [26]. There are many survey introductions about parameter estimation methods published by Isermann [24][26][38] [39]. The estimation methods were divided into two parts: state estimation and parameter estimation [24][40][41]. At this stage, some filters were introduced to detect faults under model-based condition monitoring approach [42][43][44]. The concepts of residual generation and parity space are also both introduced in some research articles [45][46]. In this period, the first book on model-based methods for condition monitoring in chemical processes was written by Himmelblau, D.M. (1978) [47].

When applying the model-based condition monitoring approach in real systems, one of the difficulties is the robustness of the residual generation [26][48][49]. In order to avoid the lack of parametric information about the expert systems, some techniques including the Kalman filter [50][51], neural networks [52][53][54], and fuzzy logic control system [55][56][57] were introduced. Since the fuzzy logic control method is lack of the capability of learning [58], while the neural networks method requires high quality data and long processing time [59], based on this research objectives, the Kalman filter method is chosen for further research. Based on the necessity of methods that improve the residual generation for fault prediction, model-based condition monitoring methods are receiving more attention step by step [60]. And some other adaptive methods were taken into account for residual generation and threshold design as well [61].

Nowadays, more and more research articles and industrial application achievements based on the model-based condition monitoring approach have been published in engineering journals [13] [62] [63]. These all makes the improvement steps of the research and application of model-based condition monitoring techniques come to mature.

## 2.1.2 Basic Theory of the Model-based Approach

The model is a mathematical representation of a system or a plant [13]. A model can be used to represent the desired behaviour of a system under test, or to represent testing strategies and a test environments [64]. The residual is the differences between the model outputs and the actual outputs [65]. During the operating process of a system, the residual will not be zero if there is a fault or faults occur in the system [13]. In practice, however, it is too difficult to build a model which can describe the actual system exactly, and, the best alternative is to design a threshold [13]. If the residual does not exceed the given threshold or thresholds, the system is considered as a healthy one. If, however, the residual exceeds the threshold or thresholds, it is indicative of a fault or faults occurring in the system [13][66].

### 2.1.2.1 The Representation of a Control System

Set a linear system with input  $u$  and output  $y$ . The representation of the system without fault and noise is [13]:

$$\dot{x}(t) = Ax(t) + Bu(t) \quad (2.1)$$

$$y(t) = Hx(t) \quad (2.2)$$

where  $x$  is the state variable matrix and  $A$ ,  $B$  and  $H$  are the coefficient matrices. Since the measurement of the system is discrete, the diagnostic computations are normally performed on sampled data. Therefore, the discrete equations of the system are usually used with a time instant  $k$  as follows:

$$x(k+1) = Ax(k) + Bu(k) \quad (2.3)$$

$$y(k) = Hx(k) \quad (2.4)$$

where  $x$  is the  $n \times 1$  state vector,  $u$  the  $l \times 1$  input vector,  $y$  the  $m \times 1$  output vector, and  $A, B, H$  are the matrices of  $n \times n, n \times l$  and  $m \times n$  dimensions respectively.

### 2.1.2.2 The Representation of System Faults

In practice, faults and disturbances may exist in systems [26]. The structure of a system with disturbances and faults is shown in Figure 2.1. Model errors act on the actuators, processes and sensors directly, whilst disturbances affect the system as random inputs to actuators, processes and sensors [26]. In majority situations, the noises can be included in disturbances. But the faults are different from disturbances or model errors [26]. Model errors exist all through the operation period but faults do not. Faults may occur inside the actuators, processes (including control components) or sensors but, however, disturbances come from outside of the system. Because of this, the disturbances affect the system in the same way as system inputs. Besides this, the disturbances are usually represented by unknown inputs in the system model for not known during the system operation [26][66].

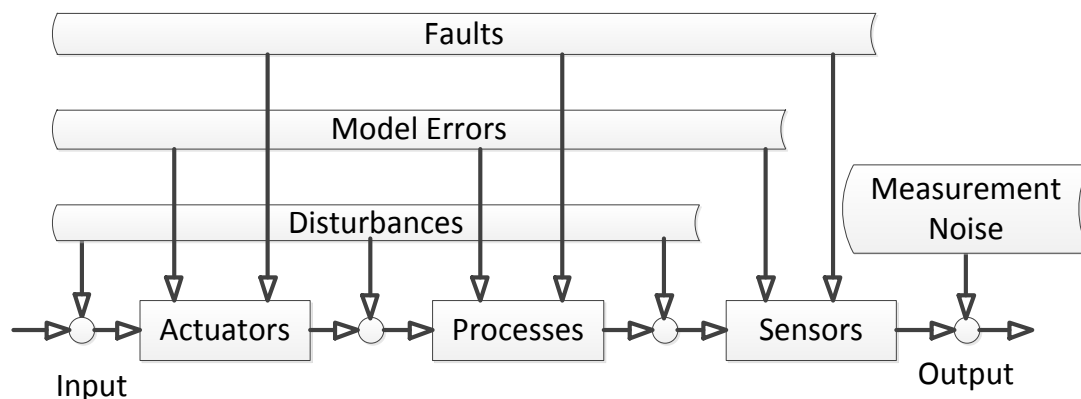


Figure 2.1 Factors applied on the actual system [26]

Figure 2.1 also indicates that the model-based approach can deal with the three possible influences from the disturbances (including noises), model errors and faults, which affect the system behaviour through the actuators, the processes, and of course, the sensors.

When the system encounters certain types of fault and disturbances, the model of the system of Equation (2.1) and Equation (2.2) becomes [13]:

$$\dot{x}(t) = Ax(t) + Bu(t) + Ed(t) + Kf(t) \quad (2.5)$$

$$y(t) = Hx(t) + Fd(t) + Gf(t) \quad (2.6)$$

where  $Ed$  represents the unknown inputs to the actuators and to the dynamic process,  $Kf$  represents actuator and component faults,  $Fd$  represents the unknown input to a sensor, and  $Gf$  represents sensor faults. The discrete form of the system model will change Equation (2.5) and Equation (2.6) by replacing continuous time ( $t$ ) to discrete time ( $k$ ).

$$x(k+1) = Ax(k) + Bu(k) + Ed(k) + Kf(k) \quad (2.7)$$

$$y(k) = Hx(k) + Fd(k) + Gf(k) \quad (2.8)$$

### 2.1.2.3 The Model-based design method

The model-based design method is significantly different from traditional design methodology [67][68]. It is based on model-based approach. The model-based design method defines models with advanced functional characteristics using either

‘continuous-time’ or ‘discrete-time’ building blocks [68][69]. The task consists of the detection of faults in the processes, actuators and sensors by using the dependencies between different measurable signals [68].

#### **2.1.2.4 Steps for Applying a Model-based Approach**

Based on the principle of the model-based condition monitoring approach, the model output should be the same as that of the real actual system under healthy conditions. As previously mentioned, the difference between the outputs of the reference signal and that of the actual system is called the residual. The process used to create a residual is called residual generation [13][26]. By using the residual with threshold, it is possible to figure out whether there is a fault occurring in the system or not. This is called fault detection [70][71].

In model-based condition monitoring of control systems, development is manifested in the following four steps [13][35][26]:

##### **1. Modelling the actual process or system.**

This is because the residual is generated from a comparison of model prediction and real measurement. The model of actual process or system is necessary. On the other hand, the relevant sensors are required for preparation of measurement for the monitored system.

##### **2. Residual generation.**

Residual is used to detect a fault if it occurs in the system. Theoretically, when the system is under normal conditions, the residual will be zero. It is an, often time-varying, signal that is used as a fault detector. An appropriate choice of residual generation method is necessary in order to generate residual that are sensitive to faults.

### 3. Threshold design.

When the residual is generated, an appropriate decision method is needed, which can involve a threshold. There are two criteria to evaluate the decision making methods: sensitiveness and robustness. They are conflicting in most cases, and therefore, a trade-off is necessary.

### 4. Report the condition.

The final step is to report the condition of the system, healthy or faulty, and to identify a fault if one occurs.

Figure 2.2 shows the scheme of the model-based condition monitoring.

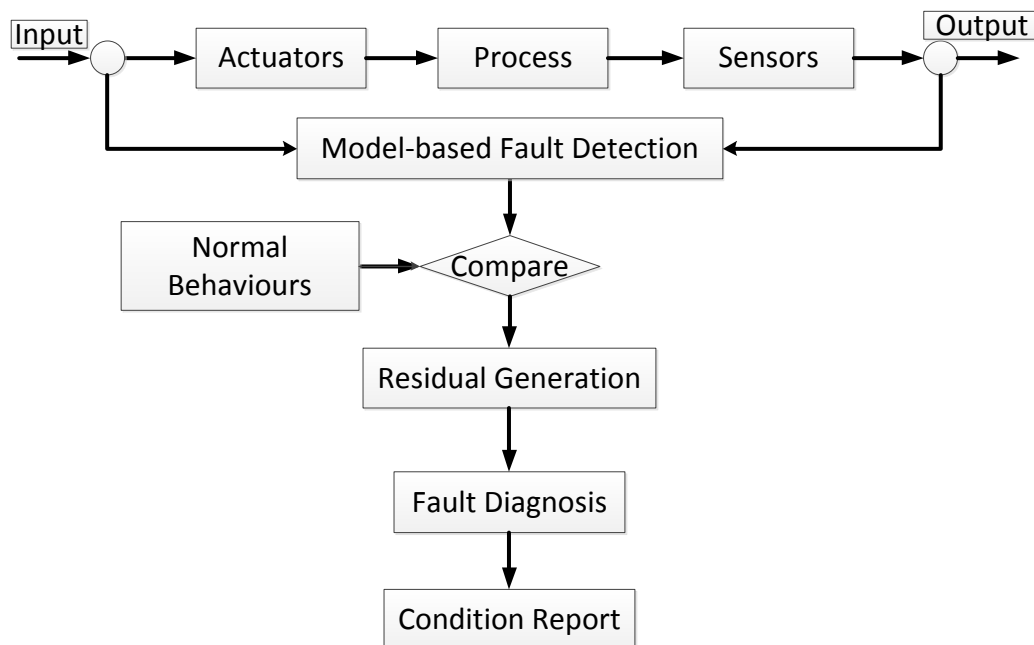


Figure 2.2 The scheme of the model-based condition monitoring approach

## 2.1.3 A General Introduction to Residual Generation in the Model-based Approach

In order to eliminate the shortcomings of the traditional methods, the most significant contribution in modern model-based condition monitoring approaches is the

introduction of residuals, which are independent of the system operating state and which respond to faults in characteristic manners [13][71]. Residuals are quantities that represent the inconsistency between the actual system variables and the mathematical model [13]. Based on the mathematical model, many invariant relations (dynamic or static) among different system variables can be derived, and any violation of these relations can be used as residuals [13].

The residual generation can be interpreted in terms of redundant signal structure as illustrated in Figure 2.3 [72] [73]. In this structure, the system (processor or algorithm)  $F_1(u, y)$  generates an auxiliary (redundant) signal ( $z$ ), which, together with  $y$  generates the residual  $r$  which satisfy the following invariant relation for a fault-free case:

$$r(t) = F_2(y(t), z(t)) = 0 \quad (2.9)$$

When any fault occurs within the system, this invariant relation will be violated and the residual will be non-zero.

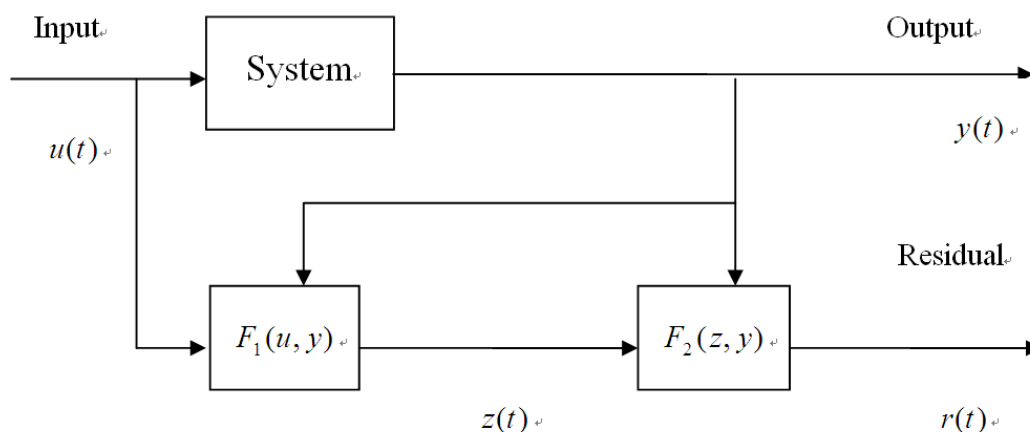


Figure 2.3 Redundant signal structure in residual generation [13]

## 2.1.4 Fault Modelling and Fault Testing

A fault model is a formal representation of the knowledge of possible faults and how they influence the process [74]. It can be used in almost all branches of engineering [75]. From the model, some target faults can be simulated by test equipment, especially those faults that are most likely to occur during operations in real systems [76]. Fault models simplify complexity of testing by reducing number of faults that have to be considered [77]. Normally, fault models can be categorized as single-fault models and multiple-faults models, depending on the number of fault(s) present in the system [77]. Fault model makes effectiveness measurable by experiments. The fault coverage can be computed for specific test patterns to reflect its effectiveness.

There are some useful concepts of the fault modelling and fault testing for model-based approach listed in Table 2.1.

Table 2.1 Useful concepts of the model-based approach

Fault	A fault is defined as an un-permitted deviation of at least one characteristic property of a parameter of the system from the acceptable or standard condition.
Failure	A permanent interruption of a system's ability to perform a required function under the specified operating conditions.
Malfunction	An intermittent irregularity in the fulfillment of a system's desired function.
Error	A deviation between a measured or computed value and the true, specified or theoretically correct value.

The fault testing is basically used for fault detection in model-based condition monitoring approach [77]. The fault testing can be performed either online or offline

[78]. Both the fault modelling and the fault testing make analysis possible with specific test patterns.

## **2.1.5 Advantages of using a Model-based Approach for Condition Monitoring**

This project focuses on the applications of the model-based approach using the Kalman filter method on the ABS system. The reasons for using the model-based condition monitoring approach for fault detection on the ABS system are listed below [7][8][13][79]:

Firstly, the control strategy of ABS can only be accessed by the manufacturer and is never declared to the customers, including maintenance organisations. The ABS cannot easily be operated under fault conditions by using normal methods such as loading extra component on it.

Secondly, the Kalman filter is a classic model-based approach which can solve the problems of not only disturbance but also random noise.

Thirdly, the system performance usually varies with different control operation. Without a model, it is difficult to say if a deviation is caused by a fault or by a control operation.

Fourthly, a model-based approach compares the measurement with the model prediction to generate residual signals. An incipient fault can be detected by checking the residual signals beyond a threshold limit.

Fifthly, the threshold can be designed under different accuracy requirements. The higher the model accuracy is, the smaller the thresholds. The tighter the thresholds are,

the more sensitive the diagnostic scheme.

Finally, the model-based condition monitoring approach can detect not only system faults but also sensor faults.

## **2.2 OVERVIEW OF ABS**

### **2.2.1 Introduction**

An anti-lock braking system (commonly known as ABS, from the German name "Antiblockiersystem" given to it by its inventors at Bosch) is a system on automobiles which prevents the wheels from locking while braking [80]. ABS is one of the important components of a modern automotive braking system. It prevents the wheel from fully locking in the vehicle braking process. As a safety device, its main functions are:

- (1) To improve the direction stability of a braking vehicle
- (2) To ensure that the driver can still control the steering wheel in the braking process, thereby avoiding obstacles
- (3) To shorten the braking distance

### **2.2.2 The Development of ABS**

With the rapid development of the automotive industry and the continuous increases in vehicle speed, many people pay more attention to the safety performance of vehicles. The ABS system can automatically adjust the brake torque in the automotive braking process, in order to prevent the wheel locking. Because the wheel slip rate is

maintained in the vicinity of the optimal slip rate, the ABS can improve the automotive braking efficiency and stability. Therefore, as an effective vehicle active safety device, the application of ABS is more and more popular. The question of how to improve the braking performance between the tyre and the road's surface adhesion, in order to meet the requirements of traffic safety, has always been the goal of researchers.

The first motor driven vehicle was developed in 1769 and the occurrence of the first driving accident happened in 1770. Since then, the engineers started to research on reducing driving accidents and improving the safety of vehicles [81]. Since then, the experts focused on the efficient design of braking systems in the purpose of reducing accidents. The German firm of Robert Bosch GmbH had been developing anti-lock braking technology since the 1930s [80]. The first set of ABS brakes were put on a Boeing B-47 to prevent spin outs and blown tyres in 1945 [81]. Later in 1950s, ABS brakes were commonly installed in aircraft fitted with fully mechanical system [80][81]. The Dunlop Maxaret anti-skid system was in widespread aviation use in the UK, with aircraft such as the Handley Page Victor, Vickers Viscount, Vickers Valiant, English Electric Lightning, de Havilland Comet 2c, and later aircraft, such as the Vickers VC10, Hawker Siddeley Trident, Hawker Siddeley 125, Hawker Siddeley HS 748 and derived British Aerospace ATP, and BAC One-Eleven being fitted with Maxaret as standard [82]. In the 1960s, only the high end automobiles were fitted with rear-only ABS, which only installed on limited automobiles for the reason of expensive cost [80][81][82]. The first test on experimental configuration was carried out on all wheel drive Ford Zodiac [82][83]. In 1970, Ford added an ABS called "Sure-track" to the rear wheels of Lincoln Continentals as an option; it became standard in 1971 [82]. With the significant development of computers and electronics technologies, the ABS techniques exploded in the 1980s. Nowadays, all-wheel ABS can be found on the majority of later model vehicles and even on select motorcycles [81] [82] [83].

Obviously, ABS is an important component to road safety as it is designed to keep a vehicle steerable and stable during heavy braking by preventing wheel lock [81]. ABS equipped vehicle has a safe side during crashes particularly in the emergency braking condition [82]. The wheels are easily to slip and lockup during emergency braking, especially on a slippery road surface such as snow or ice. The main purposes of ABS are already established at the beginning of this section. The ideal situation is that the ABS can control the wheel slip in order to meet the maximum friction between the wheel and road surface. The ABS mainly prevents skidding of the vehicle and thereby reduces the possibility of any unwanted crashes due to emergency braking [82]. And of course, the ABS can reduce the braking distance.

The typical ABS components is shown in Figure 2.4 [81].

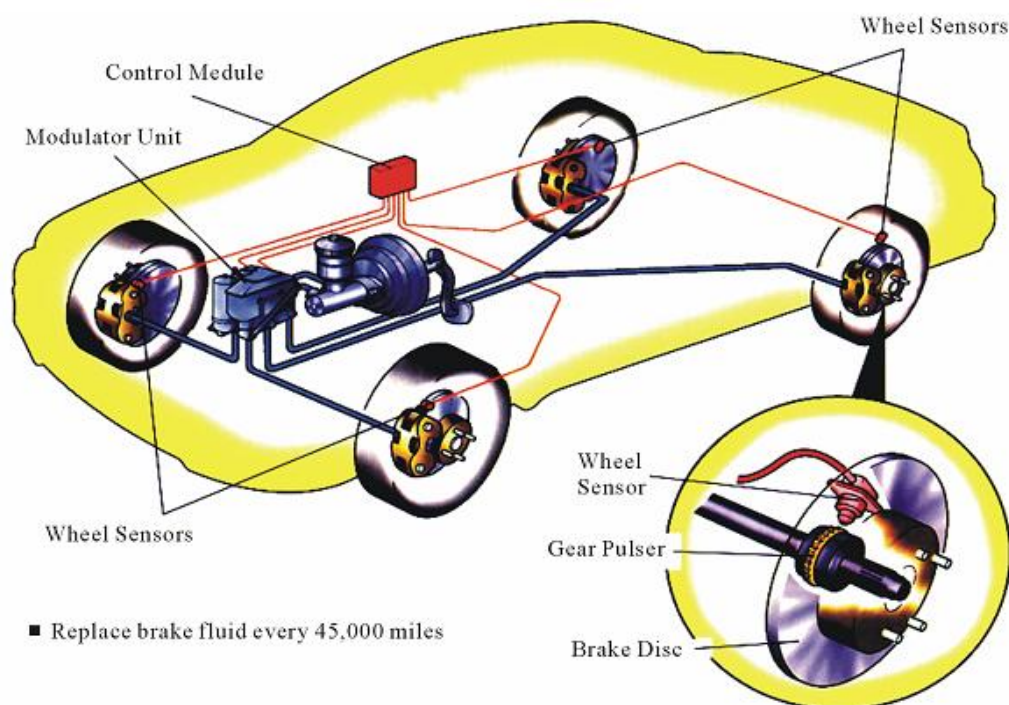


Figure 2.4 Typical ABS components [81]

## 2.2.3 The Basic Theory of ABS

### 1. Wheel Brake Dynamics

Normally, vehicle models include a general vehicle model, a four wheel vehicle model, a half vehicle model and a quarter vehicle model. The one chosen for this research is the quarter vehicle model. This model has the advantage that ignores the interactions between the four wheels and the vehicle's body, and also the additional phenomenon that complicates it. The quarter model describes the braking performance, which is suitable for ABS braking performance analysis. It can, however, also simplify the problem.

In the actual running process of an automotive, the longitudinal motion of vehicles on a road can have two different forms: rolling and sliding. A wheel during braking has two primary torques acting on it, the brake torque and the tyre torque. Figure 2.5 shows the simplified model of a braking wheel. As shown in Figure 2.5,  $v$  refers to vehicle velocity and  $\omega$  refers to wheel angular speed.

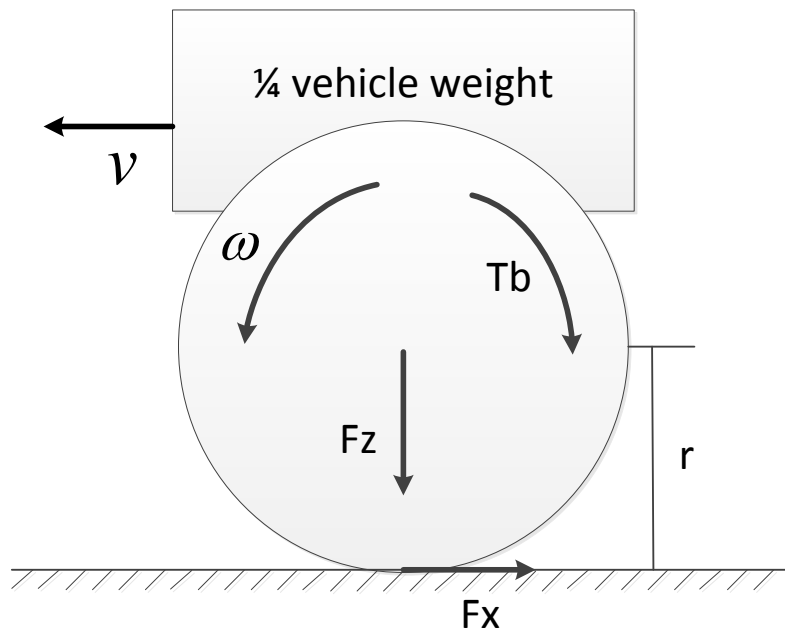


Figure 2.5 The simplified model of a wheel

From Figure 2.5, we get the dynamic functions of a braking wheel:

$$J\dot{\omega} = F_x \cdot r - T_b \quad (2.10)$$

$$F_x = \mu_b \cdot F_z \quad (2.11)$$

where  $F_x$  is the friction force,  $F_z$  is the normal force,  $\mu_b$  is the longitudinal friction coefficient,  $J$  is the moment of inertia of the wheel,  $r$  is the rolling radius of the wheel, and  $T_b$  is the braking torque.

As introduced by Tom Denton, the reason for the development of an ABS system is in essence very simple. Under braking, if one or more of a vehicle's wheels locks (begins to skid) then this has a number of consequences [84]:

- Braking distance and time increases
- Steering control is lost
- Abnormal tyre wear

The obvious result is that an accident is far more likely to occur [84]. The maximum deceleration of a vehicle is achieved when the maximum energy conversion is taking place in the brake system. A good driver can pump the brakes on and off to prevent locking but, electronic control of ABS can achieve even better result [84].

From Equation (2.10)  $J\dot{\omega} = F_x \cdot r - T_b$  both the braking force torque and the longitudinal force torque decide the behaviour of wheel. When braking, the wheel is subject to the braking force generated by friction pads and the braking force of the brake, as well as the longitudinal force generated by both tyre and road surface friction. When the braking force is less than the longitudinal force, the speed of the wheel decreases and wheel slip occurs. Together with the increase of braking pressure,

the percentage of wheel slip increases. When the braking force is greater than the longitudinal force, the wheel is locked and slips. The longitudinal force generated by a tyre depends on the non-dimensional parameter wheel slip ratio  $S_\lambda$  and the vertical load on the tyre. As a basic concept, the longitudinal wheel slip ratio  $S_\lambda$  is given by:

$$S_\lambda = \frac{v - \omega r}{v} * 100\% \quad (2.12)$$

where  $\omega$  is the wheel angular velocity,  $r$  is the radius of the wheel rolling, and  $v$  is the forward linear velocity of the vehicle. In normal driving conditions,  $v = \omega r$ , therefore  $S_\lambda = 0$ .

In severe braking, it is common to have  $\omega = 0$  whilst  $S_\lambda = 100\%$ , which is called wheel lockup. Lockup means the wheel slips on the road without rolling. Wheel lockup is undesirable since it increases the stopping distance and causes loss of direction control [85][86]. When the wheels skid and slip on road, part of the central longitudinal velocity of the wheel is caused by the wheel skidding whilst the other part is caused by wheel slippage. In this case,  $v > \omega r$  and  $0 < S_\lambda < 100\%$ . The greater the percentage of the wheel slipping, the larger slipping ratio  $S_\lambda$  is.

Together with slipping ratio, the rolling ratio  $S_\eta$  is given by:

$$S_\eta = \frac{\omega r - v}{\omega r} * 100\% \quad (2.13)$$

When rolling, the longitudinal velocity of the wheel is  $v = \omega r$  and the rolling ratio is

$S_\eta = 100\%$  . When the wheels rolling and slipping on the road, parts of the central longitudinal velocity of the wheel are caused by wheel rolling whilst the other parts are caused by wheel slippage. In this case,  $\omega r > v$  and  $0 < S_\eta < 100\%$  . The greater the percentage of the wheel rolling, the bigger the rolling ratio  $S_\eta$  is.

## 2. Tyre Friction Force

Braking happens only when the tyre is in contact with the road surface.  $F_x$  is the tyre friction force, which causes the deceleration of a moving vehicle.

$$F_x = F_z \mu_b \quad (2.14)$$

where  $F_z$  and  $\mu_b$  are the vertical force and the longitudinal friction coefficient in the brakes separately. The fundamental ‘grip’ between the road surface and the tyre is called the friction coefficient [87]. This is a non-linear function with a typical dependence on the slip shown in Figure 2.6 [81].

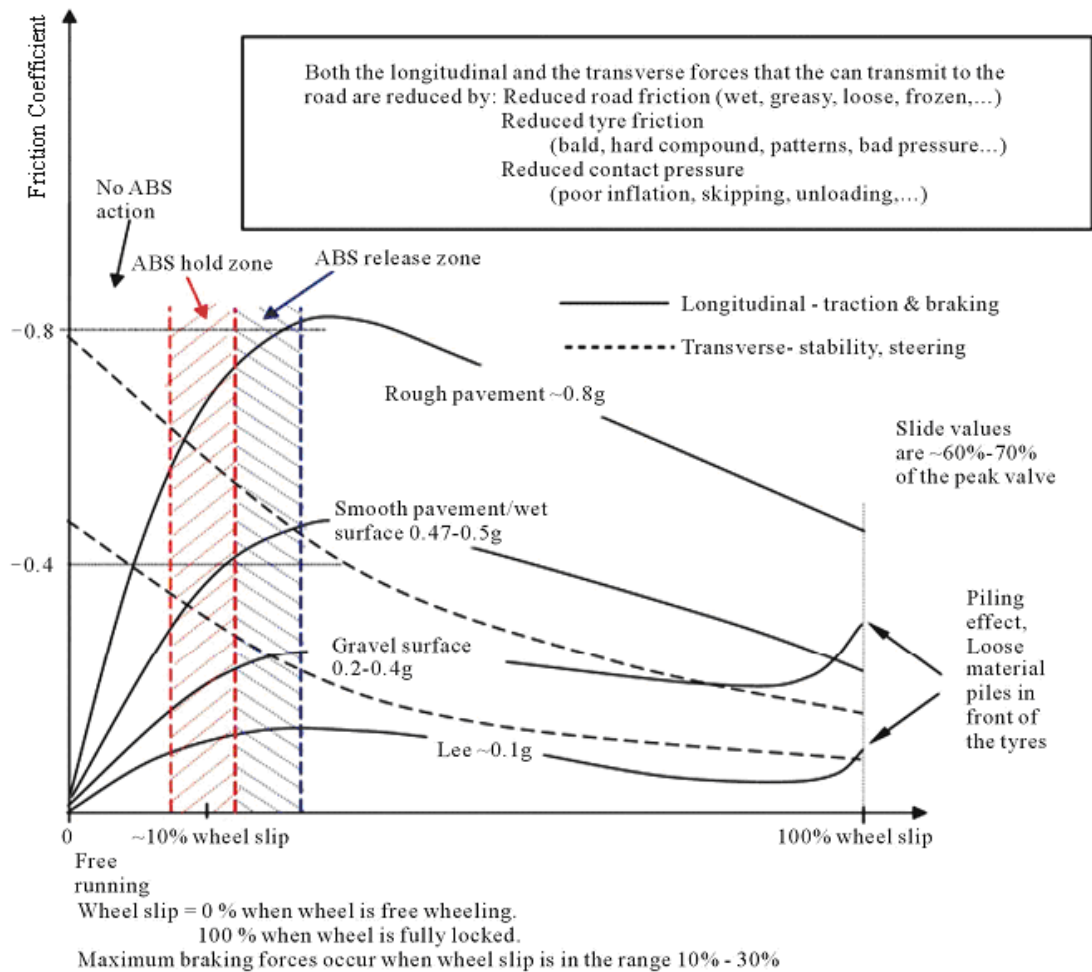


Figure 2.6 Illustration of the relationship between the braking coefficient and wheel slip [81]

Figure 2.6 shows how the friction coefficient varies with wheel slip rate for different road surfaces. A computer program that represents this graph is stored in the ECU memory so that it can be used as a reference [87]. It is shown that the slide values for stopping/traction force are proportionately higher than the slide values for cornering/steering force [81]. It is generally believed that optimum braking performance in difficult conditions is achieved when the slip rate is in the range of 10% to 30% [81] [85] [87]. Consequently, the ABS can help to maintain steering control even under very heavy braking conditions [84]. In rare circumstances the stopping distance may be increased; however, the directional control of the vehicle is substantially greater than if the wheels are locked up [81].

## **2.2.4 Technical Requirements and Evaluation Methods of ABS**

The main difficulty in the design of ABS control arises from the strong nonlinearity and uncertainty of the problem [81]. The braking process in terms of minimum stopping distance would be optimum if the slip rate of the brake type could always be kept at values corresponding to peak friction levels [88]. The ABS control logic is based on the objective of keeping the wheel from locking up and to maintain the friction between the braking tyre and road surface at an optimal maximum [81]. In practical, the wheel speed sensor measures the wheel angular velocity and feeds back to the ECU. The brake actuator control unit then receives an output signal, which is based on an underlying control approach of ABS from the ECU to the brake actuator. The angular velocity of the wheel, the braking slip rate of the tyre and the velocity difference between the tyre and the vehicle are necessary for the ABS control algorithm.

### **1. Design Requirements of ABS**

The steering force, stability and optimum braking distance are the main indicators for evaluation of ABS. The design requirements are shown below:

- (1) The car steering capability and driving stability must be guaranteed during the brake process.
- (2) Steering reaction should be as small as possible, even if the adhesion coefficients of two sides of the wheels are not the same.
- (3) Can be adjusted within the entire speed range of the vehicle.
- (4) Effective use of the adhesion of the wheels on the road surface.
- (5) The vehicle must be able to stop completely on the road in any condition within a

reasonable distance.

- (6) The ABS must be able to identify the different road conditions and make the right response for braking.

## **2. Quality guidelines of ABS**

- (1) Good driving stability
- (2) Good steering ability
- (3) High utilization of the adhesion force coefficient
- (4) Must be comfortable

## **3. Main evaluation index of ABS**

- (1) Good resistance to external electromagnetic interference
- (2) Avoid lockup of wheels when braking
- (3) High utilization of the adhesion coefficient
- (4) Adaptive ability of road condition changes
- (5) Stop ABS from working when an electrical fault occurs

## **2.3 THE BASIC COMPOSITION AND WORKING PRINCIPLES OF ABS**

### **2.3.1 The Components of ABS**

As shown in Figure 2.7, the ABS consists of a conventional hydraulic brake system plus anti-lock components [81]. The conventional brake system includes a vacuum

booster, master cylinder, front disc brakes, rear drum brakes, interconnecting hydraulic brake pipes and hoses, a brake fluid level sensor and a brake indicator [81]. There are a few variations between manufacturers involving a number of different components [84]. However, there are some main components of a typical ABS system as listed below [81] [82] [83] [84]:

1. Wheel speed sensors: up to four wheel speed sensors produce signals with a frequency proportional to wheel speed. Most of these devices are simple inductance sensors and work in conjunction with a toothed wheel.
2. Electronic control unit (ECU): monitors the wheel speed signals, computes the slip-performance on the sensed wheels and operated the modulator valves. The function of the ECU is to take in information from the wheel speed sensors and calculate the best course of action for the hydraulic modulator.
3. Valves: driven by ECU to either opened or closed position. There are two valves for one wheel as normally opened (supply) valve and normally closed (release) valve.
4. Pump: restores the pressure to the hydraulic brakes after the valves have released it. The ECU sends out a signal for releasing the valve at the detection of wheel slip. The pump is used to restore a desired amount of pressure to the braking system.
5. Other components: the vehicle's physical brake pedal, a brake master cylinder, and some of the advanced ABS systems also include an accelerometer to determine the deceleration of the vehicle.

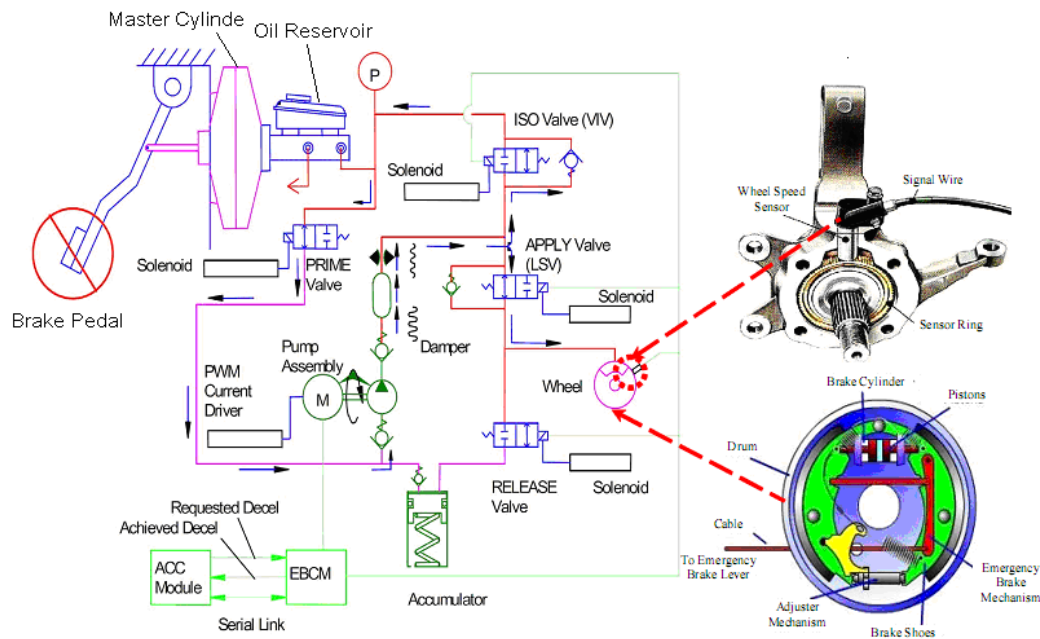


Figure 2.7 Structure of an Anti-lock Braking System [81]

### 2.3.2 Working Process of ABS

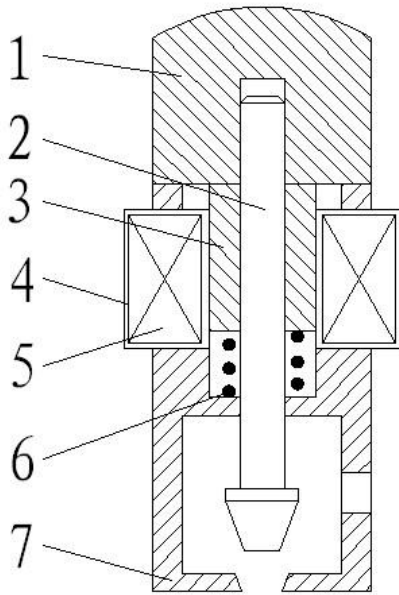
Wheel speed sensors constantly measure and send wheel speed signals to the ECU, in which the wheel deceleration is calculated. When a wheel lockup is indicated, the ECU signals to the modulation valve to regulate the braking pressure and maintain maximum braking without risking wheel lockup.

There are many configurations for ABS from different ABS manufacturers worldwide such as Bosch, TRW, Denso, Continental Teves, Lucas – Girtings, Delco, AisinSeiki, etc. [7]. The key to the operation of ABS hydraulic modulator is to consider three operating positions [84]. The solenoid valve has two positions, which control the three operating phases of ABS [84]:

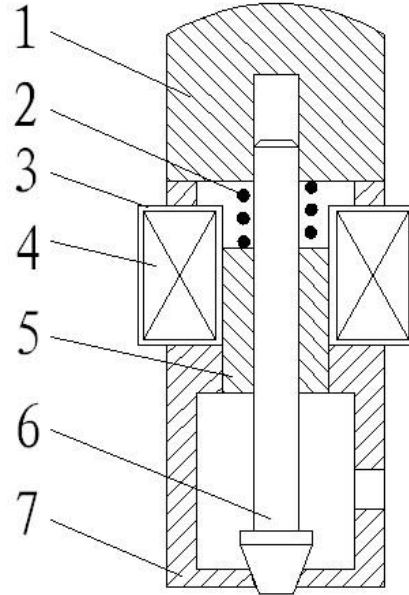
- Pressure increase / Pressure build up
- Pressure hold
- Pressure decrease / Pressure reduction

As shown in Figure 2.7, it can be seen that the wheel is modulated by an individual solenoid valve and that the supply solenoid valve and the release solenoid valve share the return pump with two check dampers and an accumulator [7]. The valves are controlled by electrical solenoids, which have a low inductance so they react very quickly. The motor of ABS only runs when the ABS is activated [84]. Because the supply valve and release valve are important parts of the ABS system, they are taken to demonstrate the modelling of the ABS system. Figures 2.8 (a) and 2.8 (b) show the solenoid valves of both supply (normally opened) and release (normally closed).

Table 2.2 lists the components of both the Normally Opened Solenoid Valve and Normally Closed Solenoid Valve.



(a) Normally Opened Solenoid Valve Structure Diagram



(b) Normally Closed Solenoid Valve Structure Diagram

Figure 2.8 Sketch of solenoid valve [89]

Table 2.2 Components list of Figure 2.8

NORMALLY OPENED SOLENOID VALVE		NORMALLY CLOSED SOLENOID VALVE	
No.	NAME	No.	NAME
1	FIXED IRON	1	FIXED IRON
2	PUSH ROD	2	RETURN SPRING
3	MOVING IRON	3	COIL YOKE IRON
4	COIL YOKE IRON	4	COIL
5	COIL	5	MOVING IRON
6	RETURN SPRING	6	PUSH ROD
7	VALVE BODY	7	VALVE BODY

## 2.4 THE CONTROL PRINCIPLES OF ABS

ABS brake controllers pose unique challenges to the designer as follows [90]:

- For optimal performance, the controller must operate at an unstable equilibrium point
- Depending on the road conditions, the maximum braking torque may vary over a wide range
- The tyre slippage measurement signal, crucial for controller performance, is both highly uncertain and noisy
- On rough roads, the tyre slip rate varies widely and rapidly due to tyre bouncing
- Brake pad coefficient of friction changes
- The braking system contains transport delays which limit the control system's bandwidth

As stated in the previous section of this chapter, the ABS consists of a conventional hydraulic brake system plus anti-lock components which affect the control characteristics of the ABS. ABS control has a highly non-linear control problem due to the complicated relationship between direction and slip. Another impediment in this control problem is that the linear velocity of the wheel is not directly measurable and it must therefore be estimated. Friction between the road and tyre is also not readily measurable or potentially requires complicated sensors. Researchers have employed various control approaches to tackle this problem. One of the technologies which has been applied to the various aspects of ABS control is soft computing. A brief review of the ideas of soft computing and how they are employed in ABS control is given below.

## **2.4.1 Control Methods**

The ABS system has its own characteristics. In addition to the requirements of the system anti-interference ability and the high reliability, an important requirement is the high-speed control of the process. The majority of ABS systems require a response within milliseconds from the control system. This is a limitation of the algorithm design. More complex algorithms based on the modern control theory are used in application of ABS [82] [85] [86][91].

### **1. Frequency Response**

The transfer function of a control system is the core of the classical linear control theory. Normally, it uses a system with a single-input, single-output (SISO) as the object. The classic control research model is the differential equations.

### **2. Linear optimal control theory**

The state-space method is another way to describe a linear system which uses first-order differential equations to describe the dynamic system characteristics. The state-space methods including Pole Control, Condition Monitoring and Optimal Control can deal with the problem of not only a linear system but also a non-linear or stochastic control system.

### **3. Adaptive Control System**

The design of the controller is done offline. When the structure of the controller is determined, the parameters of dynamic model can be estimated through the online system identification of the adaptive control. From a practical point of view, the more identification parameters required, the more complex the procedures are going to be. These become more difficult for adaptive control.

## **4. Fuzzy Logic Control System**

The model is not based on a mathematical model, but based on how the designers understand the system and summarize the rules of the ABS system. Fuzzy logic control is applicable to the control system in a similar way to the system controlled by human beings. Fuzzy logic control systems, however, lack a theoretical foundation, such as the stability of the control system.

### **2.4.2 Control Channel Layout on Vehicle Dynamics**

With four wheels, many combinations are possible for grouping the wheels into channels. This may be done as a result of cost, performance, or complexity of the system. The number of channels in the system can vary from one to four. The layout refers to the pair of wheels that are grouped together [84] [87] [91].

#### **1. One Channel: Select Rear Axle Control**

One channel systems have been exclusively used to control only the rear wheels because the vehicle stability is more dependent on the forces on the rear wheels. Although such systems prevent the vehicle swerving in many situations, their basic shortcoming is the lack of steerability during an emergency stop due to the uncontrolled front wheels. Consequently, full braking during cornering and evasive manoeuvres may result in loss of control. This system configuration by no means meets the present traffic safety requirements.

#### **2. Two Channel: Diagonal Split Control**

In a diagonal split system there are two circuits: one is connecting the front-left wheel and the rear-right wheel and the other one is connecting the front-right wheel and the rear-left wheel. Diagonal split control independently modulates brake pressure in each of the diagonal circuits based on the information received from the four wheel speed

sensors. The front to rear braking ratio is controlled by a separate proportioning valve for each channel.

### **3. Three Channel: ABS with Individual Front wheel Control and Select Rear Axle Control**

Four system configurations are possible with three channel systems. This system configuration assures full vehicle steerability and stability with braking in a turn, or evasive manoeuvre. Due to the dynamic wheel load distribution during braking in a turn, the higher brake forces available on the front wheels are fully utilized. Only the lower brake force of the outer rear wheel is adjusted to the inner rear wheel. This method also minimizes the brake force differences on the rear axle on roads with different friction coefficients or during turning. Although the system does not offer all the advantages of an individual four wheel control system, its performance is considered satisfactory.

### **4. Four Channel: Individual Wheel Control**

All the wheels are controlled independently of each other. This allows the brake forces on each wheel to be optimized. The stopping distance, steerability and stability is then dependent on the control philosophy used. This system is more expensive because of the extra controls that are required. This system is the only one to pass the current stringent test requirement.

## **2.5 MODEL-BASED CONDITION MONITORING OF ABS**

As discussed in the former sections, the ABS is one of the most important components related to driving safety in modern vehicles. It is a device integrating complicated electronic systems, hydraulic systems and mechanical components. To improve

reliability, safety and economy of the ABS system, fault detection is becoming increasingly important [92].

By now, there is no effective method to predict or check the ABS's mechanical condition routinely to ensure its functionality. Due to the ABS system only works above a certain velocity during harsh braking, current brake test systems are not adequate to test ABS systems. Besides this, it is forbidden to test ABS capability performance on roads.

There are not quite a lot published research achievement on either the analysis of system efficiency performance or the detecting of the physical layer performance of the ABS system [93]. One important reason is that this kind of researches requires for the details of internal signal flow and technical information of the ABS, which are commercially confidentiality of all the ABS manufactures.

Although there are so many difficulties need to face up, the research of ABS condition monitoring and fault diagnosis never stops. In 1990s, a Germany research team with leader of Prof. Struss started exploring the mechanism of the health status of the ABS system. He published some articles related to '*Fundamentals of model-based diagnosis of dynamic systems*', '*Parameter analysis of ABS models*' and '*Fault isolation in the hydraulic circuit of an ABS*' [93] [94] [95]. Rapid Control Prototyping (RCP) is a process that lets engineers quickly test and iterate their control strategies [96]. Consequently, the mathematical models under both fault-free and faulty conditions are automatically imported with MATLAB/Simulink on the ABS system with I/O interfaces to connect to systems in this research project. Both RCP and Hardware-in-the-loop (HIL) simulation technique are used in the development and test of complex real-time embedded systems [97]. In order to solve the problems of ABS system with vehicle road test, some researchers presented the method of RCP and HIL for simulating the vehicle dynamic performance using models [98]. Only the ABS hydraulic components, together with the electronic modules are included in the

test facility. All the other complexity of the ABS system is included in the test and development by adding the mathematical representation of the dynamic system [97] [98]. Besides this, Prof. Isermann also tried to establish the model-based condition monitoring of ABS system using current and voltage signals from the solenoid valves [99][100]. Researcher Marcus from Germany expressed model based fault detection methods can be used to compare with the fault-free state for ABS solenoid valves by using parameter estimation, state estimation [92]. This leads to a number of symptoms, indicating the occurrence of faults [92]. Researcher Gajek from U.K. carried out his research of ABS system performance in standard conditions using advanced drum test rig [101].

In this project, a model-based condition monitoring approach is going to be used for the ABS system. One approach towards model-based methods is parameter monitoring, where online estimated physical parameters of the process are compared to reference values [102]. Both simulation results and measurement results are necessary for this research. Some filtering techniques will also be used for filtering measurement signal. The comparison results between healthy and faulty conditions need to be analyzed using model-based approach. Model-based condition monitoring and fault detection has progressed to maturity of current research on model-based methods, which are necessary in order to detect not only sensor failure, but also the faults of mechanical components and hydraulic components [102].

## **2.6 SUMMARY**

In this chapter, the state-of-art model-based approach to condition monitoring was introduced. The development and basic theory, together with technical requirements and evaluation methods of ABS are reviewed. The components and working process, as well as the control methods of typical ABS on vehicle were also introduced in both words and figures. Some difficulties of application of ABS fault detection and

diagnosis were listed. In order to deal with these problems, a model-based condition monitoring method was carried out for ABS fault detection and diagnosis.

---

## CHAPTER THREE

# THEORETICAL MODEL OF THE ANTI-LOCK BRAKING SYSTEM

---

**In this chapter, the theoretical model of ABS system is developed. Firstly, the dynamic analysis of three steps of ABS control, including pressure-increasing, pressure-holding and pressure-decreasing are introduced with associated mathematical analysis. Secondly, the control cycle of ABS is introduced by using different thresholds at different stages. Thirdly, a number of general faults, including speed sensor failure, solenoid valve sticking or stuck, fluid leakage, pump efficiency loss, pressure hysteresis and air blister inclusion in brake fluid are discussed. Finally, the friction coefficient calculation method and the Kalman filter technology for calculation of both wheel velocity and vehicle velocity are also introduced in this chapter.**

## 3.1 DYNAMIC ANALYSIS OF THE THREE STEPS OF ABS CONTROL

### 3.1.1 The Pressure Increasing Mode

During emergency manoeuvres, most drivers react by stepping on to the brake to come to a stop as soon as possible. Depending on road surface conditions, the wheels eventually lock and begin to slide [103]. The braking force of the ABS occurs when the driver steps on to the brake pedal. When the Electronic Control Unit (ECU) determines that the pressure within a wheel brake cylinder needs to be increased, the fluid within it undergoes a process of pressurization. The supply/inlet valve is in the open position, whilst the release/outlet valve is in the closed position. The brake fluid is pumped from the accumulator into the master cylinder by an electric hydraulic pump. The master cylinder transfers the hydraulic oil from the solenoid valve to the brake cylinder when the driver steps on the brake pedal. The pressure of the hydraulic oil is also raised at the same time.

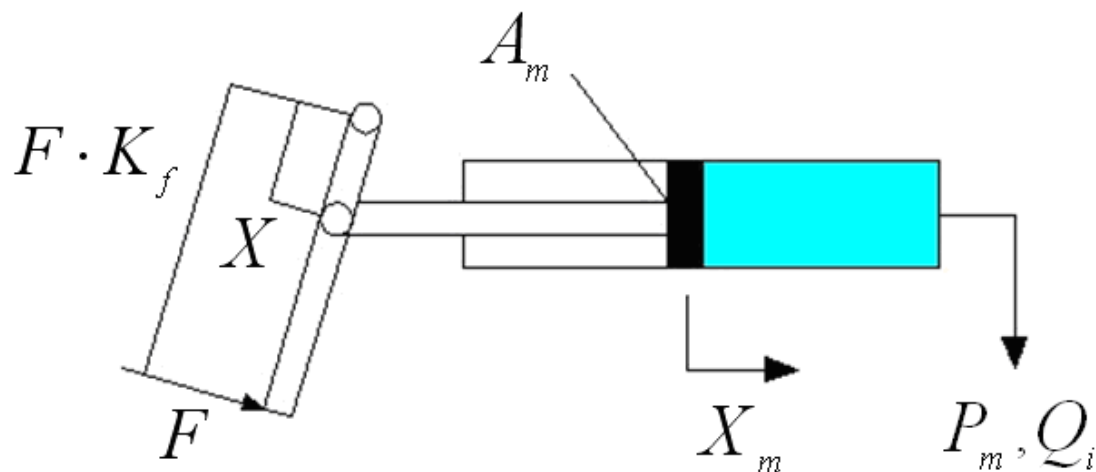


Figure 3.1 Schematic diagram of brake pedal and master cylinder

Figure 3.1 shows the structure the master cylinder operated by the brake pedal. Once the brake pedal is depressed, the pressure builds up in the master cylinder immediately. The master cylinder then transfers pressure to the braking cylinder through

appropriate piping to the apply/inlet valve [6]. From Figure 3.1 the dynamic equations of the model of the master cylinder with the brake pedal can be obtained and are given below:

$$P_m A_m = F \cdot K_f \quad \text{or} \quad P_m = F \cdot K_f / A_m \quad (3.1)$$

$$A_m \dot{X}_m = Q_i \quad (3.2)$$

The parameters are explained below:

$F$  -- The force on brake pedal from the driver

$K_f$  -- The gain of the force on the brake pedal (pedal ratio)

$P_m$  -- The pressure generated in the master cylinder when braking

$A_m$  -- The effective area of the piston inside the master cylinder

$X_m$  -- The displacement of the piston inside the master cylinder

$Q_i$  -- The volumetric flow rate from the master cylinder to the supply/inlet valve

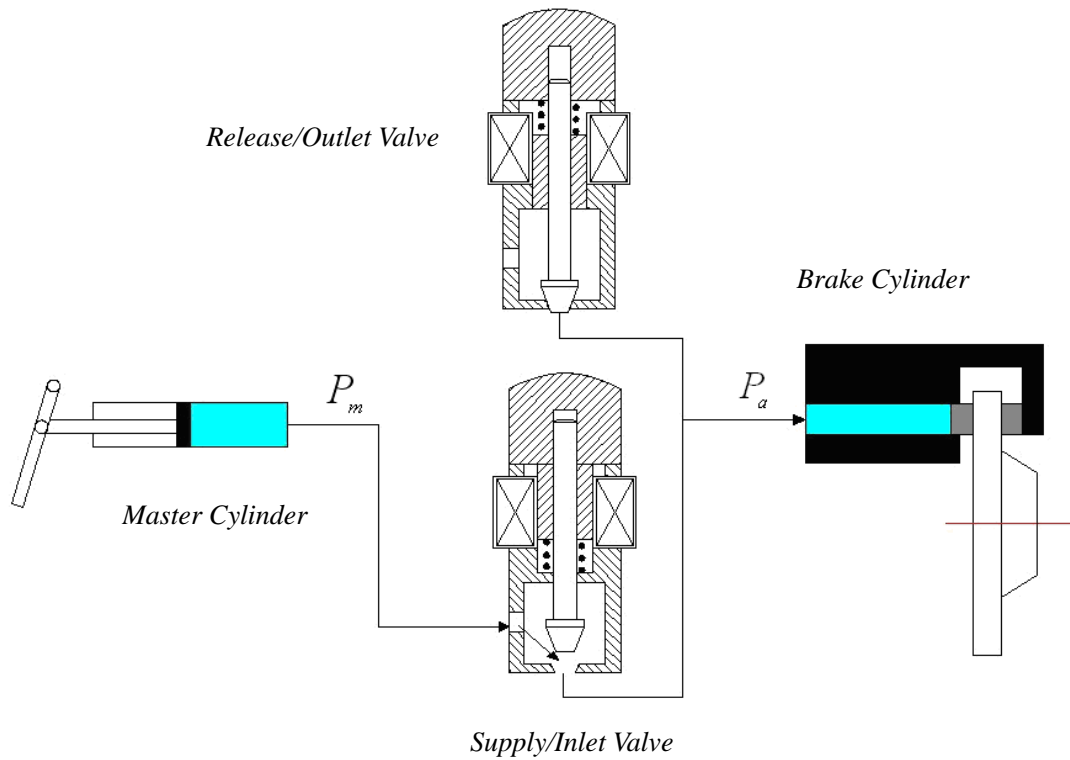


Figure 3.2 Sketch of the pressure increasing process of ABS

Figure 3.2 shows the process of increasing the pressure of the ABS. The hydraulic oil is pumped into the supply/inlet valve, which is normally opened via the master cylinder. At the same time, the release/outlet valve is closed. From Figure 3.2 the liquid flow equation can be obtained as defined below [104]:

$$Q_i = C_T A_T \Delta P_i^k \quad (3.3)$$

where  $C_T$  is the flow rate coefficient,  $A_T$  is the flow area of the valve,  $k$  is the index of the solenoid valve with a value from 0.5 to 1.0 of the supply/inlet valve respectively, and  $\Delta P_i$  is the pressure difference between the front and rear of the supply/inlet solenoid valve.

The flow rate from the master cylinder is restricted by the supply/inlet valve orifice. The hydraulic fluid loses pressure when pumping from the master cylinder to the

brake cylinder through the solenoid valve. Assuming the upstream pressure is  $P_m$  and the downstream pressure is  $P_a$ , then the equation of pressure loss can be described as:

$$\Delta P_t = P_m - P_a \quad (3.4)$$

When braking action starts, brake fluid is compressed and the pressure is increased. The continuous flow equation during the pressure-increasing stage is given by Equation (3.5).

$$Q_w = KV \frac{dP_a}{dt} \quad (3.5)$$

where  $K$  is the fluid bulk modulus, and  $V$  is the total volume of the brake cylinder and fluid pipes.

Theoretical, the flow rate of  $Q_i$  and  $Q_w$  should be the same. From equations (3.3), (3.4) and (3.5), the rate of change of pressure of the brake cylinder during the pressure-increasing stage is given by

$$\frac{dP_a}{dt} = \frac{C_T A_T}{KV} (P_m - P_a)^k \quad (3.6)$$

### 3.1.2 The Pressure Decreasing Mode

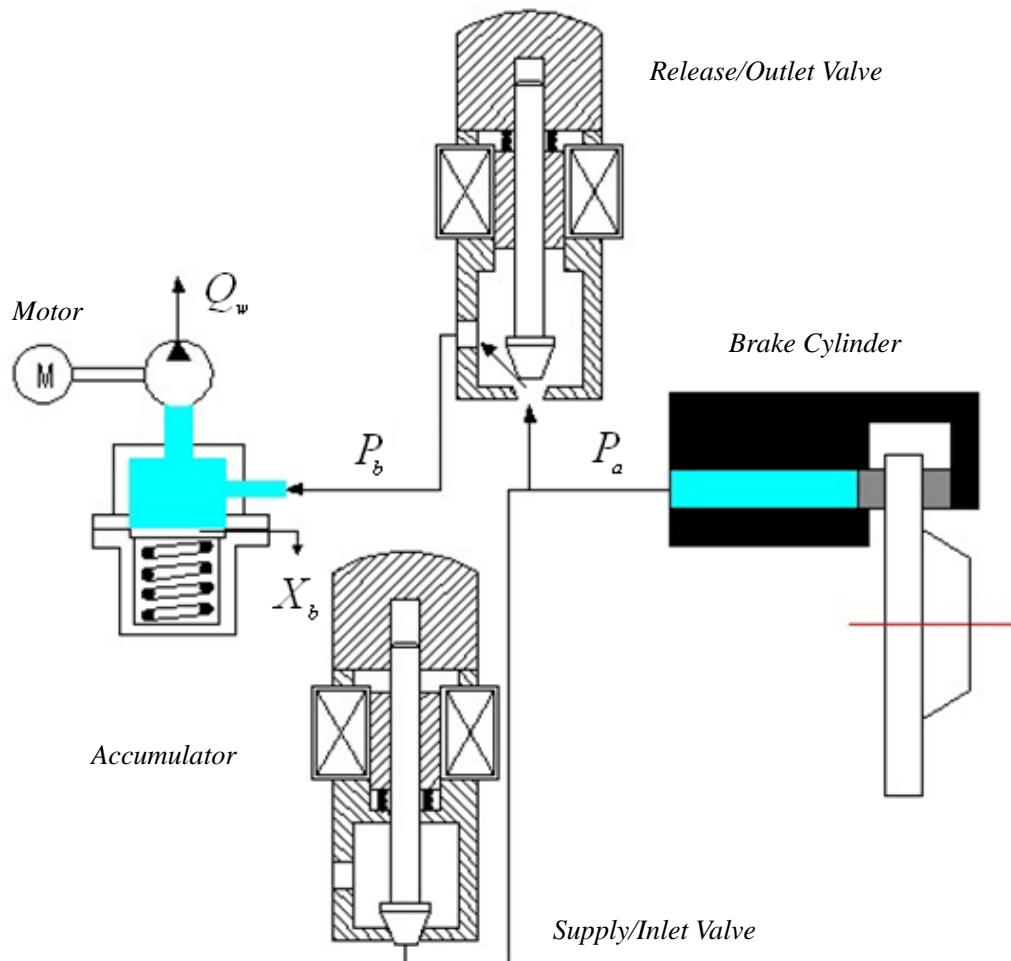


Figure 3.3 Sketch of the pressure decreasing process of ABS

When the Electronic Control Unit (ECU) determines that the pressure of a wheel brake cylinder needs to be reduced, the fluid within it will be decompressed. A command is sent to control the supply/inlet valve to close and to the release/outlet valve to open. The brake fluid flows out of the brake cylinder into the accumulator through the release/outlet valve. At the same time, the pressure of the brake oil inside the brake cylinder is decreased because the pump is activated to return the oil from the accumulator to the master cylinder. The flow circuit of the pressure-decreasing process is shown in Figure 3.3.

Given that the pump speed is far higher than the solenoid operating frequency, the

pump flow rate can be assumed to be constant. However, even for this simplified model, the model is more complex than that of a pressure build-up mode because more components are involved.

During the pressure-decreasing process, the supply valve is closed whilst the release valve is open. The brake fluid inside the brake cylinder flows into the fluid reservoir and the rate of change of pressure of the brake cylinder during the pressure decrease stage is given by:

$$\frac{dP_a}{dt} = \frac{C_B A_B}{KV} P_a^\phi \quad (3.7)$$

where  $C_B$  is the flow rate coefficient,  $A_B$  is the flow area of the valve,  $\phi$  is the index of the release/outlet valve during the pressure decrease stage.

### 3.1.3 The Pressure Holding Mode

When the Electronic Control Unit (ECU) determines that the pressure of a wheel brake cylinder is constant, the brake oil is in the process of maintaining and holding pressure. The ECU controls both the supply/inlet valve and the release/outlet valve in the closed-loop to the corresponding wheel brake cylinder. The brake oil in the brake cylinders is enclosed, and the fluid pressure remains constant. The model shows no leakage and the structure diagram for the pressure-holding process is shown in Figure 3.4.

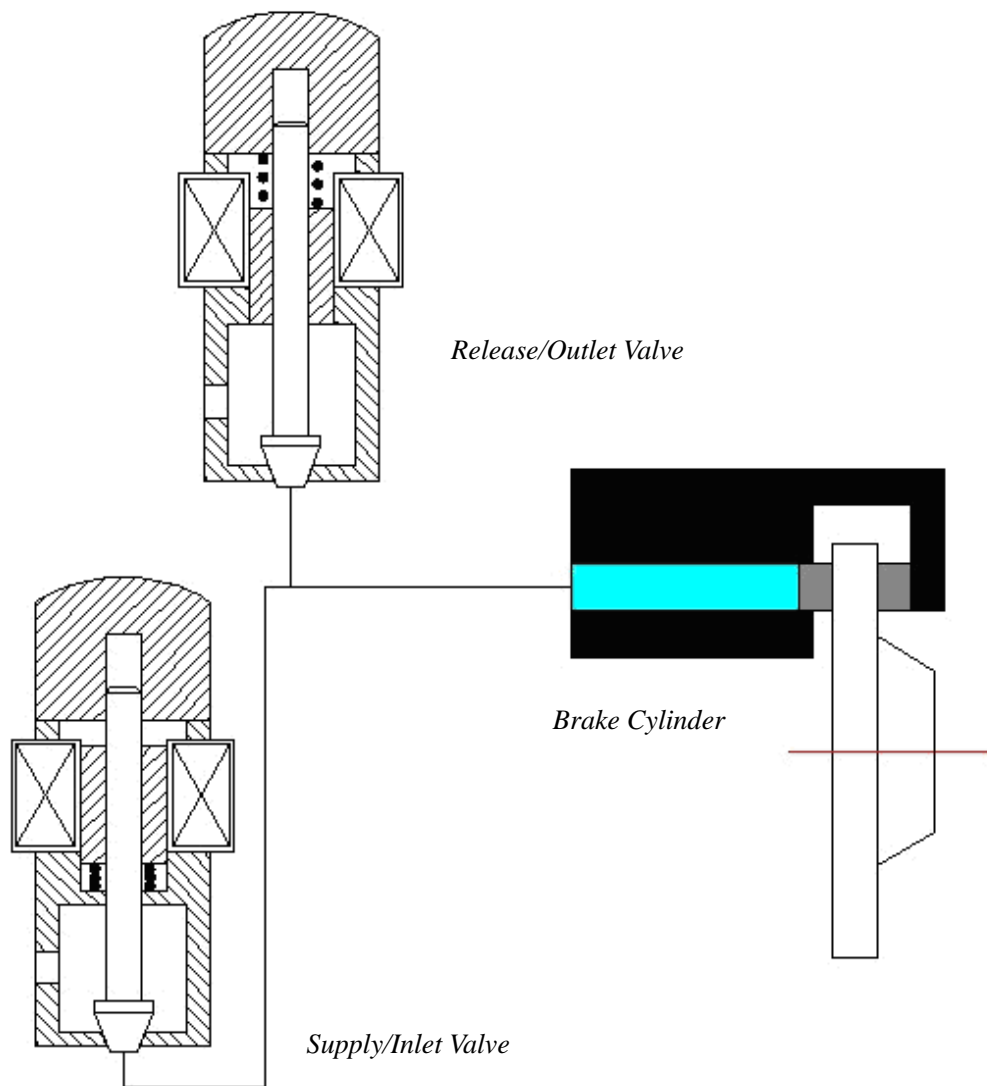


Figure 3.4 Pressure holding process structure diagram

In the pressure holding stage, the braking pressure is unchanged and given by:

$$\frac{dP_a}{dt} = 0 \quad (3.8)$$

### 3.1.4 Parameter Setting for the Three Steps of the ABS

According to the experimental data by L.Zhang [105], the characteristic model of the hydraulic throttle system can be identified as shown in Equation (3.9).

$$\begin{cases} 37.2162 \cdot (P_m - P_a)^{0.54} & \text{Pressure\_Increase} \\ 0 & \text{Pressure\_holding} \\ -35.5261 \cdot P_a^{0.95} & \text{Pressure\_Decreasing} \end{cases} \quad (3.9)$$

The brake torque  $T_b$  can be described as [106]:

$$T_b = K_{pb} P_a \quad (3.10)$$

where  $K_{pb}$  is the braking efficiency coefficient [107]. Equation (3.10) means that the braking torque of braking cylinder equals to braking efficiency coefficient times the brake oil pressure of the brake cylinder.

## 3.2 CONTROL CYCLES OF ABS

According to the relationship between the braking pressure, wheel speed and the friction coefficient of the road, the control cycle of the ABS can be described in three steps: pressure-increase, pressure-holding and pressure-decrease as described in Section 3.1. The characteristics of the first step mean that the pressure-increase can be divided into first-pressure-increase and step-pressure-increase. The setting values of the threshold parameters come from a summary of the road test [108]. The definition of the threshold parameters are shown in Table 3.1.

Table 3.1 Definition of threshold parameters

Threshold Parameter	Meaning
$S_1$	Slip rate threshold of first pressure-decrease
$S_2$	Slip rate from pressure-holding to step-pressure-increase
$S_3$	Slip rate from step-pressure-increase to pressure-decrease
$A_1$	Wheel acceleration threshold of first pressure-decrease
$A_2$	Wheel acceleration threshold from pressure-decrease to pressure-holding
$A_3$	Wheel acceleration threshold from pressure-holding to pressure-decrease

As the calculation of wheel speed is a real-time property during the braking process, the calculations of wheel speed, vehicle speed, acceleration and the slip rate are discrete in nature [109].

In the first control cycle, when the vehicle brakes in an emergency, the pressure of the braking cylinder builds quickly and the speed of the wheel decreases rapidly. When the acceleration of the wheel  $\dot{\omega}$  is less than the acceleration threshold  $A_1$ , the ABS cycle starts to work, whilst braking pressure is maintained. During the pressure-holding process, the slip rate continues to rise. If the slip rate  $S_2$  is bigger than the threshold  $S_1$ , this will lead to an unstable area of slip rate and the pressure will start to decrease (Phase 3). During the pressure-decrease process, the acceleration of the wheel  $\dot{\omega}$  is increased again. When  $\dot{\omega}$  is greater than the acceleration threshold  $A_1$ , the braking pressure is held constant in the pressure-holding process (Phase 4). When  $\dot{\omega}$  is bigger than  $A_3$ , the braking pressure is increased in order to prevent the wheel returning to too small slip values (Phase 5). When  $\dot{\omega}$  is between

$A_3$  and  $A_2$ , the pressure is held constant (Phase 6). Due to inertia and the low level of brake pressure, the wheel speed will continue to increase until  $\dot{\omega}$  exceeds the acceleration threshold  $A_2$ . When wheel acceleration  $\dot{\omega}$  is between  $A_1$  and  $A_2$ , the braking pressure is slowly raised (Phase 7). During the step-pressure-increase process, the slip rate  $S_\lambda$  is around  $S_{opt}$  (optimal slip rate). Running through such cycles, the rotational speed of the wheel,  $\omega$ , is kept in a range where the wheel slip rate  $S_\lambda$  is close to that of the maximum friction coefficient. This allows braking distance to be minimized [110]. The control cycles of the ABS system with hydraulic brakes is shown in Figure 3.5. The related introduction about transfer condition and pressure status of each phases are listed in Table 3.2.

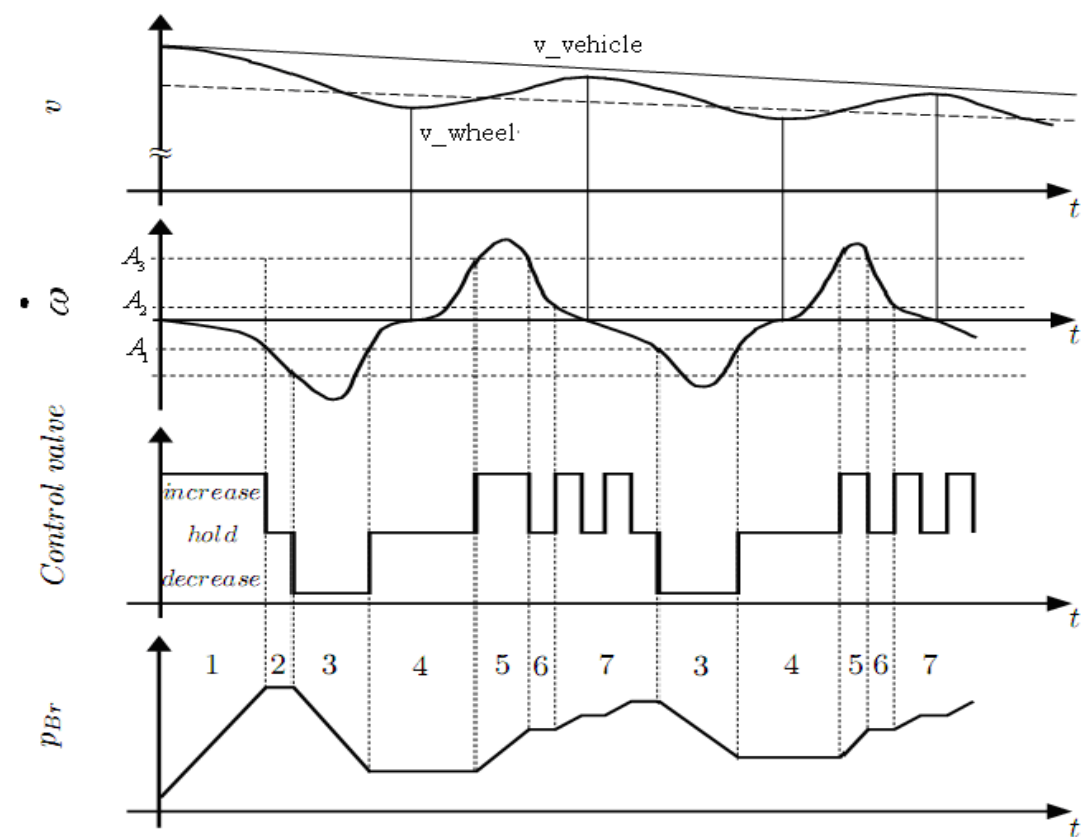


Figure 3.5 Control cycles of the ABS system with hydraulic brakes [110]

Table 3.2 Control phases with transfer conditions and pressure status

Phase	Transfer Conditions	Pressure Status
1	$\dot{\omega}$ decrease	Pressure-increase
2	if $\dot{\omega} < A_1$	Pressure-holding
3	if $S_\lambda > S_1$	Pressure-decreasing
4	if $A_1 < \dot{\omega} < A_3$	Pressure-holding
5	if $\dot{\omega} > A_3$	Pressure-increase
6	if $\dot{\omega} < A_3$	Pressure-holding
7	if $A_1 < \dot{\omega} < A_2$	Step-pressure-increase
Repeat 3	if $\dot{\omega} < A_1$	Pressure-decrease

### 3.3 GENERAL FAULTS OF ABS

In order to provide a fault prediction, the general faults of the ABS system are analyzed and modeled in this section. This includes wheel speed sensor failure, pump efficiency loss, fluid leakage, oil air blister inclusion, pressure hysteresis and sticking solenoid valves.

#### 3.3.1 Wheel Speed Sensor Failure

Speed sensor failure leads to bogus feedback to the vehicle's ECU during the braking process. As part of the control loop, wheel speed sensors provide the controllers with necessary information about the actual system state and vehicle dynamics, following which the controllers are activated in such a way that the vehicle remains stable in

extreme situations. In other words, successful vehicle control strongly depends on the performance of the sensors [111][112].

### **3.3.2 Solenoid Valve Sticking or Stuck**

Theoretically, when restarting the solenoid valve after lack of use, only a small force is required to overcome the friction resistance in order to move the spool. However, in practical application, the resistance is considerable especially in medium or high pressure systems. This phenomenon is called the solenoid valve sticking or stuck phenomena [98].

This phenomenon is due to geometry errors and centerline inconsistency between the spool and the valve body where fluid between the spool and the valve body produces an unbalanced radial force [113]. This forces the valve body and valve orifice to press against one another and leads to the phenomena of solenoid valve sticking or stuck. If it is slightly sticky, the action of the valve will be delayed and the transient pressure signal will be different from normal.

### **3.3.3 Fluid Leakage**

In a hydraulic system, the working fluid flows or is temporarily stored in hydraulic components or pipes. However, due to various reasons such as pressure and gaps, there is still some fluid discharge from the sealed cavity, which is called a fluid leakage [114].

Leakage is a serious problem, which cannot be ignored and causes problems including lack of pressure required by the system, in-stability of the speed of the actuator, waste oil, energy consumption, reduced efficiency, raised temperature, environment pollution, etc.. In the most serious cases, the external leakage may cause a fire as a

result of the fluid being combustible.

### **3.3.4 Pump Efficiency Loss**

Plunger-type hydraulic pumps suck and press the fluid by changing the volume of the sealed working chamber, in which the plunger creates a linear reciprocating motion.

If the pump fails completely, it will not return oil back to the master cylinder although the Electronic Control Unit (ECU) tries to control it to do so [6]. In this case, braking oil from the brake cylinder can only go into the accumulator during the ABS course. The accumulator has its limit as designed. After the spring of the accumulator is completely depressed, the accumulator cannot accept any additional braking oil meaning that the pressure-decrease process cannot be accomplished [6].

In practice, however, what happens most frequently is that the pump efficiency decreases with age and extensive use [6] [110]. In this case, the oil that is charged into the accumulator cannot be returned to the master cylinder completely and a small amount of oil is left in the accumulator at the end of each pressure reduction mode. In addition, because the pressure reduction cannot be completed, the following pressure increasing mode will be also slowed down [6]. The accumulator will sooner or later reach its limitation and the pressure reduction will fail [6] [110].

### **3.3.5 Pressure Hysteresis**

Lining friction causes hysteresis loss and brake gear hysteresis may limit the cyclic frequency of the ABS operation [115]. This situation may also occur as a result of the difference between the supply/inlet valve and the release/outlet valve. Theoretically, the supply/inlet valve and the release/outlet valve should behave identically but there may be a slight difference due to necessary manufacturing tolerances [6]. Fluid

damping of the armature motion may also differ from upward motion to downward motion and consequently, pressure hysteresis may be experienced.

### 3.3.6 Air Blister Inclusion in Brake Fluid

An air blister may occur if the pump pressure reduces below a specific level resulting in pump cavitation [6] [110]. When this occurs, the compressibility of the brake oil will increase significantly and there will be a consequential reduction in the bulk modulus [6].

## 3.4 FRICTION COEFFICIENT CALCULATION

The Burckhardt method is used for calculation of friction forces. The friction behaviour of the wheels can be approximated with parametric characteristics, as shown in Figure 3.6.

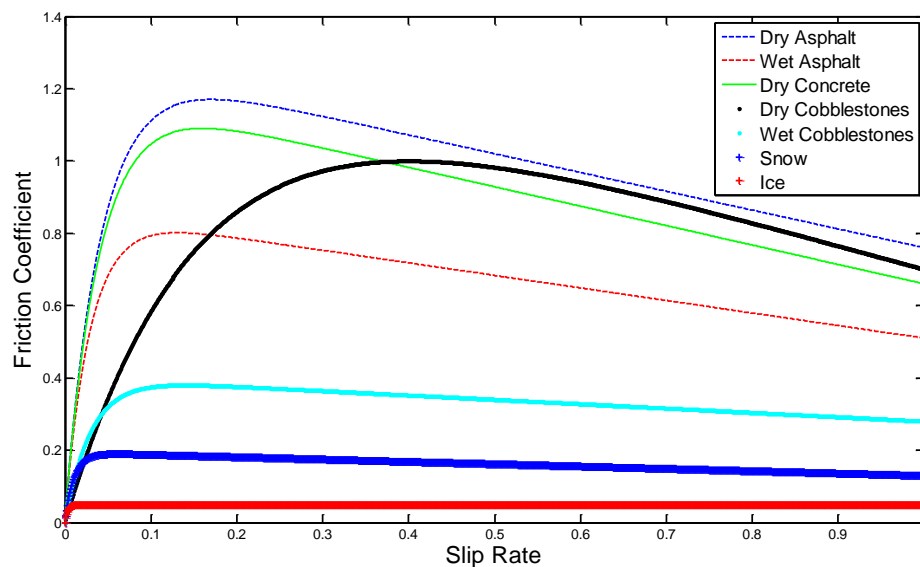


Figure 3.6 Typical slip rate – friction coefficient characteristics

The calculation of friction forces can be carried out using the method of Burckhardt

[116].

$$F(S_\lambda) = c_1(1 - e^{-c_2 S_\lambda}) - c_3 S_\lambda \quad (3.11)$$

The parameters  $c_1$ ,  $c_2$  and  $c_3$  for various road surfaces are given in Table 3.3. By using the extreme value method, the optimal slip rate and the maximum friction coefficient from Equation (3.11) can be described as follow [117].

$$\left\{ \begin{array}{l} S_{opt} = \log \frac{c_1 c_2}{c_3} \\ \mu_{max} = c_1 - \frac{c_3}{c_1} (1 - \log \frac{c_1 c_2}{c_3}) \end{array} \right. \quad (3.12)$$

Table 3.3 Parameters for friction coefficient characteristics (Burckhardt) [116]

Road Type	$c_1$	$c_2$	$c_3$	$S_{opt}$	$\mu_{max}$
Asphalt, dry	1.2801	23.99	0.52	0.17	1.1709
Asphalt, wet	0.857	33.822	0.347	0.13	0.8019
Concrete, dry	1.1973	25.168	0.5373	0.16	1.090
Cobblestones, dry	1.3713	6.4565	0.6691	0.15	0.950
Cobblestones, wet	0.4004	33.7080	0.1204	0.14	0.380
Snow	0.1946	94.129	0.0646	0.08	0.190
Ice	0.05	306.39	0.001	0.06	0.050

With the exception of wet cobblestones the Burckhardt characteristics correspond very precisely to measured characteristics [118]. A measured friction coefficient characteristic for cobblestones exhibits a higher initial gradient which levels out at friction values of about 0.4, and then runs with a smaller gradient to the maximum value, where it can once again be well approximated [116].

## 3.5 THE KALMAN FILTER FOR VELOCITY ESTIMATION

### 3.5.1 The Kalman Filter Algorithm

A Kalman filter is a set of mathematical equations that provide an efficient recursive solution [28]. It is powerful in several aspects: namely, it supports estimations of past, present, and even future states, even when the precise nature of the modelled system is unknown. The Kalman filter estimates a process by using a form of feedback control: the filter estimates the process state at some time and then obtains feedback in the form of (noisy) measurements [119]. The equations for the Kalman filter fall into two groups: time update equations and measurement update equations.

The equations of process and observation equations are

$$\begin{cases} x_k = Ax_{k-1} + Bu_{k-1} + w_{k-1} \\ y_k = Hx_k + z_k \end{cases} \quad (3.13)$$

where  $k$  denotes the discrete point in time domain,  $u_k$  is a vector of inputs,  $x_k$  is a vector of the process states,  $y_k$  is a vector of the actual process outputs,  $w_{k-1}$  and  $z_k$  are process and measurement noise respectively. They are assumed to be zero mean Gaussian with covariance  $Q_k$  and  $R_k$  respectively. The  $n \times n$  matrix ( $A$ ) in Equation (3.13) relates the state at the previous time step ( $k-1$ ) to the state at the current step ( $k$ ) in the absence of either a driving function or process noise. Note that in practice  $A$  may change with each time step, but here it is assumed that it is constant. The  $n \times l$  matrix  $B$  relates the optional control input  $u \in R^l$  to the state  $x_k$ . The  $m \times n$  matrix  $H$  in the measurement equation relates the state to the

measurement  $y_k$ . In practice  $H$  may change with each time step or measurement, but again it is assumed that it is constant.

Define  $(\hat{x}_k^-)$  to be a priori state estimate at step  $k$  given knowledge of the process prior to step  $k$ , and  $(\hat{x}_k)$  to be a posteriori state estimate at step  $k$  given measurement  $y_k$ .

The equations for the Kalman filter fall into two steps: time update equations and measurement update equations [13] [50]. The first step involves projecting both the most recent state estimate and an estimate of the error covariance (from the previous time period) forwards in time to compute a predicted (or a-priori) estimate of the states at the current time [120]. The second step involves correcting the predicted state estimate calculated in the first step by incorporating the most recent process measurement to generate an updated (or a-posteriori) state estimate [120].

The Kalman filter computation procedure is shown in Equation (3.14).

$$\left\{ \begin{array}{l} \hat{x}_k^- = A\hat{x}_{k-1} + Bu_{k-1} \\ P_k^- = AP_{k-1}A^T \\ K_g = P_k^- H^T (HP_k^- H^T + R_k)^{-1} \\ \hat{x}_k = \hat{x}_k^- + K_g (y_k - H\hat{x}_k^-) \\ P_k = (I - K_g H)P_k^- \end{array} \right. \quad (3.14)$$

where  $P_k$  is an estimate of the covariance of the measurement error,  $I$  is the identity matrix, and  $K_g$  is called the Kalman gain.

The reason for applying the Kalman filter approach for vehicle velocity estimation is because the Kalman filter provides a convenient and efficient solution for filtering and

fusing sensor data as well as estimating noise error covariance [121]. Accurate estimates of the absolute speed can be achieved even under significant braking skid and traction slip conditions by using the Kalman filter method [122].

Using the Kalman filter method to estimate velocity, as a basic concept, the

longitudinal wheel slip ratio is given by Equation (2.12)  $S_{\lambda} = \frac{v - \omega r}{v} * 100\%$ ,

where  $\omega$  is the wheel angular velocity,  $r$  is the wheel rolling radius, and  $v$  is the vehicle forward linear velocity. Generally, a situation in which the wheel velocity is bigger than vehicle velocity during braking process will not occur. If, however, the pressure decreases too much and the pressure-increasing process does not execute in time, the wheel may be rotated by inertia drive during the pressure recovery process. From a practical point of view, this phenomenon occurs more frequently on high friction coefficient roads.

### 3.5.2 The Kalman Filter of Wheel Velocity

As discussed in Section 3.5.1, the Kalman filter computation procedure is shown Equation (3.14). The Kalman filter can be used to estimate wheel velocity. Assuming the wheel acceleration  $a_{w,k}$  is calculated by the wheel velocity increment divided by the sampling interval time  $T_s$ , at time  $k$ , then:

$$a_{w,k} = \frac{v_{w,k} - v_{w,k-1}}{T_s} \quad (3.15)$$

where  $v_{w,k}$  presents wheel velocity at time  $k$ .

The state variable matrix  $x_k$  can be defined as

$$x_k = \begin{bmatrix} v_{w,k} \\ a_{w,k} \end{bmatrix} \quad (3.16)$$

Assume that the input variable  $u_{w,k}$  is the time derivative of the wheel acceleration as shown in Equation (3.17).

$$u_{w,k} = \dot{a}_{w,k} \quad (3.17)$$

Then, the coefficient matrices can be described as follows [123]:

$$A = \begin{bmatrix} 1 & T_s \\ 0 & 1 \end{bmatrix}$$

$$B = \begin{bmatrix} \frac{1}{2} T_s^2 \\ T_s \end{bmatrix}$$

$$C = [1 \quad 0]$$

By using the Kalman filter, the input vehicle velocity from the measurement can be filtered without distortion of the signal. Assume that the input  $u_{w,k}$  is zero, meaning that the effect of input is included in process noise  $w_{k-1}$ . The estimated wheel velocity  $\hat{v}_{w,k}$  and the estimated wheel acceleration  $\hat{a}_{w,k}$  at time  $k$  are provided.

### 3.5.3 The Kalman Filter of Vehicle Velocity

The vehicle velocity and wheel velocity can be described as follows:

$$\left. \begin{aligned} \dot{u}_{v,k} &= a_{v,k} \\ v_{w,k} &= u_{v,k} + \xi_k \end{aligned} \right\} \quad (3.18)$$

where  $\xi_k$  is the effect of wheel slip on the wheel velocity,  $a_{v,k}$  the vehicle acceleration,  $u_{v,k}$  the vehicle velocity and  $v_{w,k}$  the wheel velocity. It can be described as:

$$\xi_k = -S_\lambda \bullet u_{v,k} \quad (3.19)$$

In order to establish a Kalman filter equation for the vehicle velocity  $u_{v,k}$ , the estimated wheel velocity  $\hat{v}_{w,k}$  and the estimated wheel acceleration  $\hat{a}_{w,k}$  must be substituted into Equation (3.18) in order to obtain the dynamic model as described in Equation (3.20).

$$\left. \begin{aligned} \dot{u}_{v,k} &= \hat{a}_{v,k} + w_k \\ \hat{v}_{w,k} &= u_{v,k} + z_k \end{aligned} \right\} \quad (3.20)$$

where  $\hat{a}_{v,k}$  is the estimate vehicle acceleration, while  $z_k$  is not the real measurement noise but the sum of measurement noise and effect of wheel slip on the wheel velocity as shown below.

$$z_k = z_{v,k} + \xi_k \quad (3.21)$$

where  $z_{v,k}$  is the real measurement noise.  $\xi_k$  is the deviation for using vehicle velocity as wheel velocity, which is caused by wheel slip. Assuming that the measurement noise and process noise are zero mean and individual Gaussian noises, Equation (3.20) can be discretized into the form of Equation (3.13). The  $\dot{u}_{v,k}$  is

substituted by the first-order differential quotient  $\frac{u_{v,k+1} - u_{v,k}}{T_s}$ , then Equation (3.20)

can be discretized as:

$$\left. \begin{aligned} u_{v,k+1} &= u_{v,k} + T_s \hat{a}_{v,k} + T_s w_k \\ \hat{v}_{w,k} &= u_{v,k} + z_k \end{aligned} \right\} \quad (3.22)$$

Equation (3.22) can be considered as process and observation equations with parameters of  $A=1$ ,  $B=T_s$  and  $H=1$ . The covariance of process noise  $Q$ , the covariance of measurement noise  $R_k$ , together with the covariance of error  $P_k$  are set up as scalar. The Kalman filter estimation of vehicle velocity can be described as

$$\left. \begin{aligned} \hat{u}_{v,k+1} &= \frac{Q(\hat{u}_{v,k} + T_s \hat{a}_{v,k}) + (P_k + S_w) \hat{v}_{w,k+1}}{P_k + Q + R_k} \\ P_{k+1} &= \frac{(P_k + Q)R_k}{P_k + Q + R_k} \end{aligned} \right\} \quad (3.23)$$

If the covariance of process noise  $Q$ , the covariance measurement noise  $R_k$ , together with the covariance of error  $P_k$  are constant,  $\hat{u}_{v,k+1}$  can be considered as weighted sum of  $\hat{a}_{v,k}$  and  $\hat{v}_{w,k+1}$ .

### 3.5.4 Parameter Adaptive Kalman Filter

In order to get better estimation results, the covariance of process noise  $Q$  and covariance measurement noise  $R_k$  will be calculated separately under different conditions [122] [123].

The covariance of measurement noise  $R_k$  can be calculated separated depending on whether the wheel is slipping or not.

$$R_k = R_{k1} + R_{k2} \quad (3.24)$$

$$R_{k1} = \begin{cases} 0.05 + 40\left(1 - \frac{\hat{v}_{w,k+1}}{\hat{u}_{v,k}}\right) & \text{when } (\hat{v}_{w,k+1} < \hat{u}_{v,k}) \\ 0.05 & \text{when(others)} \end{cases} \quad (3.25)$$

$$R_{k2} = \begin{cases} 20\left(\frac{|\hat{a}_{v,k} - \hat{a}_{w,k-1}|}{g} - 0.2\right) & \text{when } (|\hat{a}_{v,k} - \hat{a}_{w,k-1}| > 0.2g) \\ 0 & \text{when(others)} \end{cases} \quad (3.26)$$

The covariance of process noise  $Q$  can be calculated separated depending on whether the wheel velocity is greater than vehicle velocity.

$$Q = \begin{cases} 0.05 & \text{when } (\hat{v}_{w,k+1} < \hat{u}_{v,k}) \\ 5 & \text{when(others)} \end{cases} \quad (3.27)$$

The Kalman filter results of both vehicle velocity and wheel velocity will be further discussed in Chapter Seven.

### 3.6 SUMMARY

In this chapter, a theoretical model of ABS was introduced, together with its control algorithm. The dynamic analysis of pressure status in the hydraulic components of ABS was carried out with functions. The transfer conditions of seven phases of ABS control were introduced not only in words, but also with figures and table list. A number of general faults of ABS were discussed. The Burckhardt method for

calculation friction coefficient was introduced with seven different road types. In addition, the Kalman filter with adaptive parameters for estimation of both vehicle velocity and wheel velocity were introduced. With all these theoretical analysis, the simulation models under both fault-free condition and faulty conditions are able to be built up, which will be introduced in the next chapter.

---

## CHAPTER FOUR

# THE SIMULATION MODEL OF THE ANTI-LOCK BRAKING SYSTEM

---

The simulation models of the ABS system are based on the mathematical models as discussed in Chapter Three. These are listed in this chapter using the Simulink method. The control modules for slip rate, the friction coefficient calculation, and the dynamic model of the vehicle are developed separately. The simulation model without ABS together with its parameter results is listed. The simulation models of ABS with or without pressure-holding are then developed using control logic. The faults introduced in Chapter Three including speed sensor failure, solenoid valve sticking or stuck, fluid leakage and pump efficiency loss are also seeded in the models for simulation.

## 4.1 THE ABS CONTROL MODEL

### 4.1.1 The Calculation Module of Slip Rate

As discussed in Chapter Two, the longitudinal wheel slip rate is described in Equation

(2.12) as  $S_{\lambda} = \frac{v - \omega r}{v} * 100\%$ , where  $\omega$  is the wheel angular velocity,  $r$  is the

wheel rolling radius, and  $v$  is the vehicle forward linear velocity. According to Equation (2.12), the Simulink model of slip rate can be described diagrammatically as shown in Figure 4.1.

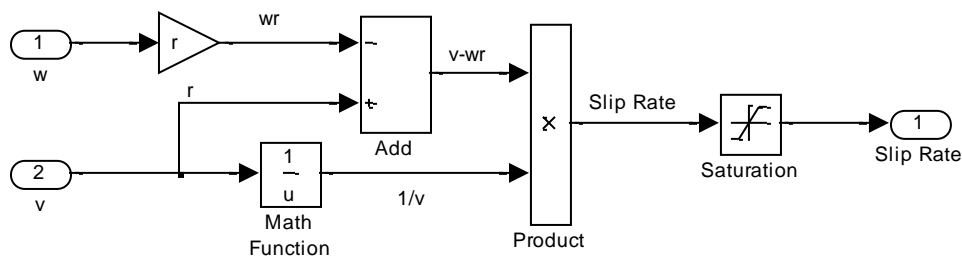


Figure 4.1 Simulation module of slip rate

### 4.1.2 The Dynamic Model of the Vehicle

The Simulink of the dynamic model based on Equation (2.10) and Equation (2.11) is shown in Figure 4.2.

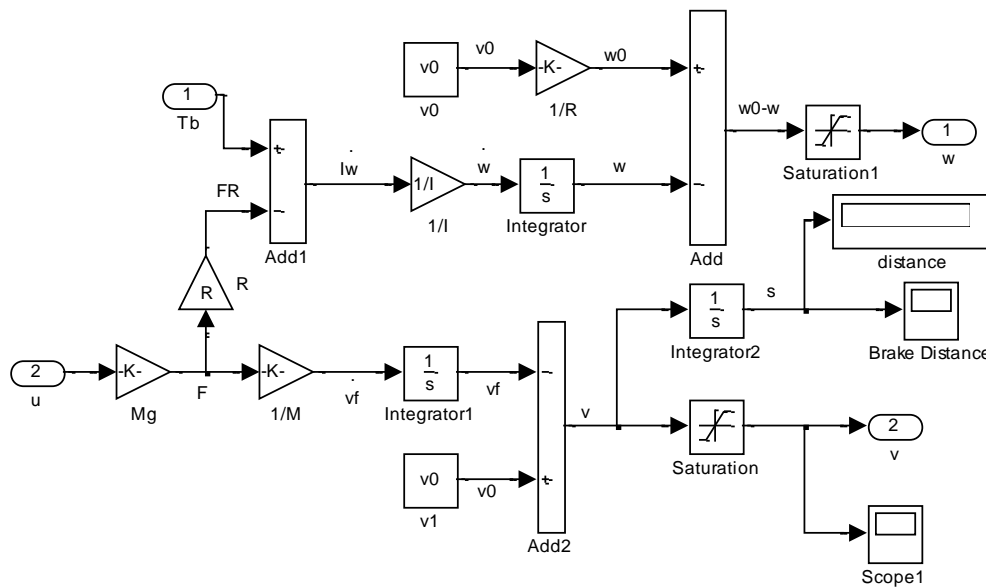


Figure 4.2 Simulation model of the vehicle

The inputs shown are: braking torque  $T_b$  and longitudinal friction coefficient  $\mu_b$ . Similarly, the outputs are: wheel angular velocity  $\omega$ , vehicle forward linear velocity  $v$  and braking distance  $S$ .

### 4.1.3 Friction Coefficient Calculation

As discussed in Section 3.4, the Burckhardt method is used for calculation of friction force. The Simulink model of both the slip rate and friction coefficient is shown in Figure 4.3. By choosing the road surface condition as shown in Figure 4.3, the model can simulate different coefficients of friction. The numerical assignments of road conditions are as follows:

1. Dry asphalt road
2. Wet asphalt road

3. Dry concrete road
4. Dry cobblestone road
5. Wet cobblestone road
6. Snow road
7. Ice road

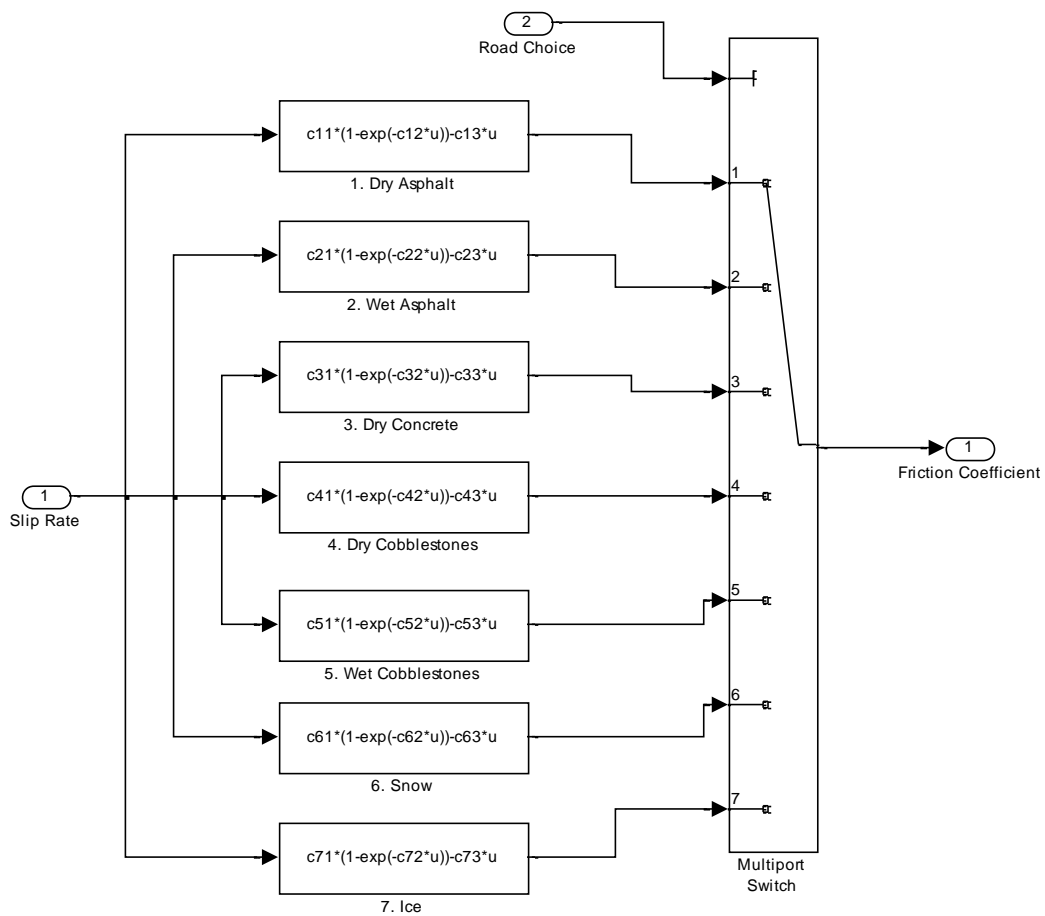


Figure 4.3 Simulink module of friction coefficient with input of slip rate

### 4.1.4 The Braking Simulation without ABS

In this section, the Simulink model without ABS is shown in Figure 4.4. The simulation results will be established in Chapter Five, which calculates the importance of a hydraulic ABS component. The initial braking torque  $T_b$ , was assumed to be 1800 Nm.

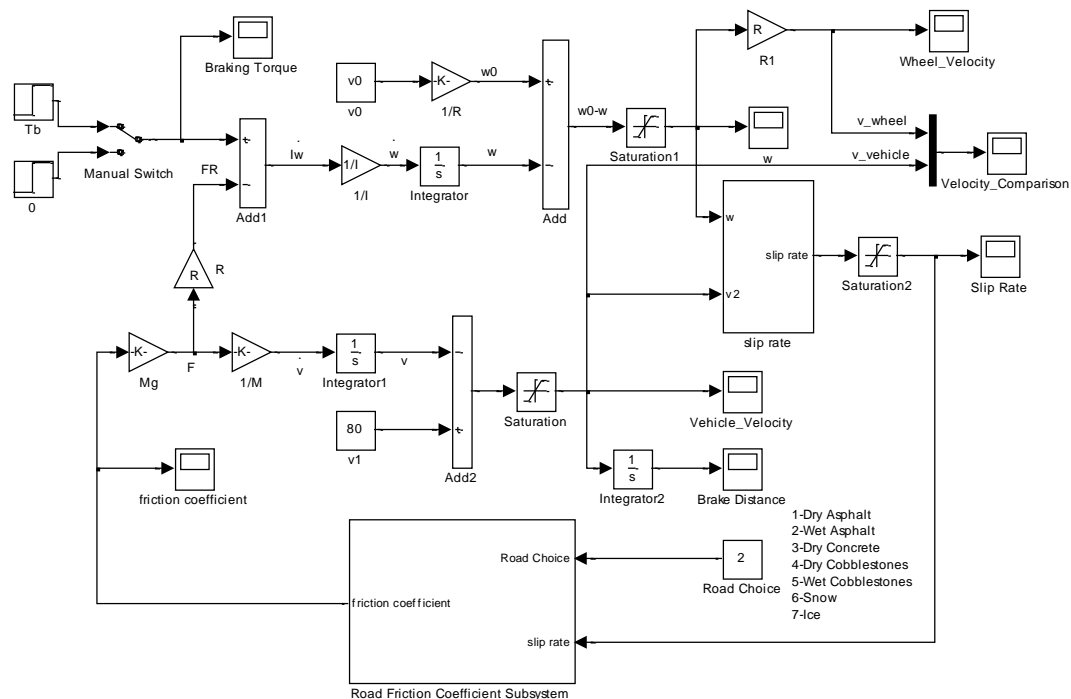


Figure 4.4 Simulation model of hydraulic pressure braking without ABS

The simulation results will be shown in Chapter Five.

## 4.2 THE SIMULATION MODEL WITHOUT PRESSURE-HOLDING PROCESS

The ABS system adjusts the state of motion of the wheel by controlling the pressure in the brake cylinder. Therefore, a study pertaining to the influence of hydraulic

characteristics is the foundation of research and evaluation of the ABS. The research of hydraulic characteristics focuses mainly on performance as the pressure within the brake cylinders is increased and decreased.

In order to develop a model of an ABS hydraulic actuator, we need [124]:

- (1) Ignore the pressure loss due to the reduced flow of brake fluid inside the hydraulic pipe.
- (2) Assume that the internal surface of the hydraulic pipe is sufficiently smooth.
- (3) Ignore the instant impact of the brake fluid during solenoid valve switching.
- (4) Ignore the elastic deformation of the braking hydraulic pipe and wheel cylinder body.

As discussed in Chapter Three, the characteristic model of the hydraulic throttle system can be identified as follows:

$$\begin{cases} 37.2162 \cdot (P_m - P_a)^{0.54} & \text{Pressure\_Increase} \\ -35.5261 \cdot P_a^{0.95} & \text{Pressure\_Decreasing} \end{cases} \quad (4.1)$$

The brake torque  $T_b$  can be described as:

$$T_b = K_{pb} P_a \quad (4.2)$$

where  $K_{pb}$  is the braking efficacy coefficient [107].

By using the principles shown above, the braking torque subsystem, without the

pressure-holding process, can be built up as shown in Figure 4.5. The Memory Block output is the input from the previous time step, applying a one integration step sample-and-hold to the input signal. As shown in Figure 4.5, the brake torque  $T_b$  is generated differently for either pressure-increasing or pressure-decreasing mode and chosen by the slip input, with a threshold of 0.2 (the optimal slip rate for wet asphalt road is about 0.1, 0.2 is the maximum limitation) in the Switch Block.

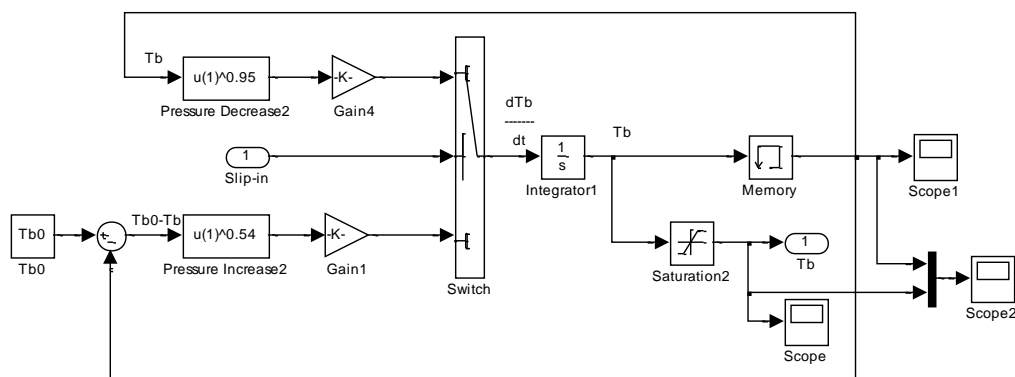


Figure 4.5 Braking torque logic controller module without the pressure-holding process

Simulation model without the pressure-holding process is shown in Figure 4.6.

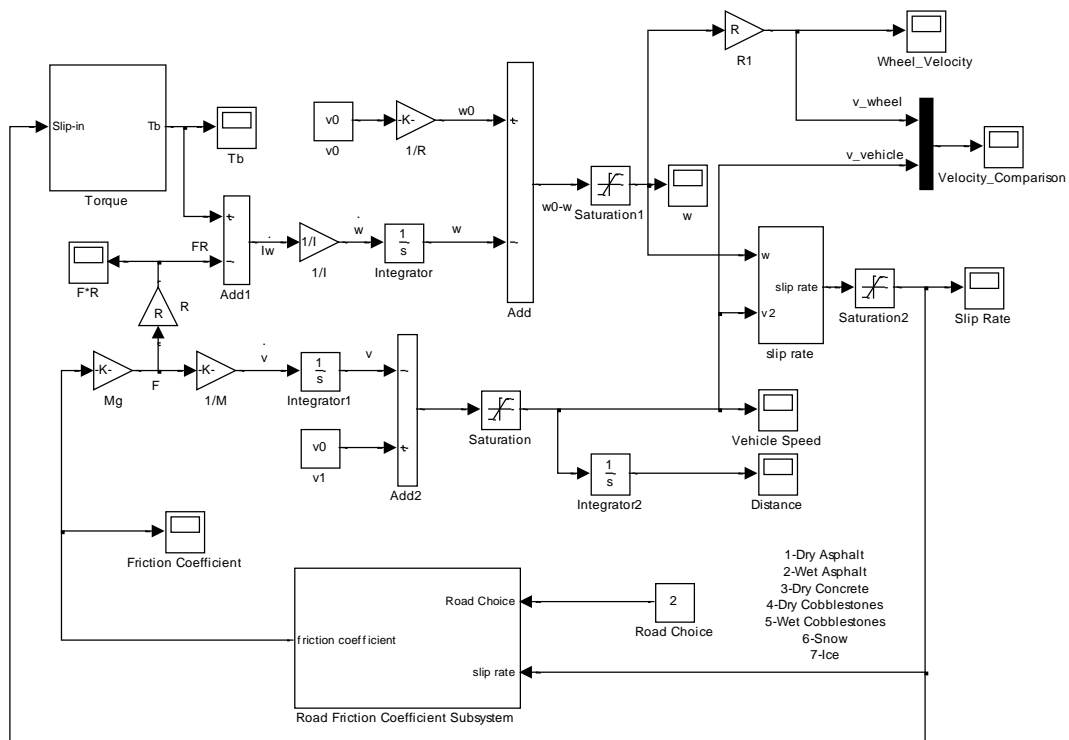


Figure 4.6 Simulation model of logic control without the pressure-holding process

As shown in Figure 4.5, the subsystem “Torque” receives a real-time slip rate from the vehicle. The module of the switch is set up with a threshold of 0.2, which is called the “Optimal Slip Rate”. If the real-time slip rate is bigger than the threshold, the switch turns to the pressure decrease module. On the contrary, if the real-time slip rate is less than the threshold, the switch turns to the pressure increase module.

### 4.3 THE SIMULATION MODEL WITH PRESSURE-HOLDING PROCESS

The test braking system includes a brake drum with radius of 0.13m. The braking efficacy coefficient is 2.42 as derived from the test [105].

$$T_b = K_{pb} P_a = K_{pb} \cdot p_a \cdot A_d \quad (4.3)$$

where  $P_a$  is the brake oil pressure of the brake cylinder,  $p_a$  the fluid pressure inside the pipe, and  $A_d$  is the area of the brake drum. If the braking efficacy coefficient  $K_{pb} = 2.42$  with  $A_d = \pi \cdot (0.013)^2$ , the fluid pressure  $P_a$  is about 3MPa from test, and the braking torque  $T_b$  is 1800Nm as set in the Simulink model.

As discussed in Chapter Three, the characteristic model of the hydraulic solenoid system can be identified as shown in Equation (4.4) [105].

$$\begin{cases} 37.2162 \cdot (P_m - P_a)^{0.54} & \text{Pressure\_Increase} \\ 0 & \text{Pressure\_holding} \\ -35.5261 \cdot P_a^{0.95} & \text{Pressure\_Decreasing} \end{cases} \quad (4.4)$$

The brake torque  $T_b$  can be described as:

$$T_b = K_{pb} P_a \quad (4.5)$$

where  $K_{pb}$  is the braking efficacy coefficient [107].

To evaluate the suggested approach, the simulation model of the ABS with the pressure-holding process is shown in Figure 4.7. The subsystem of braking torque is shown in Figure 4.8. The outputs of ‘Multiport Switch’ module in Figure 4.8 with definitions of: 0 for pressure-decrease, 1 for pressure-holding, 2 for pressure-increase and 3 for step-pressure-increase.

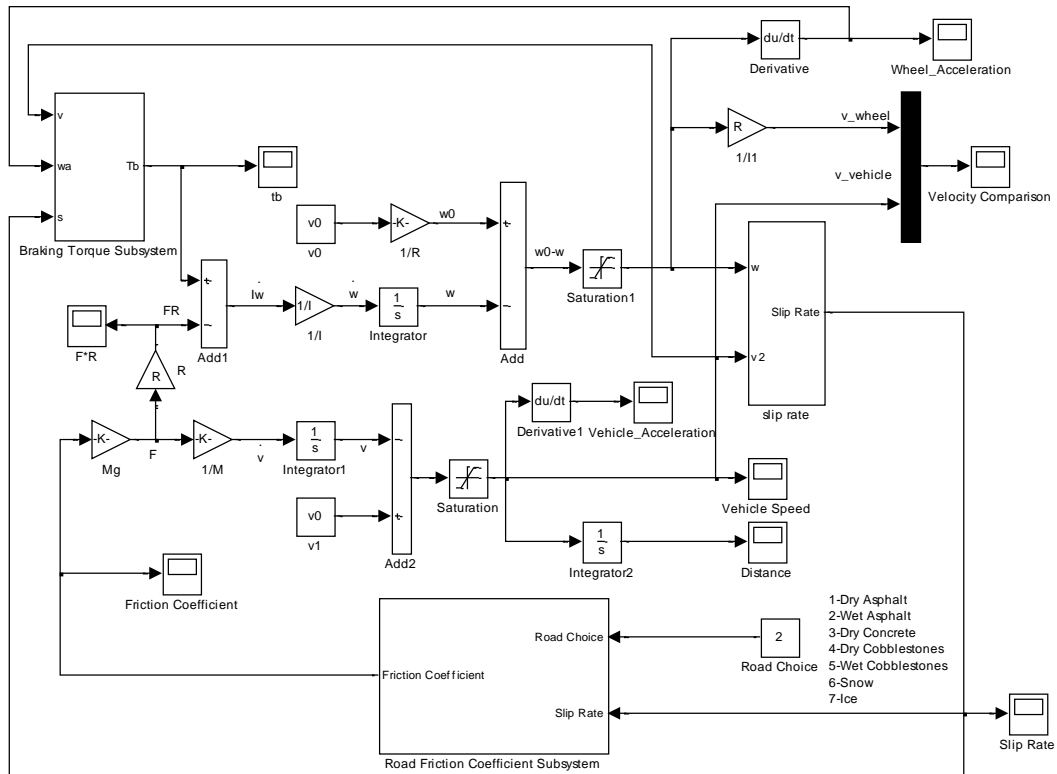


Figure 4.7 Simulation model of logic control with the pressure-holding process

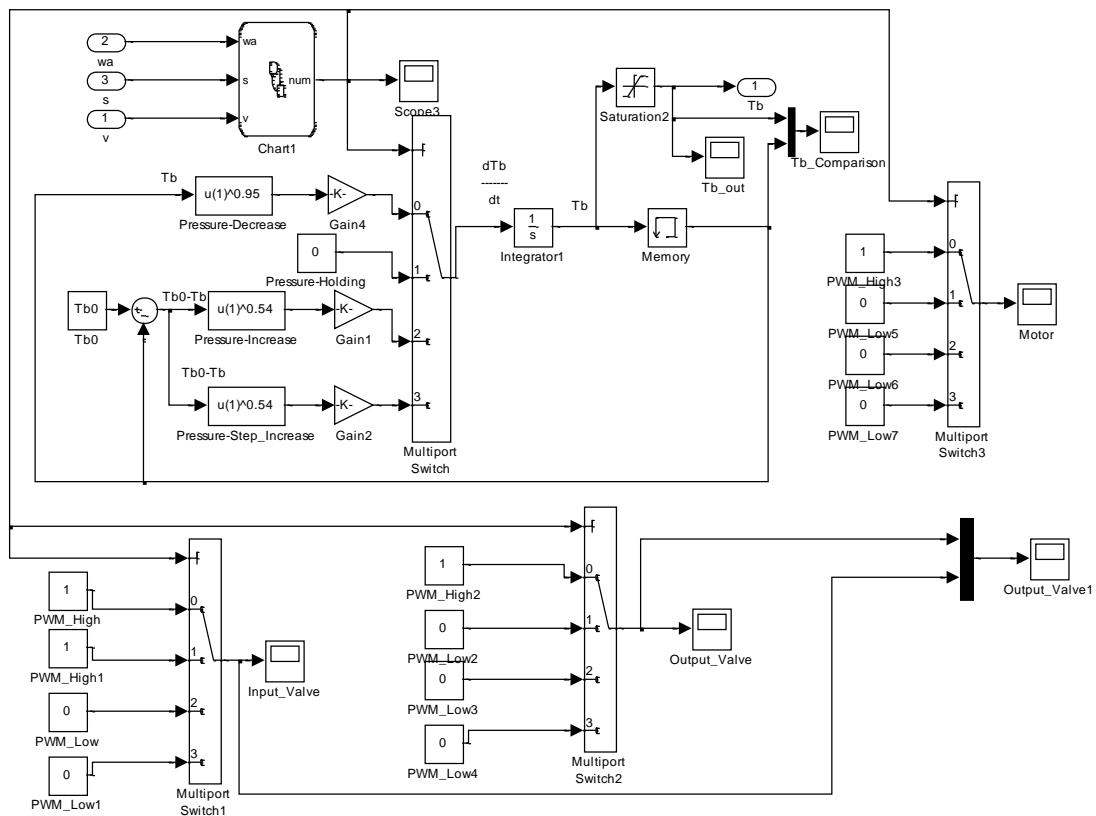


Figure 4.8 Braking torque controller with pressure-holding process

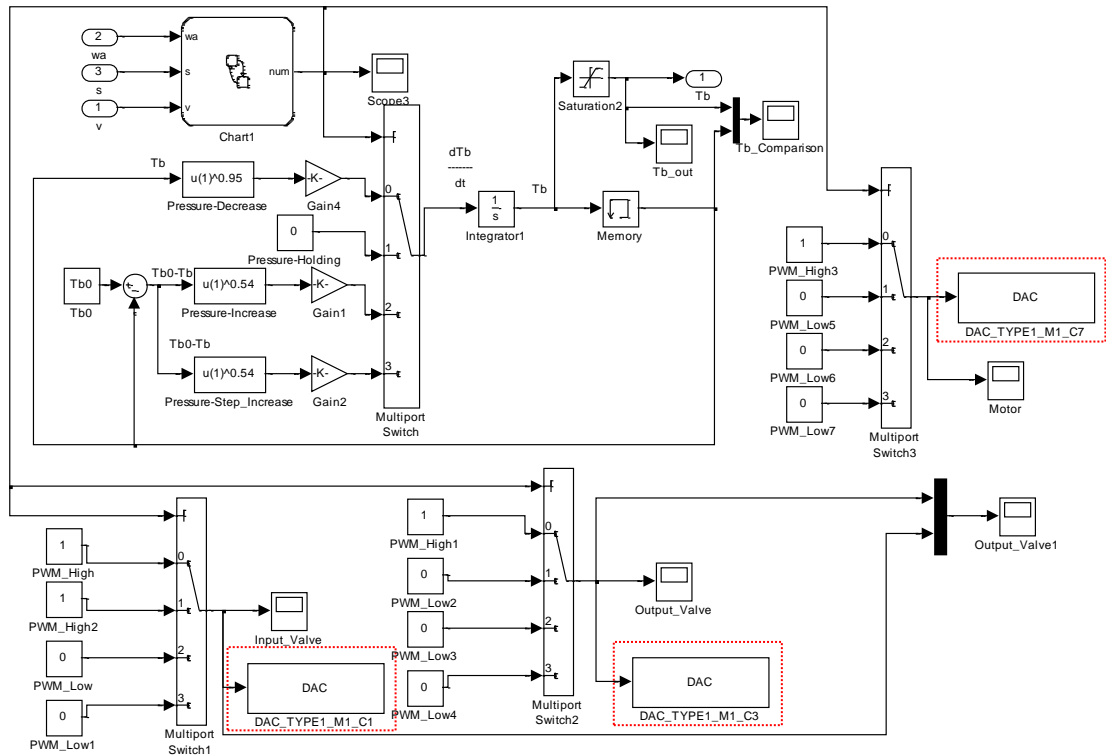


Figure 4.9 Braking torque subsystem with dSpace DAC module

Figure 4.9 shows the braking torque subsystem with the dSpace DAC Module. If the dSpace component is disconnected or has no power supply, it will turn red as shown in Figure 4.10. In this situation, it is necessary to check the connection of the system.

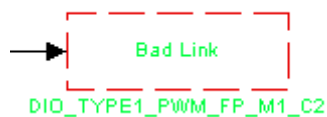


Figure 4.10 Disconnection problem of dSpace

The controller module encapsulates the ABS control logic with a compiled program. The representation of the ABS control logic algorithm can be expressed in two ways using Matlab. Firstly, it can be programmed by an S-function in Simulink. Secondly, it can be described using Stateflow. A Stateflow chart is a graphical representation of a finite state machine, where states and transitions form the basic building blocks of the system [125].

Because Stateflow has a better readability of logic design and more convenient logic control in implementation, it has been used for logic control design in this project. When the control thresholds are decided, the logic control of the ABS can be developed using Stateflow. By using Stateflow, control logic is informed by operating conditions, whilst action can be triggered by status. By using high friction coefficient control, the control logic of the ABS logic threshold is shown in Table 4.1.

Table 4.1 Control logic of ABS logic threshold

State Before Transfer	Transfer Condition	State After Transfer
Pressure-holding	$\dot{\omega} < A_1 \ \&\& \ S_\lambda > S_1$	Pressure-decrease
Pressure-holding	$\dot{\omega} > A_3$	Pressure-increase
Pressure-holding	$A_1 < \dot{\omega} < A_2$	Step-pressure-increase
Pressure-decrease	$\dot{\omega} > A_1$	Pressure-holding
Pressure-increase	$\dot{\omega} < A_3$	Pressure-holding
Step-pressure-increase	$\dot{\omega} < A_1$	Pressure-decrease

The logic control Stateflow based on a high friction coefficient road is shown in Figure 4.11. There are three general states in this Stateflow: ABS non-work state, ABS working state and ABS quit state. The ABS working state includes four sub-states: pressure-increasing state, pressure-decreasing state, pressure-holding state and step-increasing state as shown in Figure 4.11.

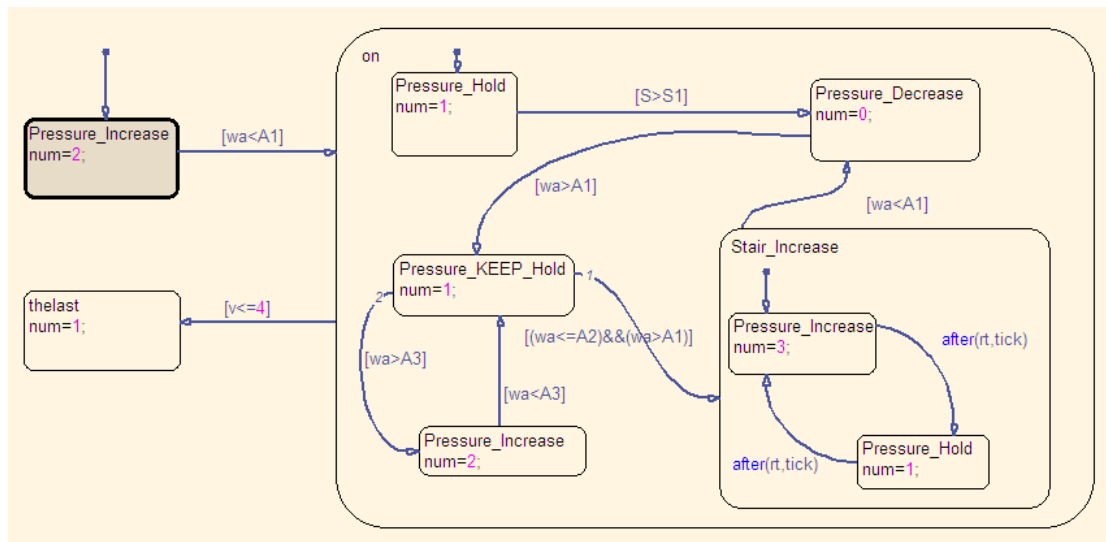


Figure 4.11 Stateflow of logic control on high friction coefficient road

## 4.4 THE FAULT SIMULATION

Conventionally, a model-based approach compares the model prediction and the actual measurement to generate residuals for fault diagnosis. In this project, however, this is virtually implemented in Simulink, in the first instance to evaluate the feasibility of the proposed method. In this Matlab/Simulink evaluation, the actual measurement is modelled by different faulty simulations. The normal behaviour of the system is simulated in a masked program in which the residual generation and fault prognosis are also carried out. Because these phases use different thresholds, they are discussed separately in following sections.

### 4.4.1 Wheel Speed Sensor Failure

When wheel speed sensor failure occurs, there is no feedback of wheel speed from sensor to the control unit. According to the slip rate function of  $S_{\lambda} = \frac{v - \omega r}{v} * 100\%$ , the slip rate will be 100% under the speed sensor failure condition. The control unit will consider that the wheel is locked. Figure 4.12 shows the Simulink model of speed

sensor failure in a vehicle braking system. The manual switch can then convert between two different states of normal and faulty.

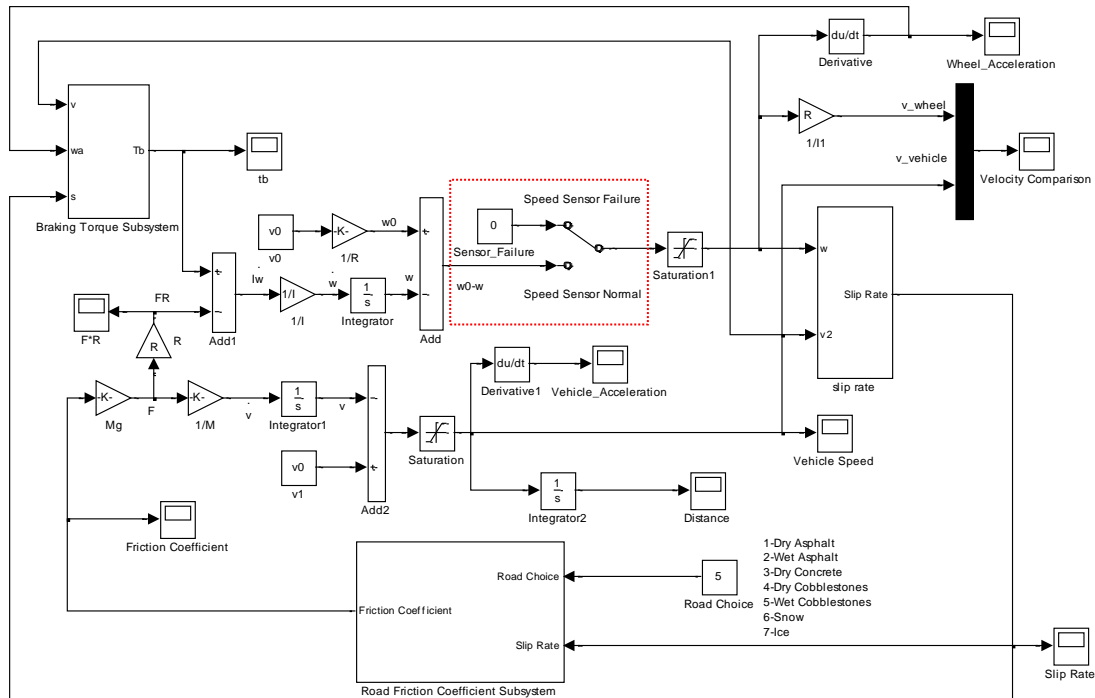


Figure 4.12 Simulink model of speed sensor failure in braking torque subsystem

## 4.4.2 Solenoid Valve Sticking or Stuck

If one of the solenoid valves sticks completely, there is no action within the valve. If it is slightly sticky, the valve's actions will be delayed and the transient pressure signal will be different from normal. This can be modelled using a delay function as shown in Figure 4.13.

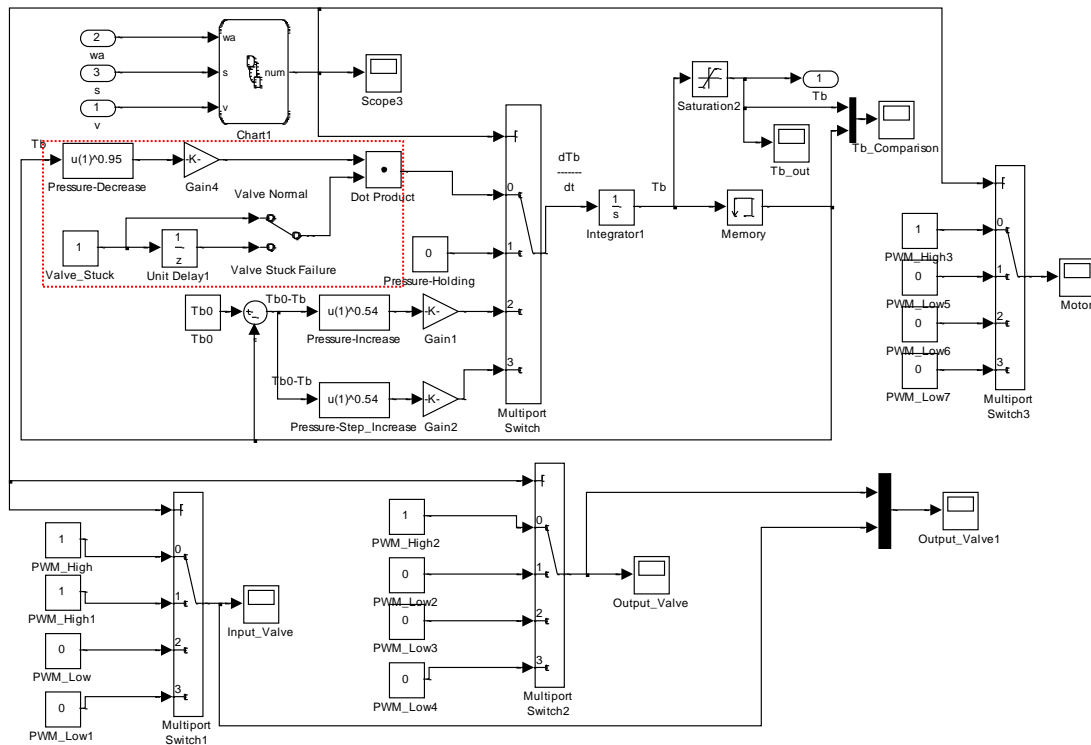


Figure 4.13 Simulink model of valve stuck failure in braking torque subsystem

### 4.4.3 Fluid Leakage

When leakage occurs, the leakage flow rate is determined by the size of the leaking hole and the pressure inside the cylinder. It is normally simplified into a linear model. If leakage is present, the ABS model in either the pressure increasing process or pressure decreasing process will be affected. Figure 4.14 shows a Simulink model of fluid leakage in the braking torque subsystem. The leakage amount can be changed by varying the module value of ‘Gain’.

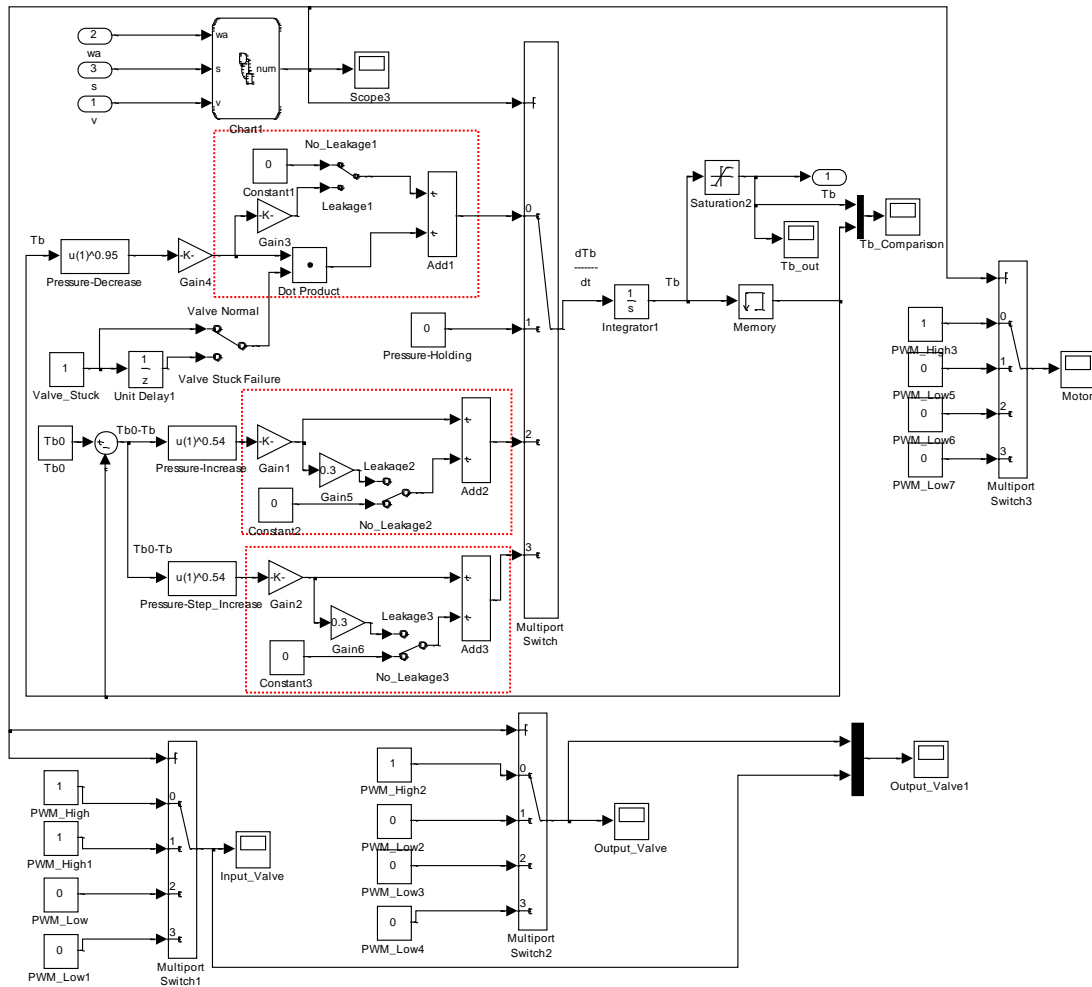


Figure 4.14 Simulink model of liquid leakage in braking torque subsystem

#### 4.4.4 Pump Efficiency Loss

If the pump fails completely, it will not return fluid back to the master cylinder although the ECU tries to control it to do so. In this case, the fluid from the brake cylinder can only go into the accumulator during the ABS cycle. The accumulator has a limit level meaning that after its spring is completely depressed, it cannot accept any additional liquid. In this case, the pressure decreasing cannot be accomplished.

In practice, however, what happens most frequently is that the pump efficiency decreases with age and extensive use. In this case, the fluid that is charged into the

accumulator cannot be returned to the master cylinder completely leaving a small amount of fluid in the accumulator at the end of each pressure decreasing mode. In addition, because the pressure decreasing cannot be completed, the following pressure increasing mode will be also slowed down. The accumulator will sooner or later reach its limitation and the pressure-decreasing process will not take place. Figure 4.15 shows the model with a fault simulation of the pump efficiency loss.

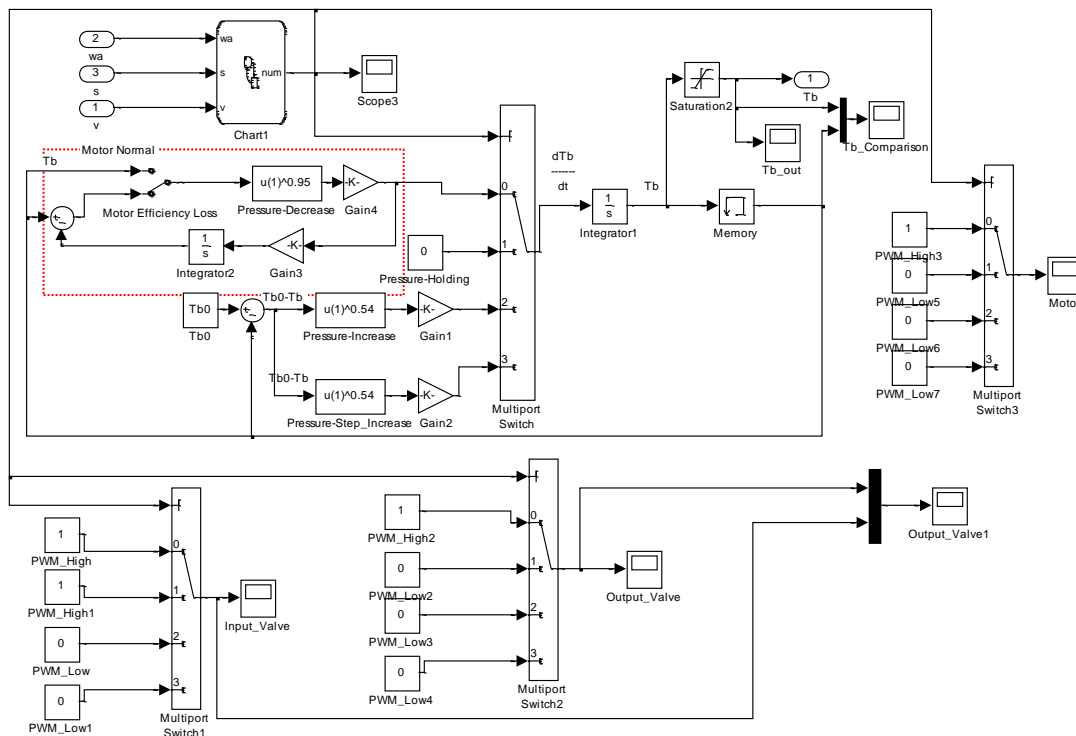


Figure 4.15 Simulink model of pump efficiency loss in braking torque subsystem

## 4.5 SUMMARY

In this chapter, the simulation models of ABS system were built up based on the mathematical model introduced in Chapter Three. Some important subsystems such as slip rate calculation subsystem, vehicle dynamic performance subsystem and friction coefficient subsystem were built up separately. Three different simulation models of braking system including braking without ABS, ABS without pressure-holding

process and entire braking system with ABS were developed with parameters. The simulation results of braking system without ABS were exposed in velocity, braking distance, slip rate and braking torque separately. The control logic of ABS was applied by using Stateflow with transfer conditions. The faulty models of speed sensor failure, solenoid valve sticking or stuck, fluid leakage and pump efficiency loss were developed in this chapter. The simulation results will be carried out in the next chapter.

---

## CHAPTER FIVE

# SIMULATION RESULTS OF THE ANTI-LOCK BRAKING SYSTEM

---

The simulation results of ABS without the pressure-holding process and ABS with pressure-holding process are discussed separately. The comparison results of vehicle velocity, wheel velocity, braking distance, slip rate and braking torque between no-ABS, ABS without pressure-holding and ABS with pressure-holding are going to be discussed. Meanwhile, the simulation results with four different faults using the simulation models as developed in Chapter Four are analyzed, and conclusions are summarized.

## 5.1 SIMULATION RESULTS WITHOUT ABS

The simulation results of braking system without ABS as discussed in Section 4.1 are shown below. The simulation model refers to Figure 4.4 as shown in Chapter Four. With an initial speed  $v_0 = 25\text{ m/s}$ , which can also be considered as  $v_0 = 90\text{ km/h}$  or  $v_0 = 55.92\text{ mile/h}$ , and braking torque  $T_b = 1800\text{ Nm}$ , Figures 5.1 to 5.4 show that wheel speed reduces sharply, with a zero value in 0.137s, whilst slip rate rises synchronously for a vehicle braking on a wet asphalt road. The wheel is lockup and begins to slip. In this condition, the steering capability and operability of the vehicle is entirely lost, potentially leading to a traffic accident. The braking distance is about 113.3m, with a braking time of 9.087s. The braking torque remains at 1800 Nm throughout the whole braking progress without ABS. All these initial parameters are set up under realistic condition[105] [126].

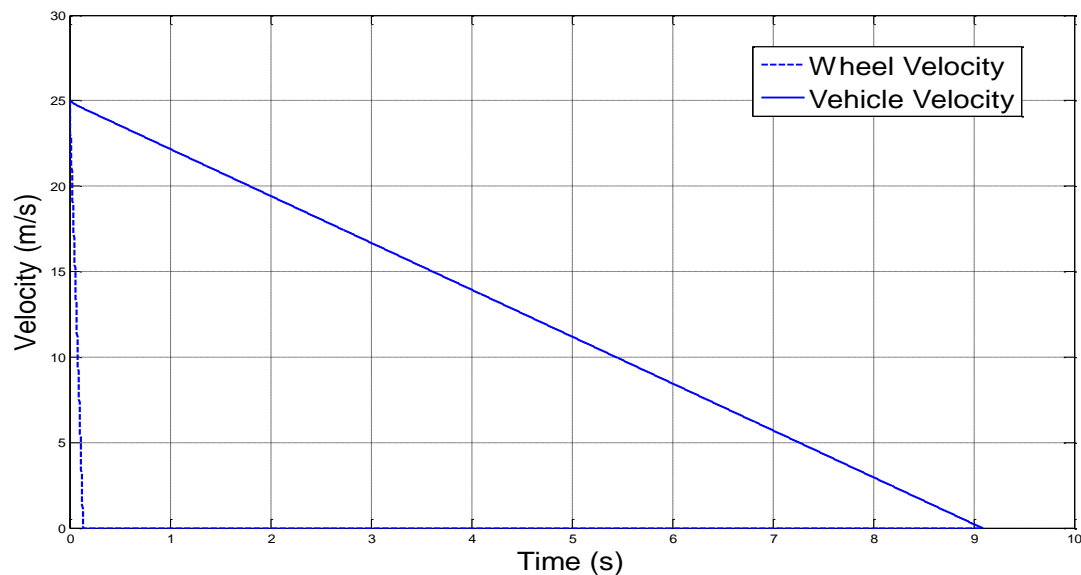


Figure 5.1 Velocity in braking without ABS

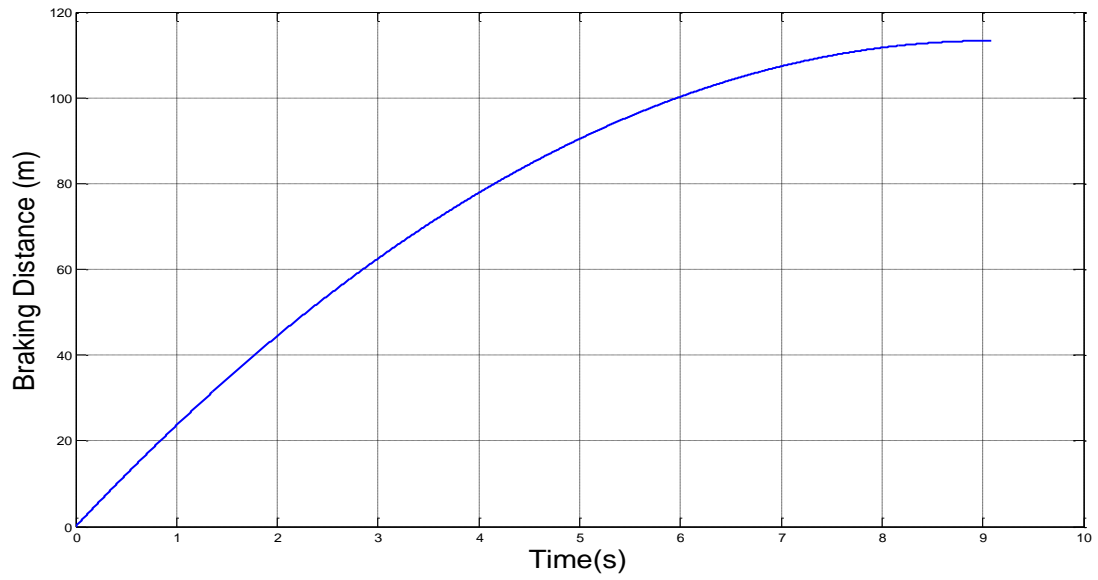


Figure 5.2 Braking distance without ABS

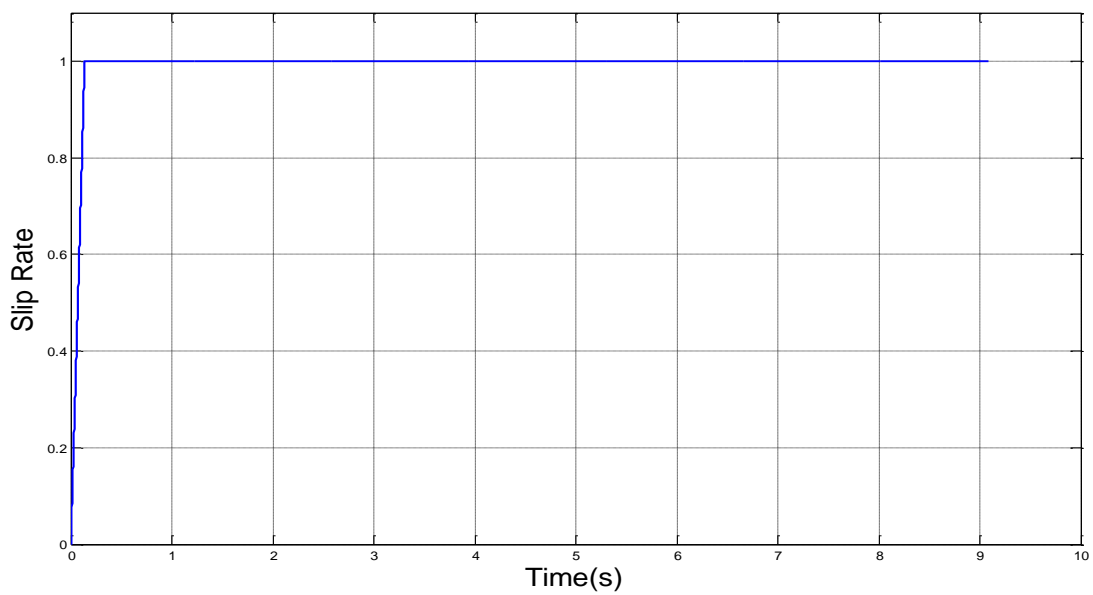


Figure 5.3 Slip rate in braking without ABS

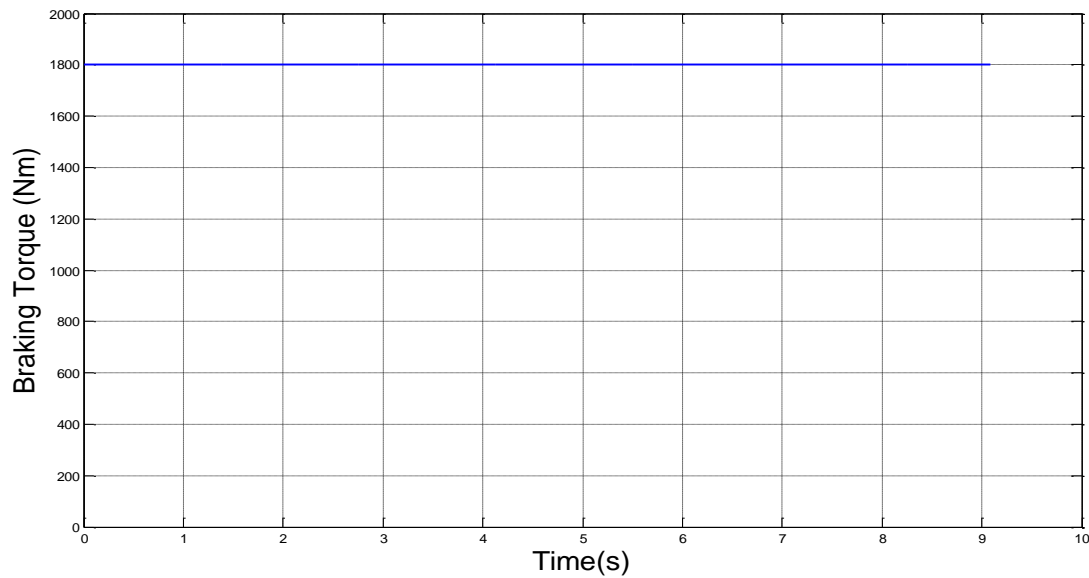


Figure 5.4 Braking torque without ABS

## 5.2 SIMULATION RESULTS WITHOUT PRESSURE-HOLDING PROCESS

By using the Simulink model as developed in Section 4.2, the simulation results are shown in Figure 5.5 to Figure 5.10. The simulation results are based on an initial velocity of  $v_0 = 25m/s$ , which can also be considered as  $v_0 = 90km/h$  or  $v_0 = 55.92mile/h$ , and a braking torque of  $T_b = 1800Nm$  on wet asphalt road.

Because the ABS starts to work during the braking process, without the pressure-holding process, the wheel is not locked during the entire braking process. The braking distance is about 95.66m, with a braking time of 7.402s.

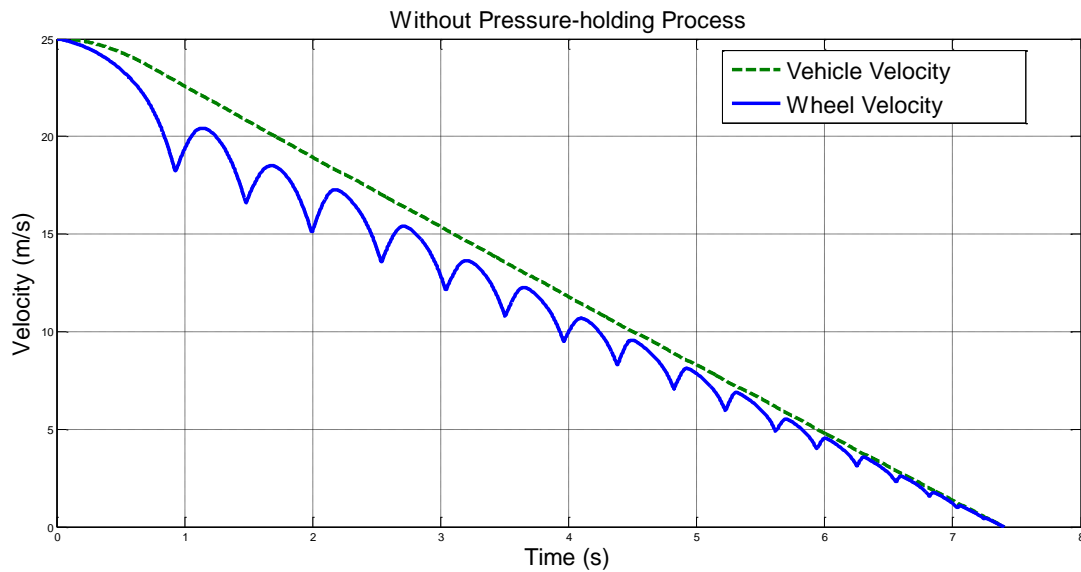


Figure 5.5 Velocity under logic control without the pressure-holding process

The vehicle velocity decreases continually from the start of the braking action. The wheel velocity shows a trend of decreasing, but with fluctuations. The fluctuations appear because when the ABS starts working, the modes of pressure-increase and pressure-decrease switch due to the threshold as shown in Figure 4.9.

Figure 5.6 shows the braking distance is about 95.66m, which is 17.64m less than the braking distance without ABS. This shows a distance reduction achieved of 15.57%, which is significant improvement.

Figure 5.7 shows the slip rate of the ABS without the pressure-holding process. The slip rate varies up to the optimal slip rate limitation value of 0.2 as designed in Section 4.2. The final value is 1 because the vehicle stops and the wheel is locked at the end of the braking process.

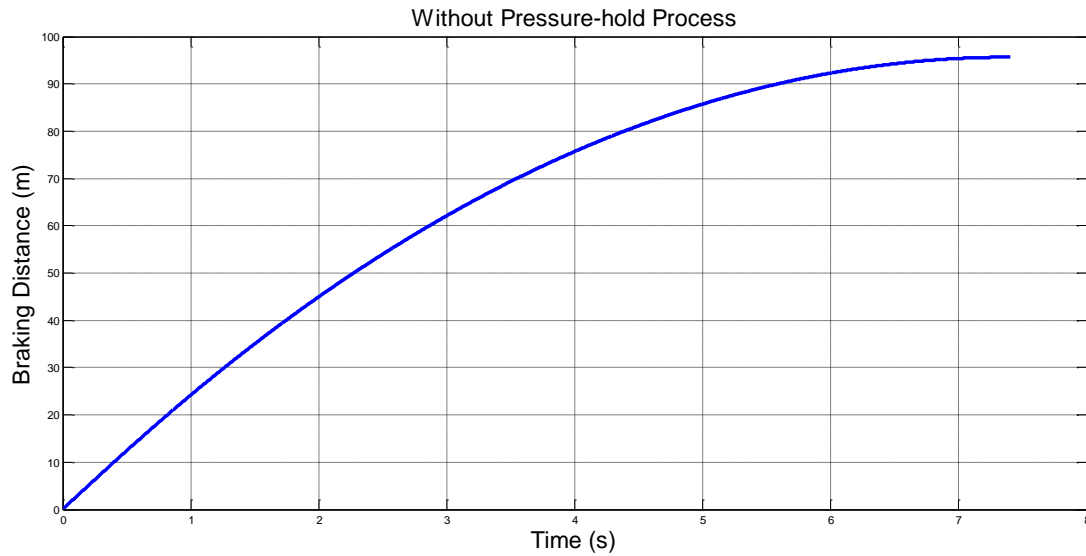


Figure 5.6 Braking distance under logic control without the pressure-holding process

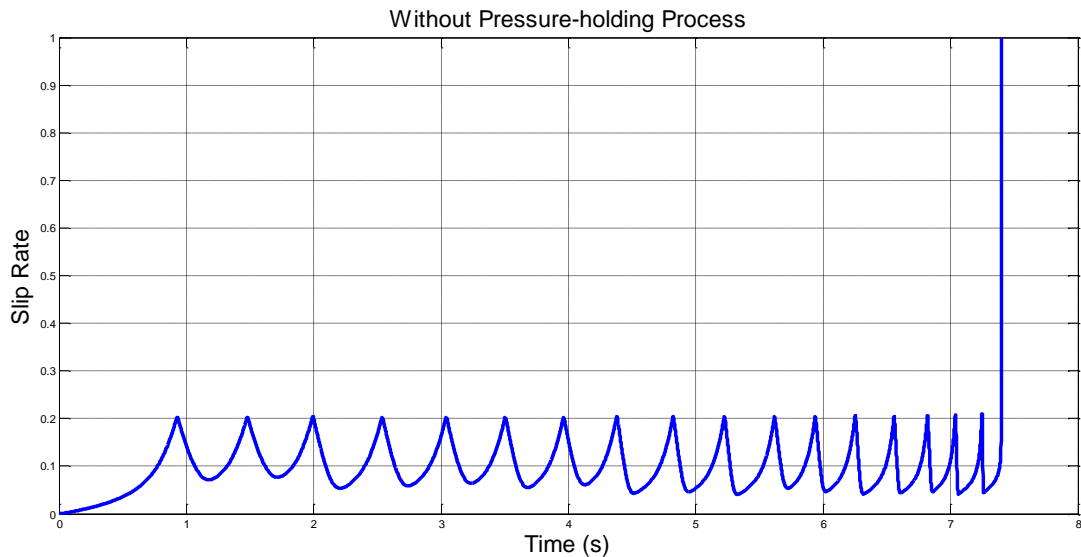


Figure 5.7 Slip rate under logic control without the pressure-holding process

The Figure 5.8 shows the braking torque changes of ABS without the pressure-holding process. The value changes significantly because there is no pressure-holding process during the braking. The biggest value of braking torque is about 600 Nm and the smallest value is about 250 Nm during the whole braking process.

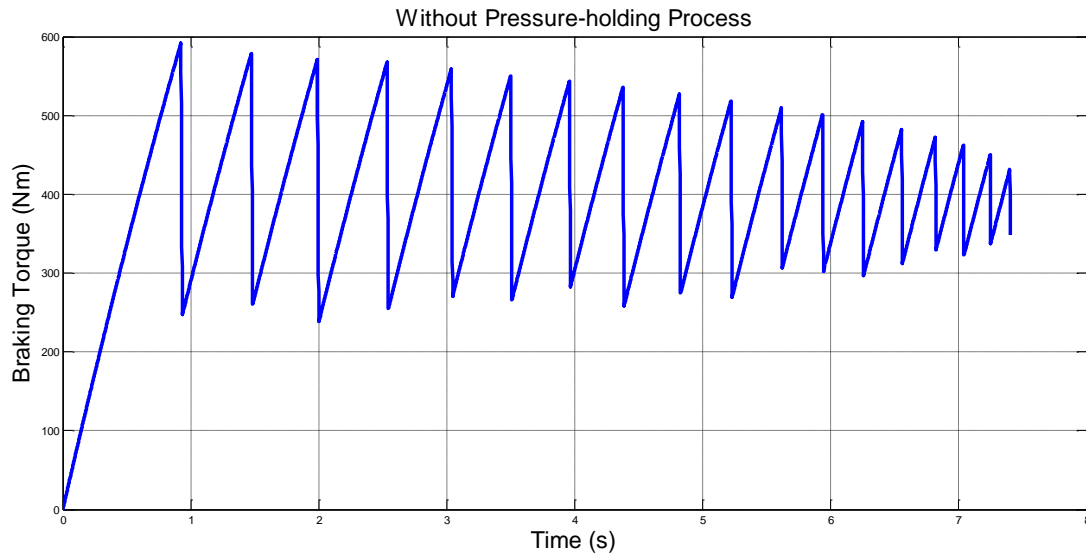


Figure 5.8 Braking torque under logic control without the pressure-holding process

Figure 5.9 shows the braking torque comparison with memory and real-time without the pressure-holding process as discussed in Section 4.3. It is based on the Braking Torque Controller model of Figure 4.12. The memory result is delayed one step behind the real-time result for feedback to the controller. From Figure 5.10, it is easy to find the difference between these two results.

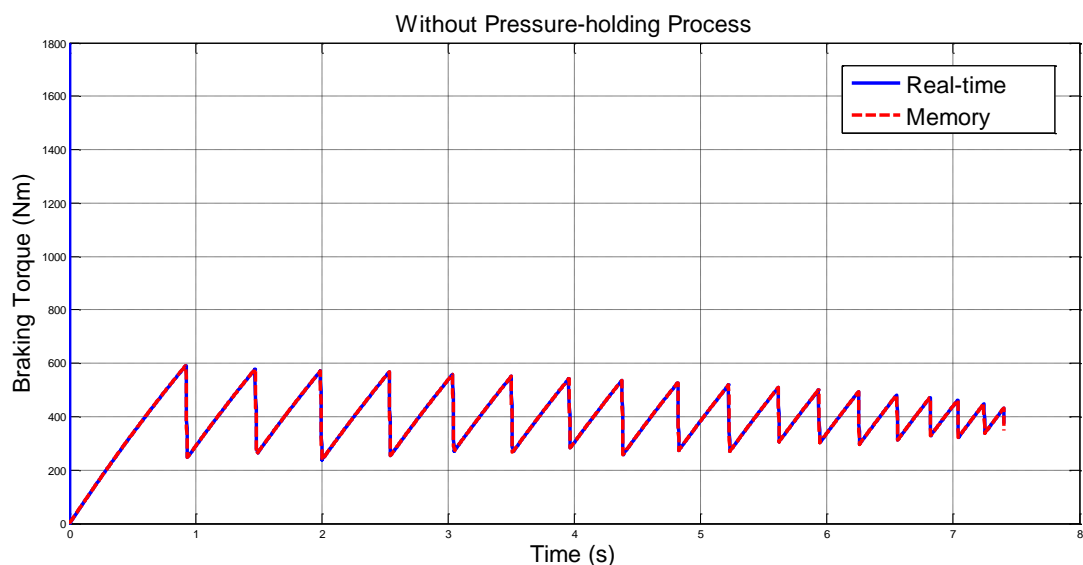


Figure 5.9 Braking torque comparison with memory and real-time without the pressure-holding process

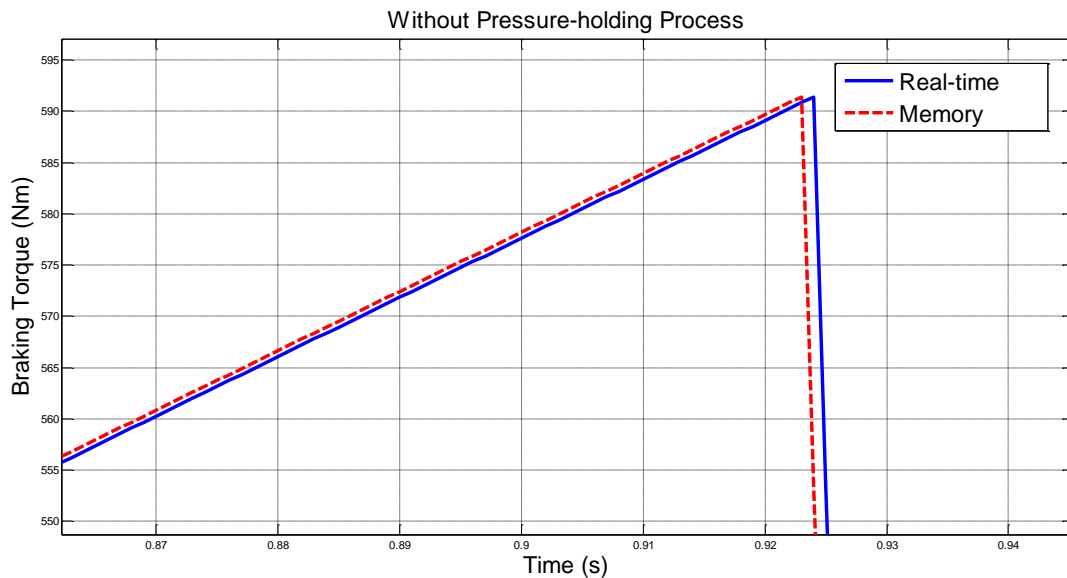


Figure 5.10 Zoom in of Figure 5.9

### 5.3 SIMULATION RESULTS WITH PRESSURE-HOLDING PROCESS

By using the Simulink model as developed in Section 4.3, the simulation results are shown from Figure 5.11 to Figure 5.16. The simulation results are based on the initial velocity of  $v_0 = 25m/s$ , which can also be considered as  $v_0 = 90km/h$  or  $v_0 = 55.92mile/h$ , and braking torque  $T_b = 1800Nm$  on a wet asphalt road.

Figure 5.11 describes wheel velocity together with the vehicle velocity from 25 m/s until the vehicle has stopped. It stops at time of 7.183s without wheel locking. The ABS stops working at about 5.95s because the vehicle velocity  $v_{vehicle} < 4m/s$ . The control algorithm is settled in Stateflow as shown in Figure 4.11. The vehicle stops at 7.183s after the braking process starts, which is 1.904s less than the time taken without ABS. The stopping time is reduced by 20.59%, a significant improvement than the stopping time without ABS.

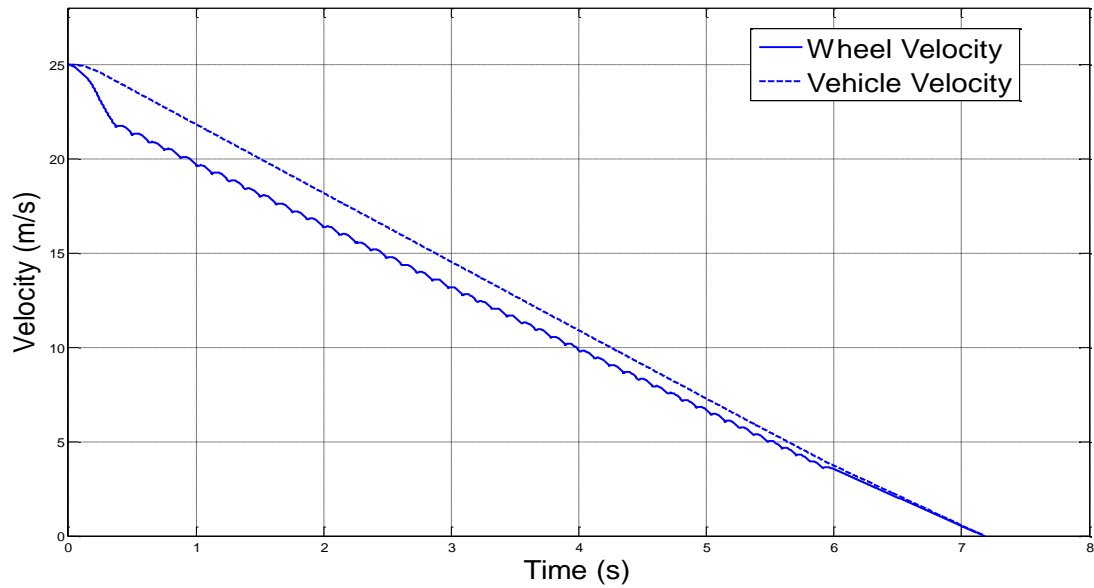


Figure 5.11 Velocity under logic control with the pressure-holding process

Figure 5.12 shows the result of the braking distance from the initial velocity of 25 m/s until stopping. The braking distance of ABS with the pressure-holding process is 89.528m from the point at which the ABS begins to work, which is 20.98% less than without ABS.

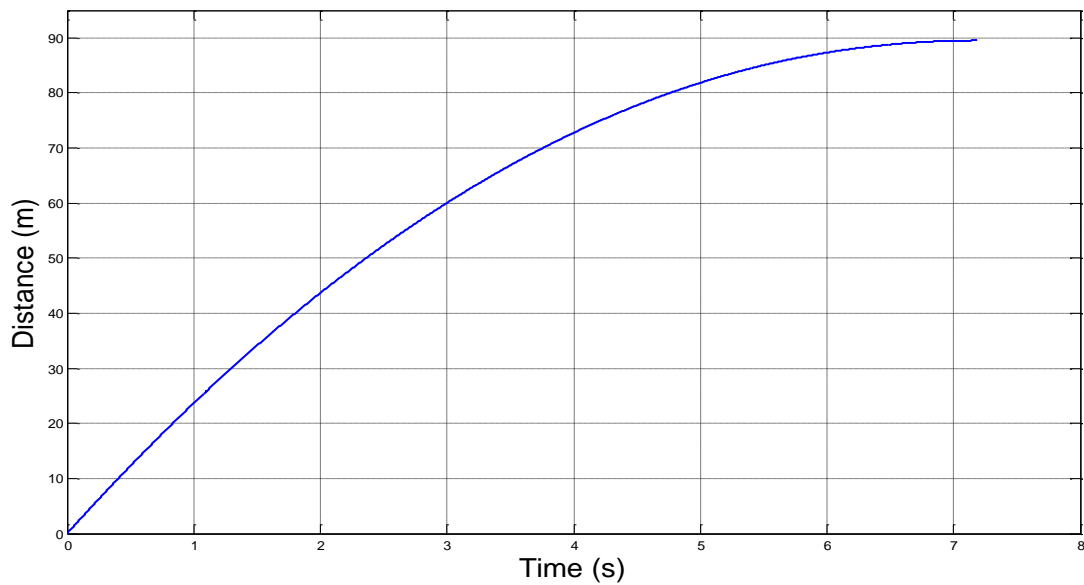


Figure 5.12 Braking distance with the pressure-holding process

Figure 5.13 shows the result of the slip rate from the initial velocity of 25 m/s until stopping. During the whole process, the wheel is not locked. The amplitude of the slip

rate with the pressure-holding process changes more slightly than the one without the pressure-holding process. In this situation, the vehicle can be more stable and easier to handle.

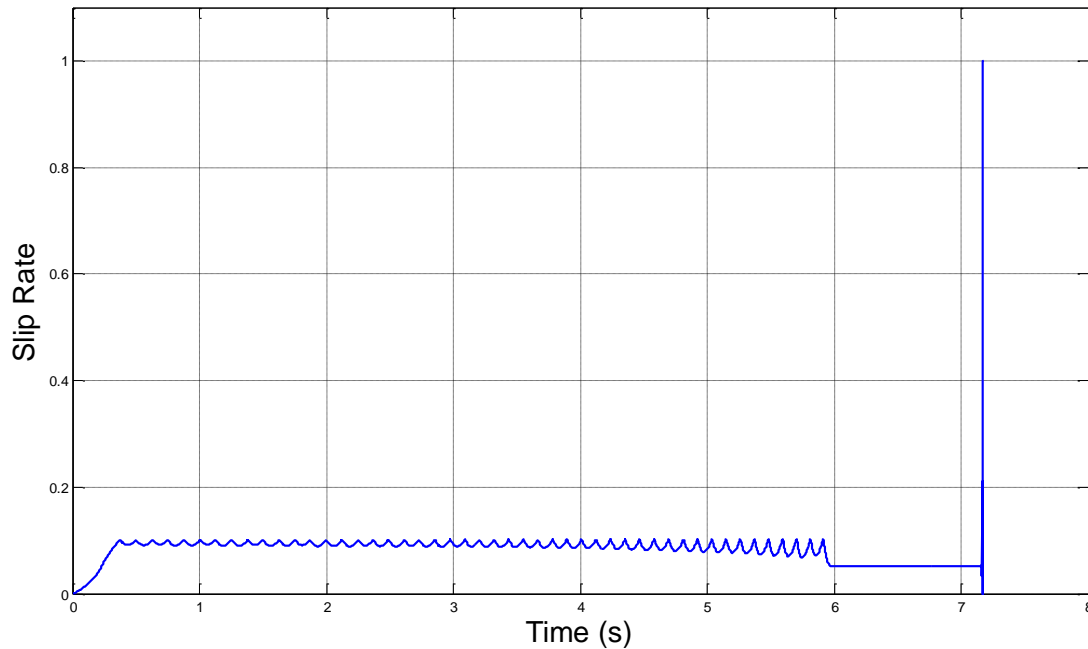


Figure 5.13 Slip rate under logic control with the pressure-holding process

Figure 5.14 shows the result of the braking torque from an initial velocity of 25 m/s until stopping. The ABS brakes 8 times/sec in average, which matches the regular braking control rules. The braking torque is controlled in the range of 360 Nm to 470 Nm, which is more stable than the ABS without the pressure-holding process.

Figure 5.15 shows the result of wheel acceleration from an initial velocity of 25 m/s until stopping. The wheel acceleration changes in the range of  $-30rad / s^2$  to  $+10rad / s^2$ . The change is caused by switching between the three modes of pressure states.

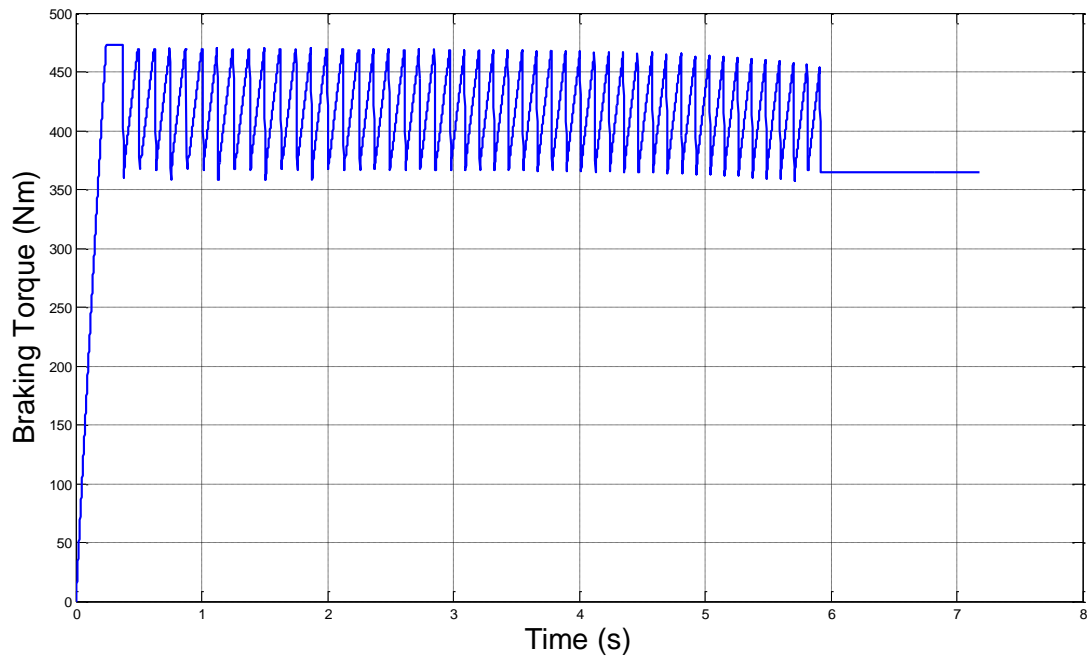


Figure 5.14 Braking torque under logic control with the pressure-holding process

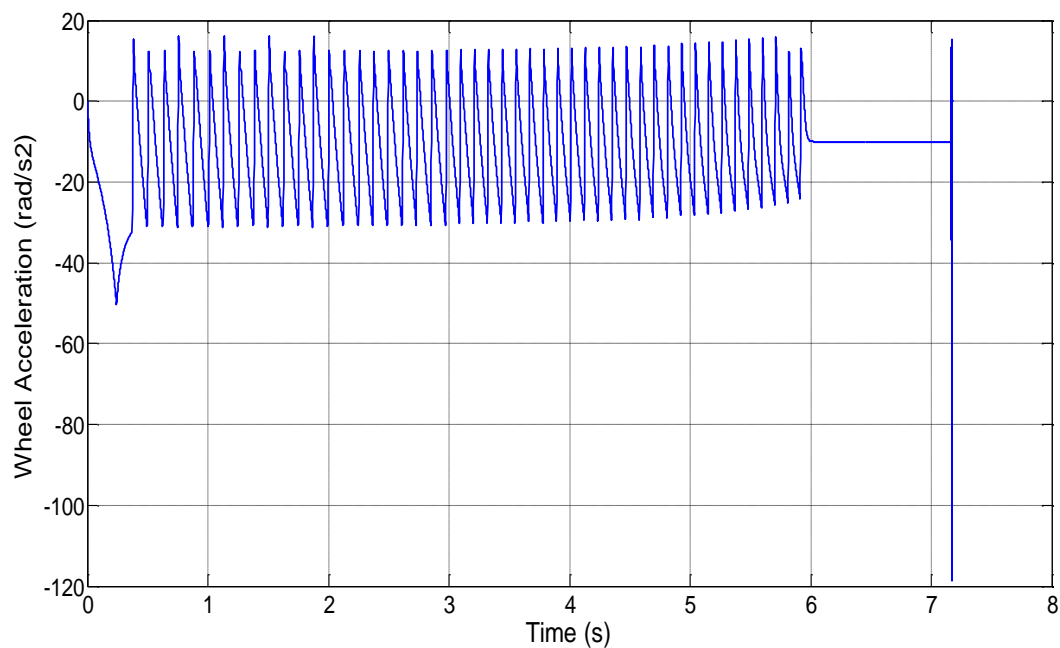


Figure 5.15 Wheel acceleration under logic control with the pressure-holding process

Figure 5.16 shows the ABS action choice based on the Stateflow control result shown in Figure 4.11. The meanings of the outputs are: 0 for pressure-decrease, 1 for

pressure-holding, 2 for pressure-increase, and 3 for step-pressure-increase. The final value is 1, which means when the ABS stops working, and the braking pressure remains stable until the vehicle has stopped.

By using the output values among 0, 1, 2 or 3, the block of the multiport switch as shown in Figure 4.13 switches to pressure-increase, pressure-decrease, pressure-holding or step-pressure-increase branches in order to control the ABS. The output results are shown in Figure 5.16.

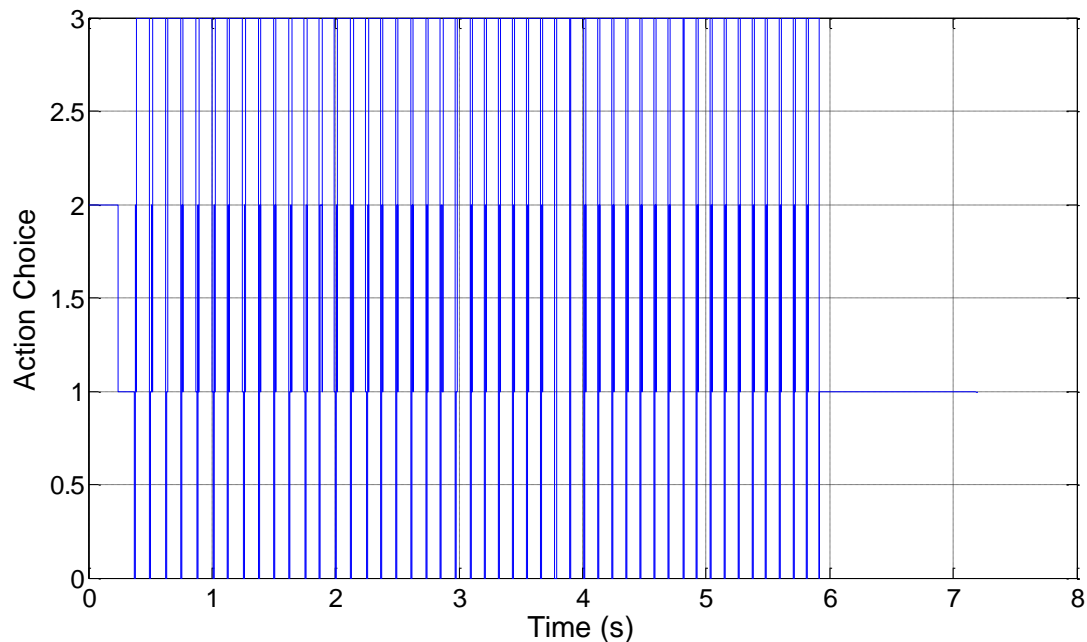


Figure 5.16 Action choice of Stateflow with the pressure-holding process

## 5.4 COMPARISON RESULTS

Based on the contents discussed above, three different control algorithms will be discussed in this chapter. All test results are based on an initial velocity  $v_0 = 25m/s$ , which can also be considered as  $v_0 = 90km/h$  or  $v_0 = 55.92mile/h$ , with initial braking torque  $T_b = 1800Nm$  on a wet asphalt road.

Figure 5.17 shows comparison results of the vehicle velocity from 25 m/s to 0 m/s. The blue solid line of the ABS with the pressure-holding process stops at 7.183s as a result of the ABS beginning to work. The red dashed line of ABS without the pressure-holding process stops at 7.402s since the ABS is similarly beginning to work. The green dotted line without the ABS stops at 9.087s, which is much longer than with ABS.

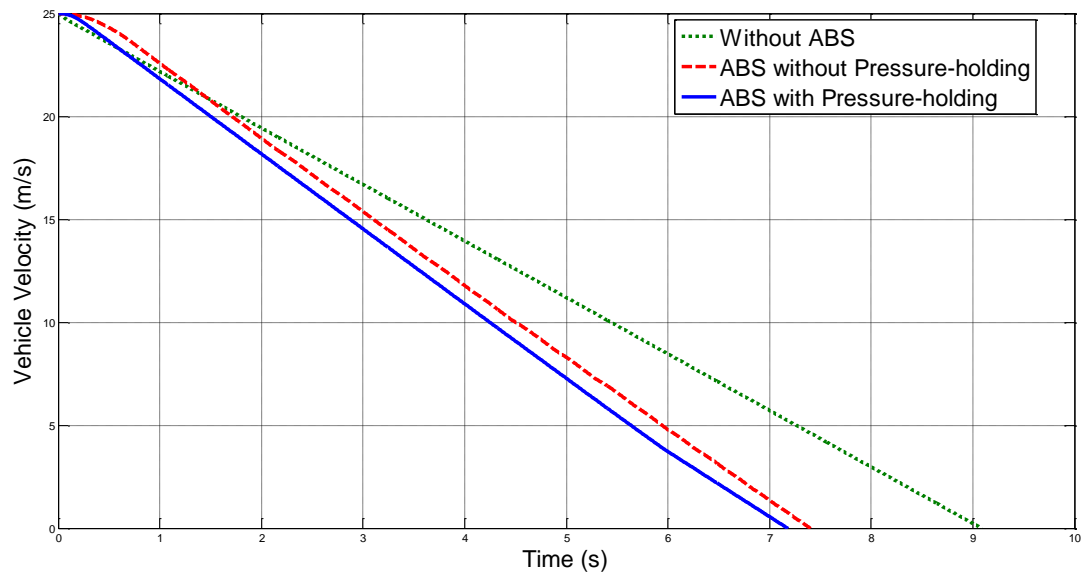


Figure 5.17 Comparison of vehicle velocity

Figure 5.18 shows comparison results of the wheel velocity from 25 m/s to 0 m/s. Without ABS it is easy to see that the wheel starts slipping at 0.137s until the vehicle stops at 9.087s. In contrast, no matter whether the systems of ABS are using the pressure-holding process or not, both show excellent performance during braking. There is no slipping phenomenon throughout the entire braking procedure of the systems using ABS.

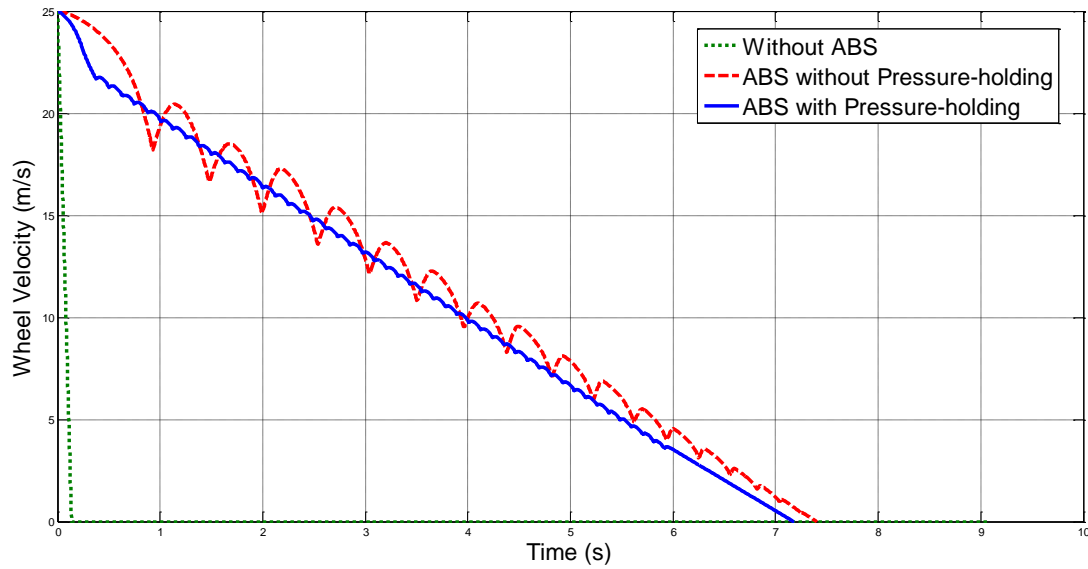


Figure 5.18 Comparison of wheel velocity

Figure 5.19 shows the comparison results of braking distance from the initial velocity of 25 m/s until stopping. The braking distance of ABS with the pressure-holding process is 89.53m from the point at which the ABS begins to work. ABS without the pressure-holding process stops at 95.66m, which is slightly longer. The braking distance of the system without ABS is 113.3m, much longer than the other two.

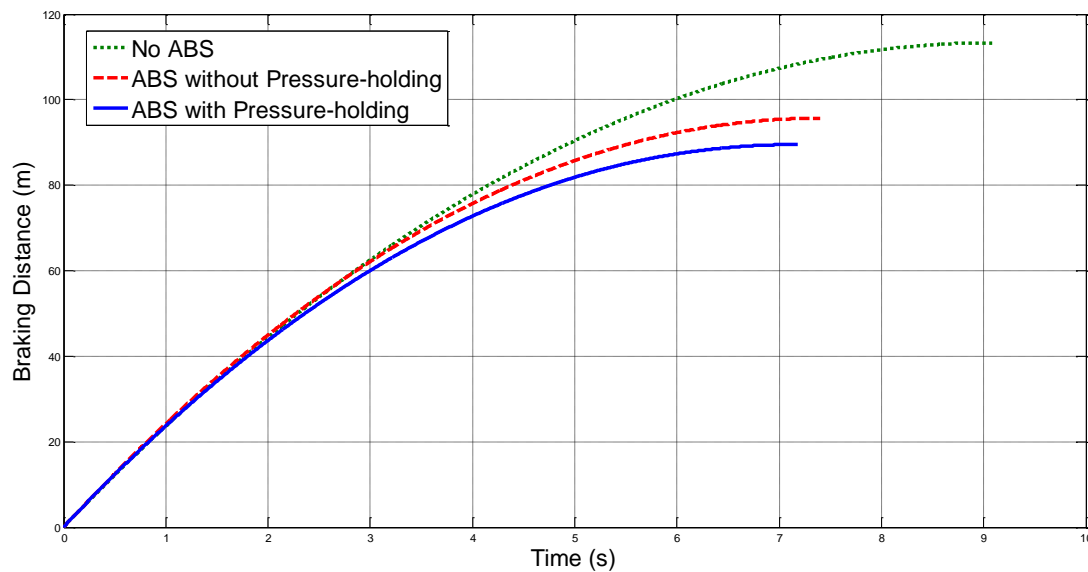


Figure 5.19 Comparison of braking distance

Figure 5.20 shows the comparison results of the slip rate from initial velocity of 25 m/s until stopping. The slip rate of the system without ABS rises rapidly at 0.137s, since this is when the vehicle wheel begins to slip. The performance of the slip rate with the ABS pressure-holding process is more stable than the one without, although both of them have volatility.

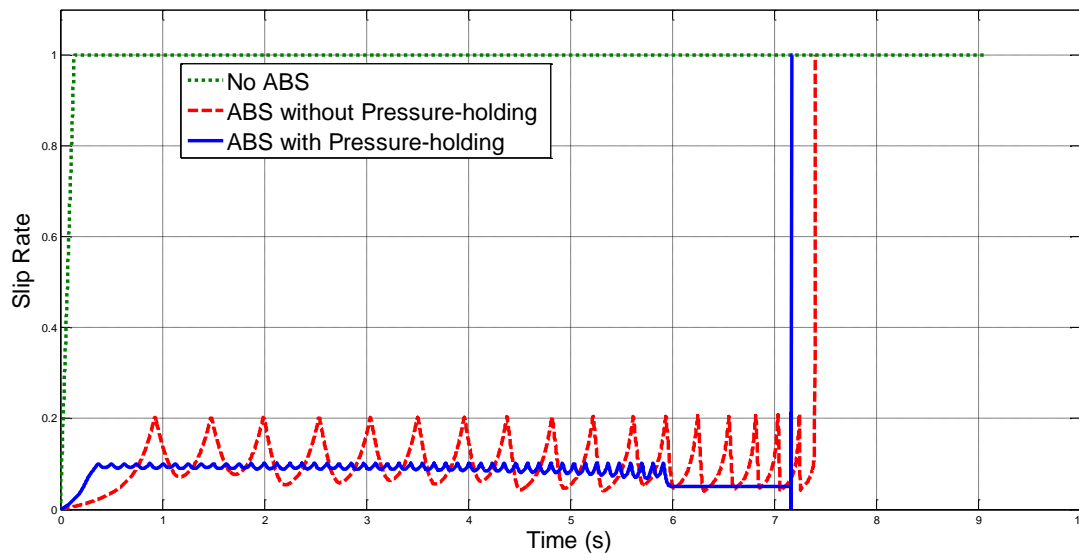


Figure 5.20 Comparison of slip rate

Figure 5.21 shows the comparison results of braking torque from an initial velocity of 25 m/s until stopping. ABS with pressure-holding process shows a better and more stable performance than the one without. The system without ABS maintains the initial braking torque value of 1800Nm through the whole process.

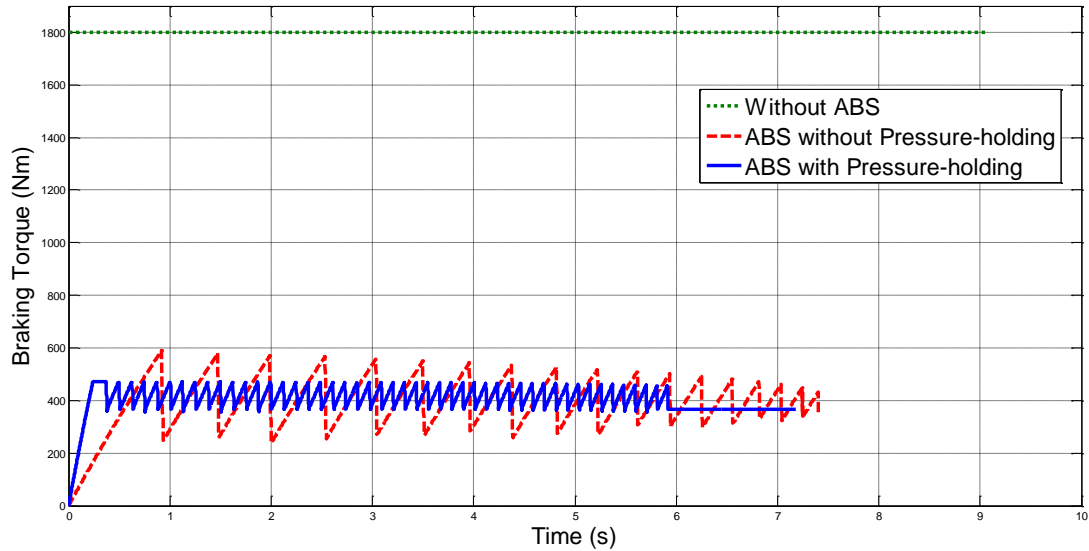


Figure 5.21 Comparison of braking torque

## 5.5 THE SIMULATION RESULTS WITH SPEED SENSOR FAILURE

As discussed in Section 4.4.1, speed sensor failure can be simulated using the Simulink model as shown in Figure 4.12. The switch block can control the condition of whether speed sensor failure occurs or not during the entire braking process. When speed sensor failure occurs, it will send incorrect feedback to the ECU of the vehicle. As a result, the control instructions which are sent to the actuators are also incorrect.

Figures 5.22 to 5.28 show the comparison of the Simulink results of speed sensor failure. The red line refers to the result with speed sensor failure, whilst the blue line refers to normal condition.

Figure 5.22 shows the vehicle velocity differences with regards to speed sensor failure and normal condition. Before 0.5372s, the speed of the sensor failure decreases more rapidly than under normal condition. After this, the situation is reversed. Compared

with normal condition results, the braking time with speed sensor failure increases by 26.84% and stops at 9.111s.

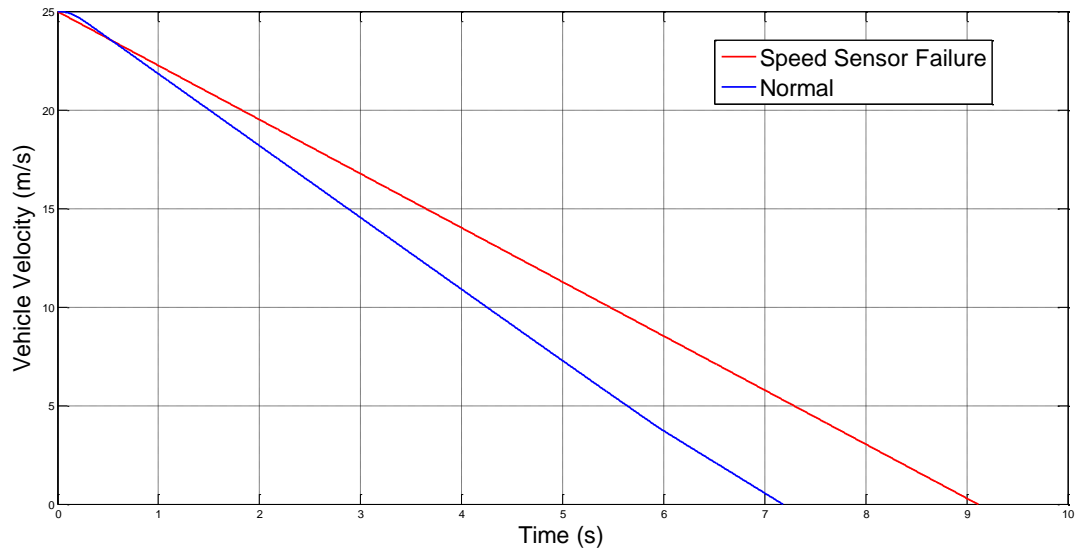


Figure 5.22 Vehicle velocity with speed sensor failure

Figure 5.23 shows the residual of the vehicle velocity with sensor failure. The peak value of 5.292m/s occurs at a time of 7.183s, which is the time point at which vehicle stops under normal condition. Because the speed sensor failure occurs during braking, the vehicle continues moving until stopping at 9.111s.

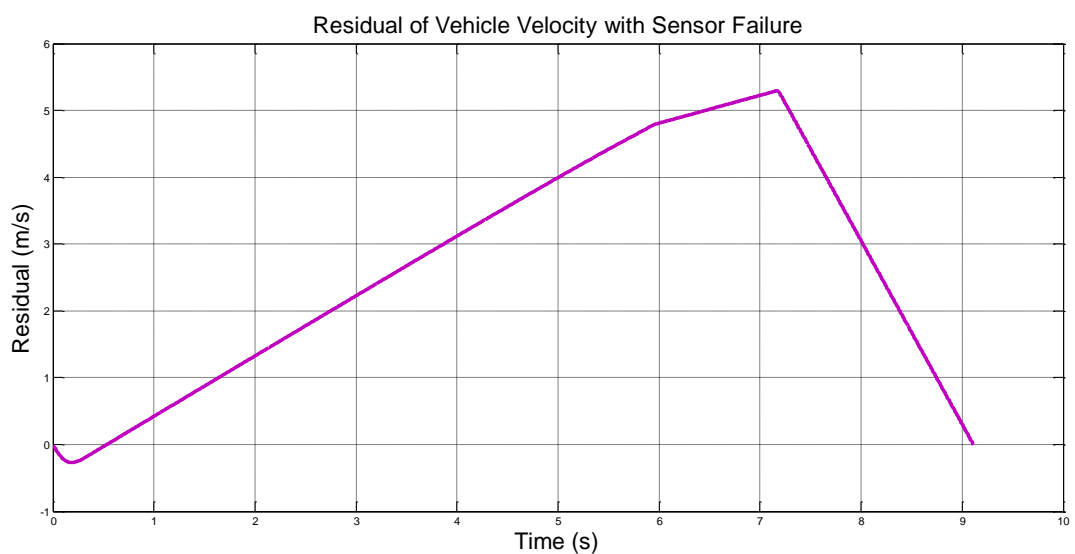


Figure 5.23 Residual of vehicle velocity with speed sensor failure

Figure 5.24 shows the wheel velocity differences between speed sensor failure and normal condition. The wheel velocity in a sensor failure situation remains at 0 during the whole braking process.

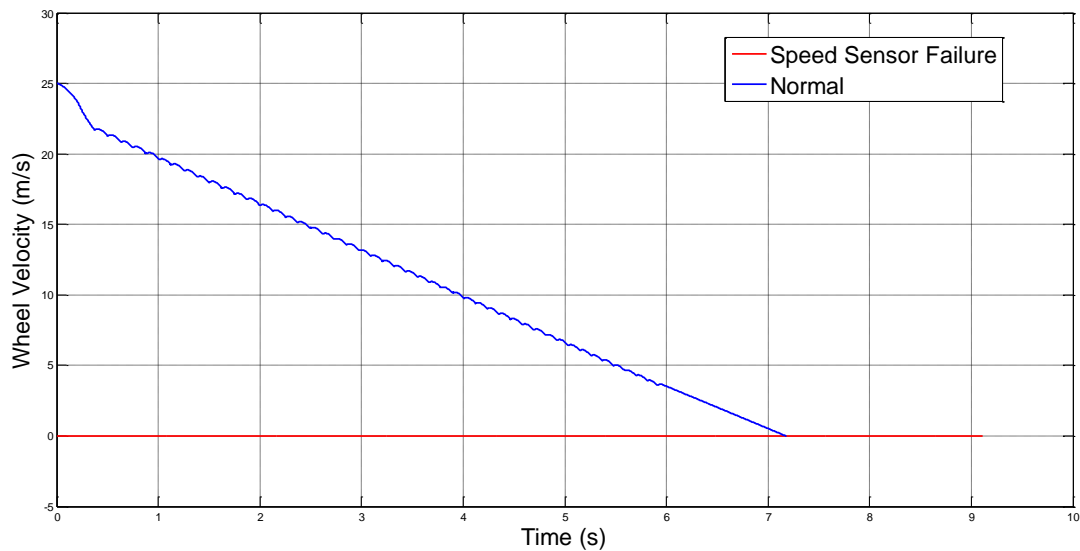


Figure 5.24 Wheel velocity with speed sensor failure

Figure 5.25 shows the residual of the wheel velocity with a speed sensor failure. Because the feedback of the speed sensor to the ECU remains 0, the residual is actually the negative value of wheel velocity under normal condition.

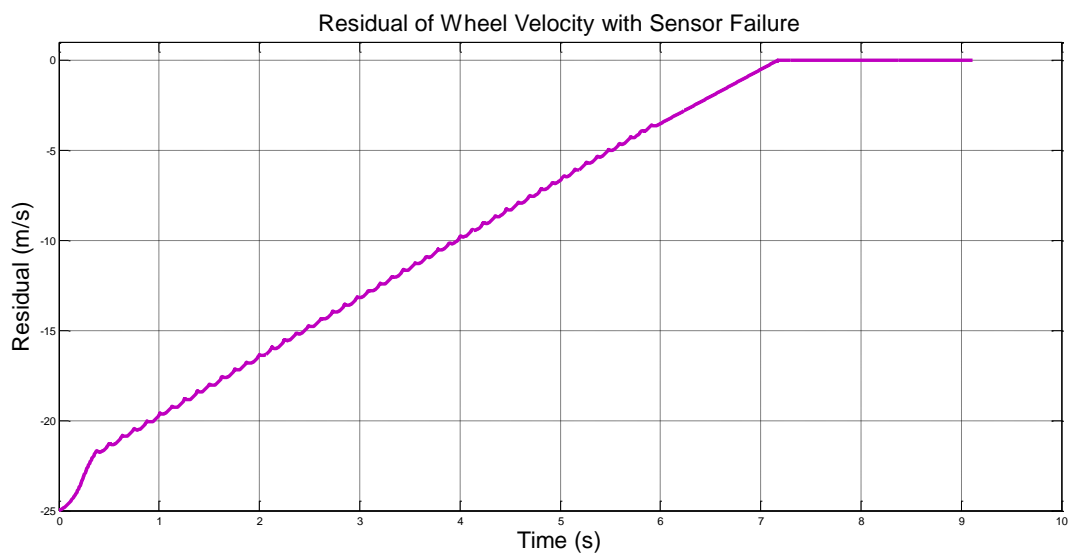


Figure 5.25 Residual of a wheel velocity with speed sensor failure

Figure 5.26 shows the difference in braking distance between speed sensor failure and normal condition. The braking distance increases by 27.22% to 113.897m when compared with a normal condition of 89.53m.

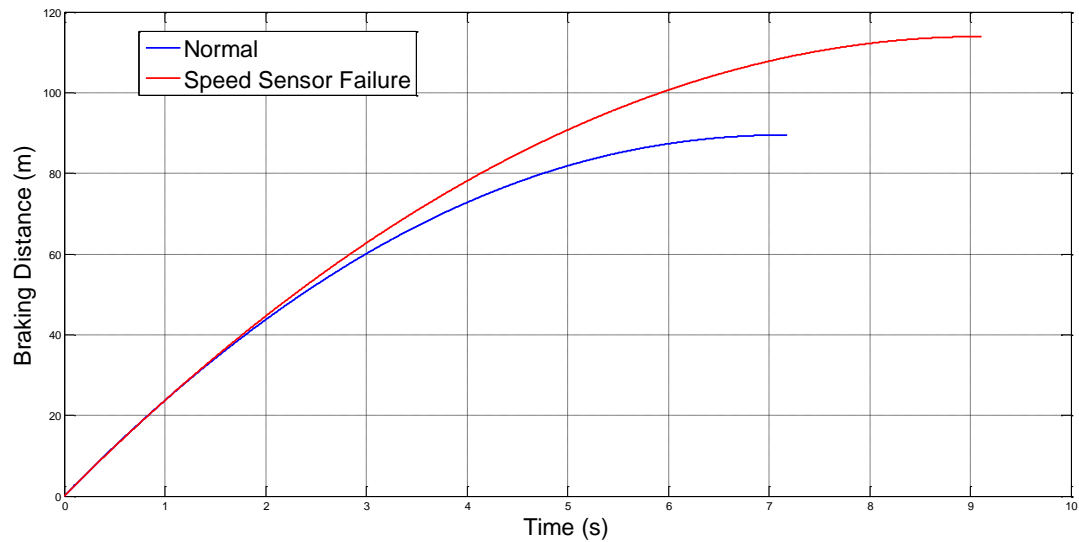


Figure 5.26 Braking distance with speed sensor failure

Figure 5.27 shows the slip rate differences between the speed sensor failure and normal condition. Because the feedback value of the wheel velocity remains at 0 during all of the braking, the ECU determines that the wheel has been locked since the very beginning. The slip rate under the speed sensor failure condition remains at a value of 1 during the entire braking process.

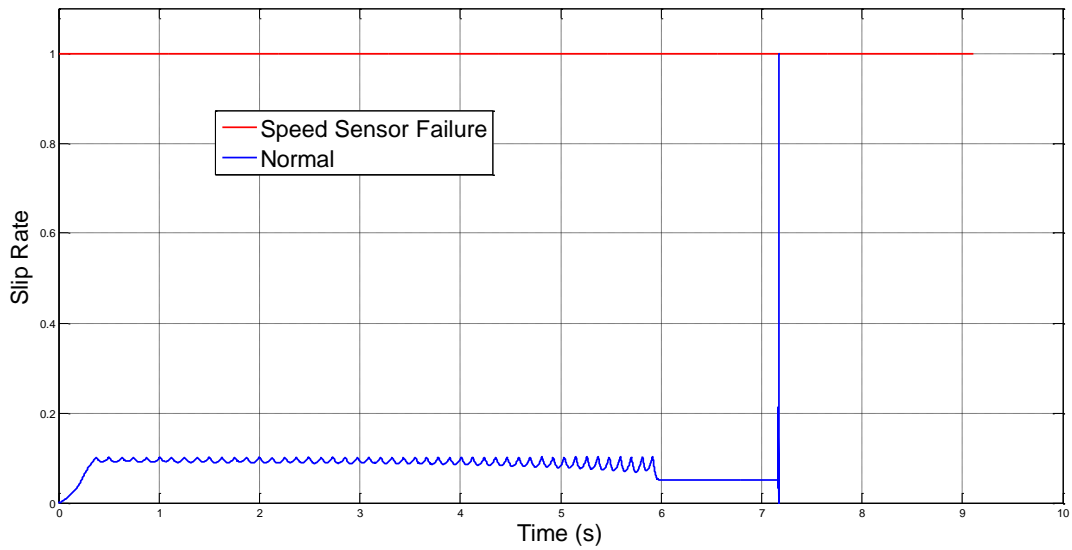


Figure 5.27 Slip rate with speed sensor failure

Figure 5.28 shows the braking torque differences between the speed sensor failure and normal condition. The braking torque with the speed sensor failure rises rapidly until at 1.8s it reaches a peak value of 1800 Nm which is the same as the initial braking torque value. The value of the braking torque remains constant until the vehicle stops.

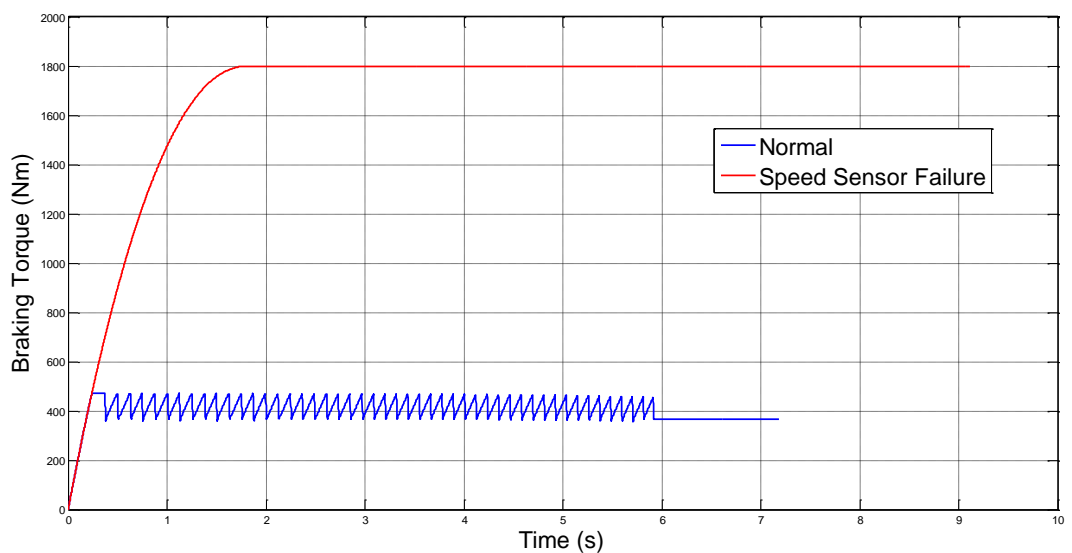


Figure 5.28 Braking torque with speed sensor failure

## 5.6 THE SIMULATION RESULTS WITH SOLENOID VALVE STICKING OR STUCK

As discussed in Section 4.4.2, the solenoid valve stuck condition can be simulated by using the Simulink model as shown in Figure 4.13. The switch block can control the condition as to whether or not the stuck condition occurs during the braking process. When the solenoid valve stuck condition occurs, it will send an incorrect feedback to the ECU of the vehicle. As a result, the control instructions sent to the actuators are similarly incorrect.

Figures 5.29 to 5.35 show the comparison of the Simulink results regarding solenoid valve stuck failure. The red line refers to the result with the solenoid valve stuck fault, whilst the blue line refers to normal condition.

Figure 5.29 shows the vehicle velocity differences between the solenoid valve stuck and normal condition. Before 1.2s, there is no notable difference between these two conditions, which because that the braking oil is not going back to the oil reservoir, but the accumulator of the ABS. The performance of the vehicle velocity is not affected by the valve fault until the spring inside the accumulator compressing to the limitation position. After that, the differences between these two conditions are obvious. The braking time increases by 5.65%, and the vehicle stops at 7.589s.

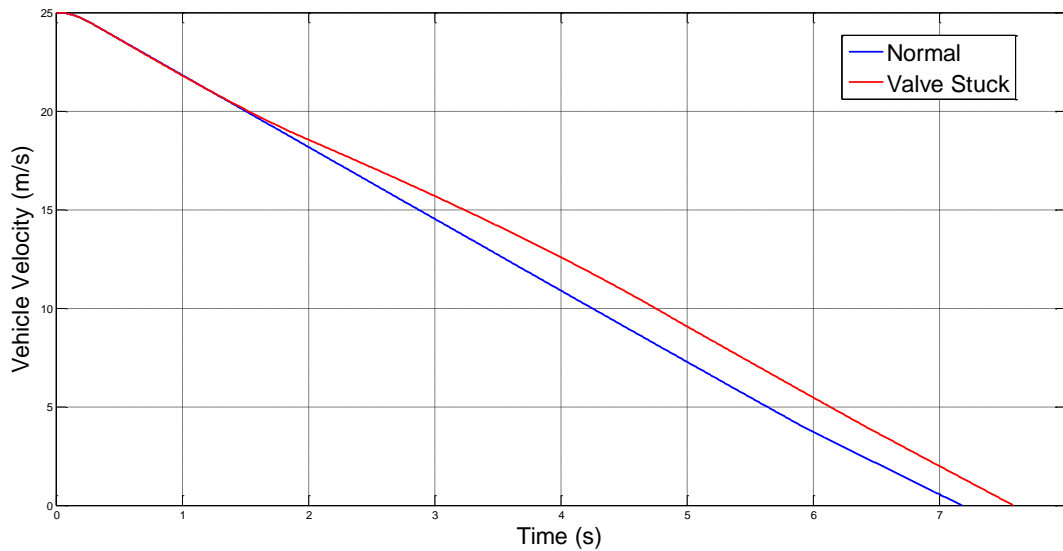


Figure 5.29 Vehicle velocity with valve stuck

Figure 5.30 shows the residual of the vehicle velocity with the solenoid valve stuck. The peak value of 1.82m/s occurs at time of 4.71s. At 7.183s after braking starts, the residual value decreases sharply because the vehicle should stop under normal conditions. Because of the solenoid valve stuck condition which occurs during braking, the vehicle continues moving until stopping at 7.589s. The solenoid valve is sticking, which means that the action of the valve will be delayed. After some time, the valve returns to normal action.

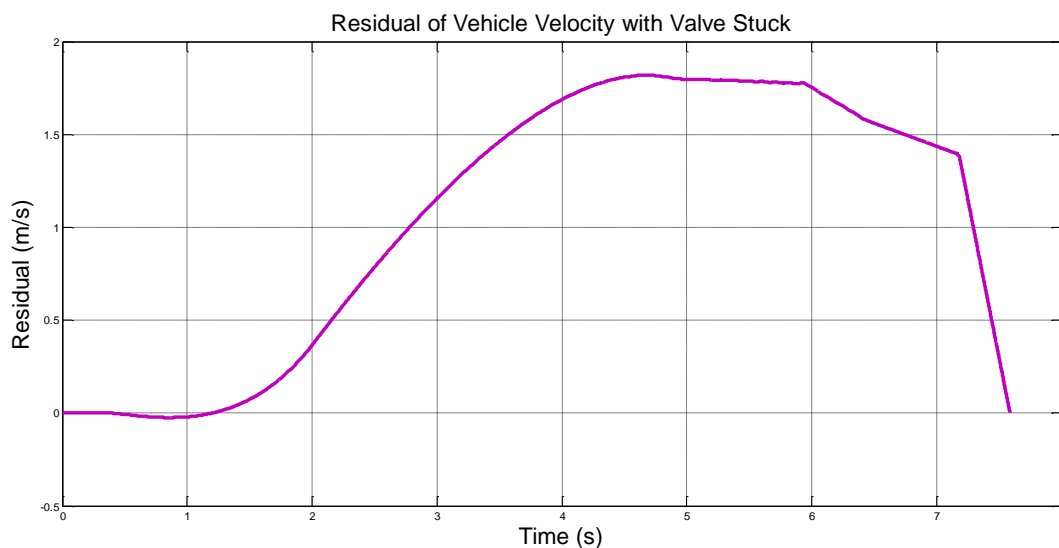


Figure 5.30 Residual of vehicle velocity with valve stuck

Figure 5.31 shows the wheel velocity differences between solenoid valve stuck and normal condition. The wheel velocity in the solenoid valve stuck situation changes significantly during the whole braking process. The wheel shows signs of locking at 2.013s, an unstable region for driving.

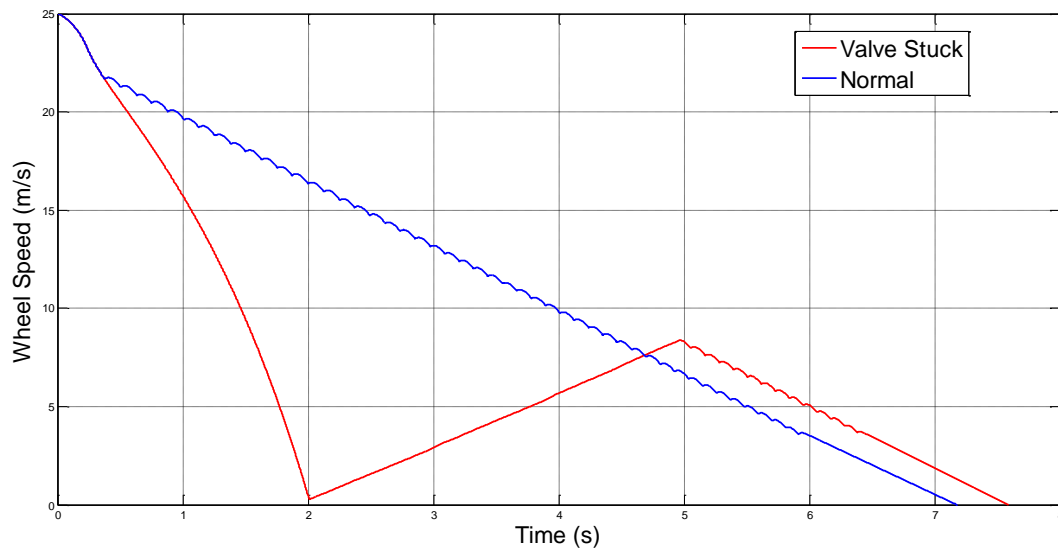


Figure 5.31 Wheel velocity with valve stuck

Figure 5.32 shows the residual of the wheel velocity with the solenoid valve stuck. The peak absolute value occurs at 2.013s, when the wheel is most unstable during the entire braking process.

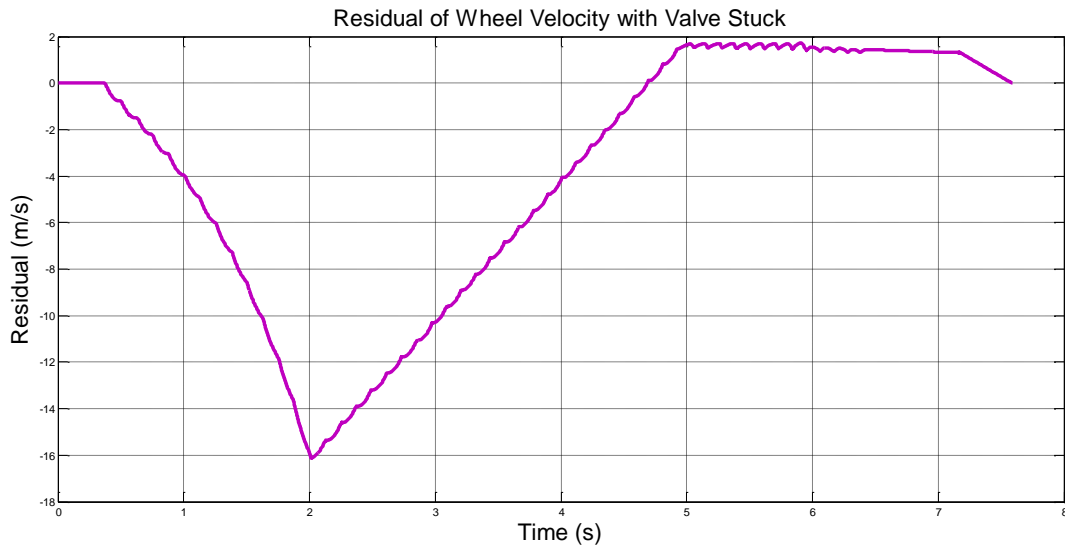


Figure 5.32 Residual of wheel velocity with valve stuck

Figure 5.33 shows the difference in braking distance between solenoid valve sticking or stuck and normal condition. The braking distance increases to 97.53m, 8.94% more than normal stopping condition of 89.53m.

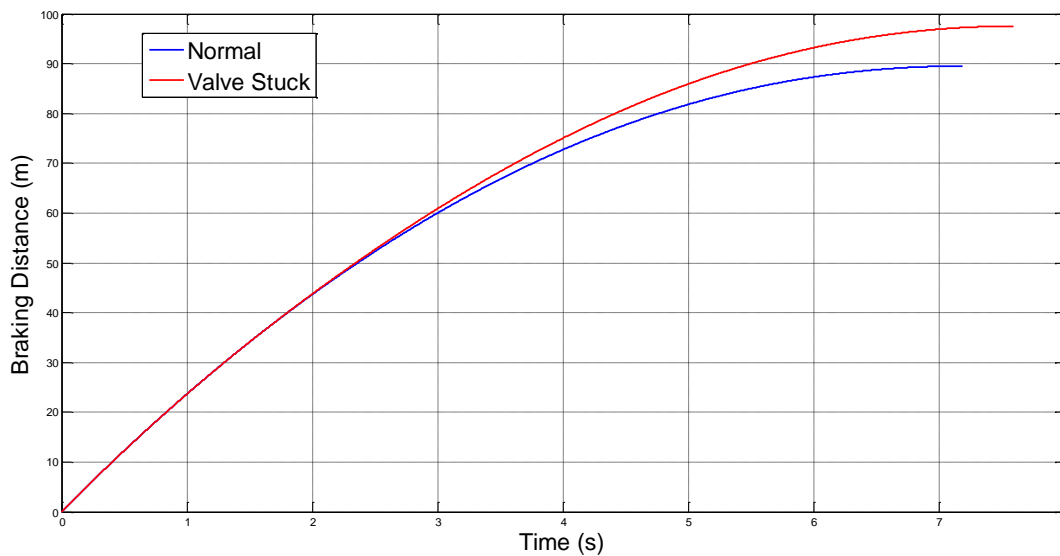


Figure 5.33 Braking distance with valve stuck

Figure 5.34 shows the slip rate differences between the solenoid valve stuck and normal condition. Normally, the optimal slip rate is 0.2, at which point the longitudinal adhesion coefficient reaches its peak value. If the slip rate is in the range

of 0.15 to 0.3 during braking, the vehicle is stable enough to control. Otherwise, wheel locking or some other condition occurs, which will lead to unstable situations during braking.

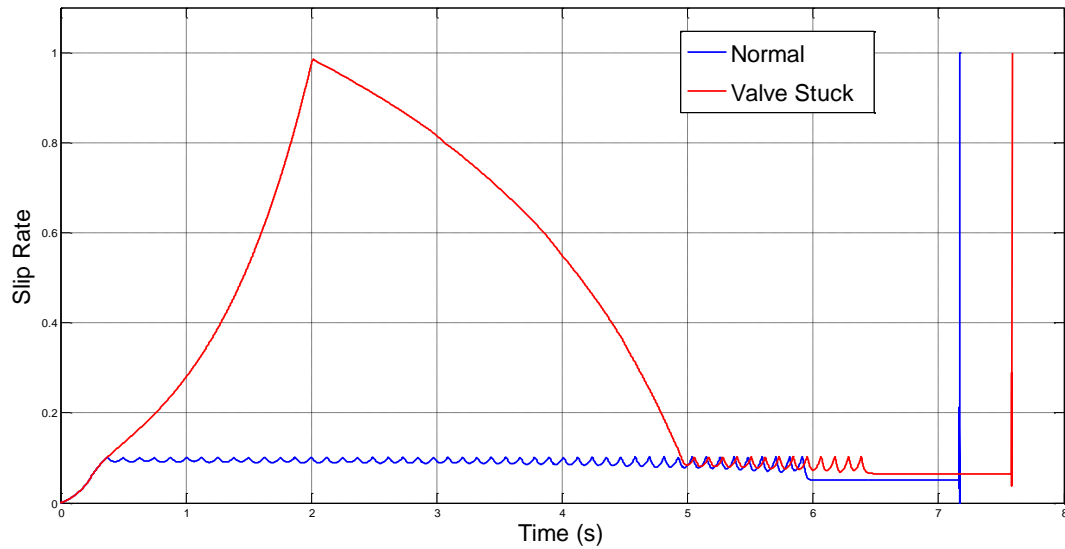


Figure 5.34 Slip rate with valve stuck fault

Figure 5.35 shows the wheel acceleration differences between the solenoid valve stuck and normal condition. The wheel acceleration with the solenoid valve stuck shows a significant difference than from the one under normal condition.

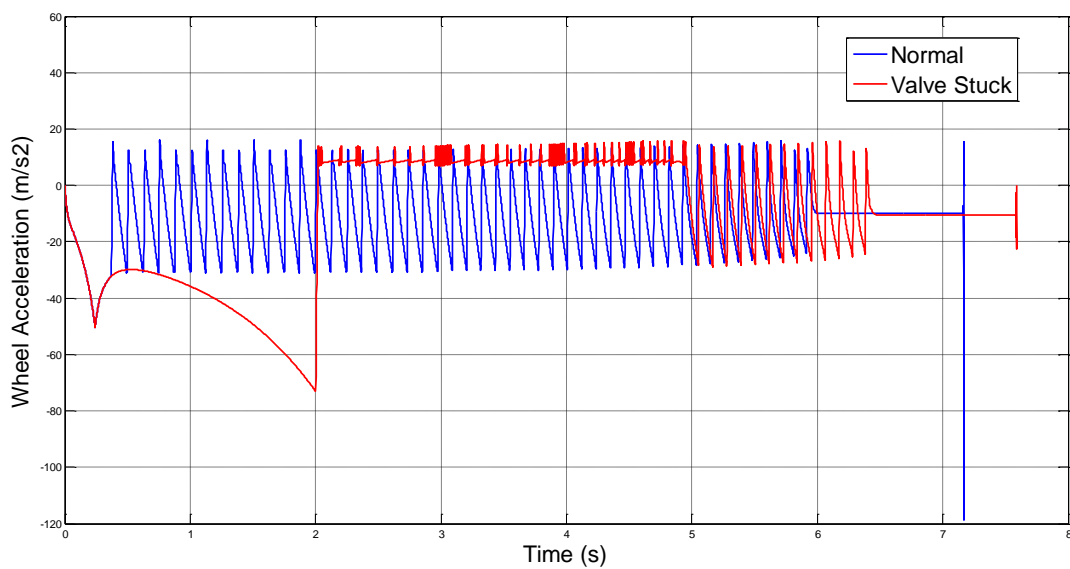


Figure 5.35 Wheel acceleration with valve stuck

## 5.7 THE SIMULATION RESULTS WITH FLUID LEAKAGE

As discussed in Section 4.4.3, a fluid leakage fault can be simulated using the Simulink model shown in Figure 4.14. The switch blocks can control the condition of whether fluid leakage occurs during the entire braking process. It is not only the pressure-decrease module which contains a fluid leakage switch; they can also be found in the pressure-increase module and the pressure-step-increase module. By using these three switches, the fluid leakage fault can be simulated during the whole braking procedure. When fluid leakage occurs, it will send incorrect feedback to the ECU of the vehicle. As a result of this, the control instructions sent to the actuators are incorrect as well.

Figures 5.36 to 5.41 show the comparison Simulink results of fluid leakage. The red line refers to the result with a speed sensor failure, whilst the blue line refers to normal condition.

Figure 5.36 shows the vehicle velocity differences between the fluid leakage fault and normal condition. The braking time increases by 1.38%, and the vehicle stops at 7.282s. The wheel locks at 6.545s and the vehicle slips until it stops at 7.282s. Although the difference between the conditions of both leakage and the normal is not significant from Figure 5.36, the uncertainty or error from the model is much smaller than typical value of the residual in this case. If the leakage amount is larger than the one as shown in Figure 4.14 (Chapter Four), then the performance will be even worse.

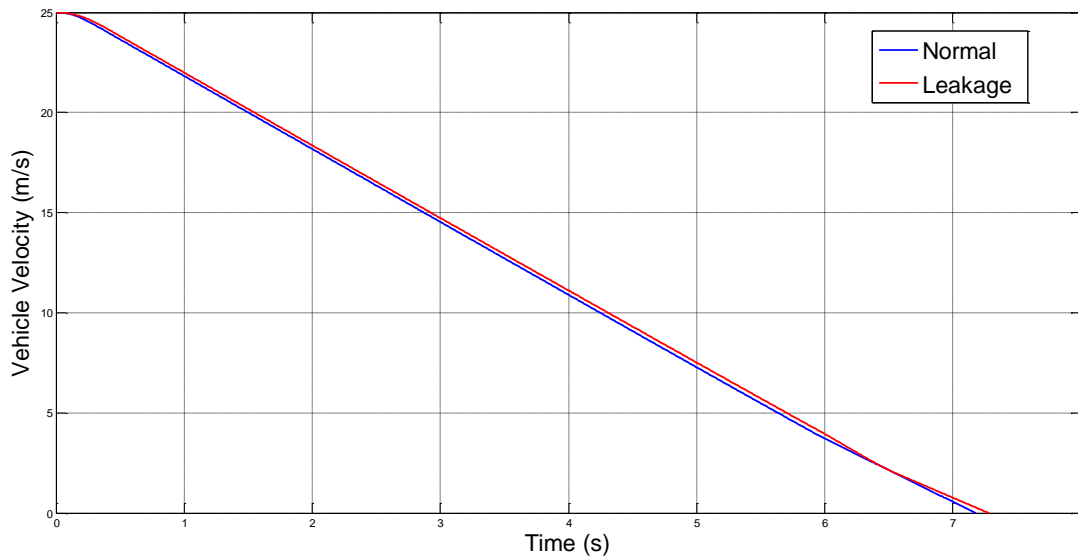


Figure 5.36 Vehicle velocity with fluid leakage

Figure 5.37 shows the residual of the vehicle velocity with fluid leakage. There is a significant decrease after 6s. The trough value of 0.005m/s occurs at time of 6.545s, as this is when the wheel is locked and begins to slip, as seen in Figure 5.37. During the slipping period, the braking control is not stable.

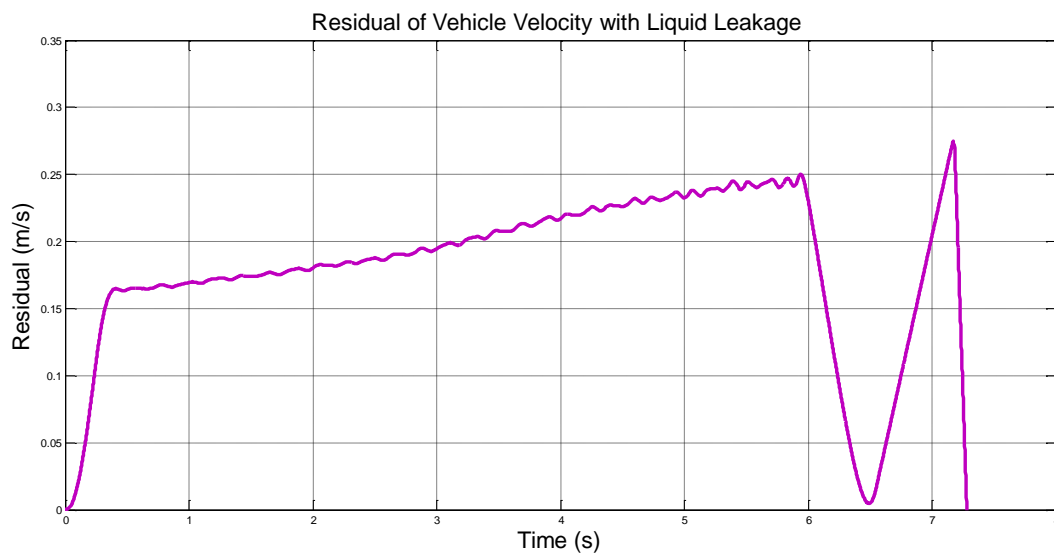


Figure 5.37 Residual of the vehicle velocity with fluid leakage

Figure 5.38 shows the wheel velocity differences between the fluid leakage fault and normal condition. The wheel velocity in the fluid leakage situation shows a completely different performance from approximately 6s after the braking starts. At

6.545s, the wheel is locked and starts slipping.

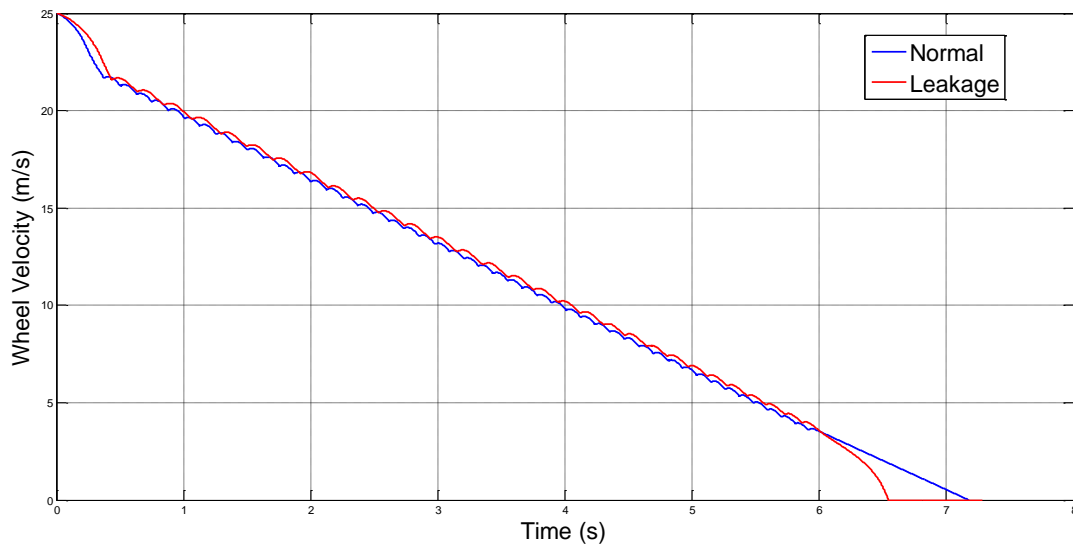


Figure 5.38 Wheel velocity with fluid leakage

Figure 5.39 shows the residual of the wheel velocity with a fluid leakage fault. The largest absolute residual occurs at 6.545s with a value of 1.9 m/s, which is also the time the wheel starts slipping. If the leakage is worse, the wheel lockup happens earlier and last for a longer time.

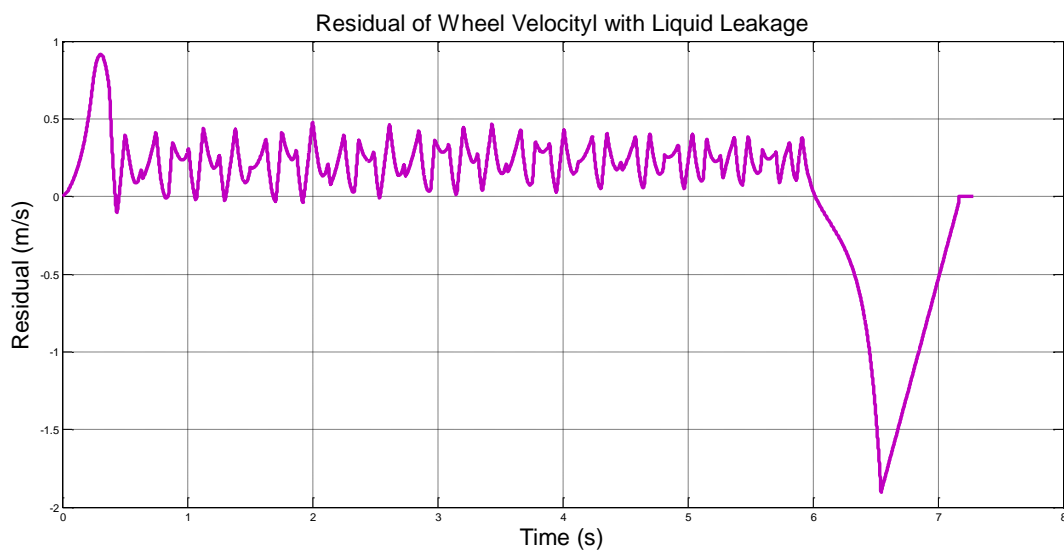


Figure 5.39 Residual of wheel velocity with fluid leakage

Figure 5.40 shows the difference in braking distance between the fluid leakage fault

and the normal condition. The braking distance increases by 1.5% more than the normal condition of 89.53m, to 90.85m.

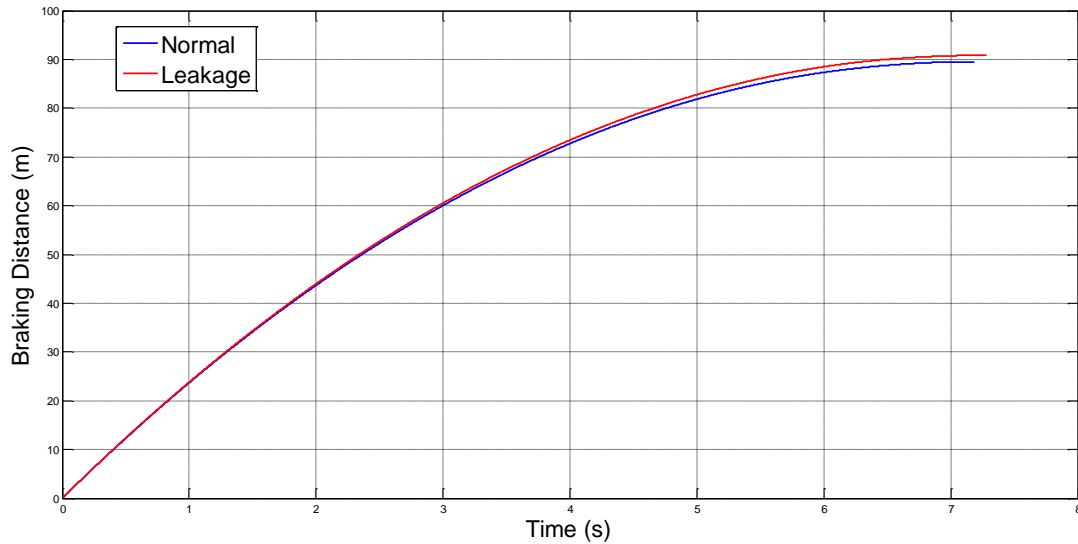


Figure 5.40 Braking distance with fluid leakage

Figure 5.41 shows the slip rate differences between the fluid leakage fault and normal condition. After 6s of braking, the slip rate result shows unstable characteristics of the wheel. The slip rate under the fluid leakage condition remains at a value of 1 from 6.545s until stopping at 7.282s.

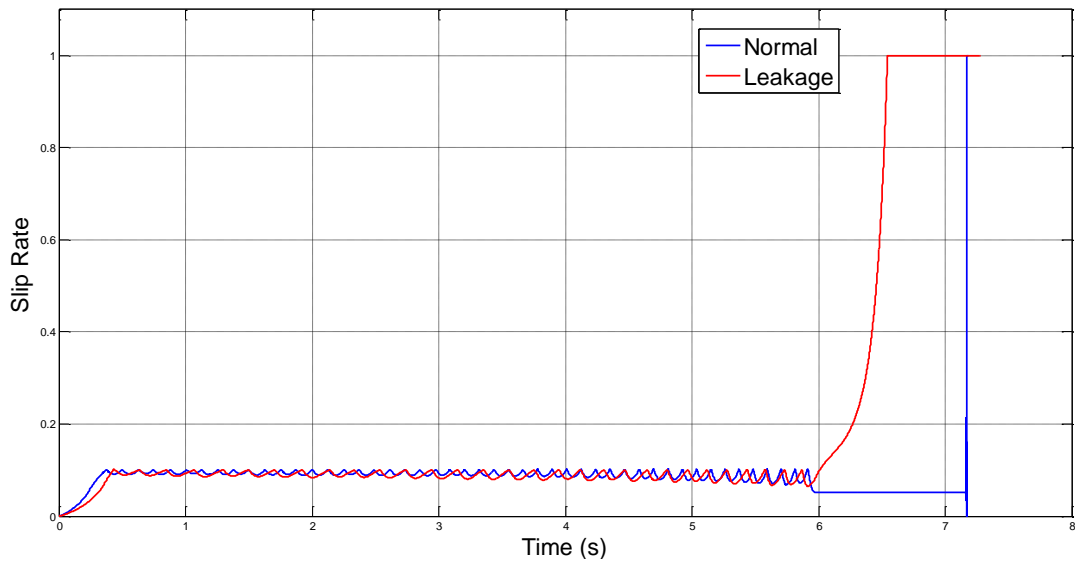


Figure 5.41 Slip rate with fluid leakage

Figure 5.42 shows the braking torque differences between the fluid leakage fault and normal condition. The braking torque with the fluid leakage fault shows a lack of performance when compared with the normal one, potentially leading to a longer braking time.

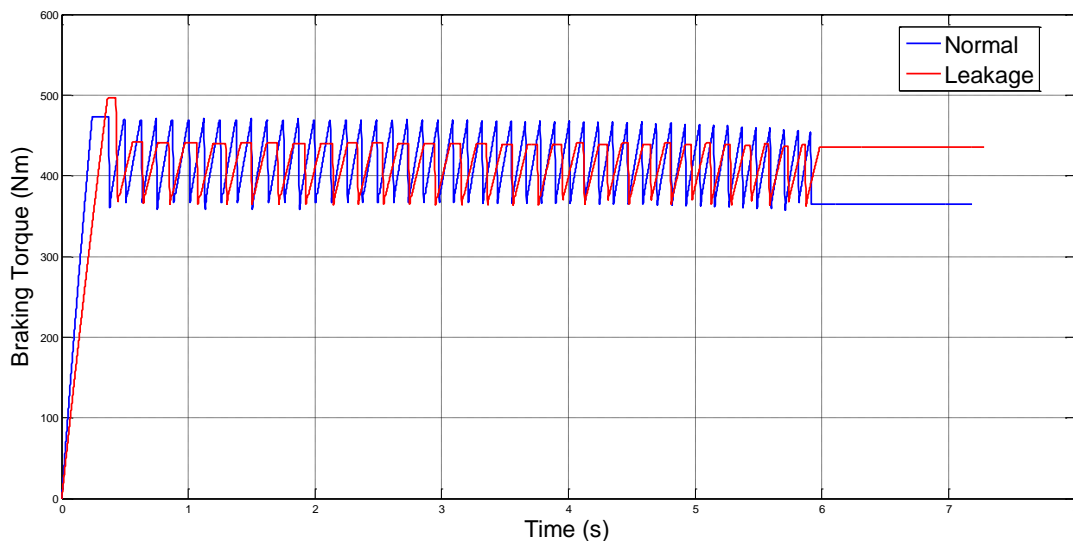


Figure 5.42 Braking torque with fluid leakage

Figure 5.43 shows the wheel acceleration differences between fluid leakage and normal condition. The wheel acceleration with fluid leakage shows a trough at 6.545s, which is the time at which the wheel is locked and starts slipping.

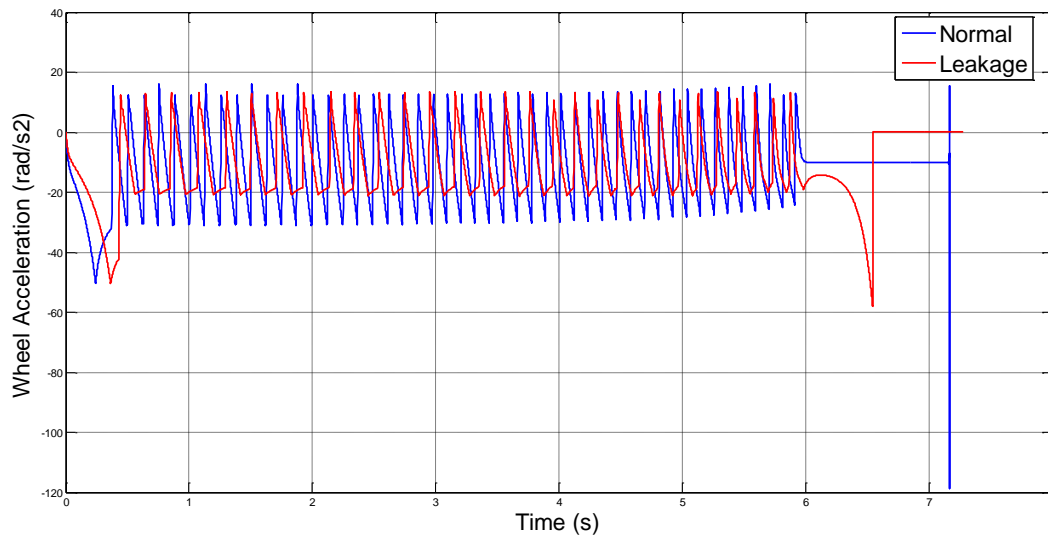


Figure 5.43 Wheel acceleration with fluid leakage

## 5.8 THE SIMULATION RESULTS WITH PUMP EFFICIENCY LOSS

As discussed in Section 4.4.4, the pump efficiency loss fault can be simulated using the Simulink model shown in Figure 4.15. The switch blocks can control the condition and select whether pump efficiency loss occurs or not during the braking process. By changing the parameters of the control block, the efficiency loss can be changed as required. When pump efficiency loss occurs, it will send an incorrect feedback to ECU of the vehicle. This means that, the control instructions sent to the actuators are incorrect as well.

Figures 5.44 to 5.51 show the comparative Simulink results of pump efficiency loss. The red line refers to the result with the speed sensor failure, whilst the blue line refers to normal condition. Both stopping time and braking distance are increased as a result of pump efficiency loss.

Figure 5.44 shows the vehicle velocity differences between the pump efficiency loss

fault and normal condition. The braking time increases by 4.6%, stopping at 7.467s. Although the braking time does not increase greatly, other characteristics show that the pump efficiency loss also increases the risk of a traffic accident during braking.

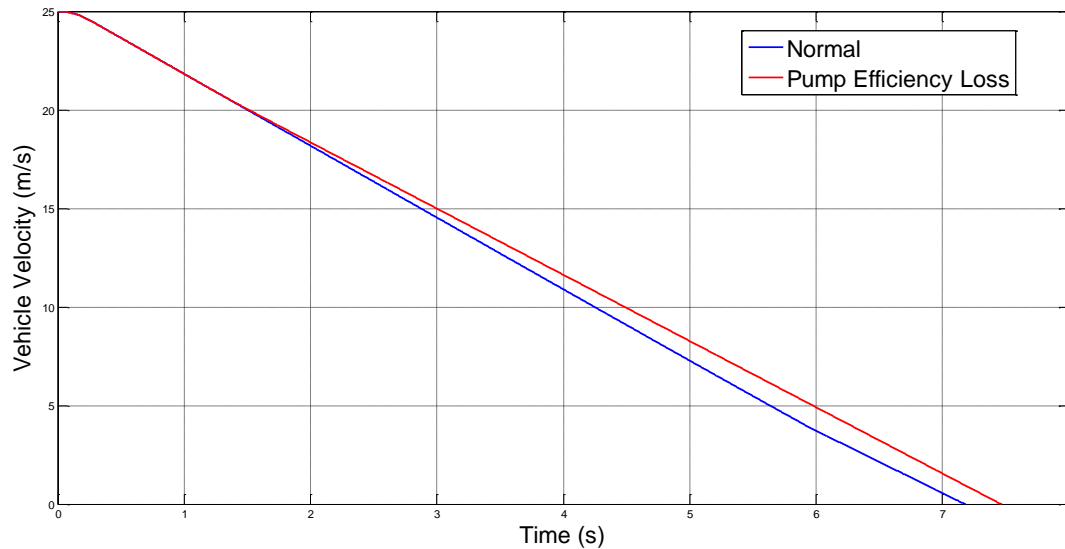


Figure 5.44 Vehicle velocity with pump efficiency loss

Figure 5.45 shows the residual of vehicle velocity with pump efficiency loss. The residual increases from 1.233s because the ABS stops working since then. Due to pump efficiency loss occurring during braking, the vehicle continues to move until stopping at 7.467s. The pump efficiency loss does not show a significant difference at the beginning of braking, but will show up as time passes.

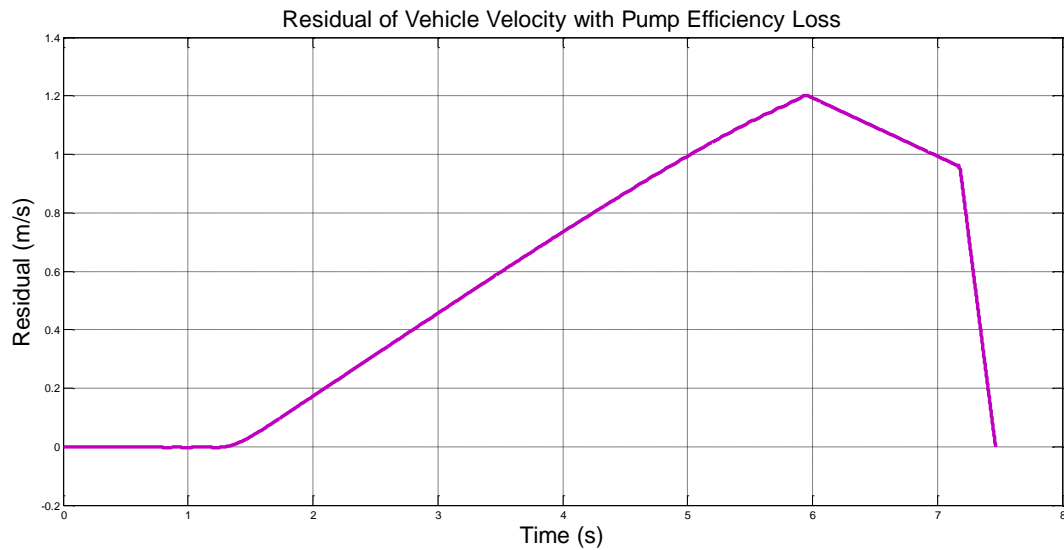


Figure 5.45 Residual of vehicle velocity with pump efficiency loss

Figure 5.46 shows the wheel velocity differences between pump efficiency loss and normal condition. The wheel velocity in the pump efficiency loss condition does not fluctuate as regularly as the normal condition. Since the ABS stops working at 1.233s, the performance of wheel velocity shows a similar performance to the one without ABS discussed in Section 4.1.4. The ABS stops working during braking process with fault of pump efficiency loss because the pressure-decreasing stage cannot be completed, whilst the next stage of pressure-increasing cannot starts working of the whole ABS working cycle.

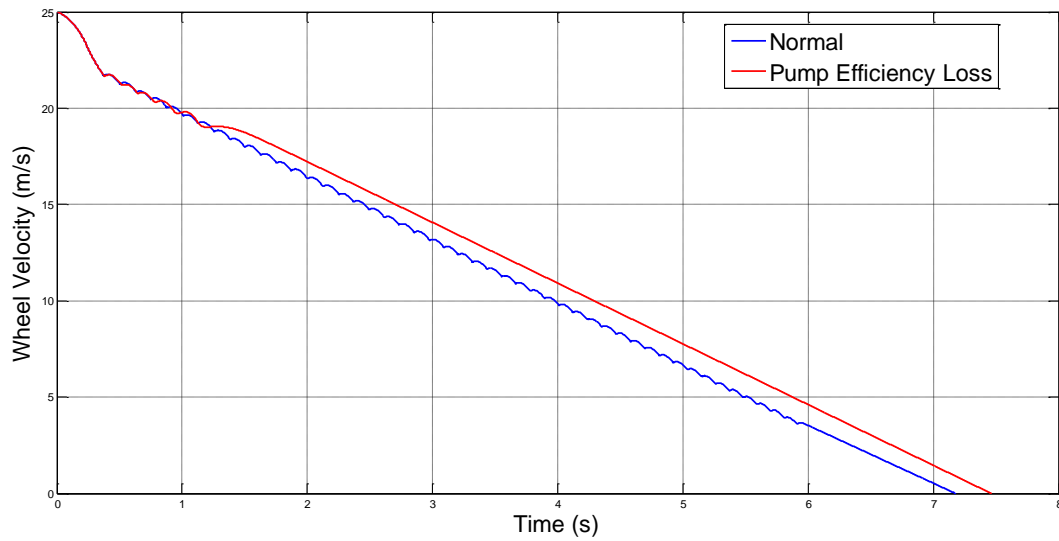


Figure 5.46 Wheel velocity with pump efficiency loss

Figure 5.47 shows the residual of the wheel velocity with a pump efficiency loss fault. The residual increases significantly from 1.233s, when the ABS stops working. After the wheel stops under normal conditions at 7.138s, the residual decreases sharply until 7.467s.

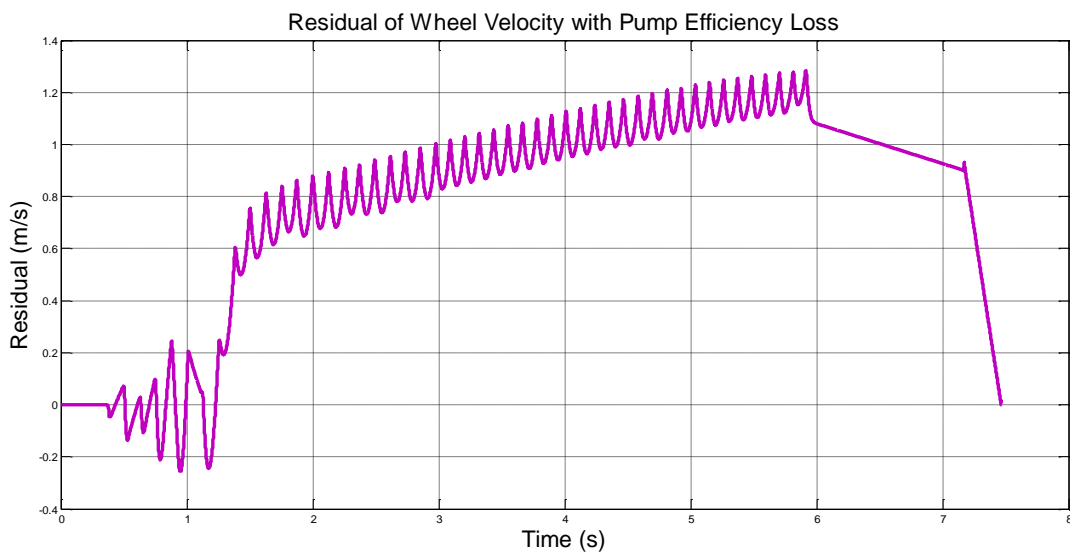


Figure 5.47 Residual of wheel velocity with pump efficiency loss

Figure 5.48 shows the difference in braking distance between the pump efficiency loss and normal condition. The braking distance increases by 4.9% to 93.87m rather than the normal condition of 89.53m.

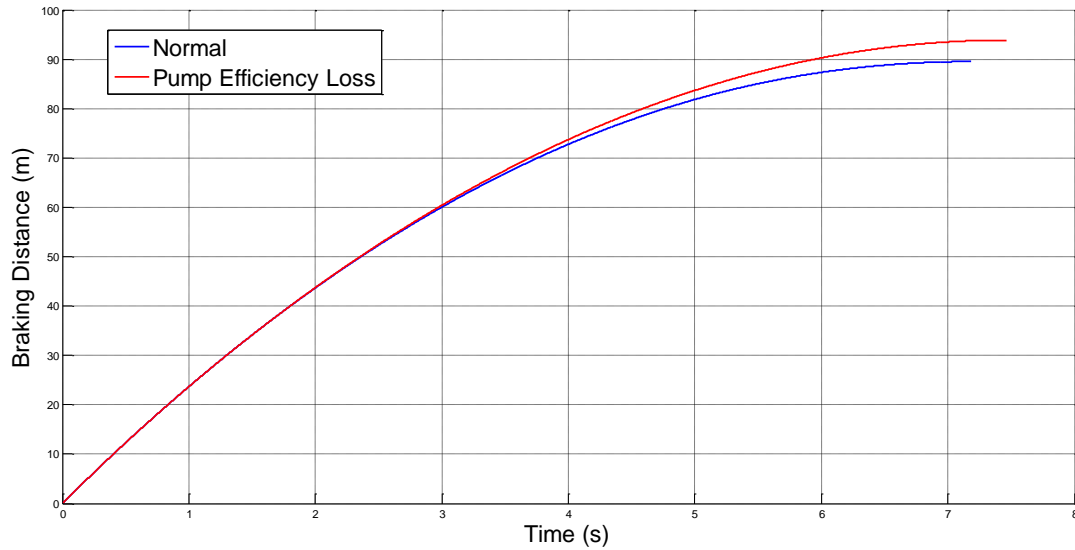


Figure 5.48 Braking distance with pump efficiency loss

Figure 5.49 shows the slip rate differences between pump efficiency loss and normal condition. The slip rate with the pump efficiency loss remains at a constant level from 1.233s until the end, which shows no signs of the ABS working.

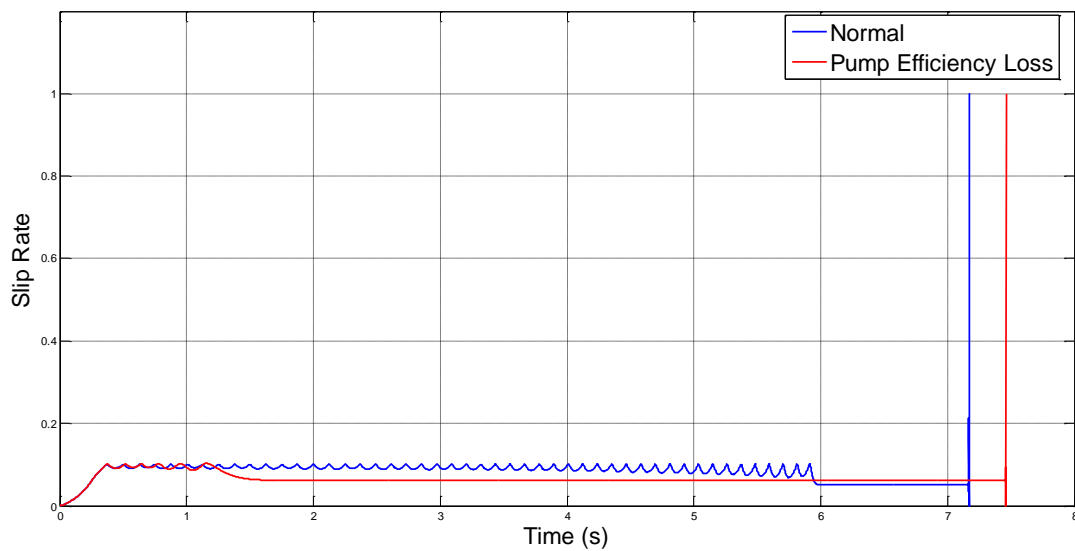


Figure 5.49 Slip rate with pump efficiency loss

Figure 5.50 shows the braking torque differences between the pump efficiency loss and normal condition. At 1.233s the ABS stops working and, from then on, the

pressure maintains a constant level of 387.7 Nm until stopping.

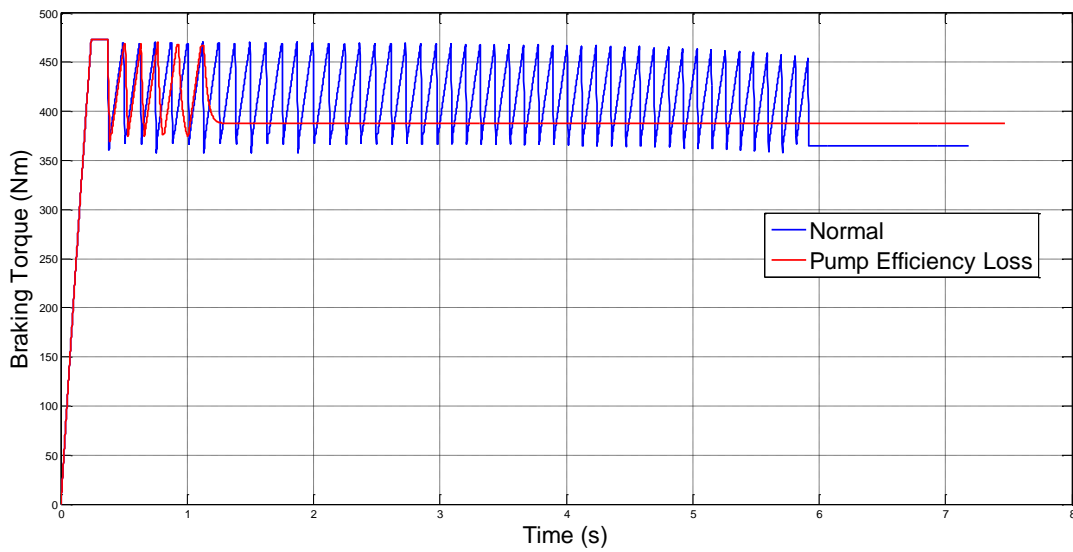


Figure 5.50 Braking torque with pump efficiency loss

Figure 5.51 shows the wheel acceleration differences between pump efficiency loss and normal condition. The wheel acceleration with pump efficiency loss shows a constant value since the ABS stops at 1.233s.

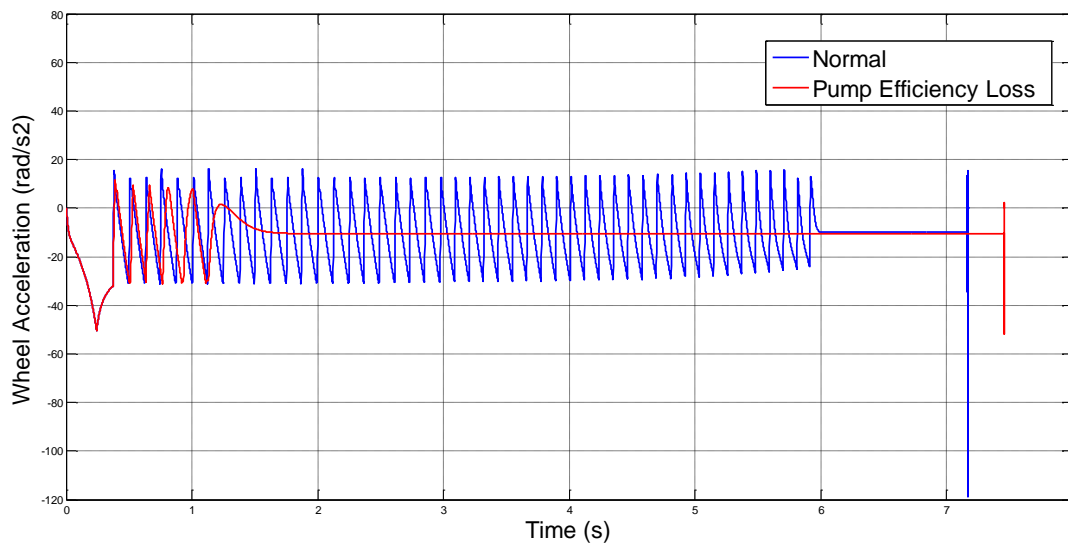


Figure 5.51 Wheel acceleration with pump efficiency loss

## 5.9 SUMMARY

This chapter showed the simulation results of both ABS without pressure-holding process and ABS with pressure-holding process. The comparison results of above two status, together with the results of braking system without ABS as discussed in last chapter, showed a better performance of the system with ABS in not only shorter the braking time and distance, but also more stable in slip rate and braking torque performance. After describes the simulation results under healthy condition, the results of ABS system under faulty conditions were carried out. The simulation results under four different faults of wheel speed sensor failure, solenoid valve sticking or stuck, fluid leakage and pump efficiency loss were discussed in wheel velocity and vehicle velocity, braking distance, slip rate and braking torque. No matter which type of fault existed in the ABS system, the braking time and distance were longer than normal condition; the slip rate and braking torque are not as stable as that under normal condition. The results showed that it would be not safe and stable to control the vehicle during emergency braking process if some faults existing in the ABS system.

---

## CHAPTER SIX

# TEST RIG DEVELOPMENT OF THE ANTI-LOCK BRAKING SYSTEM

---

**In order to validate the developed theoretical model, an Anti-lock Braking System test rig has been developed. Within this test rig, an autonomous control strategy based on dSpace MicroAutoBox II is developed and applied. A data acquisition device based on NI Labview is used for braking signal displacement. The motion of an ABS system can be monitored using a model-based approach.**

## **6.1 THE OBJECTIVES OF THE TEST RIG**

In order to carry out condition monitoring of an Anti-lock Braking System, a real system is necessary. The first objective is to design a system which enables implementation of the model-based approach on an indoor ABS system. In order to demonstrate as many industrial fields as possible, the system is designed out to be a typical ABS system which is ideally similar to most vehicle braking applications.

The second objective is to induce ABS faults for monitoring in the ABS test rig. The induced faults should have the following features [13]. Firstly, they should be selected from those that commonly occur in a typical ABS system. Secondly, the fault induction should not cause any damage to the ABS system; otherwise, the test rig either cannot be used for long or will have to be repaired from time to time. Thirdly, in order to investigate the fault performance, the induced faults should be arbitrarily repeatable. Finally, it should be possible to run the ABS test rig in both healthy and faulty conditions.

The third objective is to provide a visual interface for implementation of a model-based fault diagnosis approach [13]. This relates to software development in simulation, comparison and panel display. This may be implemented either locally for a local model-based approach or remotely for a remote model-based approach [13] [26].

## **6.2 DSPACE MICROAUTOBOX II**

The dSpace MicroAutoBox II is a real-time system for performing fast function prototyping in fullpass and bypass scenarios. It operates without user intervention, just like an ECU. MicroAutoBox II can be used for many different rapid control

prototyping (RCP) applications. The benefit of the MicroAutoBox II hardware is its unique combination of high performance, comprehensive automotive I/O, and an extremely compact and robust design.

The equipment type chosen for this project is dSpace MicroAutoBox II 1401/1505/1507. It concentrates on the bus and bypass interfaces, making it a very cost-effective solution. It contains 16 MB of main memory, 4 MB of memory exclusively for communication between the MicroAutoBox II and PC/notebook, and 16 MB of nonvolatile flash memory containing a code section and flight recorder data. Figures 6.1 to 6.3 show the appearance of the MicroAutoBox II.



Figure 6.1 Top view of dSpace MicroAutoBox II



Figure 6.2 dSpace MicroAutoBox II I/O connector



Figure 6.3 dSpace MicroAutoBox II I/O connector with hub

## 6.3 THE DESIGN OF THE ABS TEST RIG

### 6.3.1 The Overall Design

The ABS test rig is the monitoring and control system and consists of a computer, electric motors, magnetic powder clutch, reducer, anti-lock braking systems, test rig connection system including bearings, shafts, couplings, and a test bench bracket. The entire design of the ABS dynamic simulation test system is shown in Figure 6.4.

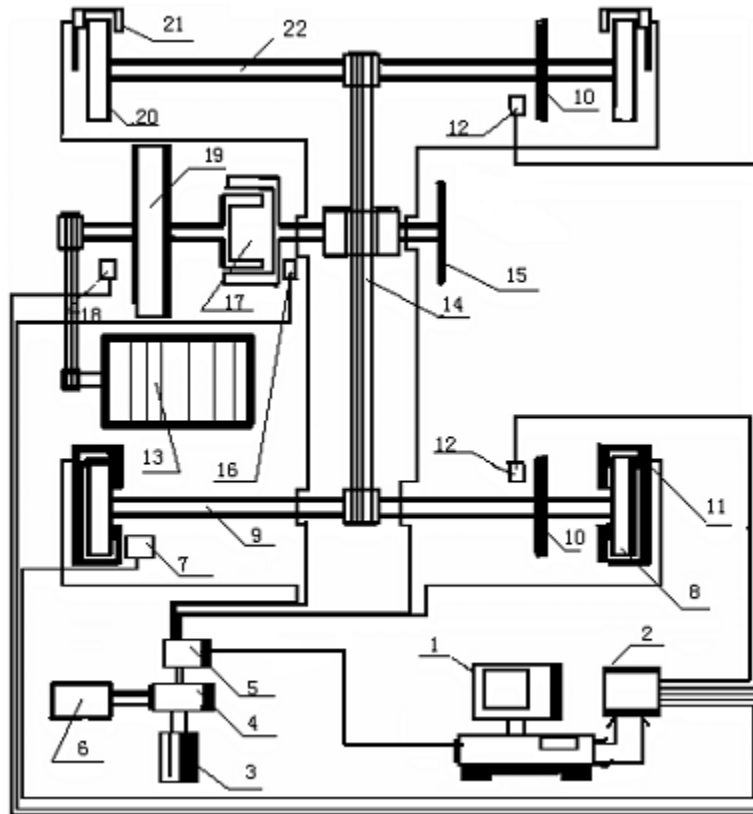


Figure 6.4 The entire design of the ABS test rig

The codes shown in Figure 6.4 are listed in Table 6.1.

Table 6.1 The appellations of components of the ABS test rig

Code	Appellation	Code	Appellation
1	PC	12	Electromagnetic Induction Sensor
2	National Instruments Data Acquisition Card	13	DC motor
3	Brake Pedal	14	Transmission Belt
4	Vacuum Booster	15	Small-size Counterweight Flywheel
5	dSpace MicroAutoBox II	16	Control Unit of Magnetic Powder Clutch
6	Vacuum Pump	17	Magnetic Powder Clutch

7	Wheel-speed Sensor	18	Wheel-speed Sensor
8	Brake Drum	19	Big-size Counterweight Flywheel
9	Rear Axle	20	Brake Disc
10	Signal Plate for Wheel-speed Collection	21	Hydraulic Modulator
11	Branch Braking Pump	22	Front Axle

Figure 6.5 shows the construction of the ABS test rig. A frame was designed to support the actuators.

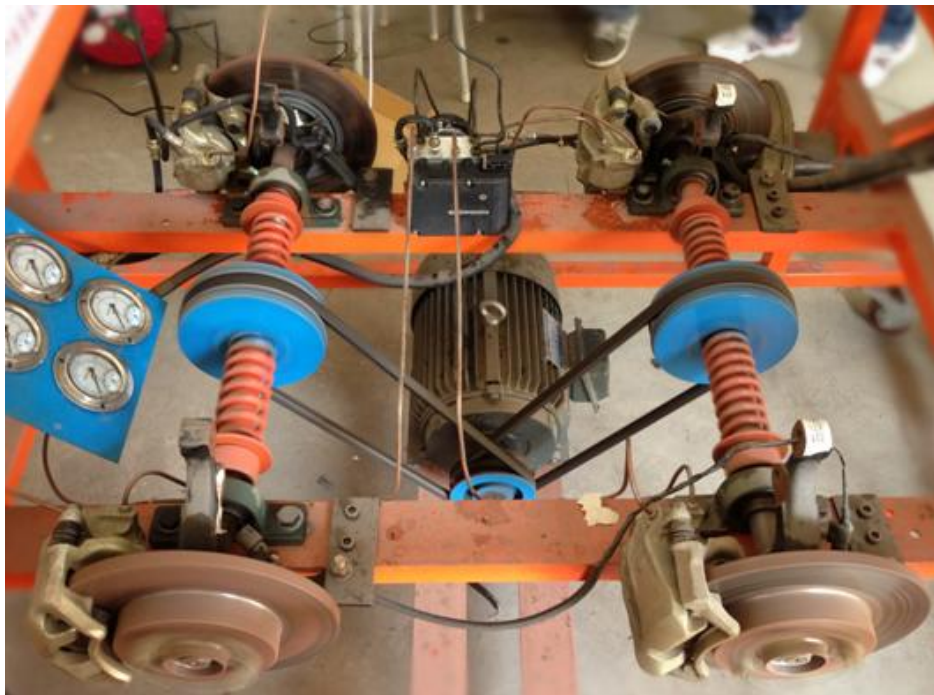


Figure 6.5 Construction of the ABS test rig

### 6.3.2 Speed Signal Collection

In the ABS test rig, wheel-speed sensors are necessary for checking the wheel speed. As with normal vehicle application, every wheel requires a wheel-speed sensor which can send a signal to the ECU for ABS control. Four gear-rings with four speed sensors on the front and rear-axle are in charge of the four wheel-speed data collection.

Figures 6.6 and 6.7 show the electromagnetic induction wheel-speed sensors of both front wheels and rear wheels separately.

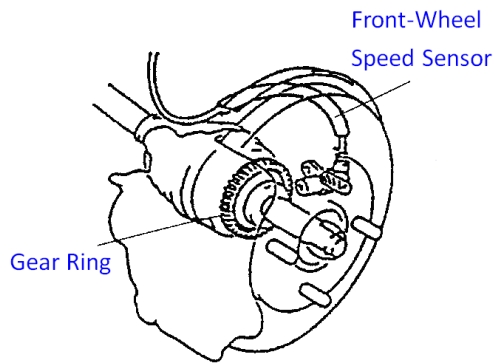


Figure 6.6 Speed sensor of front wheel

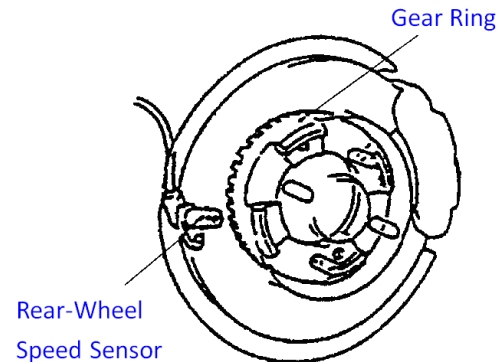


Figure 6.7 Speed sensor of rear wheel

Figure 6.8 shows the construction of the wheel-speed sensor on the ABS test rig. There are 43 teeth on the gear ring for signal collection.



Figure 6.8 Speed sensor of rear wheel on test rig

The ABS systems of modern vehicles are provided with an electromagnetic induction type wheel speed sensor. This can be installed in the main reducer or the transmission and the composition and working principle of the wheel speed sensor is shown in Figure 6.9. The sensor is composed of a magnet, coil, pole piece and the ring gear. The ring gear is rotated in a magnetic field and as the clearance between the gear top

and the electrode with a certain velocity changes, so does the magnetic inductance. The result is that the magnetic flux cycle increases or decreases and, the induction voltage across the coil is proportional to the flux rate of the increase or decrease. The AC voltage signal is transmitted to the electronic controller.

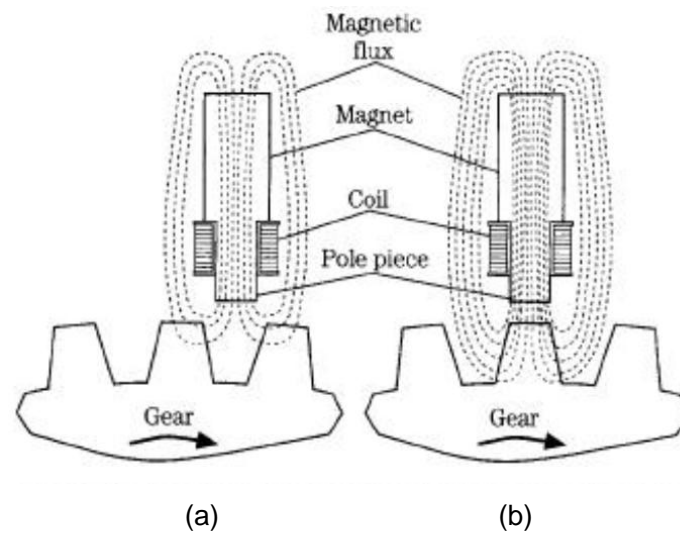


Figure 6.9 The principle of the wheel speed sensor [127]

As shown in Figure 6.9, a sinusoidal signal is produced as the gear teeth pass in front of the sensor, which causes changes in the magnetic flux. When the gap passes the sensor, the level of magnetic flux is low. When the gear tooth passes the sensor, the magnetic flux increases. The frequency of the voltage signal is proportional to the speed and the number of ring gear teeth. When there are a certain number of ring gear teeth, the frequency of the wheel speed sensor output signal is only proportional to the speed of the corresponding wheel [127]. Figure 6.10 describes the voltage differences between high speed and low speed from the speed sensor signal.

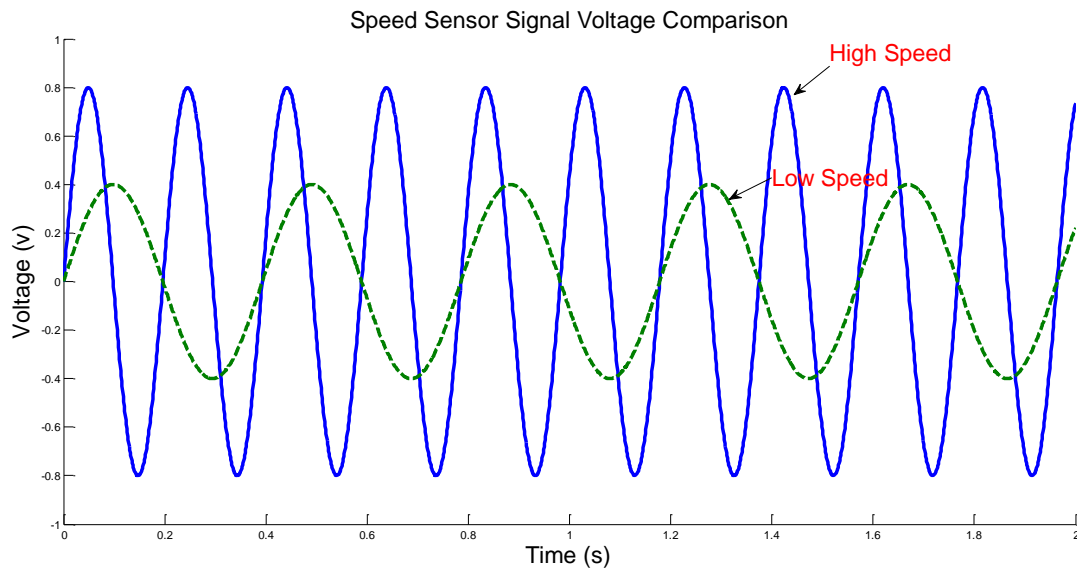


Figure 6.10 Wheel speed sensor signal voltage comparison

The characteristics of the electromagnetic induction wheel speed sensor are [87] [88] [128] [129] [130]:

- The signals generated by the sensor are close to the sine wave with mean value of zero.
- The amplitude of the sine wave signal increases with the decrease of the air gap between the sensor head and ring gear, or an increase in wheel speed.
- The signal waveform is not a standard and smooth sine wave, but a sine wave with vibration. That is because the air gap between the wheel speed sensor and gear tooth are not exactly the same. The deflections between sensor and gear tooth and the vibration from test rig affect the test results significantly.

Figure 6.11 to Figure 6.13 represent the data from the speed sensor at speed of 20km/h, 30km/h and 40km/s respectively. The control signal of wheel speed is sent out by VAS 5054 equipment through On-Board Diagnostics (OBD) connector. The VAS 5054 is usually used for vehicle diagnostic manufactured from Volkswagen. In order to identify the data from the electromagnetic induction wheel speed sensor is

confident for condition monitoring in this project, a test is carried out firstly. By using the Zero-crossing method [131], the input data of these three different speeds are 19.34km/h, 29.55km/h and 40.42km/h respectively. The test results are all within  $\pm 4\%$  of the control speeds. The test results show a confident application of using the electromagnetic induction wheel speed sensor for further model-based condition monitoring of the ABS test rig.

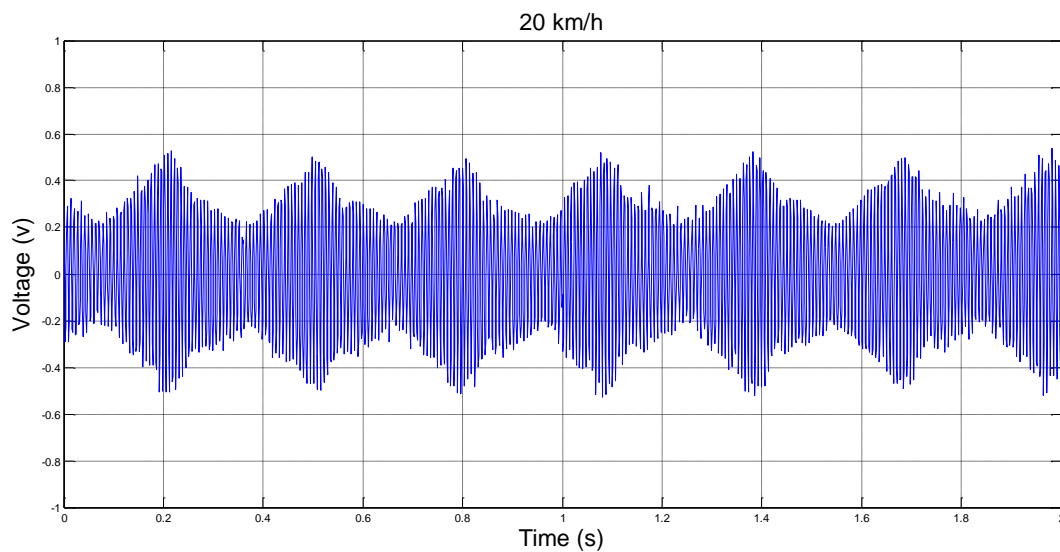


Figure 6.11 Speed sensor data of the vehicle at 20km/h

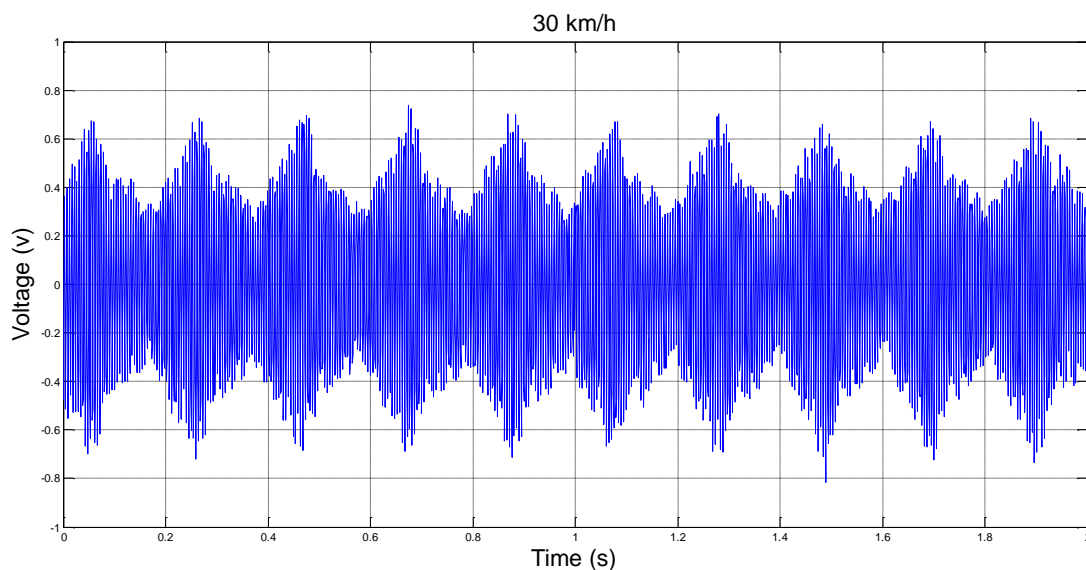


Figure 6.12 Speed sensor data of the vehicle at 30km/h

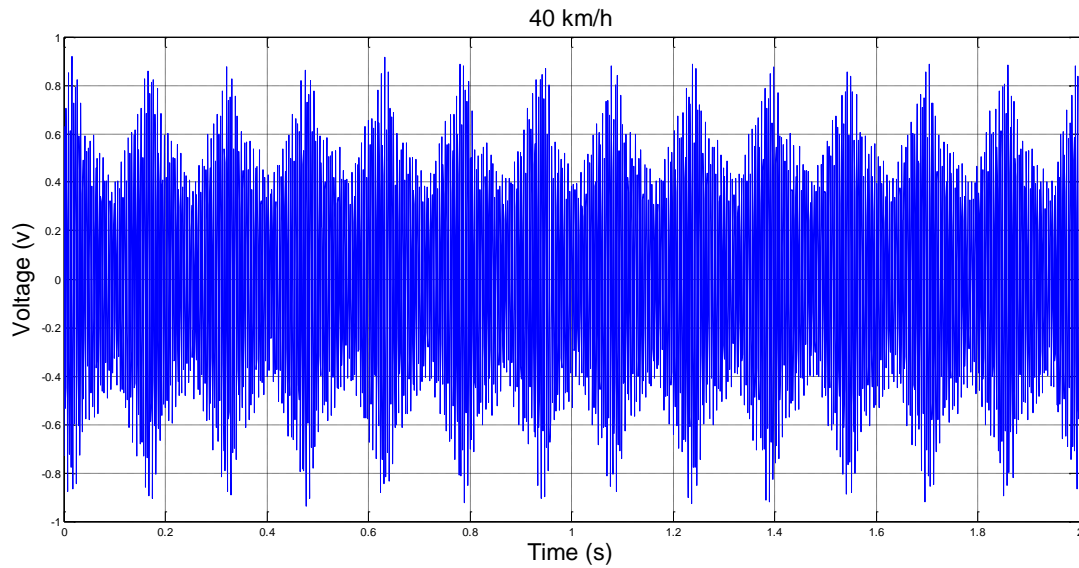


Figure 6.13 Speed sensor data of the vehicle at 40km/h

By comparing the results from Figure 6.11, Figure 6.12 and Figure 6.13 at speeds of 20km/h, 30km/h and 40km/h respectively, it is obvious that the faster the speed, the higher the frequency and the greater the amplitude. The signal is not a smooth sine wave as a result of vibration during the test as mentioned above.

### 6.3.3 Schematic Diagrams of the Three Steps

As explained in Chapter Six, there are three stages of the pressure process, pressure-increasing, pressure-holding and pressure-decreasing. Figure 6.14 shows the performance of the pressure oil inside the pipes in the pressure-increasing process.

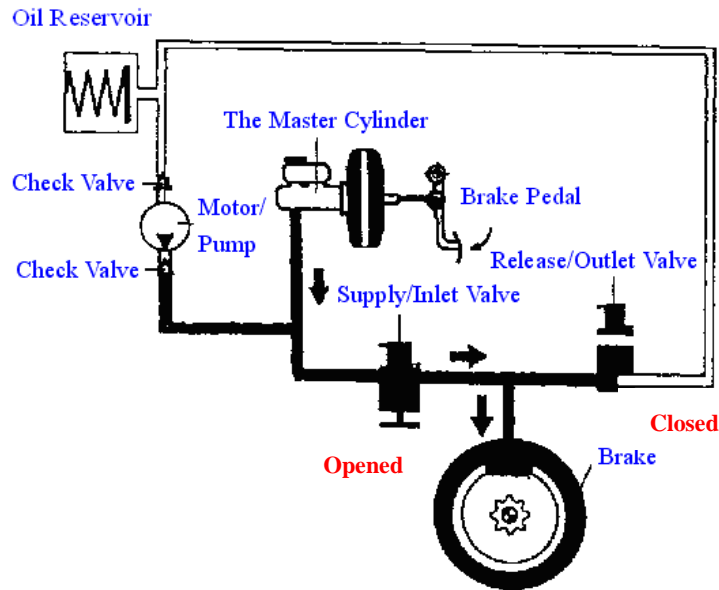


Figure 6.14 Pressure increasing sketch

Figure 6.15 shows the performance of the pressure oil inside the pipes in the pressure-holding process.

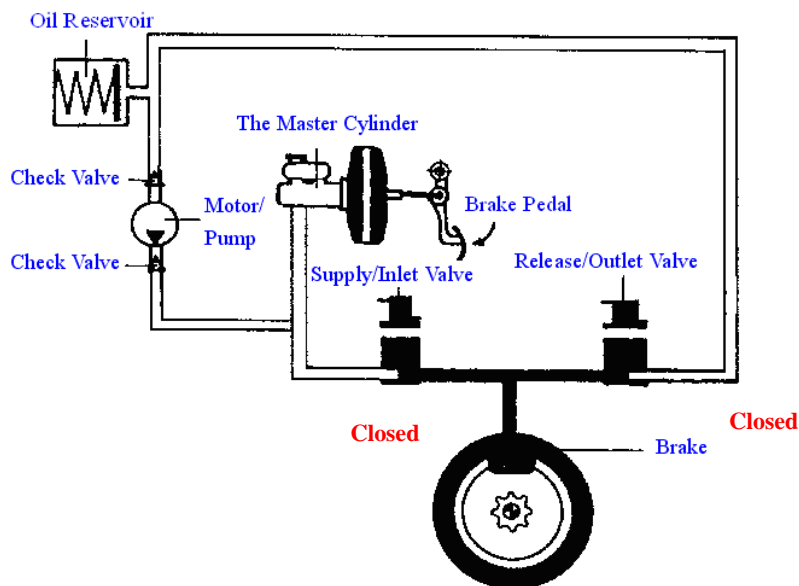


Figure 6.15 Pressure holding sketch

Figure 6.16 shows the performance of the pressure oil inside the pipes in the pressure-decreasing process.

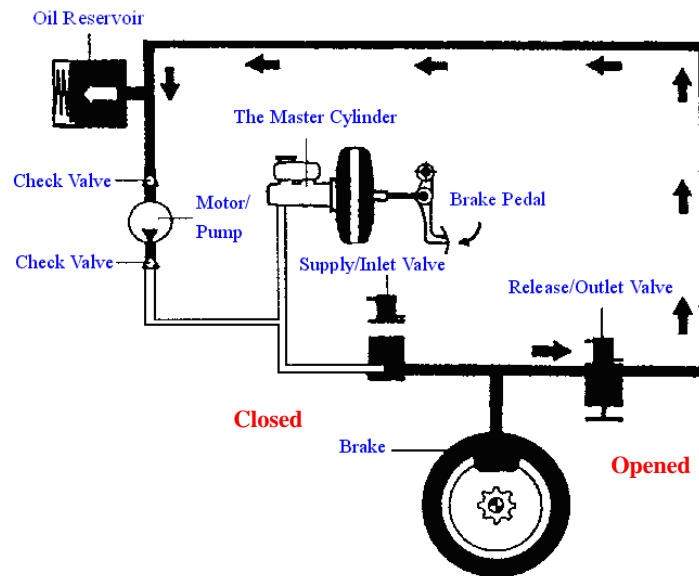


Figure 6.16 Pressure decrease sketch

### 6.3.4 Data Acquisition Component

The National Instruments (NI) Data Acquisition Card (as shown in Figure 6.17) is used for wheel-speed data collection. The NI USB-6009 is a low-cost data acquisition (DAQ) device with easy connectivity and a small form factor. With plug-and-play USB connectivity, these devices are simple enough for quick measurements but versatile enough for complex measurement applications. This NI DAQ contains:

- (1) 8 analogue inputs at 14 bits, up to 48 kS/s,
- (2) 2 analogue outputs at 12 bits, software-timed
- (3) 12 TTL/CM OS digital I/O lines
- (4) One 32-bit, 5 MHz counter
- (5) Digital triggering
- (6) Bus-powered



Figure 6.17 The National Instruments Data Acquisition Card

Figure 6.18 shows the Signal Label Application Diagram of NI DAQ. Until the signal labels are applied, the screw terminal blocks can be inserted into either of the combicon jacks.

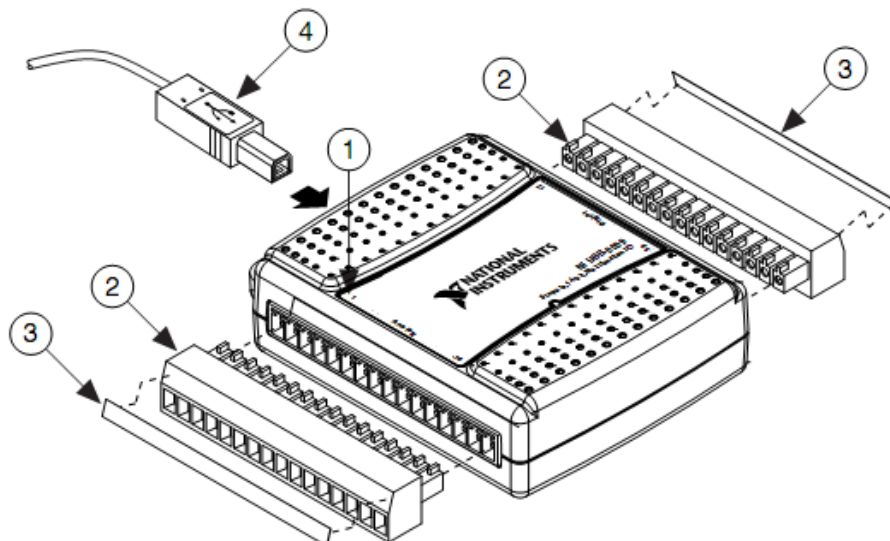


Figure 6.18 Signal label application diagram of NI DAQ [132]

- |   |                 |
|---|-----------------|
| 1 Overlay Label with Pin Orientation Guides | 2 Combicon Jack |
| 3 Signal Labels                             | 4 USB Cable     |

Once the screw terminal blocks are labeled, we must only insert into the matching combicon jack, as indicated by the overlay label on the USB-6009 device. Table 6.2 lists the analogue terminal assignments, and Table 6.3 lists the digital terminal assignments.

Table 6.2 Analogue terminal assignments of NI DAQ [132]

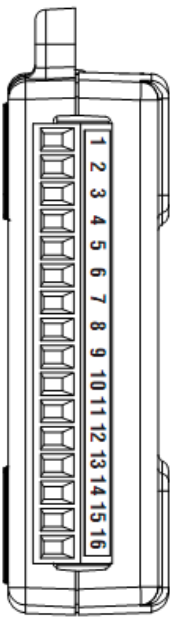
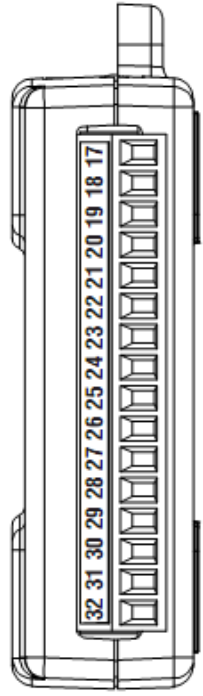
Module	Terminal	Signal, Single-Ended Mode	Signal, Differential Mode
	1	GND	GND
	2	AI 0	AI 0+
	3	AI 4	AI 0-
	4	GND	GND
	5	AI 1	AI 1+
	6	AI 5	AI 1-
	7	GND	GND
	8	AI 2	AI 2+
	9	AI 6	AI 2-
	10	GND	GND
	11	AI 3	AI 3+
	12	AI 7	AI 3-
	13	GND	GND
	14	AO 0	AO 0
	15	AO 1	AO 1
	16	GND	GND

Table 6.3 Digital terminal assignments of NI DAQ [132]

Module	Terminal	Signal
	17	P0.0
	18	P0.1
	19	P0.2
	20	P0.3
	21	P0.4
	22	P0.5
	23	P0.6
	24	P0.7
	25	P1.0
	26	P1.1
	27	P1.2
	28	P1.3
	29	PFI 0
	30	+2.5 V
	31	+5 V
	32	GND

### 6.3.5 Other Components

Figure 6.19 shows the ABS controller of the test rig.



Figure 6.19 The ABS controller

Figure 6.20 shows the ABS control unit of the test rig.



Figure 6.20 The ABS control unit

Figure 6.21 shows the Master Cylinder of the test rig.



Figure 6.21 The master cylinder

Figure 6.22 shows the vacuum booster and the accumulator of the test rig.

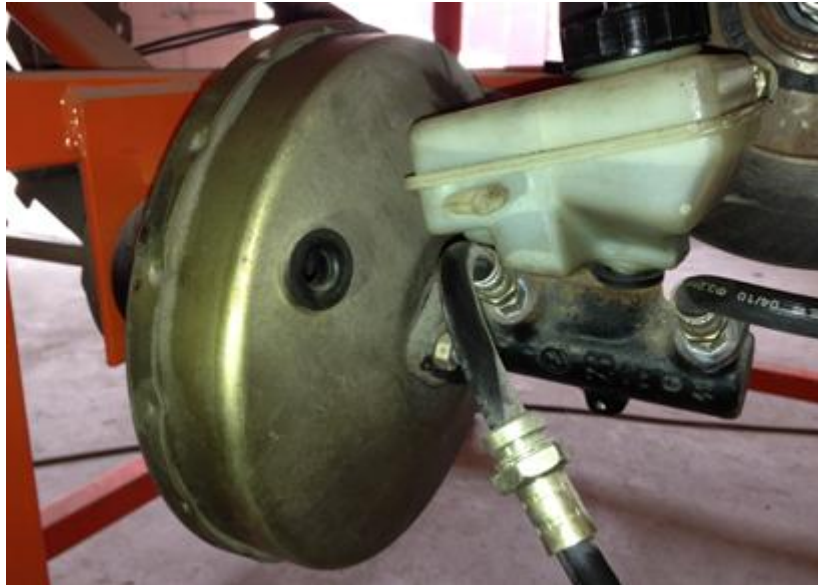


Figure 6.22 The vacuum booster and the accumulator

Figure 6.23 shows the DC motor of the test rig.



Figure 6.23 The DC motor

Figure 6.24 shows the liquid pressure sensor for collecting liquid pressure data inside pipes of the test rig.



Figure 6.24 The liquid pressure sensor

## 6.4 AUTONOMOUS CONTROL OF THE ABS SYSTEM USING THE DSPACE TOOLBOX

An autonomous control strategy has been developed to drive the ABS system operating under desired control. The dSpace MicroAutoBox II as described in Section 6.1 is utilized for this purpose. As shown in Figure 6.25, the MicroAutoBox is connected to a computer, on which a Matlab/Simulink program is developed. The program is then downloaded to the dSpace software to drive the ABS ECU which is also connected to the MicroAutoBox II through a self-designed electrical board with a power amplifier. At the same time, an interface as shown in Figure 6.26 can be developed for condition monitoring.

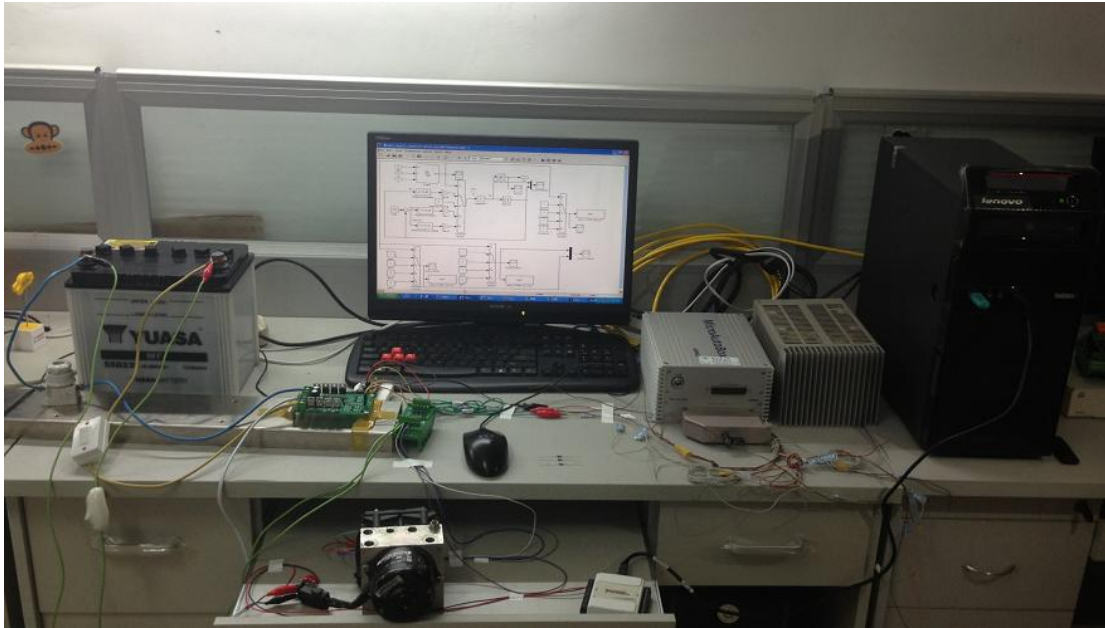


Figure 6.25 An ABS system driven by the dSpace MicroAutoBox II

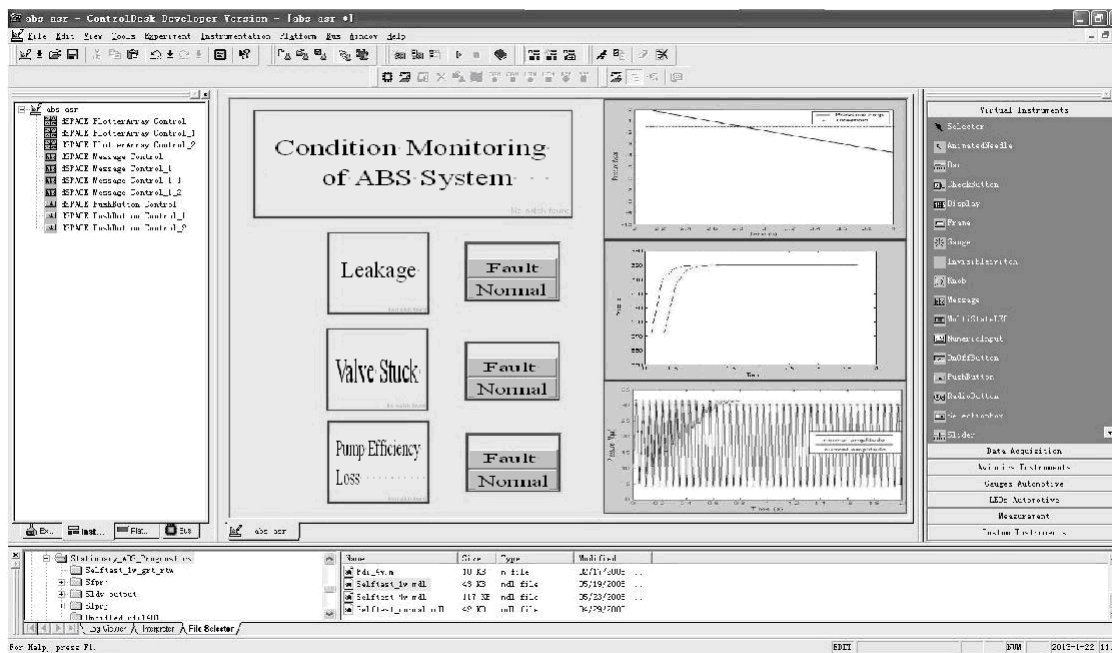


Figure 6.26 Interface for ABS condition monitoring by using dSpace toolbox

## 6.5 TEST RESULTS OF ABS SYSTEM UNDER AUTONOMOUS CONTROL

In this test, a step control strategy is used to control the ABS valve operating for one

cycle. Figure 6.27 shows the braking pressure in the ABS valve under step control. The three steps of pressure-increase, pressure-holding and pressure-decrease are carried out on the test rig. Before operation, the normally opened solenoid valve remains open, and the normally closed solenoid valve remains closed. When operation starts, the pressure increases due to a sudden force on the brake pedal. The pressure then maintains a constant level of about 1.75 MPa. In order to simulate the control stage of pressure-holding, the normally opened solenoid valve is closed. The force on the pedal is then released, but the pressure remains at the same level. When the normally closed solenoid valve is opened, the pressure is released.

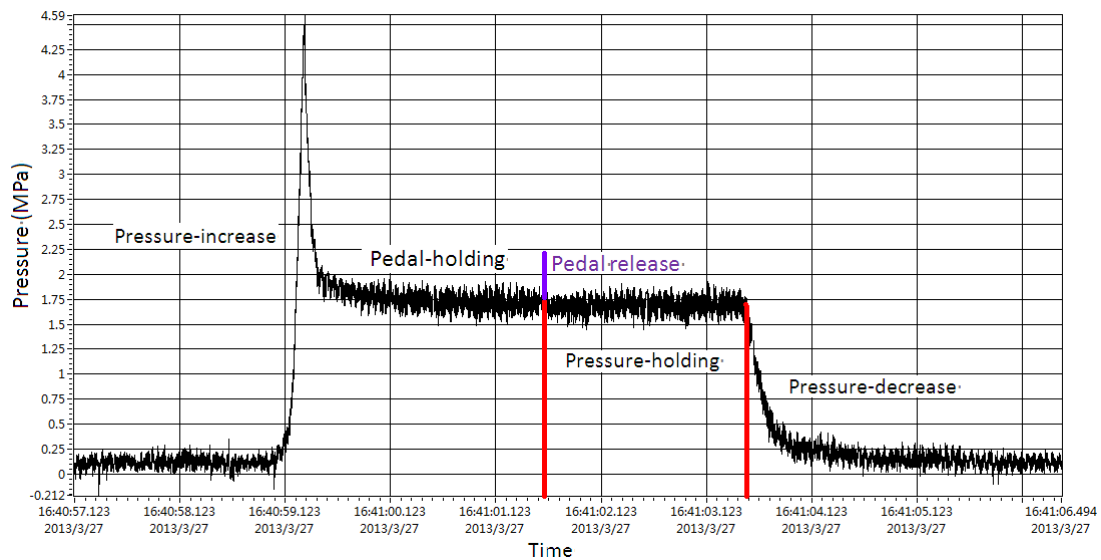


Figure 6.27 Braking pressure in the ABS valve under step control

Figure 6.28 shows the braking pressure when the normally closed solenoid valve is in the opened condition. Because the normally closed solenoid valve is open, the pressure-holding process fails. When the force on the brake pedal is released, the pressure is lost simultaneously.

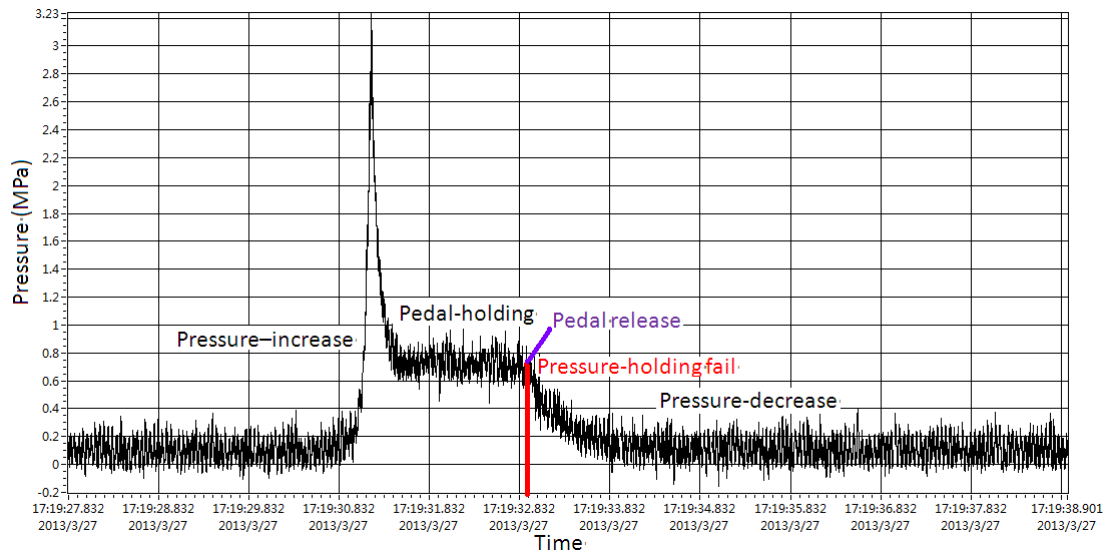


Figure 6.28 Braking pressure when the normally closed solenoid valve is in the open condition

## 6.6 SUMMARY

The test rig with components of ABS, dSpace MicroAutoBox II and data acquisition device was developed in this chapter. The design objectives were listed firstly. The entire design of the ABS test rig was then carried out with description in both figure and table. The principle of wheel speed sensor was then discussed in details. The data acquisition component of NI card was showed in both analogue terminals and digital terminals. Some other components of ABS test rig such as the master cylinder, the vacuum booster, the accumulator, the DC motor and the liquid pressure sensor were introduced as well. By using this ABS test rig, the experimental results can be carried out.

---

## CHAPTER SEVEN

# ABS MONITORING USING THE KALMAN FILTER

---

**In this chapter, the Kalman filter is used for the condition monitoring of an ABS control system. The mathematical model as described in Chapter Three is used in order to construct a Kalman filter for a typical ABS system. The Kalman filter is then used to estimate the ABS performance including vehicle velocity and wheel velocity in different cases and allows an implementation of model-based condition monitoring. The monitoring results demonstrated that the Kalman filter and associated model based condition monitoring is successful in detection and diagnosing faults from solenoid valve sticking or stuck, liquid leakage, pump efficiency loss and speed sensor failures.**

## 7.1 TEST RESULTS UNDER NORMAL CONDITION

As discussed in Section 3.5, the designed Kalman filter is for model-based condition monitoring of a typical ABS system. Using the quarter-vehicle model, the Kalman filter is applied in this project to estimate the vehicle velocity and wheel velocity respectively. The measured signals of vehicle velocity and wheel velocity are going to be used to compare with the estimated vehicle velocity and wheel velocity using the Kalman filter, and used to update the coefficient of the Kalman filter for accurate estimated results obtain. As shown in Figure 7.1, the measurement results of wheel velocity and vehicle velocity are the focus under fault-free condition.

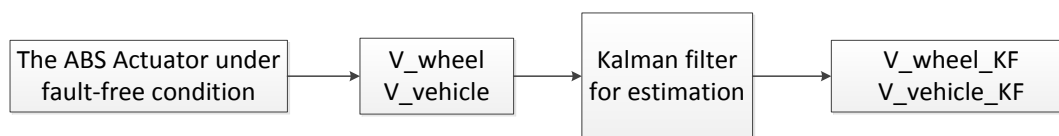


Figure 7.1 Scheme of Kalman filter application under fault-free condition

In this research, the Kalman filter is applied for estimating as baselines of both vehicle velocity and wheel velocity. When the measurement results are not enough for an entire braking process, the Kalman filter can be used to estimate the left part. This is one of the estimation features of the Kalman filter. By comparing the estimated results using the Kalman filter with measurement results, if the residual is within acceptable range, the designed Kalman filter can be used in further work as a baseline.

Figure 7.2 shows the scheme of Kalman filter application under faulty conditions. By comparing with the Kalman filter estimation results, the residuals of model-based approach will be generated from measurement results under different faults. When the residuals exceed the pre-specified thresholds, the alarm will report existing fault in the ABS system.

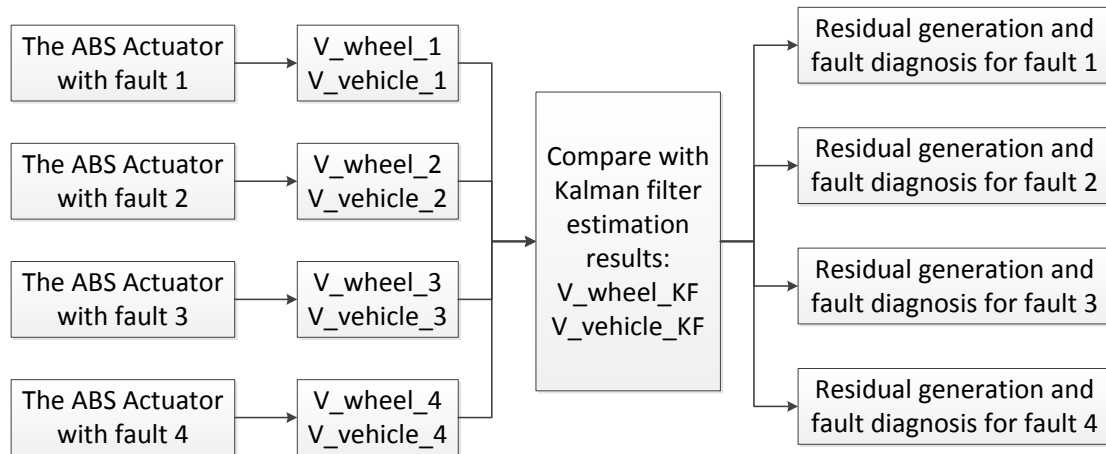


Figure 7.2 Scheme of Kalman filter application under faulty conditions

### 7.1.1 Comparison Results between the Simulation and the Kalman Filter Estimation

By using the standard deviation and tolerance intervals theory, about 68% of values drawn from a normal distribution are within one standard deviation from the mean; about 95% of the value lie within two standard deviations; and about 99.7% are within three standard deviations. This fact is known as the 68-95-99.7(empirical) rule, or the 3-sigma rule [133]. In this research, the method of three standard deviations is used for fault detection of the ABS system. The following discussions about thresholds setting are all based on this algorithm. The thresholds, including the upper limitation and lower limitation, are defined using the red dashed line as shown in Figure 7.4.

Figures 7.3 shows the vehicle velocity comparison results between the Kalman filter estimation results and the simulation results for the ABS under normal condition. The blue solid line refers to the Kalman filter estimation results. The red solid line refers to the simulation result. From Figure 7.3, there is no significant difference between these two. In order to give a quantitative measurement of the differences, the residual generated between the Kalman filter estimation results and the Simulink model results is shown in Figure 7.4. The standard deviation of vehicle velocity estimation

$stdev_{KFV}$  is calculated by

$$stdev_{KFV} = \sqrt{\frac{1}{N} \sum_{i=1}^N (diff_{v\_i} - diff_{v\_avg})^2} \quad \left. \begin{array}{l} \text{where } (diff_{v\_avg} = \frac{1}{N} \sum_{i=1}^N diff_{v\_i}) \\ diff_v = X_{KFV} - X_{modelV} \end{array} \right\} \quad (7.1)$$

where  $X_{KFV}$  and  $X_{modelV}$  represent vehicle velocity data of the Kalman filter estimation results and simulation results respectively. The vehicle velocity estimation threshold  $Dth_{KFV}$  is set up by using the three-sigma rule as

$$Dth_{KFV} = \pm 3 * stdev_{KFV} \quad (7.2)$$

The residual generated from vehicle velocity between these two is from -0.0181 m/s to 0.0181 m/s, which is within acceptable accuracy.

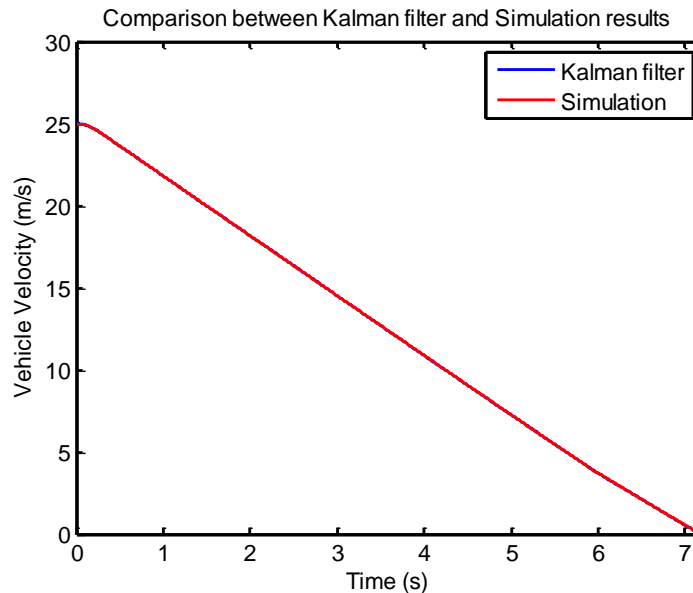


Figure 7.3 Comparison of vehicle velocity between the simulation and the Kalman filter

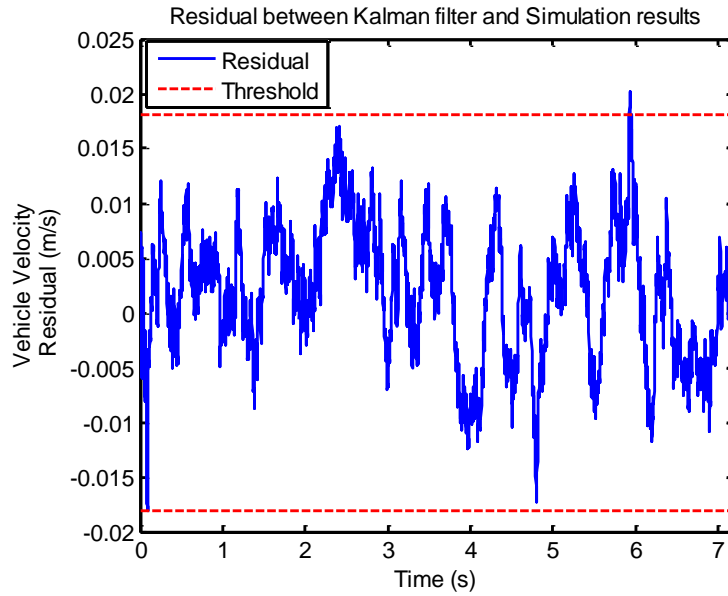


Figure 7.4 Residual of vehicle velocity between the simulation and the Kalman filter

Figure 7.5 shows the wheel velocity comparison results between the Kalman filter estimation results and the simulation results for the ABS under normal condition. The blue solid line refers to the Kalman filter estimation results. The red solid line refers to the simulation result. From Figure 7.5, there is no significant difference between these two. In order to give a quantitative measurement of the differences, the residual generated between the Kalman filter estimation results and the Simulink model results is shown in Figure 7.6. The standard deviation of wheel velocity estimation  $stdev_{KFW}$  is calculated by

$$stdev_{KFW} = \sqrt{\frac{1}{N} \sum_{i=1}^N (diff_{w\_i} - diff_{w\_avg})^2} \quad \text{where } (diff_{w\_avg} = \frac{1}{N} \sum_{i=1}^N diff_{w\_i}) \quad \left. \vphantom{\frac{1}{N} \sum_{i=1}^N} \right\} (7.3)$$

$$diff_w = X_{KFW} - X_{modelW}$$

where  $X_{KFW}$  and  $X_{modelW}$  represent wheel velocity data of the Kalman filter estimation results and the simulation results respectively. The wheel velocity estimation threshold  $Dth_{KFW}$  is set up using the three-sigma rule as

$$Dth_{KFW} = \pm 3 * stdev_{KFW} \quad (7.4)$$

The residual generated from vehicle velocity between these two is from -0.0156 m/s to 0.0156 m/s, which is also within acceptable accuracy.

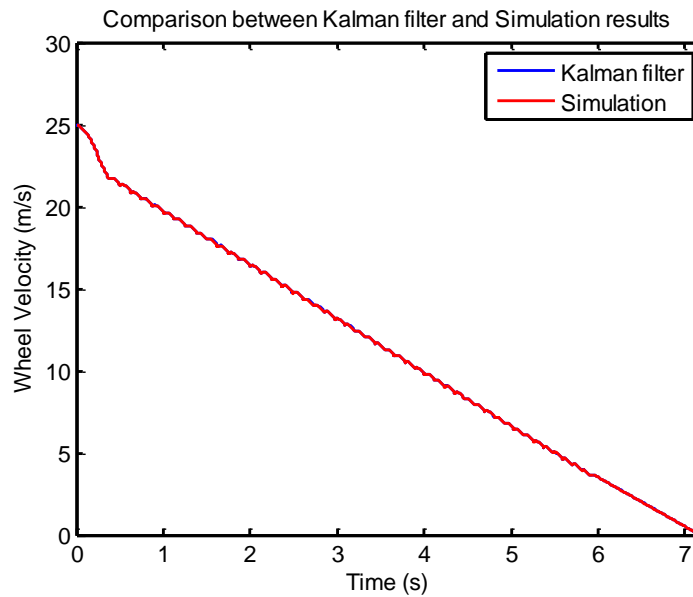


Figure 7.5 Comparison of wheel velocity between the simulation and the Kalman filter

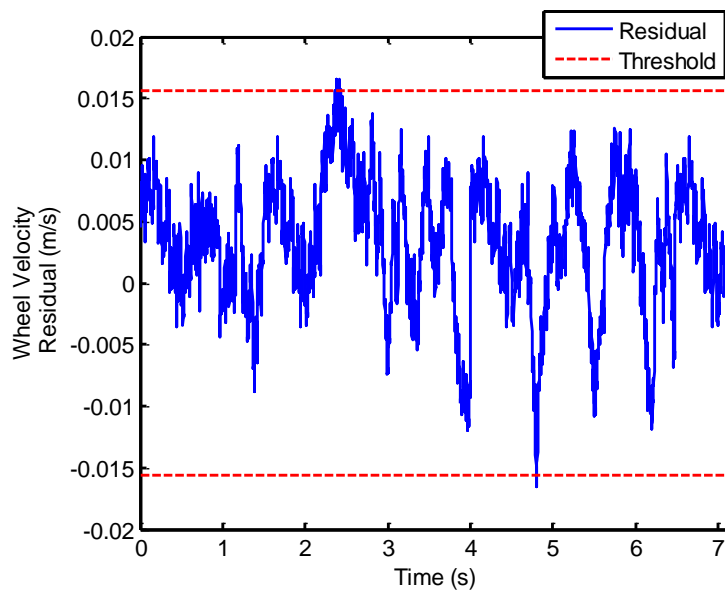


Figure 7.6 Residual of wheel velocity between the simulation and the Kalman filter

## 7.1.2 Comparison Results between the Measurement and the Kalman Filter Estimation

Figure 7.7 shows a typical vehicle velocity measured under normal condition with initial velocity of  $v_0 = 25m/s$ , which can also be considered as  $v_0 = 90km/h$  or  $v_0 = 55.92mile/h$ , and a braking torque of  $T_b = 1800Nm$  on wet asphalt road. As shown in Figure 7.7, the raw data contains a large degree of high frequency noise, which makes it difficult to compare it with estimated data from the Kalman filter. To suppress the noise, the data is smoothed using a Moving Average Filter (MAF). The MAF reduce random noise while retaining a sharp step response [134]. The MAF filters data by replacing each data point with the average of the neighboring data points defined within the span [135]. The MAF is optimal filter method for a periodic fluctuations signal with random white noise [136] [137]. Since the noise we are trying to reduce is random, none of the input points is special; each is just as noisy as its neighbor. Therefore, it is useless to give preferential treatment to any one of the input points by assigning it a larger coefficient in the filter kernel [134]. In this project, 50-point moving average MAF is applied for measurement data filtering. As shown in Figure 7.7, the MAF eliminates the high frequency noise and retains the important decreasing trend which is embedded in the original data.

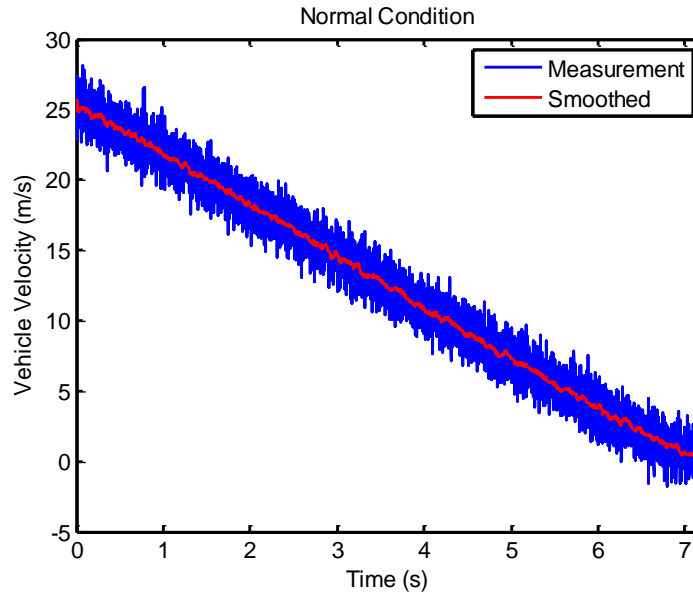


Figure 7.7 Measurement results of the vehicle velocity under normal condition

Using the smoothed data, the measured vehicle velocity results can be compared with those of the Kalman filter. Figure 7.8 shows the comparison of the results. It can be seen that the two sets of data are in close agreement. In order to obtain an accurate quantitative measure of the difference between the smoothed data and the Kalman filter data, a residual signal is obtained by subtracting the Kalman filter estimation results from the smoothed measurement results. As shown in the lower graph of Figure 7.8, the residual signal is nearly Gaussian. The standard deviation of vehicle velocity measurement  $stdev_{MV}$  is calculated using:

$$stdev_{MV} = \sqrt{\frac{1}{N} \sum_{i=1}^N (diff_{v_i} - diff_{v\_avg})^2} \quad \left. \begin{array}{l} \text{where } (diff_{v\_avg} = \frac{1}{N} \sum_{i=1}^N diff_{v_i}) \\ diff_v = X_{MV} - X_{KFV} \end{array} \right\} (7.5)$$

where  $X_{MV}$  and  $X_{KFV}$  represent vehicle velocity data of the smoothed measurement results and the Kalman filter estimation results respectively. The vehicle velocity measurement threshold  $Dth_{MV}$  is established using the three-sigma rule and is given as:

$$Dth_{MV} = \pm 3 * stdev_{MV} \quad (7.6)$$

As shown in Figure 7.8, the residual data from vehicle velocity measurement under normal condition is from -0.4038 m/s to 0.4038 m/s, showing the normal status of the system.

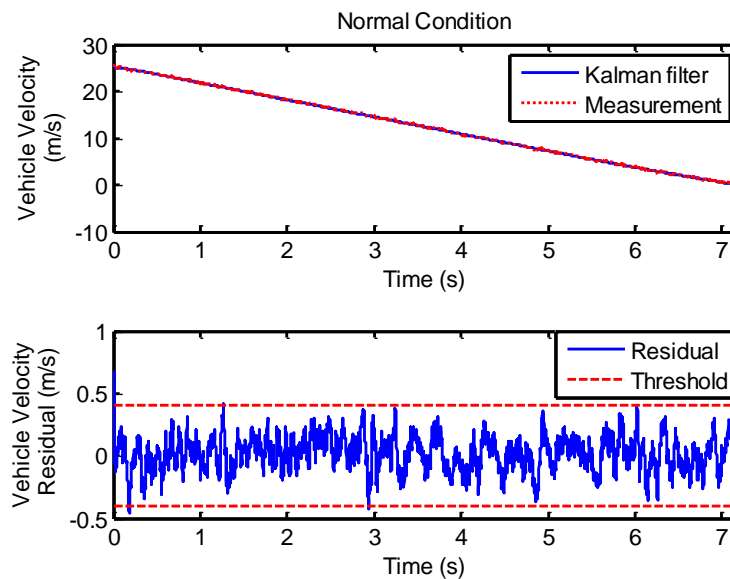


Figure 7.8 Comparison between the measurement and the Kalman filter of vehicle velocity under normal condition

Figure 7.9 shows a typical wheel velocity measured under normal condition. As discussed above, the raw data contain a high degree of high frequency noise, which makes comparison with estimated results from the Kalman filter. To suppress the noise, the data is smoothed in the same way as previously discussed by using an MAF method. As shown in Figure 7.9, the MAF eliminates the high frequency noise and retains the important decreasing trend which is embedded in the original data. The blue solid line refers to the measurement results. The red solid line refers the smoothed results.

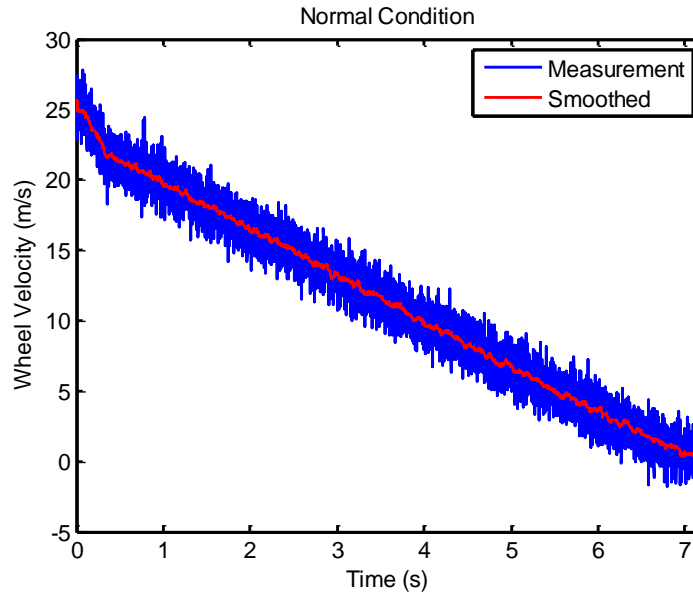


Figure 7.9 Measurement results of the wheel velocity under normal condition

Using the smoothed data, the measured wheel velocity results can be compared with those from the Kalman filter. Figure 7.10 shows the comparison results. It can be seen the two data sets are in good agreement. In order to obtain a quantitative measure for the difference, the residual is generated between the smoothed measurement results and the Kalman filter estimation results. As shown in the lower sub-figure of Figure 7.10, the blue solid line represents the Kalman filter estimation results whilst the red dotted line represents the measurement results. The standard deviation of wheel velocity measurement  $stdev_{MW}$  is calculated using:

$$stdev_{MW} = \sqrt{\frac{1}{N} \sum_{i=1}^N (diff_{w-i} - diff_{w-avg})^2} \quad where (diff_{w-avg} = \frac{1}{N} \sum_{i=1}^N diff_{w-i}) \quad \left. \vphantom{stdev_{MW}} \right\} (7.7)$$

$$diff_w = X_{MW} - X_{KFW}$$

where  $X_{MW}$  and  $X_{KFW}$  represent wheel velocity data of the smoothed measurement results and the Kalman filter estimation results respectively. The vehicle velocity measurement threshold  $Dth_{MW}$  is established using the three-sigma rule as follows:

$$Dth_{MW} = \pm 3 * stdev_{MW} \quad (7.8)$$

The residual generated from wheel velocity under normal condition is from -0.4104 m/s to 0.4104 m/s and is almost a random signal.

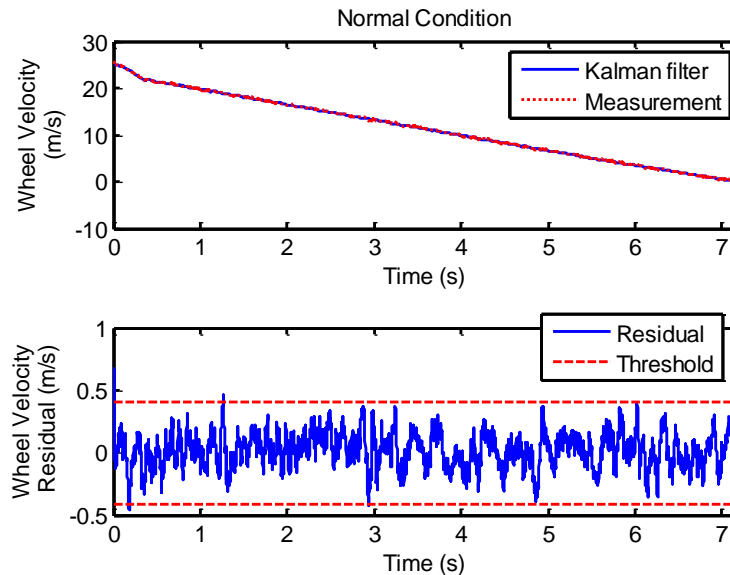


Figure 7.10 Comparison results and the residual results between the measurement and the Kalman filter of vehicle velocity under normal condition

The results show that the Kalman filter method is with good performance on filtering the signal processing of the measurements of both vehicle velocity and wheel velocity, it can therefore be used for condition monitoring of the ABS system under fault conditions.

## 7.2 TEST RESULTS OF WHEEL SPEED SENSOR FAILURE

### 7.2.1 Vehicle Velocity with Speed Sensor Failure

Figure 7.11 shows the measured results and smoothed results of vehicle velocity with the speed sensor failure in the ABS system. As shown in Figure 7.11, the raw data

contain a high degree of high frequency noise, making it difficult to compare with data from the estimate results of the Kalman filter. To suppress the noise, the data is smoothed using an MAF method. The blue solid line refers to the original measurement results whilst the red solid line refers to the smoothed results. Data was simulated using Simulink as discussed in Section 5.4, the vehicle stops at 9.111s when the speed sensor fails. This is 1.928s longer than under the normal condition.

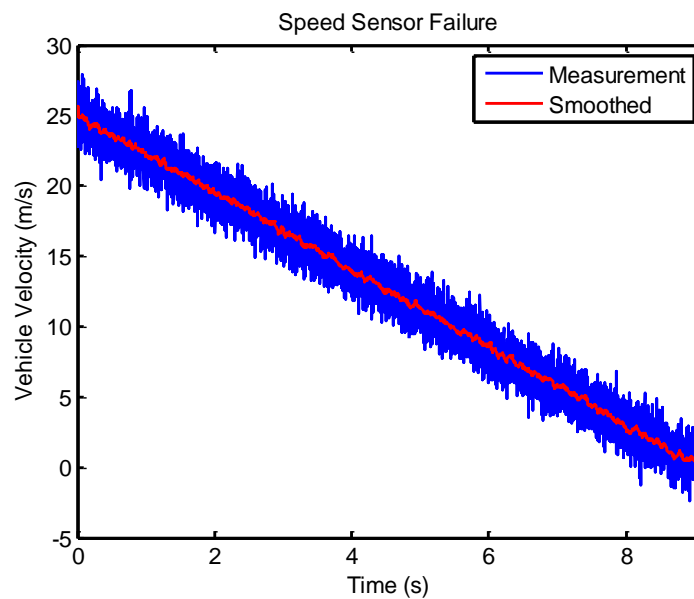


Figure 7.11 Measurement results of the vehicle velocity with speed sensor failure

Figure 7.12 shows the smoothed measurement results with speed sensor failure and the Kalman filter estimation results of vehicle velocity. As shown in the upper graph, the blue solid line refers to the smoothed measurement results whilst the red dotted line refers to the Kalman filter estimation results. The residual generated between them is shown in the lower graph. The vehicle velocity residual with speed sensor failure varies significantly and continues to increase from the beginning of the simulation. It achieves peak amplitude of 5.5512m/s at time equals 7.183s, which is the vehicle stop time under normal condition. Since then, the residual reduces until the vehicle stops.

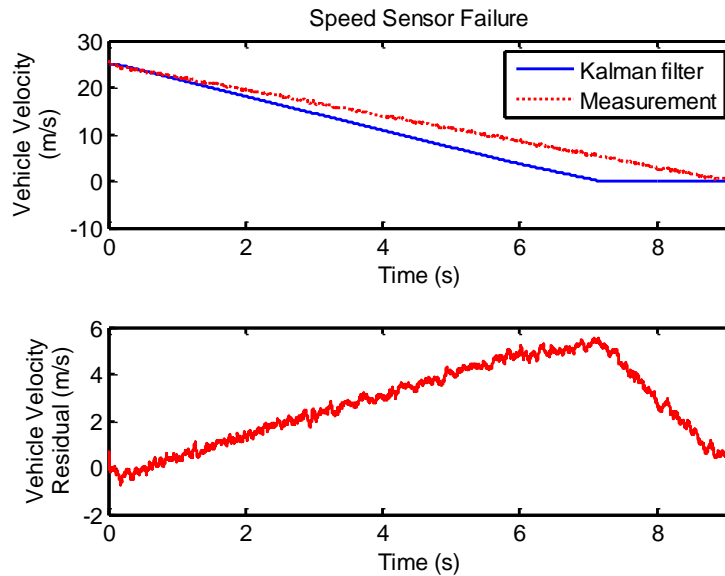


Figure 7.12 Comparison results between the measurement and the Kalman filter of vehicle velocity with speed sensor failure

Figure 7.13 shows the fault detection threshold settings of the ABS system. By using the standard deviation and tolerance intervals theory, as discussed in Section 7.2.1, the upper and lower thresholds are set up using the method of three standard deviations as described in Equations (7.5) and (7.6). As shown in Figure 7.13, the adaptive thresholds (Adaptive threshold methods are those that do not use the same threshold throughout the whole process but the same trends of the processing signal [138]) for the vehicle velocity maintain the same trends as the smoothed measurement results. In order to make it easier to observe, the residual signal with thresholds is applied for the fault detection of the ABS system under speed sensor failure. The two red dashed lines refer to the thresholds setting for vehicle velocity from  $-0.4038$  m/s to  $0.4038$  m/s. The failure alarm only works when the residual signal exceeds the thresholds' range. In the case of the speed sensor failure, as shown in Figure 7.13, the residual exceeds the threshold at time equals 1.1s when the braking commences, and the alarm starts to report the failure.

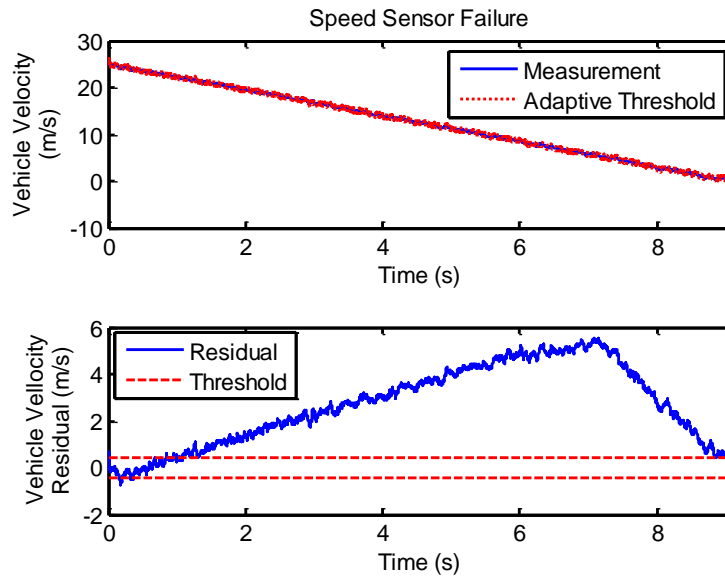


Figure 7.13 Fault detection threshold of vehicle velocity with speed sensor failure

## 7.2.2 Wheel Velocity with Speed Sensor Failure

Figure 7.14 shows the measurement results and the smoothed results of wheel velocity under speed sensor failure in the ABS system. As the speed sensor fails to work since the beginning of braking, the measurement remains a mean value of 0 for the entire process. By using the MAF method, the smoothed measurement results are obtained and shown in Figure 7.14 with the red solid line, whilst the original measurement is shown with the blue solid line.

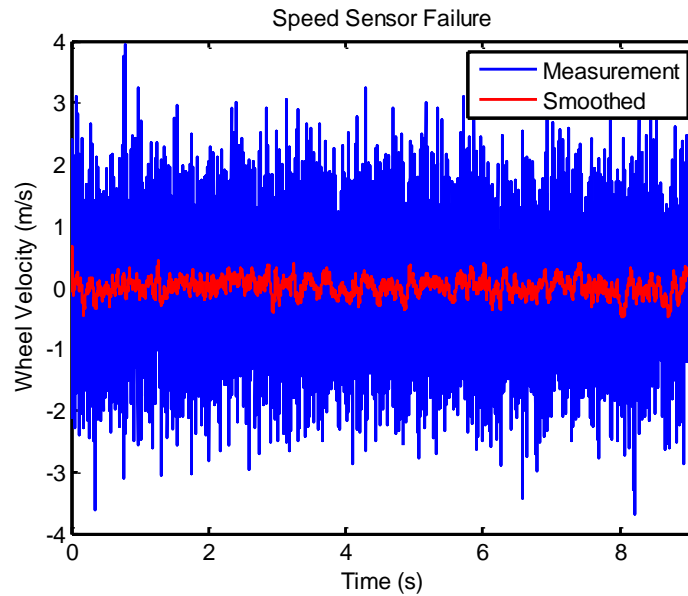


Figure 7.14 Measurement results of the wheel velocity with speed sensor failure

Figure 7.15 shows the smoothed measurement results with speed sensor failure and the Kalman filter estimation results of wheel velocity. The blue solid line refers to the smoothed measurement results whilst the red dotted line refers to the Kalman filter estimation results. The residual generated between the smoothed measurement and the Kalman filter results shows a significant value since the start of the braking process. The absolute peak value of residual is 25m/s, which appears at the start time of the braking process.

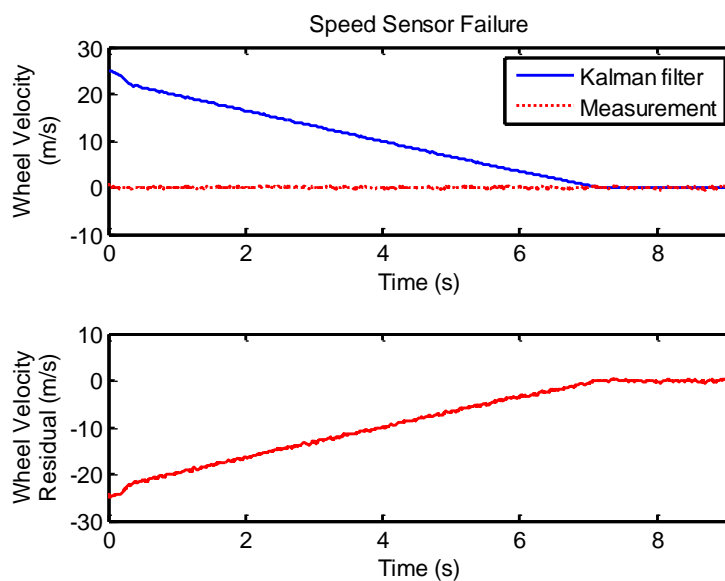


Figure 7.15 Comparison results between the measurement and the Kalman filter of wheel velocity with speed sensor failure

Figure 7.16 shows the fault detection thresholds for wheel velocity of the ABS system with speed sensor failure. By using the standard deviation and tolerance intervals theory, as discussed in Section 7.1.2, the upper and the lower thresholds are established using the method of three standard deviations as described in Equation (7.7) and (7.8). The figure shows that the adaptive thresholds for the wheel velocity maintain the same trends as the smoothed measurement results. In order to make it easier to observe, the residual signal with thresholds is applied for the fault detection of the ABS under speed sensor failure. The two red dashed lines refer to the threshold setting for wheel velocity from -0.4104 m/s to 0.4104 m/s. As the residual signal exceeds the lower threshold at start of the braking process, the alarm reports faults occurring in the ABS system immediately.

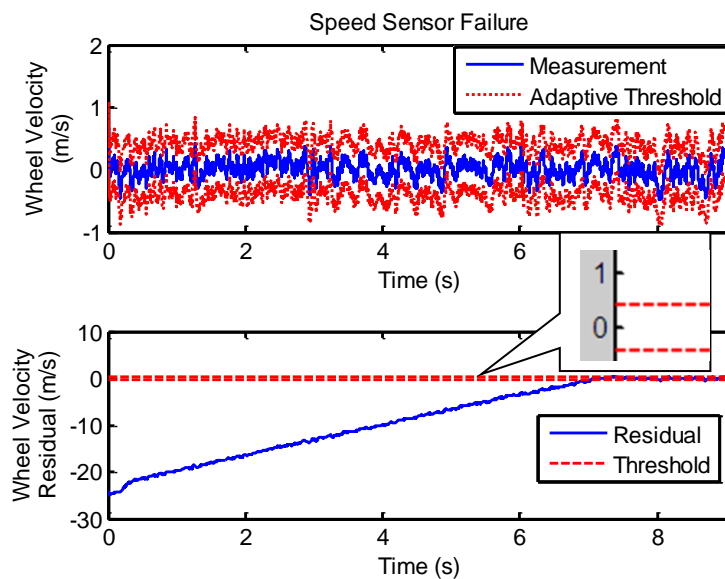


Figure 7.16 Fault detection threshold of wheel velocity with speed sensor failure

## 7.3 TEST RESULTS OF SOLENOID VALVE STICKING OR STUCK

### 7.3.1 Vehicle Velocity with Solenoid Valve Sticking or Stuck Fault

Figure 7.17 shows the measurement results and the smoothed results of vehicle velocity with a solenoid valve sticking or stuck fault in the ABS system. The figure shows the original measurement data is smoothed using an MAF method as discussed above. The blue solid line refers to the original measurement results whilst the red solid line refers to the smoothed results. When simulated using Simulink, as discussed in Section 5.5, the braking time increases to 7.589s.

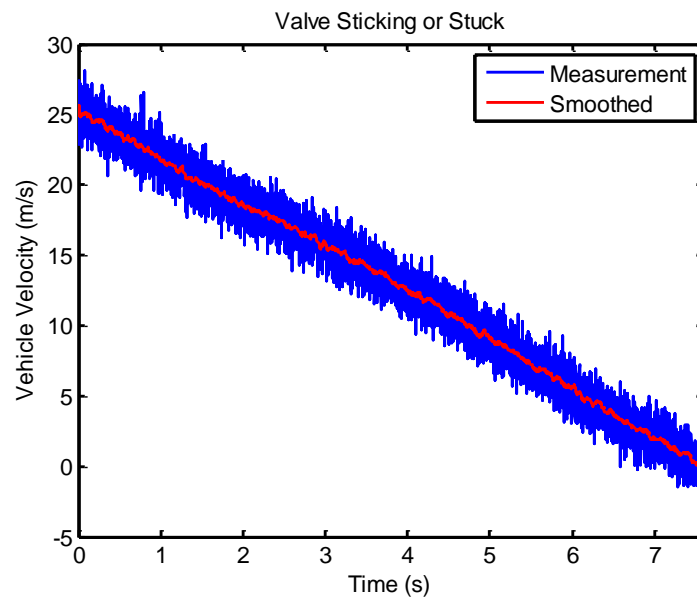


Figure 7.17 Measurement results of the vehicle velocity with valve sticking or stuck fault

Figure 7.18 shows the smoothed measurement results for the valve sticking or stuck fault and the Kalman filter estimation results of the vehicle velocity. The blue solid line refers to the smoothed measurement results whilst the red dotted line refers to the

Kalman filter estimation results. The residual signal generated between them is also shown in Figure 7.18. The vehicle velocity residual with the valve sticking or stuck fault does not show a significant value, but it continues to increase 1.5s from the start of the braking process reaching a peak value of 2.1579 m/s.

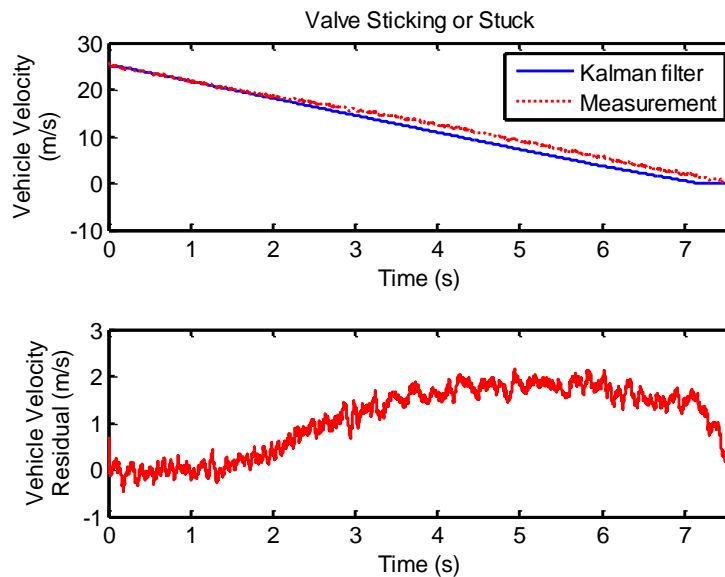


Figure 7.18 Comparison results between the measurement and the Kalman filter of vehicle velocity with valve sticking or stuck fault

Figure 7.19 shows the thresholds setting for fault detection of the ABS system. By using the standard deviation and tolerance intervals theory, the upper and lower thresholds are set up in the same way. As shown in the lower sub-figure, the red dotted lines refer to the adaptive thresholds which maintain the same decreasing trend as the smoothed measurement results for the vehicle velocity. To make it easier to observe, the residual signal with thresholds are applied to the fault detection of the ABS system with valve sticking or stuck fault. The two red dashed lines refer to the thresholds setting for vehicle velocity from  $-0.4038$  m/s to  $0.4038$  m/s. The alarm reports a fault occurring in the ABS system when the residual signal exceeds the thresholds' range at about 2s as shown in the lower sub-figure of Figure 7.19.

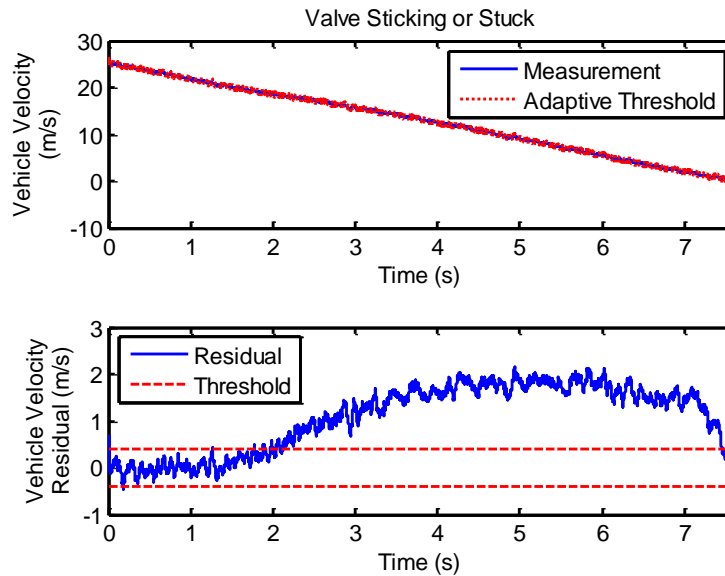


Figure 7.19 Fault detection threshold of vehicle velocity with valve sticking or stuck fault

### 7.3.2 Wheel Velocity with Solenoid Valve Sticking or Stuck Fault

Figure 7.20 shows the measurement results and the smoothed results of wheel velocity with valve sticking or stuck fault in the ABS system. The blue solid line refers to the smoothed measurement results whilst the red solid line refers to the original measurement results. As the solenoid valve is sticking or stuck, the processes of pressure-increasing, pressure-holding and pressure-decreasing cannot switch as it is designed in a control algorithm. As shown in the figure, the performance of the wheel velocity decreases to a slipping trend at 2.013s, which is an unstable region for driving.

Figure 7.21 shows the comparison results between the measurement and the Kalman filter estimation with valve sticking or stuck. The red dotted line refers to the smoothed measurement results whilst the blue solid line refers to the Kalman filter estimation results. The residual generated between these two shows a significant decreasing and increasing trend through the whole braking process. The peak absolute

value occurs at 2.013s, which is the most unstable region of driving during the whole braking process.

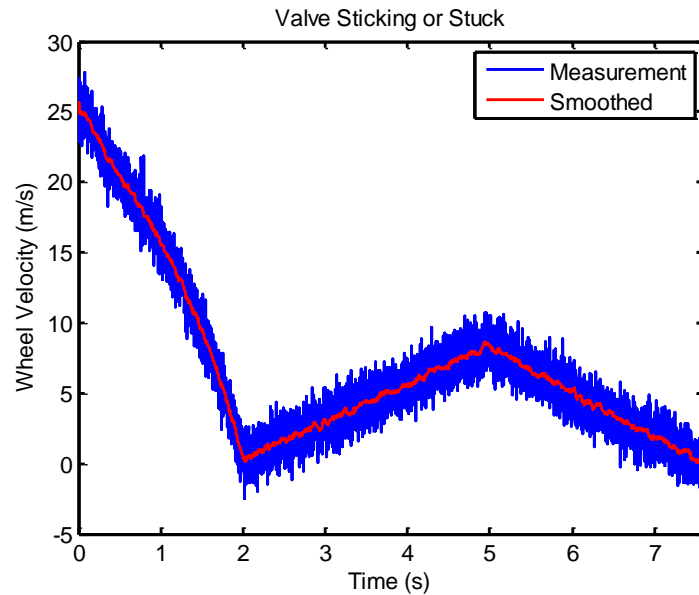


Figure 7.20 Measurement results of the wheel velocity with valve sticking or stuck fault

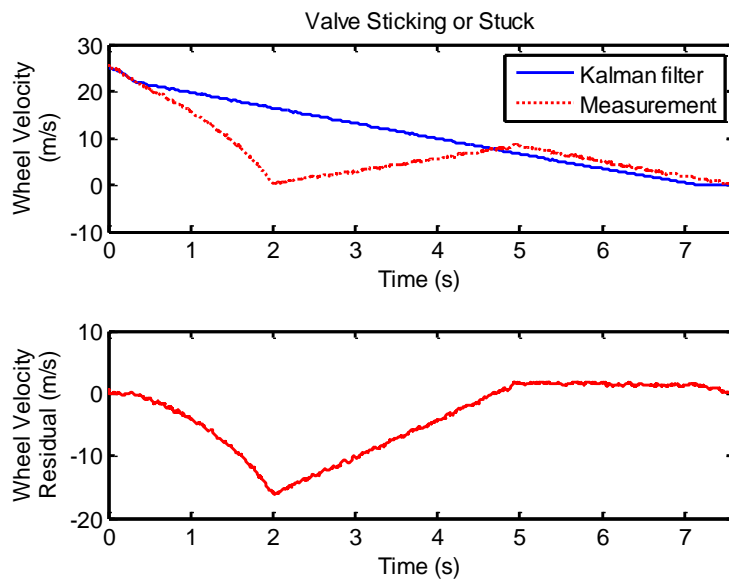


Figure 7.21 Comparison results between the measurement and the Kalman filter of wheel velocity with valve sticking or stuck fault

Figure 7.22 shows the fault detection thresholds for the ABS system with valve sticking or stuck fault. Using the three standard deviation method, the upper and lower

adaptive thresholds limits are set up as shown in the upper sub-figure with the red dotted line. For ease of observation, the residual signal with thresholds is applied. The red dashed lines refer to the thresholds setting for wheel velocity from  $-0.4104$  m/s to  $0.4104$  m/s. The blue solid line refers to the residual. The alarm reports a fault when the residual exceeds the thresholds.

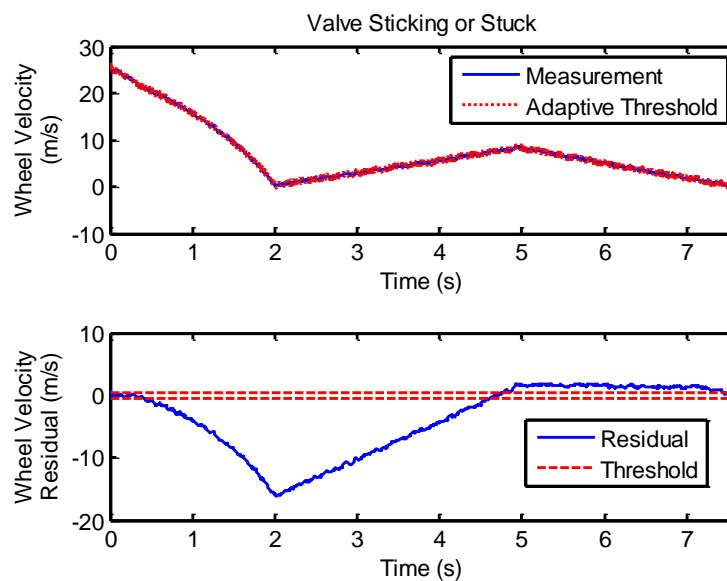


Figure 7.22 Fault detection threshold of wheel velocity with valve sticking or stuck fault

## 7.4 TEST RESULTS OF LIQUID LEAKAGE

### 7.4.1 Vehicle Velocity with Liquid Leakage Fault

Figure 7.23 shows the measurement results and the smoothed results of the vehicle velocity with the liquid leakage in the ABS system. As shown in the figure, the original measurement data is smoothed using an MAF method as previously discussed. The blue solid line refers to the original measurement results whilst the red solid line refers to the smoothed results. As liquid leakage will lead to serious and

non-reversible damage to the ABS test facility, the leakage amount setting for this project is not significant. However, it is sufficient enough to show the characteristics of the fault itself. When simulated using Simulink, as discussed in Section 5.6, the entire braking process takes 7.282s until the vehicle stops.

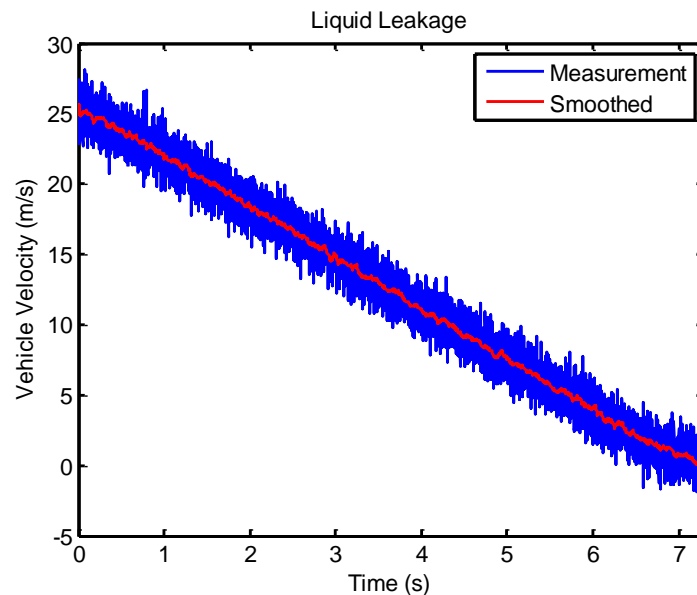


Figure 7.23 Measurement results of the vehicle velocity with liquid leakage fault

Figure 7.24 shows the comparison results between the smoothed measurement and the Kalman filter estimation. The blue solid line refers to the Kalman filter estimation results whilst the red dotted line refers to the smoothed measurement results, as shown in the upper sub-figure. The residual generated between them is shown in the lower sub-figure. The vehicle velocity residual with the liquid leakage fault does not change a great deal because the liquid amount previously set in the system is not particularly large. If the setting parameters are different, the liquid leakage amount together with the residual will be changed.

Figure 7.25 shows the fault detection thresholds setting for the ABS system with liquid leakage fault. By using the standard deviation and tolerance intervals theory, the upper and lower thresholds are set up the same way. As shown in the lower sub-figure, the red dotted lines for the adaptive threshold maintain the same

decreasing trends as the smoothed measurement results for the vehicle velocity. For ease of observation, the residual signal with thresholds is applied for the fault detection of the ABS system with liquid leakage fault. The two red dashed lines refer to the thresholds setting for vehicle velocity from  $-0.4038$  m/s to  $0.4038$  m/s. The alarm reports faults occurring in the ABS system when the residual signal exceeds the thresholds' range and can be seen in the lower sub-figure of Figure 7.25.

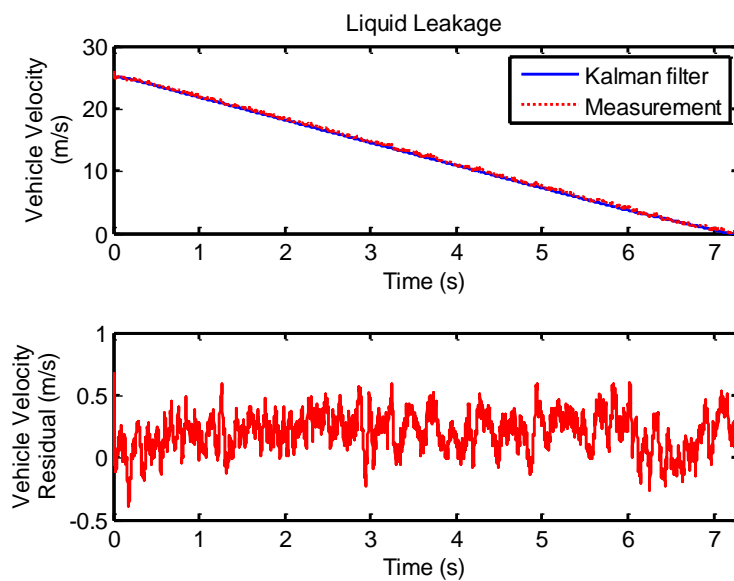


Figure 7.24 Comparison results between the measurement and the Kalman filter of vehicle velocity with liquid leakage fault

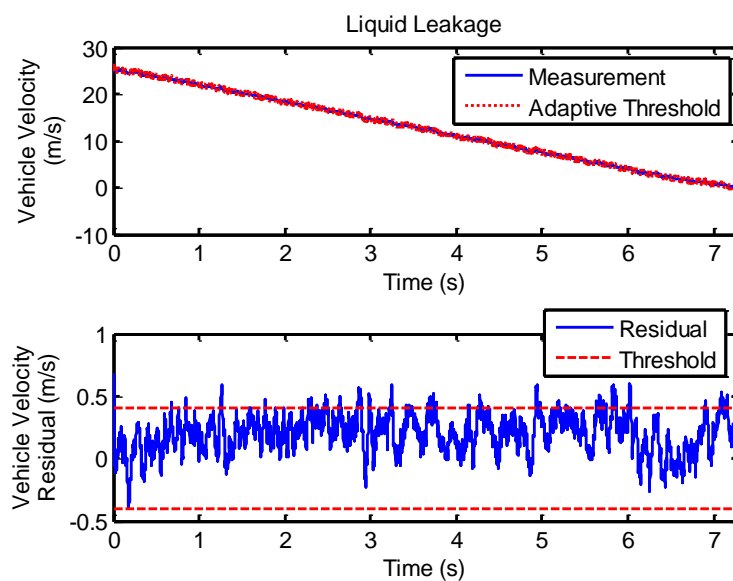


Figure 7.25 Fault detection threshold of the vehicle velocity with liquid leakage fault

## 7.4.2 Wheel Velocity with Liquid Leakage Fault

Figure 7.26 shows the measurement results and the smoothed results of wheel velocity with a liquid leakage fault in the ABS system. It can be seen that the wheel locks at about 6.5s and begins to slip until the vehicle stops. If the leakage amount is increased, then the performance will be significantly worse. The blue solid line refers to the original measurement results whilst the red solid line refers to the smoothed results.

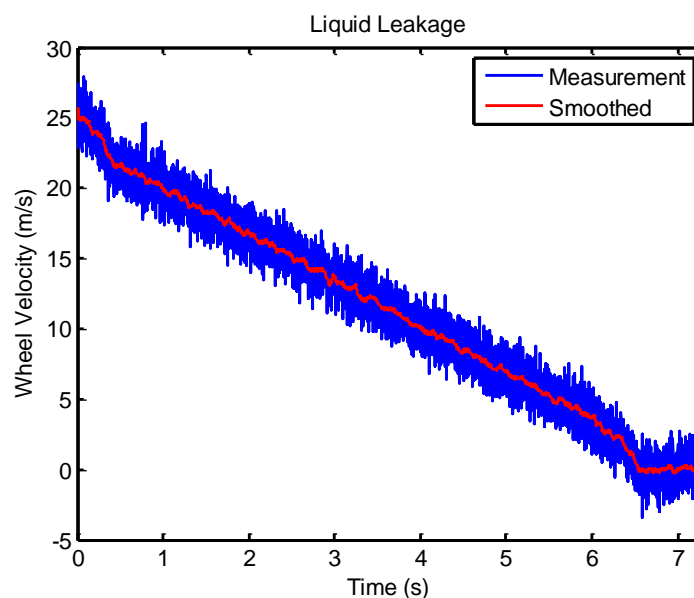


Figure 7.26 Measurement results of the wheel velocity with liquid leakage fault

Figure 7.27 shows the smoothed measurement results with liquid leakage fault and the Kalman filter estimation results of wheel velocity. The blue solid line refers to the Kalman filter results whilst the red dotted line refers to the smoothed measurement results. The residual generated between them is shown in the lower sub-figure. The peak value is 1.0566m/s and the valley value is -2.0065m/s.

Figure 7.28 shows the fault detection thresholds for the ABS system with liquid leakage fault. The upper sub-figure shows the smoothed measurement results together with adaptive thresholds. The lower sub-figure shows the residual with thresholds

settings for wheel velocity from  $-0.4104$  m/s to  $0.4104$  m/s. The alarm reports faults in the ABS system intermittently when the residual exceeds the thresholds.

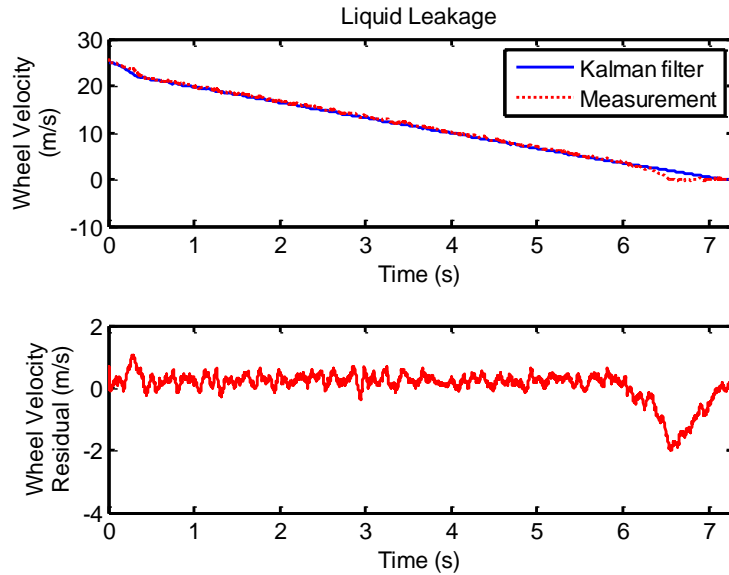


Figure 7.27 Comparison results between the measurement and the Kalman filter of wheel velocity with liquid leakage fault

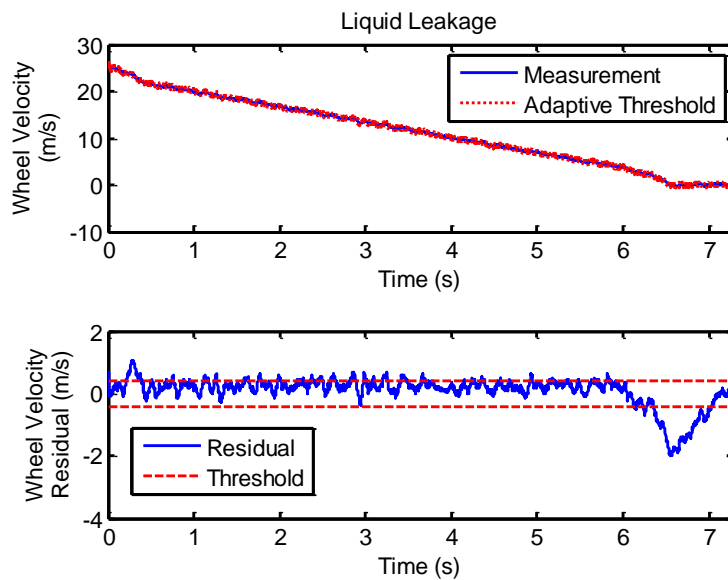


Figure 7.28 Fault detection threshold of the wheel velocity with liquid leakage fault

## 7.5 TEST RESULTS OF PUMP EFFICIENCY LOSS

### 7.5.1 Vehicle Velocity with Pump Efficiency Loss

Figure 7.29 shows the measurement results and the smoothed results of vehicle velocity with pump efficiency loss in the ABS system. The original measurement data is smoothed by using an MAF method as previously discussed. The blue solid line refers to the original measurement results whilst the red solid line refers to the smoothed results. The braking time increases to 7.467s due to the pump efficiency loss fault in the ABS system.

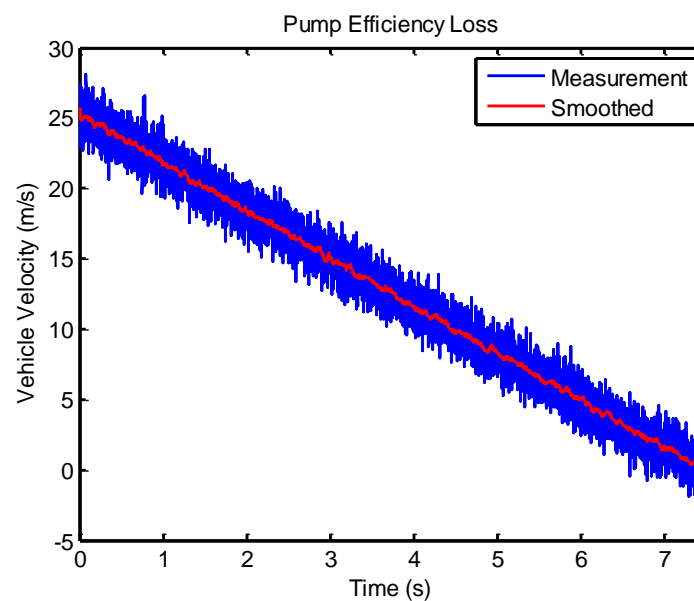


Figure 7.29 Measurement results of the vehicle velocity with pump efficiency loss

Figure 7.30 shows the smoothed measurement results with pump efficiency loss and the Kalman filter estimation results of vehicle velocity. As shown in the upper sub-figure, the blue solid line refers to the smoothed measurement results whilst the red dotted line refers to the Kalman filter estimation results. The residual generated between them is shown in the lower sub-figure. The peak value of 1.5776m/s occurs 5.9s after the start of the braking process.

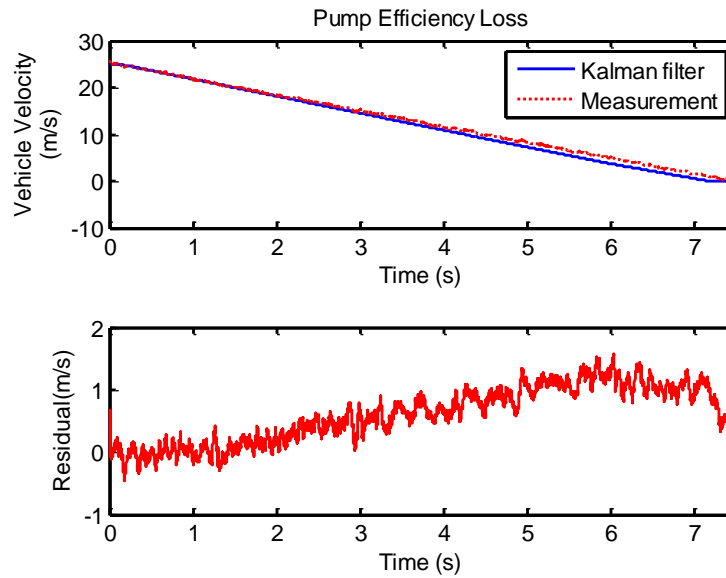


Figure 7.30 Comparison results between the measurement and the Kalman filter of vehicle velocity with pump efficiency loss

Figure 7.31 shows thresholds setting up for fault detection of the ABS system with pump efficiency loss. The red dotted lines in the upper sub-figure refer to the adaptive threshold. The blue solid line refers to the smoothed measurement results under fault conditions. The thresholds are set up with values of  $-0.4038$  m/s and  $0.4038$  m/s. The alarm reports faults of the ABS system when the residual exceeds either the upper or the lower threshold.

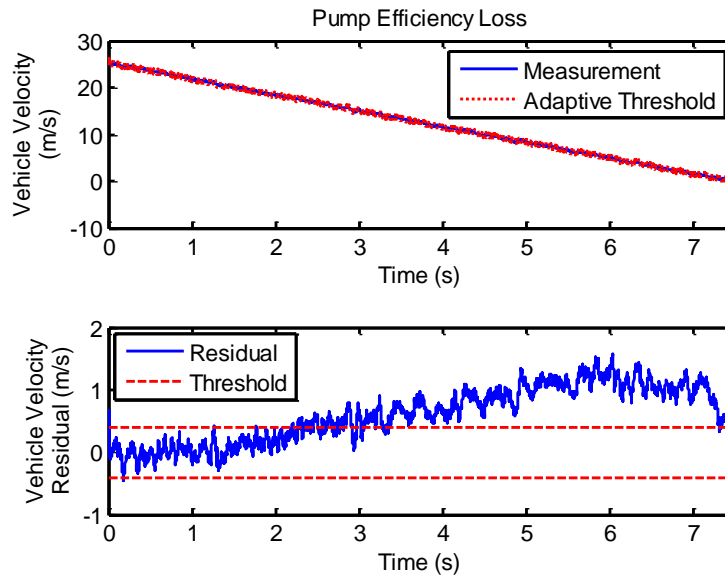


Figure 7.31 Fault detection threshold of vehicle velocity with pump efficiency loss

## 7.5.2 Wheel Velocity with Pump Efficiency Loss

Figure 7.32 shows the measurement results and the smoothed results of wheel velocity with pump efficiency loss in the ABS system. The blue solid line refers to the smoothed measurement results whilst the red solid line refers to the original measurement data with high frequency noise.

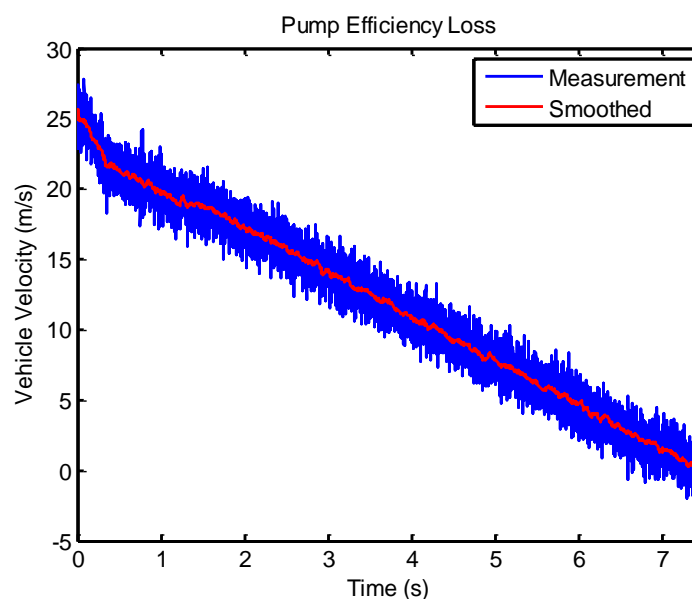


Figure 7.32 Measurement results of the wheel velocity with pump efficiency loss

Figure 7.33 shows the comparative results between the actual measurement and the Kalman filter estimation results with pump efficiency loss. The red dotted line refers to the smoothed measurement results whilst the blue solid line refers to the Kalman filter estimation results. The residual generated between these two shows a significant change during the entire braking process.

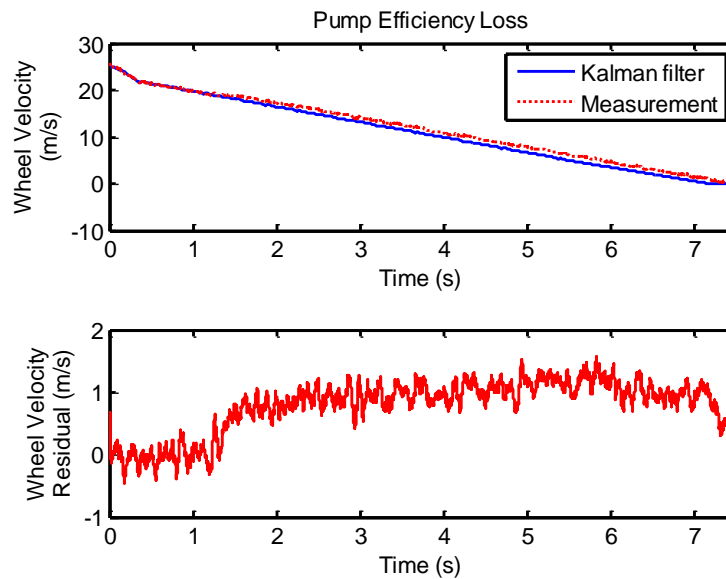


Figure 7.33 Comparison results between the measurement and the Kalman filter of wheel velocity with pump efficiency loss

Figure 7.34 shows the fault detection thresholds for the ABS system with pump efficiency loss. The threshold are set with values of  $-0.4104$  m/s and  $0.4104$  m/s. As shown in the upper sub-figure, the blue solid line refers to the smoothed measurement results whilst the red dotted lines refer to the adaptive thresholds. For ease of observation, the residual signal with thresholds is applied as shown in the lower sub-figure. The red dashed lines refer to the thresholds, whilst the blue solid line refers to the residual. The alarm starts to report faults in the ABS when the residual exceeds the thresholds after 1.4s until the wheel stops.

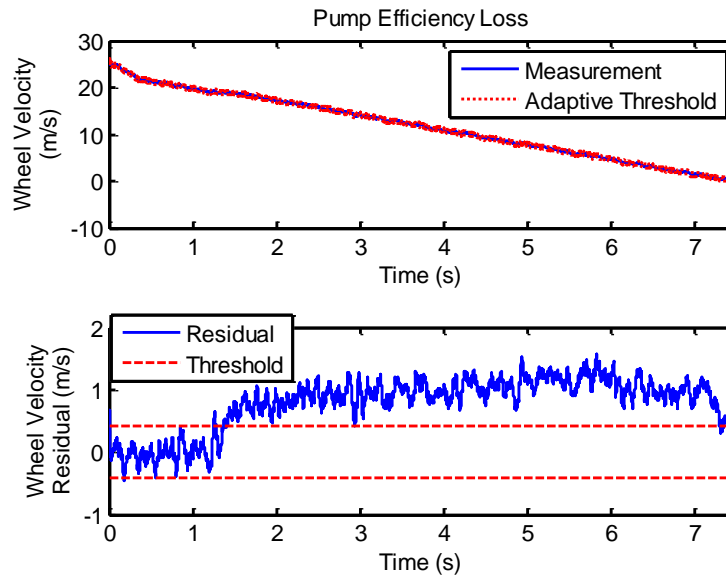


Figure 7.34 Fault detection threshold of wheel velocity with pump efficiency loss

## 7.6 SUMMARY

In this chapter, the experimental results were carried out by using the test rig that built up in Chapter Six. The Kalman filter was utilized in this project to estimate both the vehicle velocity and wheel velocity and to obtain good filtering performances. The residuals generated between the results of both the Simulink model and the Kalman filter were from  $-0.0181$  m/s to  $0.0181$  m/s and from  $-0.0156$  m/s to  $0.0156$  m/s for vehicle velocity and wheel velocity respectively. The residuals generated between the results from measurement that smoothed by MAF and the Kalman filter were from  $-0.4038$  m/s to  $0.4038$  m/s and from  $-0.4104$  m/s to  $0.4104$  m/s for vehicle velocity and wheel velocity respectively. It showed that the Kalman filter method for this project could provide excellent accuracy for condition monitoring and could be implemented to detect faults of the ABS system. By using the standard deviation method, the measurement results under four different faulty conditions were discussed with residuals and designed thresholds. With the vehicle state variables estimated by the Kalman filter, advanced ABS control strategies could be designed to improve the vehicle safety without adding additional expensive hardware to the system.

---

## CHAPTER EIGHT

# CONCLUSIONS AND FUTURE WORK

---

**In this chapter, the achievements of this research project are summarized. The findings and conclusions are presented. The contributions to knowledge have been summarized separately and proposals for future research to develop this area of work are discussed.**

## 8.1 REVIEW OF PROJECT OBJECTIVES AND ACHIEVEMENTS

The key achievements of the research documented in this thesis are described below. Care has been taken to correlate these achievements with the original objectives set out in Section 1.5.

- ★ **Objective 1:** To review and understand existing techniques in the model-based condition monitoring of control systems. A potential technique will be chosen for implementation in this project.

**Achievement 1:** The review was presented in Chapter 2. The basic principles of the model-based approach were briefly reviewed in Section 2.1.2. The advantages of a conventional model-based approach were discussed in Section 2.1.5.

- ★ **Objective 2:** To investigate the background and algorithm of the Kalman filter. New applications of the Kalman filter will be introduced in order to exploit the filter with the ABS.

**Achievement 2:** The process to be estimated and the computational origins of the Kalman filter were discussed in Section 3.5.1. Some new applications of Kalman filter, especially in velocity estimation field, were introduced in Section 3.5.1 as well. The parameters for estimation of both vehicle velocity and wheel velocity using the Kalman filter method were set up in Section 3.5.2 and Section 3.5.3. In order to get better filter results, parameter adaptive Kalman filter was introduced in 3.5.4.

- ★ **Objective 3:** To develop a normal model of a typical ABS system for

implementing ABS process control. The control strategies will focus on improving controllability, stability and stopping distance under a wide variety of driving conditions.

**Achievement 3:** The dynamic analysis of the seven steps of the control cycle of a typical ABS system with hydraulic brakes was introduced in Chapter Two. The simulation models of the entire ABS system under normal control conditions were designed using Stateflow for logic control design (Section 3.3). Simulation models without ABS (Section 3.1), ABS without the pressure-holding process (Section 3.2), and ABS with the pressure-holding process (Section 3.3) were developed for vehicle braking simulations. In ABS with the pressure-holding process, different actions of pressure-increasing, pressure-holding, pressure-decreasing and step-pressure-increasing were included in the models. The control state was transformed from one state to another using different ABS control logic thresholds.

- ★ **Objective 4:** To develop fault models for the ABS control system. The faults designed in the model should be ones which are not easily detected by common methods. The seeded faults should be fully controlled in fault type and in fault severity, and furthermore, should not cause any damage to the test facility or simulation hardware.

**Achievement 4:** Speed sensor failure (Section 3.3.1), solenoid valve sticking or stuck (Section 3.3.2), fluid leakage of the actuator (Section 3.3.3) and pump efficiency loss (Section 3.3.4) were seeded in the simulation models. These seeded faults did not cause damage to the ABS system or the hardware of dSpace MicroAutoBox II. The simulation model in fault-free condition was designed to achieve the same effect as an ABS system. The seeded faults could be turned on and off to simulate faults and to return to normal conditions. The parameters of the models could also be changed, which lead to different fault severity within the

ABS system. It was found that different faults could be active independently or in any combination.

- ★ **Objective 5:** To set up a test facility for the implementation of the ABS system. This work will allow control of the ABS system when different strategies are applied, in order to monitor and estimate the system, with the same user interface, and moreover, to seed faults in the system.

**Achievement 5:** The test facility was developed in Chapter Six. A typical Anti-lock Braking System was chosen as designed. The ABS type MK20- I , which widely applied on Volkswagen vehicles, from a Germany manufacture named *Continental Teves*, was chosen for this project and this model is a typical Anti-lock Braking System.

- ★ **Objective 6:** To design different road conditions in a Simulink model in order to test scenarios for road and driving conditions. The road type chosen for the design should be classical and realistic.

**Achievement 6:** Seven different types of road were designed using the Simulink subsystem (Section 4.1.3). The calculation of the friction forces was carried out using the Burckhardt method (Section 3.4). A number of road types were selected to simulate real road conditions. These included the high adhesion coefficient roads such as dry asphalt, wet asphalt and dry concrete and the low adhesion coefficient roads such as dry cobblestones, wet cobblestones, snow and ice.

- ★ **Objective 7:** To combine a dSpace MicroAutoBox II with the ABS system test rig together with advanced data acquisition components. The targets for the application of this hardware are flexible of design and modelling, and stability of operation and control.

**Achievement 7:** The real-time system dSpace MicroAutoBox II was combined into the ABS test rig (Section 6.2). It operated without user intervention, just like the ECU of a vehicle. It was used for rapid control prototyping (RCP). Both normal models and faulty models were downloaded into the dSpace MicroAutoBox II. The ABS actuators were operated via a PC and a National Instruments (NI) Data Acquisition Card was used for data collection (Section 6.3.4). The speed sensor data and the liquid pressure sensor data were transferred to the PC for analysis (Section 6.5).

- ★ **Objective 8:** To investigate Kalman filtering techniques for application to the condition monitoring of the ABS system. Based on this study, novel schemes will be recommended for the model-based approach.

**Achievement 8:** The Kalman filter technology was applied to the simulation model of the ABS (Section 3.5). The test results of both the vehicle velocity and the wheel velocity provided good performance for both tracking and estimation (Section 7.1). The thresholds were set for fault detection and diagnosis using the standard deviation and tolerance intervals theory. The measurements of the vehicle velocity and wheel velocity were smoothed using an MAF method (Section 7.1.1 and Section 7.1.2). The comparison results between the smoothed measurement and the Kalman filter showed an excellent accurate estimation. The Kalman filter technology can be implemented to an actual vehicle system without calculating any analytical derivatives.

- ★ **Objective 9:** To perform a comprehensive data analysis for the ABS system for fault detection and diagnosis. Both normal condition and faulty conditions are to be demonstrated based on the control algorithm designed for the ABS system.

**Achievement 9:** The data analysis using simulation results was described in Chapter 5. The simulation results without the pressure-holding process and with

the pressuring-holding process in normal condition were listed separately. Comparison of vehicle velocity, wheel velocity, braking distance, slip rate, braking torque and wheel acceleration (Section 5.1 to 5.3) were presented. The simulation results for faults including speed sensor failure (Section 5.4), solenoid valve sticking or stuck (Section 5.5), fluid leakage (Section 5.6) and pump efficiency loss (Section 5.7) were also presented and compared with normal conditions. The measurements results under healthy conditions (Section 7.1) and faulty conditions (Section 7.2 to Section 7.5) were discussed. The thresholds for fault detection of vehicle velocity and wheel velocity are set using the standard deviation method. The residuals generated from the measurements and the Kalman filter estimations under faulty conditions are listed in figures.

- ★ **Objective 10:** According to the results and experience gained during this programme of work, to suggest potential future work which will extend the research for integration of more advanced technologies in this field.

**Achievement 10:** Some possible directions for future work have been identified including unscented filter applications, residual generation in the model-based approach, acoustic model-based exploitation, fault isolation techniques and so on.

## 8.2 CONCLUSIONS

**Conclusion 1:** The Model-based method has significant advantages for condition monitoring and for fault detection for control systems. The basic algorithm of the model-based method is developed using the system model and the measurement signal to reconstruct the parameters. By using the difference between the estimation and measurement to obtain the residual, the goals of condition monitoring can easily be achieved.

**Conclusion 2:** Anti-lock Braking Systems are highly integrated systems with a high degree of commercial confidentiality. The development of these systems has accelerated during the past 30 years. The ABS system can improve braking safety and driver comfortability during emergency braking situations. The dynamic friction tyre model can provide a simplified procedure for the controller design process to obtain stable and reliable performance during the operation of the ABS systems.

**Conclusion 3:** As a consequence of this research, ABS condition monitoring and fault detection has improved significantly compared with previous research works. In the past, ABS condition monitoring and fault detection has been concerned primarily with electronic fault diagnosis. It is not easy to detect the mechanical faults of an ABS system. An ABS system only works under extreme driving conditions where severe braking is necessary to avoid accidents and endangering life. This research has focused on both the electronic faults such as speed sensor failure and, the mechanical and hydraulic faults such as solenoid valve stuck, liquid leakage and pump efficiency loss. It provides methods for carrying out regular checks of the mechanical and hydraulic components of the ABS using a specially designed test rig ensuring the capability and performance of the functioning ABS system.

**Conclusion 4:** The Kalman filter with adaptive parameters can be combined with a model-based approach for condition monitoring. In this research work, the Kalman filter estimation results are fitted to the simulation and measurement results with a high degree of accuracy, meaning that the adaptive parameter settings for the model of the Kalman filter are sufficiently accurate. Together with a model-based method, the Kalman filter can be used to estimate vehicle velocity and wheel velocity during faults occurring in the ABS system. The residuals are generated between the Kalman Filter estimation and measurement for fault diagnosis.

**Conclusion 5:** The mathematical model of the ABS system has been developed, providing a new method for the modelling of the vehicle braking system and

simplifying the design of the ABS controller. At the same time, a dynamic friction tyre model was also developed based on the Burckhardt method for generating the dynamic tyre/road interaction.

**Conclusion 6:** The Kalman filter was utilized to estimate the vehicle velocity and obtain good filtering performance of the wheel velocity. The test results showed that the Kalman filter estimation of the vehicle state matched the simulated vehicle state very well. From the vehicle state variables estimated by the Kalman filter, it is possible to design advanced ABS control strategies to improve the vehicle safety without adding additional expensive hardware to the ABS system. The Kalman filter used during this research shows a good performance when estimating both the vehicle velocity and wheel velocity.

**Conclusion 7:** The dSpace MicroAutoBox II can be combined with the ABS system for the implementation of RCP simulation. The dSpace take place of ECU in vehicle as a virtual controller. The model could be downloaded from Matlab or Simulink and communicated with the actuators as in the case of an ECU of a vehicle. As a result of this research, a number of advantages were observed such as: more comprehensive and more systematic tests in a shorter time, fewer prototypes and higher accuracy for modelling.

**Conclusion 8:** From the rig simulation of system faults, it can be concluded that faults such as speed sensor failure, solenoid valve sticking or stuck, fluid leakage and pump efficiency loss can be seeded with the following effects: Firstly, they will not cause damage to the system itself; Secondly, they will not cause distortion coding to the dSpace MicroAutoBox II; Thirdly, they can be repeated arbitrarily; Finally, their severity can be adjusted to any desired degree and finally, they can be turned on or off as required.

**Conclusion 9:** The test results show that the braking performance of a vehicle with an

ABS system is much better than the one without an ABS system. The braking performance of an ABS with the pressure-holding process is much better than one without the pressure-holding process. All comparison results such as vehicle velocity, wheel velocity, braking distance, slip rate and braking torque have been carried out for these different scenarios.

## 8.3 CONTRIBUTION TO KNOWLEDGE

The project reported on within this thesis has made several new contributions to research in the field of model-based condition monitoring using the Kalman filter. These will now be summarized:

- ★ ***Novelty 1: A new model of ABS system was developed with normal conditions and faulty conditions.***

There are several subsystems included in the simulation model of the ABS system. The slip rate calculation module using the inputs of vehicle velocity and wheel velocity is a subsystem example. It is intuitive to observe the slip rate changing throughout the whole braking process. The choice of road type is also a subsystem and seven different road types including dry asphalt, wet asphalt, dry concrete, dry cobblestones, wet cobblestones, snow and ice were simulated. The road type can be changed freely as the test requires. The most complicated subsystem of the entire ABS system is the control strategy. The control commands of not only the processes of pressure-increasing, pressure-holding and pressure-decreasing, but also the processes of the step-pressure-increasing and first round pressure-increasing are demonstrated in the ABS system. The initial vehicle velocity and initial braking torque can be modified according to requirements.

- ★ ***Novelty 2: An autonomous ABS control system was designed with a dSpace***

## **MicroAutoBox II.**

By using dSpace MicroAutoBox II and its software interface Control Desk, the simulated model of the ABS control system can be programmed without manual programming. No special expertise is necessary for implementation of the prototyping system. The designed faults can also be seeded into the Matlab/Simulink model of ABS. With dSpace's implementation software Real-Time Interface (RTI), the designed models can be implemented on the dSpace hardware automatically. A graphical block library with numerous interface functionalities is provided for configuring input and output and connecting I/O to the model, which can be easily used in Simulink. The ABS models with faults can also be implemented by dSpace MicroAutoBox II for using on ABS actuator components.

★ ***Novelty 3: The Kalman filter was applied to model-based condition monitoring of the ABS system.***

The Kalman filter method is used to estimate the vehicle velocity and wheel velocity of the ABS system under healthy and faulty conditions. The comparison results show that the Kalman filter model can match the designed ABS system with high accuracy. By using the Kalman filter model-based approach, the ABS system with faults can be monitored by inspecting the generated residual. The condition monitoring with fault detection can be carried out by analysis of residual characteristics.

## **8.4 FUTURE WORK**

★ ***Future Work 1: Liquid pressure sensors will be installed on the brake fluid pipe of the remaining three wheels for pressure monitoring.***

The sensor for measuring liquid pressure is only used on a quarter model at the

moment. The performance can suit the theoretical model as required. It is recommended that liquid pressure sensors are added to the other three wheels for pressure monitoring of the whole system.

★ ***Future Work 2: Use Fault Diagnostic Apparatus (AutoBoss V30) for the ABS test rig.***

The fault diagnostic apparatus can decode the command orders from the Electronic Control Unit (ECU) and can also send code to the ECU for testing. By using the proposed fault diagnostic apparatus, the three steps of the ABS controller can be demonstrated. At the same time, the speed signal of the vehicle and the pressure signal can then be collected for analysis.

★ ***Future Work 3: Develop a non-interference pressure sensor.***

In order to check the pressure of the brake cylinder, a non-interference pressure sensor is needed. This kind of sensor will not change any construction of the pipelines, which is required to maintain a high safety level of the braking system. The non-interference sensor should be used for ABS system condition monitoring and fault diagnosis. When a fault occurs in the ABS mechanical components, the pressure of the brake cylinder should be different from the healthy condition.

★ ***Future Work 4: Residual generation for partially known systems.***

A partially known system means that only a part of the system information can be obtained. For example, most ABS manufacturers do not provide detailed structure parameters when they sell their products. Instead, they deliver performance descriptions such as valve action frequency in their product specifications. This is usually not sufficient for a model-based application. Another example of a partially known system is when the non-linearity of a system cannot be

represented accurately with a linearized analytical model since some information has been lost.

★ ***Future Work 5: Network communications between ECU and dSpace.***

This work is important for implementation of the ABS control algorithm in the operation of real vehicle. At the moment, the majority of vehicles are using CAN communication protocol. Only a few vehicles are using other types of communication protocol. By using the packet information from CAN-High and CAN-Low, the control algorithm can be applied to vehicles through the vehicle OBD connector.

★ ***Future Work 6: Non-parametric modelling.***

The central issue of the model-based approach is the residual generation, which in turn relies heavily on the system model. However, for systems with high non-linearity and a wide operating range, the modelling is quite difficult and often inadequate for model-based application. In some systems, an analytical model cannot be built up due to the lack of sufficient information. A non-parametric model with adaptive parameters and advanced filtering technology is a possible alternative in these cases.

## REFERENCES

- [1] R. H. Madison and H. E. Riordan, "Evolution of Sure-Track Brake System," SAE International, Warrendale, PA, SAE Technical Paper 690213, Feb. 1969.
- [2] A. M. A. Soliman, M. M. S. Kaldas, and K. R. M. Mahmoud, "Active Suspension and Anti-lock Braking Systems for Passenger Cars," SAE International, Warrendale, PA, SAE Technical Paper 2009-01-0357, Apr. 2009.
- [3] L. Austin and D. Morrey, "Recent advances in antilock braking systems and traction control systems," *Proc. Inst. Mech. Eng. Part J. Automob. Eng.*, vol. 214, no. 6, pp. 625–638, Jun. 2000.
- [4] R. Jegadeeshwaran and V. Sugumaran, "Comparative study of decision tree classifier and best first tree classifier for fault diagnosis of automobile hydraulic brake system using statistical features," *Measurement*, vol. 46, no. 9, pp. 3247–3260, Nov. 2013.
- [5] T. K. Bera, K. Bhattacharya, and A. K. Samantaray, "Evaluation of antilock braking system with an integrated model of full vehicle system dynamics," *Simul. Model. Pract. Theory*, vol. 19, no. 10, pp. 2131–2150, Nov. 2011.
- [6] Z. Shi, I. Legate, F. Gu, J. Fieldhouse, and A. Ball, "Prediction of antilock braking system condition with the vehicle stationary using a model-based approach," *Int. J. Automot. Technol.*, vol. 11, no. 3, pp. 363–373, Jun. 2010.
- [7] Z. Shi, A. Higson, L. Zheng, F. Gu, and A. Ball, "Automatic Fault Detection Using a Model-Based Approach in the Frequency Domain," pp. 849–855, 2006.
- [8] L. Zheng, Z. Shi, and A. Ball, "Vehicle Anti-lock Braking System Performance using dSPACE," in *Proceedings of Computing and Engineering Annual Researchers' Conference 2013 : CEARC'13*, G. Lucas, Ed. Huddersfield: University of Huddersfield, 2013, pp. 1–6.
- [9] T. M. Hunt, *Level, leakage & flow monitoring*. Oxford: Coxmoor Pub. Co., 2001.
- [10] R. A. Collacott, *Mechanical Fault Diagnosis and Condition Monitoring*. Chapman and Hall, 1977.
- [11] B. K. N. Rao, *Handbook of Condition Monitoring*. Elsevier, 1996.
- [12] A. Davies, *Handbook of Condition Monitoring: Techniques and Methodology*. Springer, 1998.
- [13] L. Zheng, "Model-based fault detection for non-linear control system using advanced filtering techniques," MPhil Thesis, The University of Manchester, U.K., 2007.
- [14] "Condition monitoring," Wikipedia, the free encyclopedia. 28-Dec-2013.

- [15]C. W. Reeves, Power, Performance and Efficiency Handbook. Coxmoor Publishing Company, 1998.
- [16]J. T. Lenaghan and A. I. Khalil, “Condition/performance monitoring of internal combustion engine by continuous measurements of crankshaft twist angle,” in Condition Monitoring and Diagnostic Engineering Management, R. B. K. N. Rao, J. Au, and B. Griffiths, Eds. Springer Netherlands, 1990, pp. 114–119.
- [17]Proceedings of 18th COMADEM International Conference. .
- [18]R. B. Randall, “Detection and diagnosis of incipient bearing failure in helicopter gearboxes,” Eng. Fail. Anal., vol. 11, no. 2, pp. 177–190, 2004.
- [19]G. B. Q. M. and S. S. Committee, British Standard Glossary of Maintenance Management Terms in Terotechnology. British Standards Institution, 1984.
- [20]A. Kelly, Maintenance Strategy. Elsevier, 1997.
- [21]J. S. Mitchell, An introduction to machinery analysis and monitoring. PennWell Pub. Co., 1981.
- [22]R. J. Patton, “Fault-tolerant control systems: The 1997 situation,” in IFAC Symposium on Fault Detection Supervision and Safety for Technical Processes,” in IFAC SAFEPROCESS’1997, 1997, pp. 1033–1054.
- [23]P. M. Frank, “Advances in observer-based fault diagnosis in dynamic systems,” Eng. Simul., vol. 13, pp. 717–760, 1996.
- [24]R. Isermann, “Supervision, fault-detection and fault-diagnosis methods — An introduction,” Control Eng. Pract., vol. 5, no. 5, pp. 639–652, 1997.
- [25]R. Isermann and P. Ballé, “Trends in the application of model-based fault detection and diagnosis of technical processes,” Control Eng. Pract., vol. 5, no. 5, pp. 709–719, 1997.
- [26]Z. Shi, “A hybrid model-based approach to condition monitoring,” PhD Thesis, The University of Manchester, 2004.
- [27]G. Welch and G. Bishop, An Introduction to the Kalman Filter. 1995.
- [28]R. E. Kalman, “A New Approach to Linear Filtering and Prediction Problems,” J. Basic Eng., vol. 82, no. 1, pp. 35–45, 1960.
- [29]M. S. Grewal and A. P. Andrews, Kalman Filtering: Theory and Practice Using MATLAB. Wiley, 2008.
- [30]W. C. Congwei Hu, “Adaptive Kalman Filtering for Vehicle Navigation,” J. Glob. Position. Syst., vol. 2, no. 1, pp. 42–47, 2003.
- [31]L. A. Mcgee, Discovery of the Kalman filter as a practical tool for aerospace and industry. 1985.
- [32]S. Dutta, S. K. Pal, S. Mukhopadhyay, and R. Sen, “Application of digital image

- processing in tool condition monitoring: A review,” *CIRP J. Manuf. Sci. Technol.*, vol. 6, no. 3, pp. 212–232, 2013.
- [33] X. Xue, J. Tang, N. Sammes, and Y. Ding, “Model-based condition monitoring of PEM fuel cell using Hotelling T2 control limit,” *J. Power Sources*, vol. 162, no. 1, pp. 388–399, 2006.
- [34] R. V. Beard, “Failure accomodation in linear systems through self-reorganization,” Thesis, Massachusetts Institute of Technology, 1971.
- [35] R. Isermann, “Model-based fault-detection and diagnosis – status and applications,” *Annu. Rev. Control*, vol. 29, no. 1, pp. 71–85, 2005.
- [36] A. S. Willsky, “A survey of design methods for failure detection in dynamic systems,” *Automatica*, vol. 12, no. 6, pp. 601–611, 1976.
- [37] M. L. Darby and M. Nikolaou, “Identification test design for multivariable model-based control: An industrial perspective,” *Control Eng. Pract.*, vol. 22, pp. 165–180, 2014.
- [38] R. Isermann, “Advanced methods of process computer control for industrial processes,” *Comput. Ind.*, vol. 2, no. 1, pp. 59–72, 1981.
- [39] M. Börner and R. Isermann, “Model-based detection of critical driving situations with fuzzy logic decision making,” *Control Eng. Pract.*, vol. 14, no. 5, pp. 527–536, 2006.
- [40] L. Billmann and R. Isermann, “Leak detection methods for pipelines,” *Automatica*, vol. 23, no. 3, pp. 381–385, 1987.
- [41] R. Isermann, “Process fault detection based on modeling and estimation methods—A survey,” *Automatica*, vol. 20, no. 4, pp. 387–404, 1984.
- [42] A. Gryzlov, W. Schiferli, and R. F. Mudde, “Soft-sensors: Model-based estimation of inflow in horizontal wells using the extended Kalman filter,” *Flow Meas. Instrum.*, vol. 34, pp. 91–104, 2013.
- [43] H. K. Sahoo, P. K. Dash, and N. P. Rath, “NARX model based nonlinear dynamic system identification using low complexity neural networks and robust  $H_\infty$  filter,” *Appl. Soft Comput.*, vol. 13, no. 7, pp. 3324–3334, 2013.
- [44] P. Beckerle, H. Schaede, N. Butzek, and S. Rinderknecht, “Balancing filters: An approach to improve model-based fault diagnosis based on parity equations,” *Mech. Syst. Signal Process.*, vol. 29, pp. 137–147, 2012.
- [45] V. Krishnaswami, G.-Luh, and G. Rizzoni, “Nonlinear parity equation based residual generation for diagnosis of automotive engine faults,” *Control Eng. Pract.*, vol. 3, no. 10, pp. 1385–1392, 1995.
- [46] A. Zakharov, V.-M. Tikkala, and S.-L. Jämsä-Jounela, “Fault detection and diagnosis approach based on nonlinear parity equations and its application to

- leakages and blockages in the drying section of a board machine,” *J. Process Control*, vol. 23, no. 9, pp. 1380–1393, 2013.
- [47] D. M. Himmelblau, *Fault detection and diagnosis in chemical and petrochemical processes*. Elsevier Scientific Pub. Co., 1978.
- [48] D. Wang, M. Yu, C. B. Low, and S. Arogeti, *Model-based Health Monitoring of Hybrid Systems*. Springer, 2013.
- [49] F. Serdio, E. Lughofer, K. Pichler, T. Buchegger, and H. Efendic, “Residual-based fault detection using soft computing techniques for condition monitoring at rolling mills,” *Inf. Sci.*, vol. 259, pp. 304–320, 2014.
- [50] L. Zheng, “Model-based Fault Detection for a Non-linear Control System Using Advanced Filtering Techniques and Neural Networks,” *The University of Manchester, First Year Transfer Report*, 2006.
- [51] M. Jin, J. Zhao, J. Jin, G. Yu, and W. Li, “The adaptive Kalman filter based on fuzzy logic for inertial motion capture system,” *Measurement*, vol. 49, pp. 196–204, 2014.
- [52] Z. N. Sadough Vanini, K. Khorasani, and N. Meskin, “Fault detection and isolation of a dual spool gas turbine engine using dynamic neural networks and multiple model approach,” *Inf. Sci.*, vol. 259, pp. 234–251, 2014.
- [53] J. Chen and C.-M. Liao, “Dynamic process fault monitoring based on neural network and PCA,” *J. Process Control*, vol. 12, no. 2, pp. 277–289, 2002.
- [54] F. Alrowaie, R. B. Gopaluni, and K. E. Kwok, “Fault detection and isolation in stochastic non-linear state-space models using particle filters,” *Control Eng. Pract.*, vol. 20, no. 10, pp. 1016–1032, 2012.
- [55] P. Ballé, “Fuzzy-model-based parity equations for fault isolation,” *Control Eng. Pract.*, vol. 7, no. 2, pp. 261–270, 1999.
- [56] V. Puig and J. Quevedo, “Passive robust fault detection using fuzzy parity equations,” *Math. Comput. Simul.*, vol. 60, no. 3–5, pp. 193–207, 2002.
- [57] H. Taghavifar and A. Mardani, “Fuzzy logic system based prediction effort: A case study on the effects of tire parameters on contact area and contact pressure,” *Appl. Soft Comput.*, vol. 14, Part C, pp. 390–396, 2014.
- [58] Z. Wei, “Fuzzy Logic and Neural Network-aided Extended Kalman Filter for Mobile Robot Localization,” *Thesis*, 2011.
- [59] “Iscanoglu Aysegul - Credit Scoring Methods and Accuracy Ratio,” *Scribd*. [Online]. Available: <http://www.scribd.com/doc/56001811/26/Advantages-and-Disadvantages-of-Neural-Networks>. [Accessed: 03-Mar-2014].
- [60] M. A. O. Alves, D. Cabral, and K. Fitzgibbon, “Model-based failure severity

- prediction based on robust residual design,” in Mediterranean Conference on Control Automation, 2007. MED ’07, 2007, pp. 1–6.
- [61]X. Ding, L. Guo, and T. Jeinsch, “A characterization of parity space and its application to robust fault detection,” *IEEE Trans. Autom. Control*, vol. 44, no. 2, pp. 337–343, 1999.
- [62]informa, “Comadem 2014 - Implications of life cycle analysis in asset and maintenance management | Informa Conferences & Exhibitions.” [Online]. Available: <http://www.comadem2014.org/>. [Accessed: 08-Jan-2014].
- [63]“Engineering Standards News and Resources for Engineers - ASME.” [Online]. Available: <https://www.asme.org/>. [Accessed: 08-Jan-2014].
- [64]“Model-based testing,” Wikipedia, the free encyclopedia. 17-Dec-2013.
- [65]R. Izadi-Zamanabadi, M. Blanke, and S. Katebi, “Cheap diagnosis using structural modelling and fuzzy-logic-based detection,” *Control Eng. Pract.*, vol. 11, no. 4, pp. 415–422, 2003.
- [66]S. X. Ding, *Model-Based Fault Diagnosis Techniques - Design Schemes, Algorithms and Tools*. 2013.
- [67]G. Mermoud, “Model-Based Design,” in *Stochastic Reactive Distributed Robotic Systems*, Springer International Publishing, 2014, pp. 159–173.
- [68]“Model-based design,” Wikipedia, the free encyclopedia. 08-Dec-2013.
- [69]G. Franceschini and S. Macchietto, “Model-based design of experiments for parameter precision: State of the art,” *Chem. Eng. Sci.*, vol. 63, no. 19, pp. 4846–4872, 2008.
- [70]J. Chen, “Robust residual generation for model-based fault diagnosis of dynamic systems,” Thesis, University of York, 1995.
- [71]J. Chen, *Robust Model-Based Fault Diagnosis for Dynamic Systems*. Springer, 1999.
- [72]L. A. Mironovski, “Functional diagnosis of linear dynamic systems - a survey,” *Autom. Remote Control*, vol. 41, pp. 1122–1143, 1980.
- [73]M. Basseville, “Detecting changes in signals and systems—A survey,” *Automatica*, vol. 24, no. 3, pp. 309–326, 1988.
- [74]E. Frisk, “Residual Generation for Fault Diagnosis,” 2001.
- [75]“Fault model,” Wikipedia, the free encyclopedia. 04-Dec-2013.
- [76]T. Sedighi, P. Phillips, and P. d. Foote, “Model-based Intermittent Fault Detection,” *Procedia CIRP*, vol. 11, pp. 68–73, 2013.
- [77]J. Anugrah, “Fault tolerant synthesis of reversible circuits,” Dissertation, Rajasthan Technical University, Kota, 2013.

- [78]K.-T. (Tim) Cheng, W.-B. Jone, and L.-T. (L.-T. ) Wang, “Chapter 12 - Test Technology Trends in the Nanometer Age,” in *VLSI Test Principles and Architectures*, L.-T. Wang, C.-W. Wu, and X. Wen, Eds. San Francisco: Morgan Kaufmann, 2006, pp. 679–749.
- [79]L. Zheng, L. L. Wu, X. Gu, Z. Shi, and A. Ball, “Application of EKF for an Electro-Hydraulic Servo System Using Model-Based Approach,” *Appl. Mech. Mater.*, vol. 385–386, pp. 609–613, Aug. 2013.
- [80]“Anti-lock braking systems (ABS),” *Engineering*. [Online]. Available: [http://engineering.wikia.com/wiki/Anti-lock\\_braking\\_systems\\_\(ABS\)](http://engineering.wikia.com/wiki/Anti-lock_braking_systems_(ABS)). [Accessed: 10-Jan-2014].
- [81]A. A. Aly, “An Antilock-Braking Systems (ABS) Control: A Technical Review,” *Intell. Control Autom.*, vol. 02, no. 03, pp. 186–195, 2011.
- [82]“Anti-lock braking system,” *Wikipedia, the free encyclopedia*. 10-Jan-2014.
- [83]P. Hart, “Review of Heavy Vehicle Braking Systems Requirements (PBS Vehicle Aspects),” *National Road Transport Commission, National Road Transport Commission, Discussion Paper (Main Report)*, Jul. 2003.
- [84]G. Press, “Automobile Electrical and Electronic Systems: 4th Edition (Paperback) - Guilford Press.” [Online]. Available: <http://www.guilfordpress.co.uk/books/details/9780080969428/>. [Accessed: 10-Jan-2014].
- [85]M. Stan, R.-E. Precup, and A. S. Paul, “Analysis Of Fuzzy Control Solutions For Anti-lock Braking Systems,” *J. Control Eng. Appl. Inform.*, vol. 9, no. 2, pp. 11–22, Jul. 2007.
- [86]S. Drakunov, U. Ozguner, P. Dix, and B. Ashrafi, “ABS control using optimum search via sliding modes,” *IEEE Trans. Control Syst. Technol.*, vol. 3, no. 1, pp. 79–85, 1995.
- [87]A. W. M. Bonnicksen, *Vehicle electronic systems and fault diagnosis: a practical guide*. 1998.
- [88]R. Limpert, *Brake Design and Safety*. SAE International, 2011.
- [89]W. Xing, “Model-based ABS/ASR system failure prediction simulation study,” *MSc Thesis, Hebei University of Technology, Tianjin, China*, 2013.
- [90]J. A. Cabrera, A. Ortiz, J. J. Castillo, and A. Simon, “A fuzzy logic control for antilock braking system integrated in the IMM tire test bench,” *IEEE Trans. Veh. Technol.*, vol. 54, no. 6, pp. 1937–1949, 2005.
- [91]U. K. and L. Nielsen, “Automotive Control Systems: For Engine, Driveline, and Vehicle,” *Meas. Sci. Technol.*, vol. 11, no. 12, p. 1828, Dec. 2000.
- [92]M. Börner, H. Straky, T. Weispenning, and R. Isermann, “Model based fault

- detection of vehicle suspension and hydraulic brake systems,” *Mechatronics*, vol. 12, no. 8, pp. 999–1010, 2002.
- [93] P. Struss, “Fundamentals of Model-Based Diagnosis of Dynamic Systems,” presented at the 15th International Joint Conference on Artificial Intelligence, Nagoya, Japan, 1997, pp. 480–485.
- [94] P. Struss and A. Malik, “Qualitative modeling is the key: a successful feasibility study in automated generation of diagnosis guidelines and failure mode and effects analysis for mechatronic car subsystems,” in *Working Notes of the 6th International Workshop on Principle of Diagnosis*, Goslar, Germany, 1995, vol. DX-95.
- [95] M. Sachenbacher and P. Struss, “Fault Isolation in the Hydraulic Circuit of an ABS: A Real-World Reference Problem for Diagnosis,” in *IN WORKING NOTES OF THE 8TH INTERNATIONAL WORKSHOP ON THE PRINCIPLES OF DIAGNOSIS*, (DX-97), MONT-ST-MICHEL, 1997, pp. 113–119.
- [96] “Rapid control prototyping,” Wikipedia, the free encyclopedia. 03-Nov-2013.
- [97] “Hardware-in-the-loop simulation,” Wikipedia, the free encyclopedia. 24-Dec-2013.
- [98] H. Straky, M. Kochem, J. Schmitt, and R. Isermann, “Influences of braking system faults on vehicle dynamics,” *Control Eng. Pract.*, vol. 11, no. 3, pp. 337–343, 2003.
- [99] O. Moseler, “Fault Detection of a Solenoid Valve for Hydraulic System in Vehicles,” presented at the 4th, Fault detection, supervision and safety for technical processes, 2001, pp. 119–124.
- [100] R. Isermann, “Industrial application of fault diagnosis,” *Control Syst. Robotics Autom.*, vol. XVI.
- [101] A. Gajek, “A Testing of ABS Operation in Stand Conditions,” presented at the International Conference on Brakes 2000: Automotive Braking - Technologies for the 21st Century, Leeds, England, 2000.
- [102] D. Fischer, M. Börner, J. Schmitt, and R. Isermann, “Fault detection for lateral and vertical vehicle dynamics,” *Control Eng. Pract.*, vol. 15, no. 3, pp. 315–324, 2007.
- [103] A. D. Khekare, “Straight line braking performance of a road vehicle with non linear tire stiffness formulation,” CLEMSON UNIVERSITY, 2010.
- [104] J. Anderson, *Computational Fluid Dynamics*. McGraw-Hill Education, 1995.
- [105] W. Qin, “Research and development on evaluate system for vehicle ABS performance based on multi-dimension wheel force measurement,” PhD Thesis, Southeast University, China, 2005.

- [106] L. Zhang, "Simulation and studying hydraulic anti-lock braking system of vehicle ABS methods," MSc Thesis, University of Northeast, China, 2009.
- [107] W. L. Zheng, "The ABS/EBD control strategy study based on the slip rate," PhD Thesis, University of Jilin, China, 2008.
- [108] T. X. Zheng, "Automotive ABS control strategy based on logic threshold," *J. Traffic Transp. Eng.*, vol. 10, no. 2, pp. 69–74, 2010.
- [109] J. X. Li, "Study on application of speed segmentation in the ABS logic threshold control method," *Automob. Technol.*, vol. 11, pp. 5–8, 2004.
- [110] U. Kiencke and L. Nielsen, *Automotive Control Systems: For Engine, Driveline, and Vehicle*. Springer, 2005.
- [111] E. L. Ding, H. Fennel, and S. X. Ding, "Model-based diagnosis of sensor faults for ESP systems," *Control Eng. Pract.*, vol. 12, no. 7, pp. 847–856, 2004.
- [112] W. B. Na, J. Sun, and L. Li, "A method of fault type identification on ABS wheel speed sensor system," *Mach. TOOL Amp Hydraul.*, vol. 36, no. 7, pp. 191–193, 2008.
- [113] M. Karpenko, N. Sepehri, and D. Scuse, "Diagnosis of process valve actuator faults using a multilayer neural network," *Control Eng. Pract.*, vol. 11, no. 11, pp. 1289–1299, Nov. 2003.
- [114] M. Wu and M. Shih, "Simulated and experimental study of hydraulic anti-lock braking system using sliding-mode PWM control," *Mechatronics*, vol. 13, no. 4, pp. 331–351, 2003.
- [115] D. T. Valentin Ivanov, "Investigation on Hysteresis Losses into Disc Brake Gear for Heavy Vehicles," *SAE Tech. Pap. Ser.*, no. 2006–01–3212, pp. 1–7, 2006.
- [116] A. G. Ulsoy, H. Peng, and M. Çakmakci, *Automotive control systems*. Cambridge ; New York: Cambridge University Press, 2012.
- [117] B. Wang, "Optimal slip ratio on line identification of ABS," *Automob. Technol.*, vol. 5, pp. 9–12, 2006.
- [118] *Dynamik der Kraftfahrzeuge*. .
- [119] R. G. Brown and P. Y. C. Hwang, *Introduction to random signals and applied Kalman filtering: with MATLAB exercises and solutions*. Wiley, 1997.
- [120] "An Introduction to the Kalman Filter," Goddard Consulting: Modeling, Simulation, Data Analysis, Visualization. [Online]. Available: <http://www.goddardconsulting.ca/kalman-filter.html>.
- [121] M. P. Stanley, "IMPLEMENTATION OF KALMAN FILTER TO TRACKING CUSTOM FOUR-WHEEL DRIVE FOUR-WHEEL-STEERING ROBOTIC PLATFORM," Thesis, University of Maryland, 2010.

- [122] K. Kobayashi, "Estimation of Absolute Vehicle Speed using Fuzzy Logic Rule-Based Kalman Filter," presented at the American Control Conference, Seattle, Washington, USA, 1995, vol. FA6, pp. 3086–3090.
- [123] N. G. Ding, "Estimation of vehicle speed based on Kalman filter and ABS control inputs," *J. Beijing Univ. Aeronaut. Astronaut.*, vol. 37, no. 1, pp. 67–71, 2011.
- [124] K. H. Guo, "A study on hydraulic characteristics of anti-lock braking system," *J. Jilin Univ. Technol. Nat. Sci.*, vol. 29, pp. 1–25, 1999.
- [125] W. Zhang, *Stateflow logic system modeling*. Xi'an Electronic and Science University Press, 2007.
- [126] B. Danis and M. Arnis, "Research in parameters of braking for automobiles," *Eng. Rural Dev.*, vol. 28–29, pp. 124–130, 2009.
- [127] Y. F. Chen, "Experimental study on wheel speed sensor in ABS," Master Dissertation, Hefei University of Technology, China, 2008.
- [128] X. F. Zhang, "Automotive ABS wheel signal collection and analysis," *Beijing Automot.*, vol. 6, pp. 5–7, 2008.
- [129] J. Sun, "A study on testing system for wheel speed sensor in ABS," *Automot. Eng.*, vol. 29, no. 8, pp. 698–713, 2007.
- [130] Z. W. Wang, "Study on Dynamic Characteristics of Magnetolectric Wheel Speed Sensor in Anti-lock Brake System and Signal Processing," Master Dissertation, Heifei University of Technology, Heifei, China, 2006.
- [131] "Zero crossing," Wikipedia, the free encyclopedia. 13-Jan-2014.
- [132] Instruments National, "NI USB-6008/6009 User Guid and Specifications." 2006.
- [133] "Normal distribution," Wikipedia, the free encyclopedia. 09-Jan-2014.
- [134] S. W. Smith, *The Scientist and Engineer's Guide to Digital Signal Processing*. San Diego, California: California Technical Publishing.
- [135] MathWorks, "Filtering and Smoothing Data," Documentation Center. Available: <http://www.mathworks.co.uk/help/curvefit/smoothing-data.html>.
- [136] C. Yu, "Compare Analysis of Several Nonlinear Filters' Performance," *Hydrogr. Surv. CHARTING*, vol. 28, no. 6, p. 237, 2008.
- [137] H. Chen, "Analysis of different methods for denoising of high temperature raman spectra," *Spectrosc. Spectr. Anal.*, vol. 27, no. 6, pp. 1148–1151, Jun. 2007.
- [138] E. Carpentieri and S. Cuomo, "An adaptive threshold algorithm for detection of pulse radar signals," in *IEEE Radar Conference, 2008. RADAR '08*, 2008, pp. 1–5.